Efforts Towards the Synthesis of Silicon-Stereogenic Silanols

By

ADILENE BERNAL SANCHEZ

DISSERTATION

Submitted in partial satisfaction of the requirements for the degree of

DOCTOR OF PHILOSOPHY

in

Chemistry

in the

OFFICE OF GRADUATE STUDIES

of the

UNIVERSITY OF CALIFORNIA

DAVIS

Approved:

Annaliese K. Franz, Chair

Dean J. Tantillo

Cody Ross Pitts

Committee in Charge

2025

Para todos los estudiantes hijos de inmigrantes

indocumentados.

Nadie entiende lo que sufrimos en este mundo, con personas, el sistema

y situaciones que no nos apoyan.

Pero nunca se olviden que no hay mal que por bien no venga.

ACKNOWLEDGMENTS

I am the first in my family (on both sides) to graduate college, the first scientist and the first to earn a Ph.D. My education has meant the world to me since I was 4 years old. I knew at that age that I would study up until the highest degree possible. I don't even know how I knew. It took me 16 years to get through my undergraduate and graduate education. When I say it out loud it sounds wild. I am stoked that I refused to give up on what I wanted no matter what came my way. There are so many people to thank for helping me get to this point in my life. But I would like to thank myself for getting up every morning to keep at it for 30 years until I made my childhood dream a reality. It's been so punk rock.

The next person I would like to thank is my undergraduate research advisor, Prof. Steven C. Farmer. Your lectures really sparked what I call "the pull" for me for organic chemistry. I began to even wonder how and why reactions work. It was even cooler to find out you were also a first-generation college student and loved The Misfits as much as I did. Within no time, you gave me the opportunity to work on a six-step synthesis in your research lab. I truly don't know how I convinced you to take me on as your first wet lab student in years, but I am glad I did. Your mentorship and unwavering support did not stop after I graduated. You have always made yourself available through all the highs and lows that come with graduate school and life. Dr. Farmer you changed my life. You get it, every single time. This non-conforming, little punk kid thanks you from the bottom of my soul. I am honored to be your student.

To Dr. Megan D'Errico. I still remember meeting you. You had the biggest smile. You took any chance you could to help me get through anything I was going through. Your messages to ride the wave (~~~~). Those helped me beyond words. You have always been someone who just sees me. You get it, every single time.

I would also like to thank my best friends, Lucero, Tara, and Matt. I would not have been able to get through any of this without your love, support, and encouragement. It is because of you all that I realized what *true* friendships mean.

I would also like to thank, J. Ramón Villanueva, for your kindness and support of our family. The opportunities you give and continue to give my parents, who immigrated to this country with nothing more than a dream for a better life, have allowed me the privilege of my education. There are no words to describe your impact on our family's ability to make it in this country. Desde el fondo de mi corazón, muchísimas gracias Jefe.

Thank you to my doctoral advisor, Prof. Annaliese K. Franz for your enthusiastic support of all my bold ideas. I've learned a lot in my time in your lab. Thank you for allowing me to have full autonomy over my research. It helped cement what I have known about myself my entire life–that I am capable of anything I put my mind to. Thank you for allowing me the opportunity to take on some very interesting chemistry in a welcoming environment. I really have always thought silanols were so cool since I was a first-year student. Working with silanediols in my time in your lab really was full circle for me when it came to understanding why I even like organic chemistry to begin with.

I want to thank the Merck Research Award for Underrepresented Chemists of Color community that embraced all the different parts of my identity and welcomed me with open arms to the Merck family. You all came at a time when I needed it most. I am forever grateful. I want to especially thank David Thaisrivongs, Ph.D., Yon-Hee Lim, Ph.D. and Morgan Crawford, M.S. for being some of the coolest humans. To Estely: You are a breath of fresh air. It is not every day that I meet someone just as like-minded. I really admire the way you can articulate things calmly even when it is something difficult to talk about. Thank you for trusting me enough and allowing

me the privilege to be your friend. I couldn't imagine winning the Merck Award with anyone else. Vales oro mi amiga.

Thank you to my committee members, Prof. Dean Tantillo and Prof. Cody Ross Pitts. I have really valued your feedback when I needed it most. It has been so cool to talk to you both about my dreams for the professoriate. Thank you for all your encouragement.

Thank you to Prof. Jesús M. Velázquez and Prof. Osvaldo Gutierrez (UCLA). Profes he valorado demasiado todo su apoyo en mi doctorado. No hay muchas personas que se parecen como nosotros en la academia. Ni saben que tanto los admiro. Gracias por todo el ánimo y los mensajes tan bellos. ¡Para arriba y para adelante!

Thank you to the Franz group for all their support throughout the years, especially my mentor Jacob. There is no other desymmetrization partner I'd choose. Thank you, To Linnea: You have always been there for me, and I never even had to ask. You always just got it, every single time. To Yun-Pu: Wow, there are no words to describe how much I smile when I think of you. You make me want to be a better chemist each day. To Ravi: I really love your contagious laugh! You have been such a great friend to me. We had so many good times together. Do you remember me calling the phone in 309? That was the funniest thing. To Kevin: Oye hot choccy, gracias por tu amistad. Siempre he apreciado que siempre sabes decir la cosa perfecta en el tiempo más adecuado. Te aprecio demasiado. To Wendy: You're the most hard-working and coolest undergraduate student I have ever had the privilege to teach and mentor. I cherish you beyond words. To Hannah: Thank you for the honor to have had the privilege to mentor you. I learned so much and had so much fun! Don't forget that no matter what comes your way you can handle it. To David: Thank you for all the times we fixed things together. I really have always thought of you as a great co-worker who was always ready to help. To Leah: You are a shining

star. Your dedication to research is astonishing. To Andrew: Hey Mr. Sandwich thanks for all the laughs, don't forget to continue sending me pictures of your sammys! I know I will be. To Angel and Jake: Thank you both for subgroups. I learned so much about what it meant to be at the board. You grilling me really made me a better chemist. I really thank you for the hard love.

I'd also like to thank my friends in the Shaw group. To José: Gracias amigo por todo tu apoyo todos estos años. Siempre voy a valorar todos tus consejos. Cuando pienso en ti siento una calma y quiero ser una mejor persona. Vales oro. Sabes que a mí no me importa el fútbol pero que ¡viva América! To Yuan-Shin: My friend you taught me every day what it meant to work hard at my chemistry. To work smarter and think things differently. I am honored to have worked near you. I learned so much. To Cheng-En: Thanks for being the best housemate! I really loved smelling the freshly brewed coffee each day. To Garrett: I would've never been able to get through this without you. You have been such a great friend to me. Sometimes I think about how I even scored the friend lottery with you, but I am so glad I did. To Linda: It has been such a privilege to watch you grow the last few years. I still remember when you rotated with me. You have been such a great friend. I wouldn't have been able to get through this without you. Spending time with you always makes me smile.

To the UC Office of the President, thank you for seeing me and my vision. Your belief in what I hope to accomplish in academia really helped me feel like I truly belong here. I especially want to thank Pamela Jennings for being in my corner.

Thank you to everyone who sees me, *actually sees me*. You all are such gems.

Lastly, I would like to thank my four siblings, my sister-in-law, my nephew, and Nala & Django for all the love and support of my crazy idea to continue studying this long. Los quiero hasta la luna.

A mis papas,

Gracias por sus gran esfuerzos y sacrificios.

Es por ustedes que he tenido el privilegio de estudiar.

Les dedico a ustedes mis dos asociados, mis dos licenciaturas y mi doctorado.

Los quiero mucho.

ABSTRACT

Hydrogen bonding is crucial for all biological systems. This dissertation explores the importance of the synthesis and subsequent desymmetrization of silanediols and the hydrogen-bonding interactions crucial for catalysis. The introduction presents the discovery of organosilanols and introduces the properties and importance of organosilanols. Notable reactions in silica gel catalysis are presented. Finally, silanols as catalysts in the Franz group are discussed, which sets the precedent for the need for the synthesis of chiral-at-silicon compounds.

Chapter two details my contributions to the organocatalytic asymmetric synthesis of silicon-stereogenic siloxanols. The initial understanding of the organocatalyst-substrate complex was investigated by Jacob J. Dalton, Ph.D. who performed a co-crystallization experiment which revealed a two-point hydrogen-bonding interaction involving the imidazole and amide of the organocatalyst. My contributions involve the design, synthesis, and evaluation of organocatalyst analogs. Structural changes in the organocatalyst validated the crucial role of the imidazole in reactivity and selectivity. Additionally, the chapter explores the efforts towards substrate scope expansion. The hydrogen-bonding interactions present in the solid-state were verified using ^{1}H NMR binding studies and a correlation of binding affinity and enantioselectivity was discussed. This research represents my contributions to the first example of a Lewis base-catalyzed desymmetrization of prochiral silanediols.

Chapter three extends the desymmetrization of prochiral silanediols for the synthesis of chiral 1,3-disiloxanediols. The initial exploration for the synthesis of chiral 1,3-disiloxanediols gained insight into the role of the chlorosilane reaction partner. The chapter presents access to the first example of a diaryl silanediol to produce a stereogenic siloxanol in high selectivity. Additionally, the potential application of chiral 1,3-disiloxanediols as hydrogen-bonding

organocatalysts were briefly explored. ^{1}H NMR binding studies were used to probe the hydrogen-bonding interactions that alluded to the role of the chlorosilane binding partner. Moreover, ^{1}H NMR binding studies, analyzed by ^{1}H NMR, were conducted to explore the binding affinity of chiral 1,3-disiloxanediols with pyridine as a model Lewis base. The synthesis of chiral 1,3-disiloxanediols in high yields remains a priority.

List of Symbols and Abbreviations

Å	Angstrom
Ar	Aryl
BAMOL	axially chiral 1,1'-biary-2,2'dimethanol family of diols
BINOL	axially chiral 1,1'-bi-2-naphthol family of diols
CSP-HPLC	Chiral Stationary Phase High Performance Liquid Chromatography
o-DCB	1,2-Dichlorobenzene
DCC	Dicylohexylcarbodiimide
DCM	Dichloromethane
DIPEA	*N*, *N*-Diisopropylamine
DSD	1,3-Disiloxanediol
EDC	1-Ethyl-3-(3-dimethylaminopropyl) carbodiimide
eq	Equation
equiv	Equivalence
ee	Enantiomeric excess
er	Enantiomeric ratio
ESI-MSI	Electrospray Ionization-Mass Spectrometry
Et	Ethyl
EtOAc	Ethyl acetate
g	Grams
HBA	hydrogen-bond acceptor
HBD	hydrogen-bond donor
h	Hours

HPLC	High Pressure Liquid Chromatography
HOBt	1-Hyderxybenzotriazole
HRMS	High Resolution Mass Spectrometry
NMI	*N*-Methylimidazole
i-Pr	Isopropyl
i-Bu	Isobutyl
K_a	Association constant
LRMS	Low Resolution Mass Spectrometry
MALDI	Matrix-Assisted Laser Desorption Ionization
M	Molar
Me	Methyl
MeCN	Acetonitrile
2-MePh	2-Methylphenyl
MeOH	methanol
4-OMe	4-methoxy
Mes	mesityl
mg	Milligrams
MHz	Megahertz
min	Minutes
mL	Milliliters
μL	Microliters
mM	Millimolar
mmol	Millimole

mol	Mole
MS	Molecular sieves
MW	Molecular weight
m/z	Mass-to-charge ratio
n-Bu	*n*-Butyl
Np	1-Naphthyl
2-Np	2-Naphthyl
Np^F	4-Fluoro-1-Naphthyl
NS	4-Trifluoromethyl-*trans*-β-nitrostyrene
NMR	Nuclear magnetic resonance
o-Tol	*o*-tolyl
P	Product
Ph	Phenyl
PhMe	Toluene
pK_a	Acid dissociation constant
ppm	Parts per million
rt	Room temperature
SM	Starting Material
TADDOL	α,α,α',α'-tetraaryl-2,2-disubstituted-1,3-dioxolane-4,5-dimethanol
t-Bu	*tert*-Butyl
TBS	*tert*-Butyldimethylsilyl
TCCA	Trichloroisocyanuric acid
TCFH	Chloro-*N*, *N*,*N*',*N*'-tetramethylformamidiniumhexafluorophosphate

TEA	Triethylamine
TFA	Trifluoroacetic acid
THF	Tetrahydrofuran
TLC	Thin Layer Chromatography
VANOL	axially chiral 2,2’-binapthol family of diols
VAPOL	axially chiral 3,3,’-biphenanthrol family of diols
Δ	Change in indicated quantity

Chapter 1: Introduction

This introduction chapter presents a summary of organosilicon chemistry relevant to the research in this dissertation. A brief history of the early discovery of organosilanols is discussed. The properties and importance of organosilanols and early examples of silica gel catalysis are presented. Silanols as catalysts in the Franz group are introduced to set the stage for the importance of accessing silicon-stereogenic compounds in the subsequent chapters. Methods to access silicon-stereogenic compounds are highlighted.

1.1 Discovery of Organosilanols

In 1871, Landenburg reported the first synthesis of triethylsilanol.[1] Landenburg described the synthesis of **1.2** from **1.1** and stated "it is not permanent in air and is not attacked by alcohol ammonia at elevated temperature" (i.e., 250 °C) (Figure **1.1**). Landenburg reported water did not act on **1.1** until 200 °C and stated, "among the products of decompositions triethylsilico bearing silicium the same relation as triethyl-carbinol to carbon." Counterintuitive to the current knowledge of the hydrolysis of chlorosilanes producing organosilanols,[2–10] Landenburg later described that silicoheptyl chloride boiled at 153.5 °C and "has the properties of an alcohol." Landenburg concluded triethylsilanol **1.2** as possibly among the substances of high boiling point formed in Figure **1.1**, but it was not isolated. Landenburg's seminal publication garnered attention from chemists around the world to study organosilanols.[11–13]

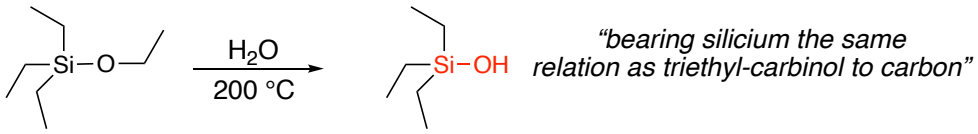

1.1 **1.2**, *not isolated*

Figure **1.1**. Landenburg's report of the first organosilanol.

1.2 Properties and Importance of Organosilanols

The properties and importance of organosilanols have been well studied.[14,15] Although carbon and silicon bear many similarities, there are noteworthy and distinct differences. In the field of organic chemistry, silanes remained established as the most commonly used protecting group.[16–18] Silicon is at the interface of organic and inorganic realms, where organosilicon molecules have unique properties that are relevant for synthesis, catalysis, and medicinal chemistry. Compared to carbon–carbon bond lengths (1.52 Å), silicon–carbon bond lengths are longer (1.86 Å). In addition, silicon has a larger dynamic radius (117 ppm vs. 77 ppm), and reversed polarity for silicon-containing bonds. The enhanced acidity of silanol groups allows for increased hydrogen bonding (Figure **1.2**A). The back-bonding of the oxygen lone pair of electrons into the carbon-silicon σ* orbital ($O_{LP} \rightarrow \sigma^*_{Si\text{-}C}$) accounts for the observed increased acidity of silanols to carbon alcohols. This trend is observed in the pK_a comparison of triphenylsilanol (**1.3**) (16.6) and the carbon analog **1.4** (17.0) (Figure **1.2**B).[19,20] The electropositivity of silicon vs carbon accounts for the observed acidity trend.

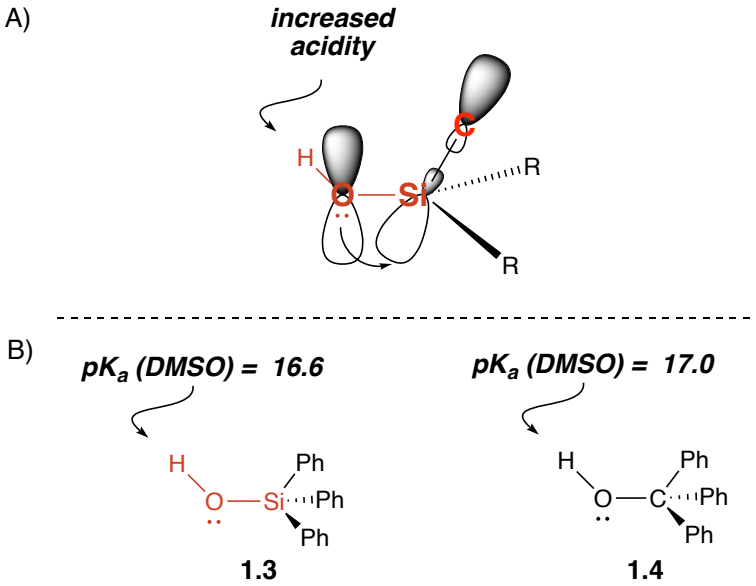

Figure **1.2.** A) Enhanced acidity of silanols compared to alcohols. B) Example of observed silanol acidity.[19,20]

Among the structures of silanols, silanediols represent a unique prochiral substrate for silicon relative to carbon. In contrast to carbon, silicon favors the geminal diol (Figure **1.3**A). In the case of carbon, a ketone (**1.6**) is thermodynamically favored over the geminal diol **1.5**. In contrast, the silanone **1.8** is thermodynamically disfavored over silanediol **1.7** due to poor p orbital overlap between oxygen and silicon in silanone **1.8**.[15,21,22] However, silanediols are prone to self-condensation due to the thermodynamic stability of siloxanes.[14] Surprisingly, stable trisilanols have been reported that overcome self-condensation.[11,12,23] Silanediols feature a common homodimeric eight-membered ring hydrogen-bonding pattern that is also found in oxoacids, boronic acids, and phosphoric acids (Figure **1.3**B).[24,25] These properties make a strong case for silanols to be explored as design features in catalysts.

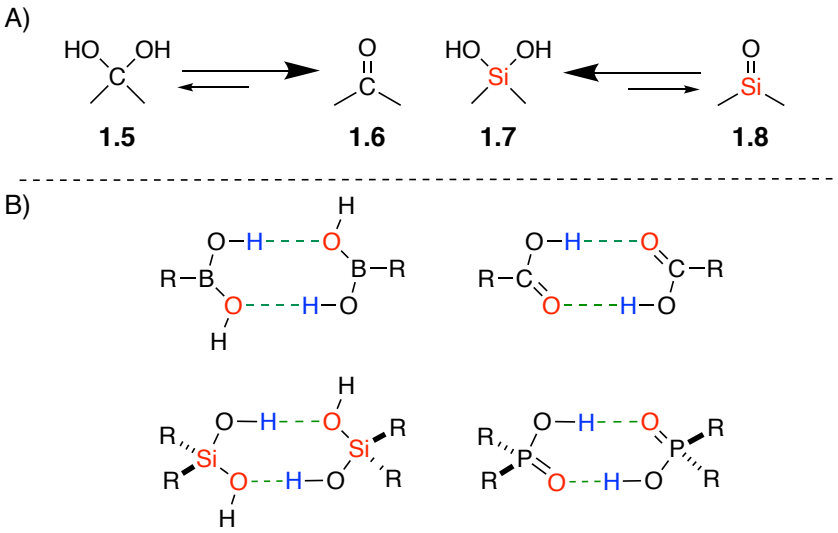

Figure **1.3** A) Carbon vs. silicon geminal diol formation. B) Comparing homodimeric eight membered ring hydrogen-bonding patterns found in oxoacids, boronic acids, phosphoric acids and silanediols.

1.3 Silica Gel Catalysis

Silicon is the second most abundant element in the Earth's crust existing primarily as silicates [$(SiO_4)^{4-}$] and quartz (sand). Silicon materials and compounds are considered less toxic, garnering attention from chemists for their use as catalysts.[26] Early interest in silanol structures began with the curiosity for their use as models of silica surfaces. The unsaturated face of silica surfaces is decorated with a mixture of monosilanols (no hydrogen bonds possible), geminal silanols (isolated) and vicinal silanols (hydrogen bonds possible) (Figure **1.4**). The surface properties of silicas are greatly influenced by the silanols and their hydrogen-bonding patterns, and are studied through a combination of vibrational spectroscopy and solid-state NMR spectroscopy.[27–29] Silsesquioxanes are considered to be a model surface structure and potential mimic for the reactivity of silica surfaces, yet simple organic silanediols have been most commonly studied spectroscopically.[10,11]

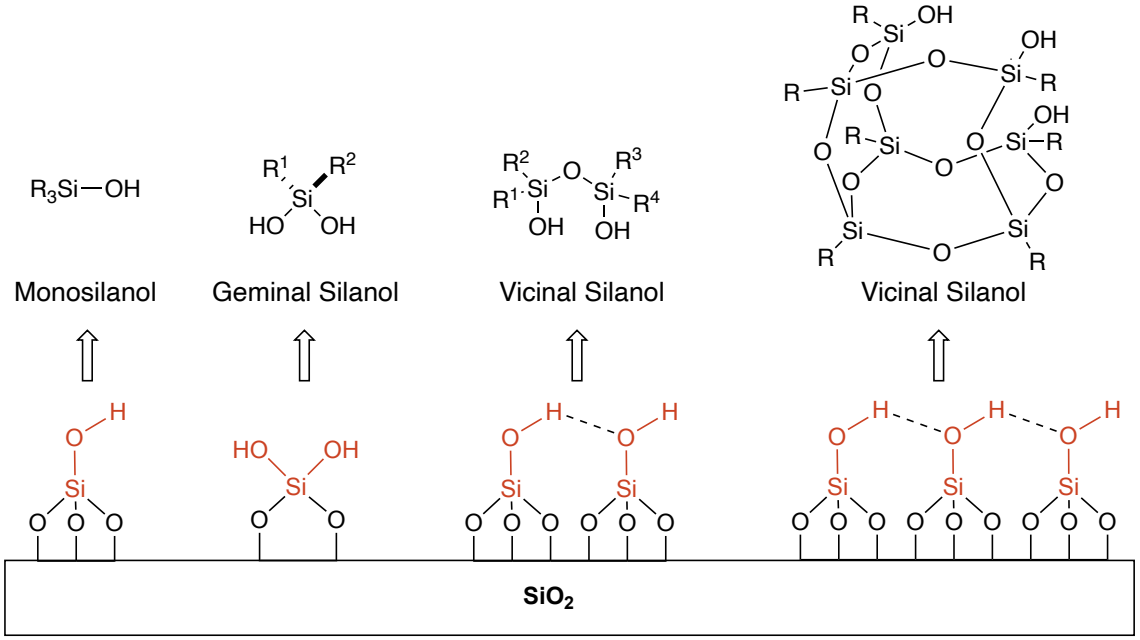

Figure **1.4**. Silica surface and the structure analogy with molecular organosilanols.

With the initial interest of silica surfaces, inorganic supports interested organic chemists for use as catalysts in synthetic transformations.[30] The beginnings in the field gave attention to aluminum oxides,[4,31–41] zeolites[42–47] and clays.[48,49] Tsukamoto and co-workers presented silica gel as an efficient catalyst for the successful condensation of arenesulfenyl chlorides and aryl chloromethyl sulfides with aromatic compounds.[50] Tsukamoto and co-workers extended this study to include the alkylation of phenols and some heterocyclic aromatic compounds (Figure **1.5**A).[51] When **1.9** was treated with sufficient excess of **1.10** in the presence of silica gel the corresponding di-*tert*-butylated product **1.11** was synthesized in high yield (92%). Heterocyclic compounds such as furan, thiophene, benzothiophene, and 1-methylindole were alkylated in good yields (50–98%). Silica gel-catalyzed reactions of epoxides with several nitrogen heterocycles was demonstrated by Nishizawa (Figure **1.5**B).[52] A long reaction time (i.e., 7 days) was required for the successful ring opening of **1.12** with indole **1.13** to produce **1.14** in 88% yield. Both high-pressure and silica gel-catalyzed ring-opening of **1.12** were reported independently, but the combination was found most efficient for the synthesis of less reactive substrates (i.e., imidazoles and pyrazoles). The silica gel-catalyzed conjugate addition of nitrogen heterocycles to electron-deficient olefins was reported by Kusurkar and coworkers (Figure **1.5**C). The addition of indole **1.13** to trans-*β*-nitrostyrene **1.15** was carried out using silica gel and resulted in high yield (92%). The method was generalized to include pyrrole with a range of monosubstituted phenyl nitroolefins with good success (up to 89% yield). Silica gel has also developed as a useful catalyst in many synthetically useful organic transformations such as aromatic nitration,[53–55] Wittig-type olefination[56,57] and Morita-Baylis-Hillman reaction.[58–60] Many advances are beyond the scope of this introduction but the select examples highlighted showcase the opportunity for the implementation of silanols in catalyst design.

(A) Alkylation of Phenols (Tsukamoto 1984)

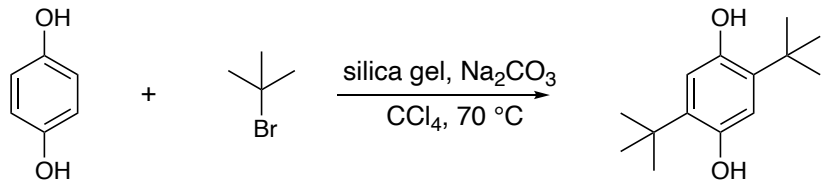

1.9 **1.10** **1.11**, 92 %

(B) High-Pressure-Promoted, Silica Gel-Catalyzed Reaction of Epoxides (Nishizawa 1996)

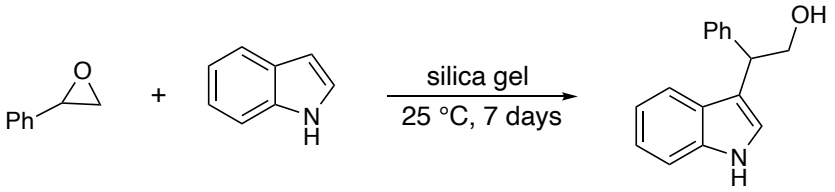

1.12 **1.13** **1.14**, 88 %

(C) Silica Gel-Catalyzed Nitrostyrene Addition to Indole (Kusurkar 2009)

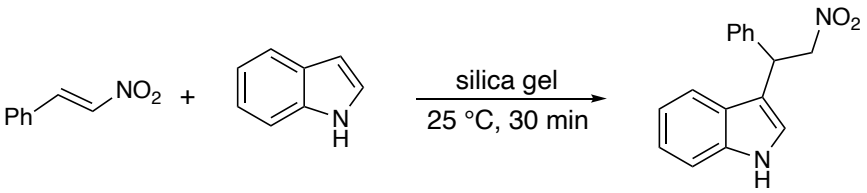

1.15 **1.13** **1.16**, 92 %

Figure **1.5**. Early advances in silica-gel catalysis.

1.4 Silanols as Catalysts in the Franz Group

The Franz group has leveraged the unique properties of silanols in their use as catalysts. Taewoo Min, Ph.D. first demonstrated the hydrogen-bonding ability of pyrrolidinylsilanol **1.19** to enable enantiocontrol for an aldol reaction between **1.17** and **1.18** (Figure **1.6**).[61] The method resulted in good yields and selectivities (up to 81% yield and 88% ee). Increasing steric bulk around the silanol center in **1.19** with two mesityl groups suppressed self-condensation and was accessible in three steps. Notably, the synthesis of **1.19** tolerated the incorporation of an amine and did not result in silanol polymerization. The carbon analog of **1.19** was demonstrated to be less reactive and less selective in the aldol reaction. ESI-MS studies indicated a hydrogen-

bonding adduct with the nucleophilic enamine which allowed for understanding of the stereochemical rationale. The electropositive nature of silicon was suggested to provide potential secondary directing effects that also contribute to enantiocontrol.

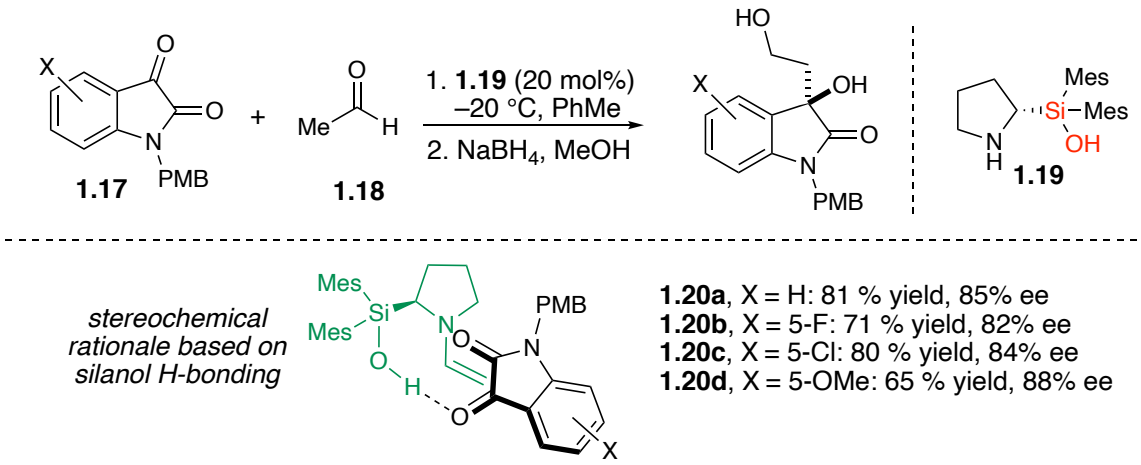

Figure **1.6**. Enantiocontrol with a hydrogen-bond directing pyrrolidinylsilanol catalyst **1.19**.

In 2011, the ability of silanols to catalyze the Diels–Alder reaction between Rawal's diene[62] **1.21** and methacrolein **1.22** was reported (Figure **1.7**). Diaryl silanediols **1.23a–b** catalyzed the reaction in good yields. Although silanediol **1.23b** was designed to be more acidic with the potential to catalyze the reaction in higher yields, disiloxanediol **1.24** showcased the best catalytic activity (72% at 20 mol % catalyst loading). The reduced yields with silanediols were attributed to self-association in solution, which impeded catalysis. More recently, Bolm and coworkers have demonstrated the use of the first planar-chiral bis silanol in the hetero-Diels–Alder reaction involving Rawal's diene with butyraldehyde in fair yield and low enantioselectivity (45% yield and 64:36 er).[63]

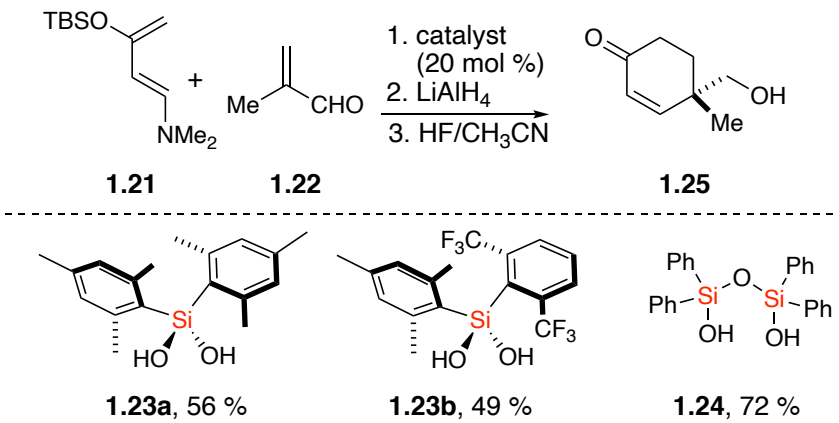

Figure **1.7**. Silanol catalyst comparison for Diels–Alder cyclization.

The indole addition to *trans*-*β*-nitrostyrene **1.15** gained attention in silica gel catalysis,[64] and was further explored by the Franz group using silanediol catalysts (Figure **1.8**).[25] A unique mode of hydrogen-bonding activation was proposed for the silanediol-catalyzed addition of **1.26** to **1.15**. Diaryl silanediols **1.23a–b** decorated with large substituents and electron-withdrawing groups performed with interesting reactivity. Notably, electron-deficient silanediols **1.23b** catalyzed the reaction in excellent yield (99%). The catalysis was attributed to the Si-OH acidification. Silanediols self-associated as cyclic dimer where the remaining external protons are acidified and behave as a single hydrogen-bond donor. Control experiments performed with alkoxy silanediols resulted in yields that matched that of no-catalyst control, confirming the catalysis *via* SiOH acidification. The Michael reaction was catalyzed efficiently by **1.23b**. The catalysis was attributed to the SiOH acidity, which existed as the cyclic dimer with enhanced hydrogen-bonding capabilities.

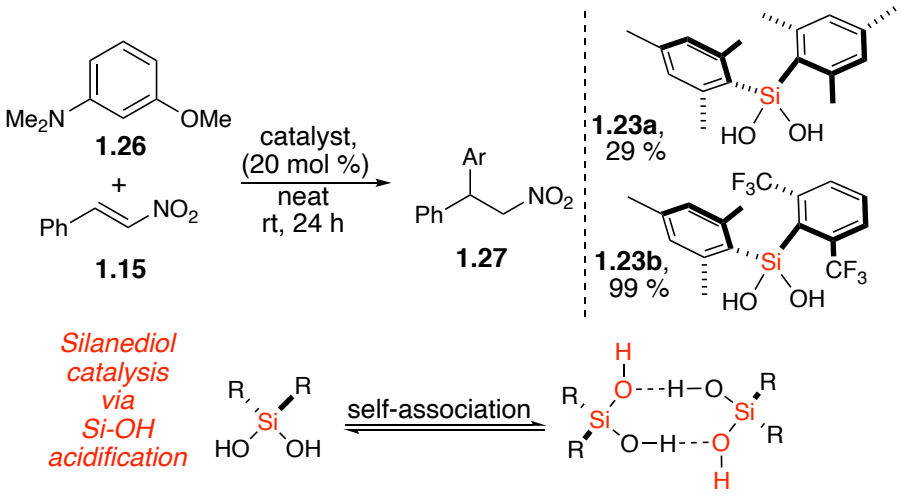

Figure **1.8**. Si-OH acidification allows for catalysis of challenging Michael donor.

The catalytic activity of various disiloxanediols was evaluated for the addition of **1.13** to **1.15** (Figure **1.9**).[65] At loadings of 20 mol % and 10 mol %, disiloxanediols **1.28a–b** catalyzed the reaction in good yields (up to 70%). Unsymmetrical disiloxanediol **1.28c** appended with electron-withdrawing groups exhibited increased catalytic activity at 5 mol% and resulted in high yield (91%). An in-depth kinetic study using a Reaction Progress Kinetic Analysis (RPKA)[66] protocol, suggested a monomeric active catalytic species with no self-association (as had previously been observed by silanediols).[24,25] Self-association of disiloxanediols was determined to not hinder activation. The catalytically active species was determined to be the monomer under all catalytically relevant conditions.

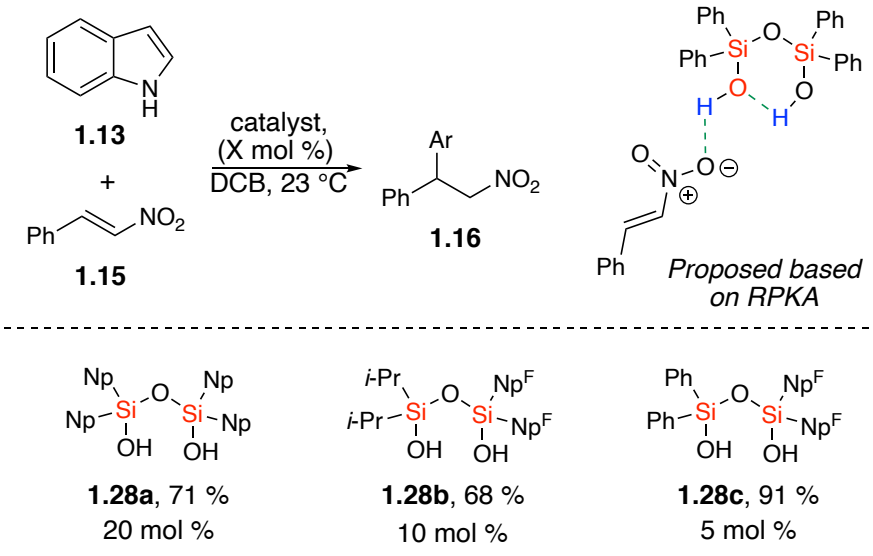

Figure **1.9**. Catalytic activity for a collection of 1,3-disiloxanediols **1.28a–c**.

Disiloxanediol catalysts were explored in the addition of silyl ketene acetal **1.29** to *N*-acyl Mannich reaction of **1.30** (Figure **1.10**). Monosilanol **1.30** and silanediol **1.23c** resulted in lower catalytic activity compared to disiloxanediol **1.28b**. Similar to the results of the *trans-β*-nitrostyrene addition to indole, this study revealed 1,3-disiloxanediols as the most effective catalyst. The study suggested that activation proceeds through a monomeric species. Prior studies have demonstrated the ability of 1,1,3,3-tetraphenyldisiloxanediol[67] and BINOL-derived silanediols to bind anions.[68] The Si-O-Si linkages present in disiloxanediols were seen as advantages to explore for hydrogen-bonding ability. Disiloxanediols were highlighted as a new class of organocatalysts.

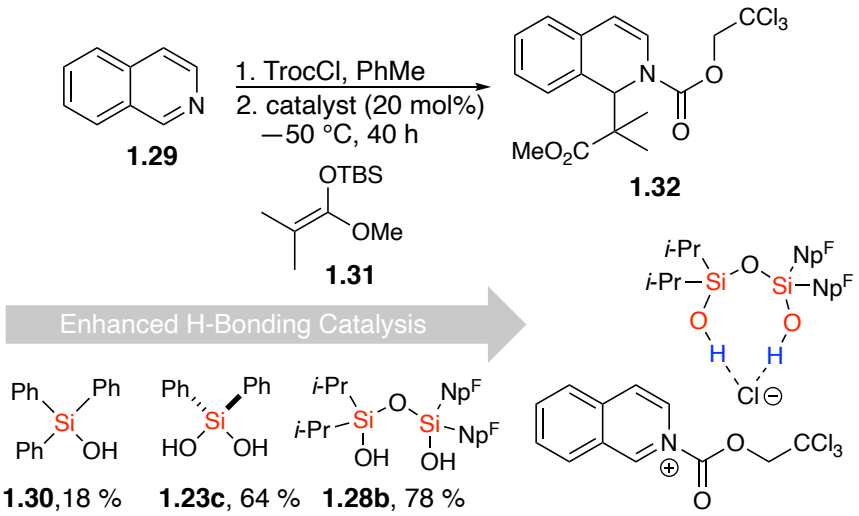

Figure **1.10**. Silanol groups of 1,3-disiloxanediols effective for anion binding catalysis.

1.5 Methods to Access Silicon-Stereogenic Silanols

The synthesis of chiral-at-silicon compounds is a topic of rapidly growing interest for application in the fields of materials science,[11,13,69,70] medicinal chemistry,[71–75] and synthetic chemistry.[25,61,76–84] Efforts towards synthesis of chiral-at-silicon compounds have primarily focused on monohydrosilanes, with Si-H insertion and hydrosilylation catalyzed by a chiral transition metal complex receiving the most attention.[82,85–90] Early work was focused in two areas described below.

Since prochiral silanones are not accessible, this has dramatically affected the approaches available for the asymmetric synthesis of silicon-stereogenic silanols. Chiral silanols have been synthesized through 1) resolution of racemates[91–93] and 2) transformations of enantioenriched stereogenic-silicon precursors.[94–98] Early advances in the resolution of racemates for the synthesis of chiral silanols was investigated by two groups (Figure **1.11**). Miyazawa and co-workers demonstrated the first example of the kinetic resolution of (±)-cyclohex-1-enylsilanol **1.33** by the Sharpless asymmetric epoxidation (Figure **1.11**A).[91] The desired 1,3-epoxycyclohexylmethylphenylsilanols **1.34** and **1.35** were prepared with a stoichiometric

Sharpless epoxidation of **1.33** and proceeded steadily to form a diastereomeric mixture (3:1) in a 43% combined yield with 32% recovery of starting material. The enantiomeric excess (ee) was determined by ^{1}H NMR spectroscopy using Eu(hfc)$_3$. Hiyama and co-workers harnessed the power of alkylative cleavage of a cyclic siloxane for the synthesis of novel chiral silanols (Figure **1.11**B).[93] Cyclic trisiloxane 1,3,5-tris(3,3,3,-trifluoropropyl)-1,3,5-trimetjylcyclotrisiloxane (D_3^F) **1.36** was treated with alkenyllithium and afforded alkenylsilanol **1.37** in 84% yield. Optical resolution of silanol **1.37** was performed by HPLC, which indicated clear separation.

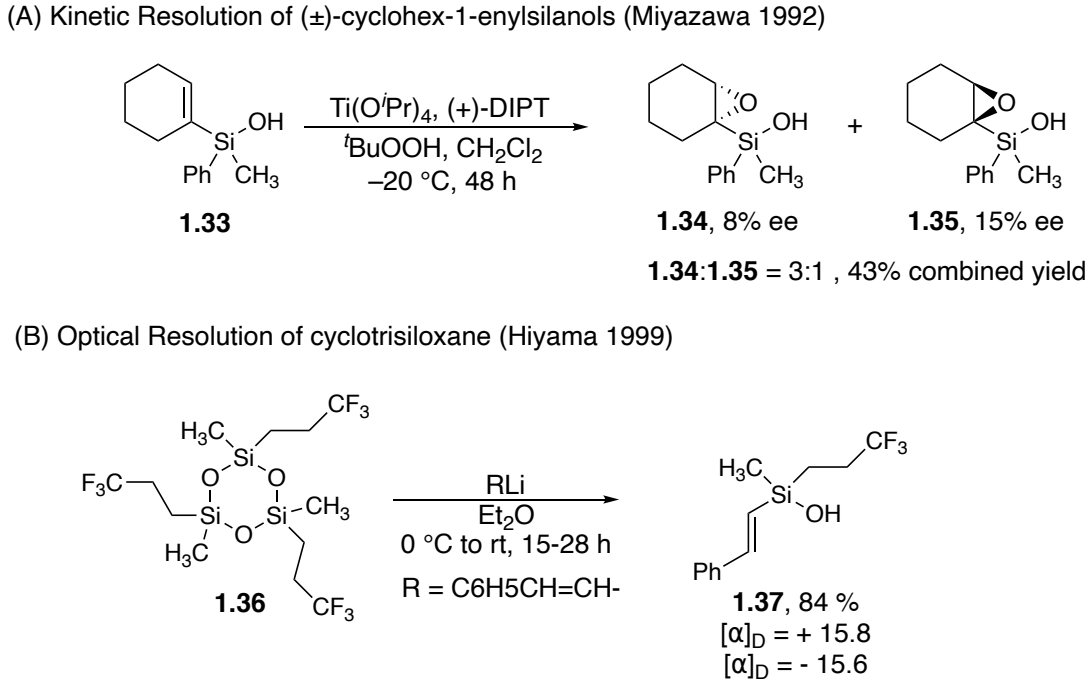

Figure **1.11**. Resolution of racemates for the synthesis of chiral silanols.

The stereoselective transformations of enantioenriched silicon-stereogenic precursors have been widely utilized[99] with interesting advances discussed below (Figure **1.12**). For example, Sommer and co-workers reported the hydroxylation of optically active methylnaphthylphenylsilane **1.38** with perbenzoic acid (Figure **1.12**A).[95] Using an excess of perbenzoic acid a 49% yield was obtained of optically active methylnaphthylphenylsilanol **1.39**. The reaction was reported to proceed with at least 93% retention of configuration based on optical purity of the

product. A mechanistic model was proposed for the hydroxylation. The electrophilic attack at the silicon-hydrogen bond was described as the essential feature of the mechanism as opposed to a nucleophilic substitution by a benzoate anion. Instead, the electrophilic attack at the silicon-hydrogen bond was described as the essential feature of the mechanism. Nakai and co-workers presented an elegant study of a novel 1,4-aryl migration that occurs on β-*tert*-butyldiphenylsiloxy cyclic heminal **1.40** that proceeded in a highly stereoselective manner (Figure **1.12**B).[96] The preparation of aminal **1.41** followed from β-*tert*-butyldiphenylsiloxy cyclic heminal **1.40** subjected to K10 clay in benzyl alcohol. To the surprise of the Nakai group, the unexpected phenyl migration from **1.41** to **1.42** proceeded in moderate yield (50%) and as a single diastereomer. Treatment of **1.21** with *n*-BuLi provided chiral benzyloxysilanol **1.43** in good yield and excellent enantioselectivity (87% yield and 95% ee). The synthesis of enantioenriched alkoxysilanols was unexpectedly discovered and allowed for efficient access to synthetically valuable compounds.

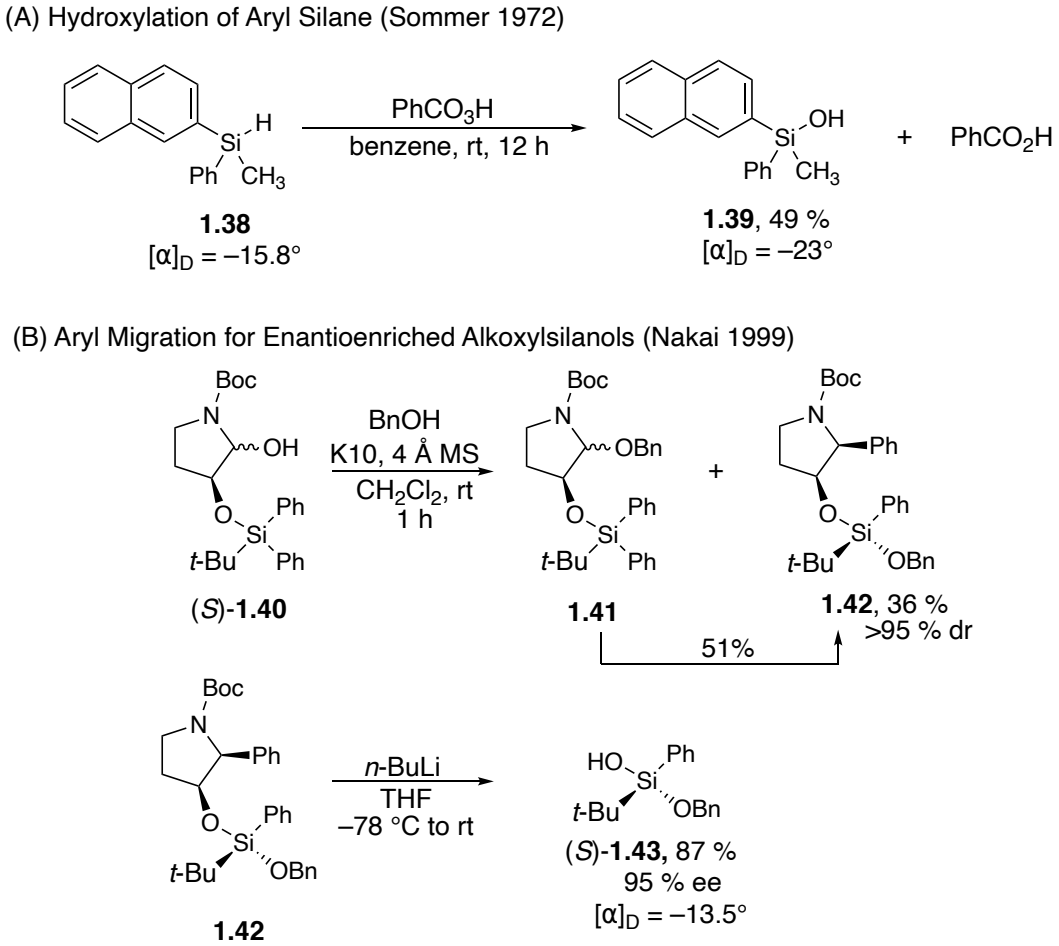

Figure **1.12**. Interesting stereospecific transformations of enantioenriched silicon-stereogenic precursors for the synthesis of chiral silanols.

Although the resolution of racemates and stereospecific transformations of enantioenriched silicon-stereogenic precursors were attractive methods to access chiral silanols, there remained a need for asymmetric methods. Notably, many methods have been investigated for the stereoselective oxidation of enantioenriched silanols (Figure **1.13**). Sommer and co-workers reported the first example that was described in detail in the previous paragraph and reiterated for completion (entry 1).[95] The stereoselective oxidation methylnaphthylphenylsilanol **1.39** using an oxaziridine was reported to proceed with 99% retention by the Adam, Mello and Curci groups (entry 2).[100] The DMDO oxidation of **1.39** was reported to proceed with excellent yield and stereoselectivity.[101] Adam and co-workers reported the synthesis of **1.39** using MTO

(methyltrioxorhenium), UHP (urea-hydrogen peroxide adduct) (entry 3).[102] Catalytic amounts of Mes_2Te[103] or $(TBA)_4[\gamma\text{-}SiW_{10}O_{34}(H_2O)_2]$[104] afforded **1.39** in high stereoretention (entries 5–6). Surprisingly, $[RuCl_2(p\text{-cymene})]_2$,[105] Raney nickel,[106] and Pd/C methods delivered chiral silanols **1.39** and **1.45** with inversion of stereochemistry (entries 7–9). Ru complex (RuHAP) produced chiral silanol **1.46** with high inversion of stereochemistry (entry 10).[107]

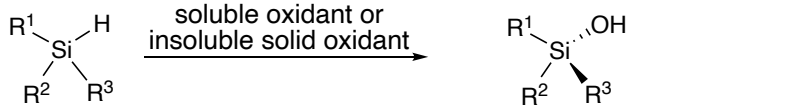

1.44

1.39, R^1 = Ph, R^2 = ^{1}Np, R^3 = CH_3
1.45, R^1 = Ph, R^2 = *t*-Bu, R^3 = *n*-Bu
1.46, R^1 = Et, R^2 = CH_3, R^3 = Ph

entry	substrate	reagent	yield (%)	stereoselectivity
1	**1.39**	$C_6H_5CO_3H$	49	93% retention
2	**1.39**	oxaziridine	N/A	99% retention
3	**1.39**	DMDO	>98	95% retention
4	**1.39**	MTO, UHP	96	94% retention
5	**1.39**	Mes_2Te, hematoporphyrin	79	93% retention
6	**1.39**	$(TBA)_4[\gamma\text{-}SiW_{10}O_{34}(H_2O)_2]$	>95	93% retention
7	**1.39**	$[RuCl_2(p\text{-cymene})]_2$	97	74% inversion
8	**1.39**	Raney nickel, H_2O	97	94% inversion
9	**1.45**	Pd/C, H_2O	96	81% inversion
10	**1.46**	RuHAP, O_2	N/A	99% inversion

Figure **1.13**. Methods for the oxidation of enantioenriched hydrosilanes.

In 2008, Tomooka and co-workers reported the first example of an enantioselective synthesis of a silanol (Figure **1.14**).[108] The Tomooka group found seven-membered cyclic silane **1.47** to provide alkoxysilanes **1.49** using bisoxazoline **1.48**. Alkoxysilanes **1.49** were converted to chiral silanols **1.50**–**1.53** *via* Birch reduction in good yields and a spectrum of enantioselectivities, ranging from 21 to 84 % ee. DFT calculations revealed the reaction was a retentive process that involved the apical attack and departure for the formation of chiral silanols.

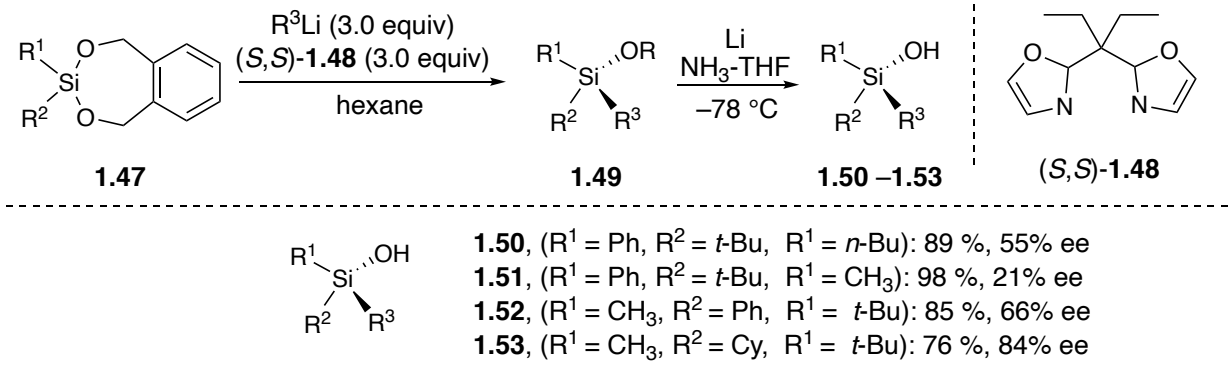

Figure **1.14**. Desymmetrization of alkoxysilanes for the asymmetric synthesis of silanols.

The asymmetric synthesis of enantioenriched silicon-stereogenic silanols from prochiral silanols was reported by Zhao and co-workers (Figure **1.15**).[109] An Ir-catalyzed enantioselective C–H silylation of prochiral diarylsilanols **1.54** was followed by a regioselective and stereospecific ring-opening. Prochiral diarylsilanols **1.54** were converted to the corresponding siloxanes **1.55**. The Ir-catalyzed asymmetric intramolecular C–H silylation gave the corresponding ring-closed product **1.57**. Organolithium reagents cleaved the Si–O bond giving enantioenriched silanols **1.58**–**1.61** in high yields and selectivities.

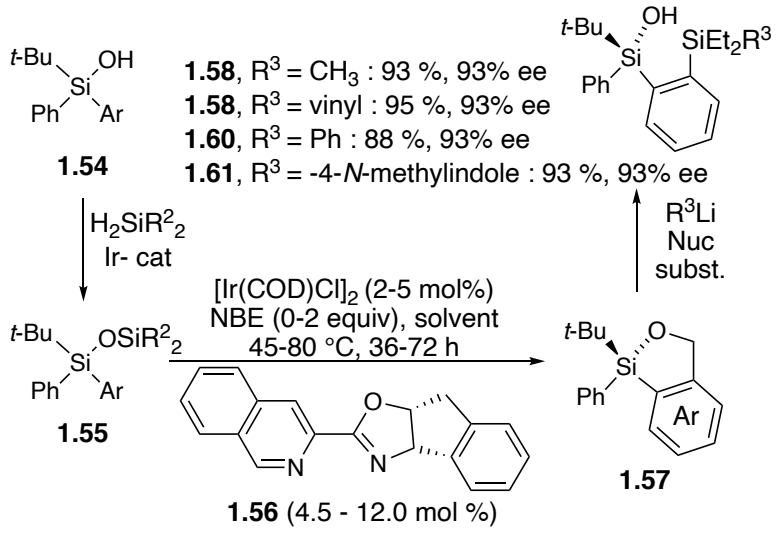

Figure **1.15**. Ir-catalyzed asymmetric synthesis of chiral silanols from prochiral silanols.

In 2022, He and co-workers developed an efficient enantioselective synthesis of silicon-stereogenic silanols involving the catalytic asymmetric hydroxylation of prochiral silanes (Figure **1.16**).[110] The hydroxylation of prochiral silanes **1.62** to enantioenriched silanols **1.63a**–**d** was achieved with a Rh catalytic system using pre-catalyst (*S,S*)-Ph-BPE. The process was efficient for electron-deficient silanol **1.63a** and proved suitable for the late-stage functionalization of complex molecules **1.63b**–**d** and many other examples not shown. Mechanistic studies suggested that water was involved in the rate-determining step. The He methodology proceeded with high atom economy, good functional-group compatibility, and provided H_2 as the sole byproduct.

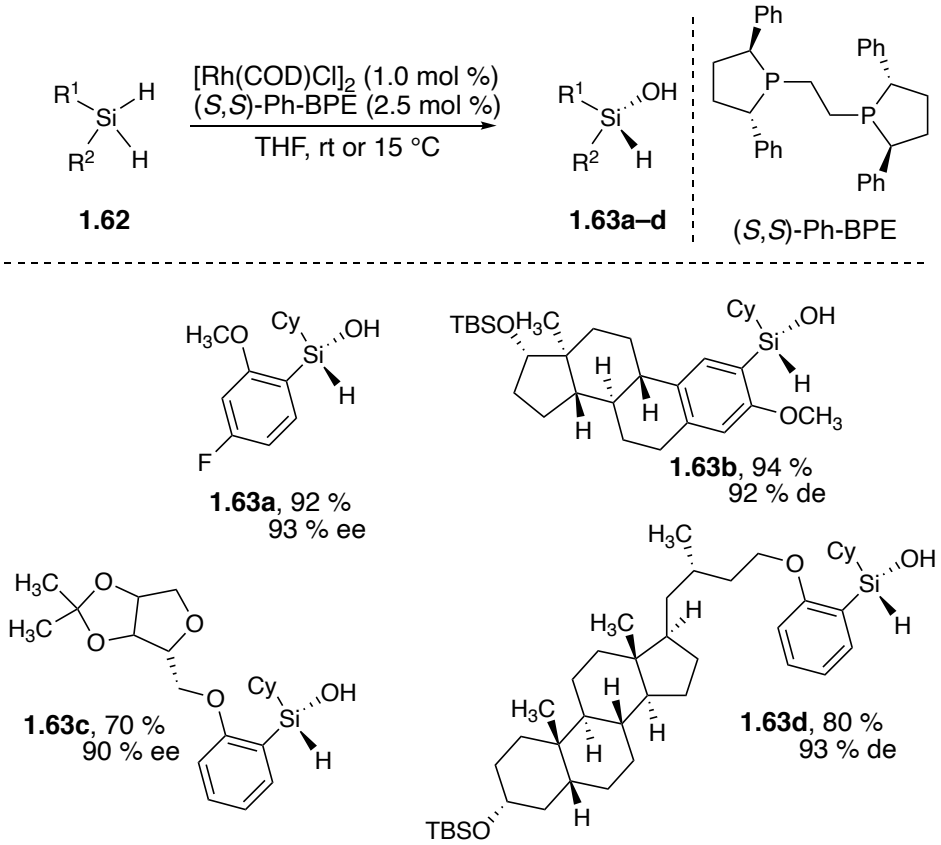

Figure **1.16**. Catalytic asymmetric hydrolytic oxidation of prochiral silanes.

Methodologies for the desymmetrization of prochiral silanediols were developed concurrently by the He [111] and Oestreich[112] groups with the development in the Franz group.[113] In 2022, the He group expanded their use of (*S*,*S*)-Ph-BPE as a pre-catalyst for the Cu-catalyzed

desymmetrization of prochiral silanediols towards enantioenriched silanols (Figure **1.16**).[111] The intermolecular dehydrogenative coupling of prochiral silanediols **1.64** with hydrosilanes **1.65** in the presence of $Cu(CH_3CN)_4PF_6$ and (*S*,*S*)-Ph-BPE successfully produced siloxanols **1.66a–f** in good to excellent enantioselectivities. Mechanistic investigations through DFT calculations revealed the process generated an active copper hydride species. Silanediols and hydrosilanes underwent a sequential σ-bond metathesis that produced chiral siloxanols. DFT calculations determined the σ-bond metathesis between silanediols, and the active copper hydride species determined the enantioselectivity of the process. The reaction featured high atom economy, yields, ranging from 53 to 80 %, and excellent enantioselectivities with H_2 as the sole byproduct.

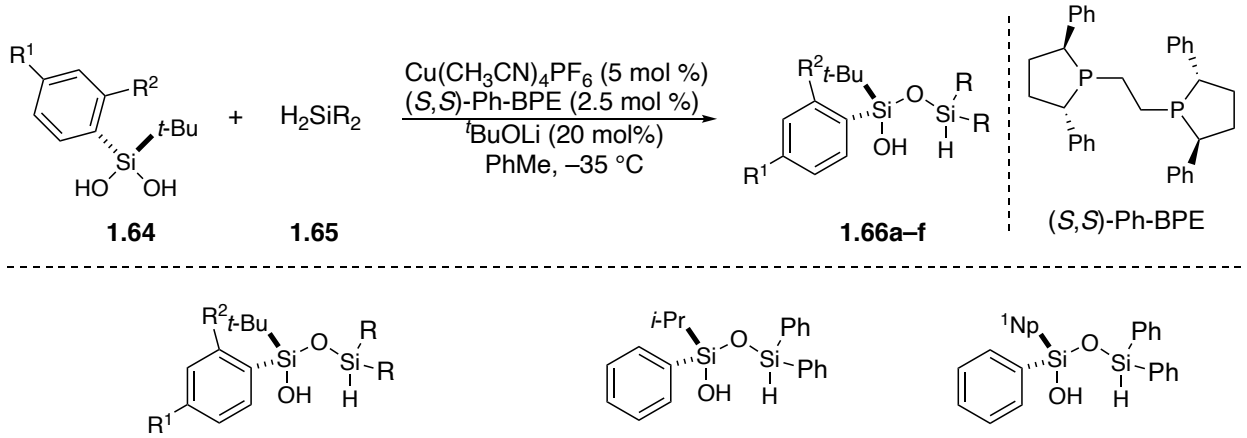

1.66a, (R^1 = R^2 = H, R = Ph): 72 %, 90 % ee
1.66b, (R^1 = H, R^2 = SCH_3, R = Ph): 63 %, 80 % ee
1.66c, (R^1 = OCF_3, R^2 = H, R = Ph): 70 %, 90 % ee
1.66d, (R^1 = R^2 = H, R = Et): 52%, 72 % ee

1.66e, 68%
79% ee

1.66f, 75%
74% ee

Figure **1.16**. Cu-catalyzed desymmetrization of prochiral silanediols.

In 2023, the Oestreich group developed the monosilylation of prochiral silanediols[112] using List's counteranion-directed silylation method (Figure **1.17**).[114] An imidodiphosphorimidate (IDPi) enabled the enantioselective discrimination of the two hydroxyl groups of the silanediols for the production of siloxanols in good to great selectivities. The strong Brønsted acidity of IDPi enabled the silylation of silanediols **1.67** through activation of

allylsilanes *tert*-butyldimethylsilyl (TBS) **1.68a** and trimethylsilyl (TMS) **1.68b**. The reaction was optimized using the He group's lead substrate phenyl(*tert*-butyl)silanediol. When paired with **1.68a**, phenyl(*tert*-butyl)silanediol was found to perform in moderate to good yields and selectivities (**1.69a–e**) and tolerated 4-position substituents well. Naphthyl(*tert*-butyl)silanediol resulted in good yield and selectivity for **1.69f** (90% yield and 80% ee). Enantioselectivity was eroded for diaryl silanediols. The loss of the *tert*-butyl group resulted in siloxanols **1.69g–i** with good yields and poor selectivity. The authors provided mechanistic insight through control experiments involving the reaction rates of the fast and slow-reacting enantiomers. The minor disiloxane enantiomer resulted in the achiral trisiloxane byproduct that enhanced the overall enantioselectivity. Thus, the high enantioselectivities obtained with *tert*-butyl-substituted silanediols were the result of a desymmetrization-kinetic resolution sequence.

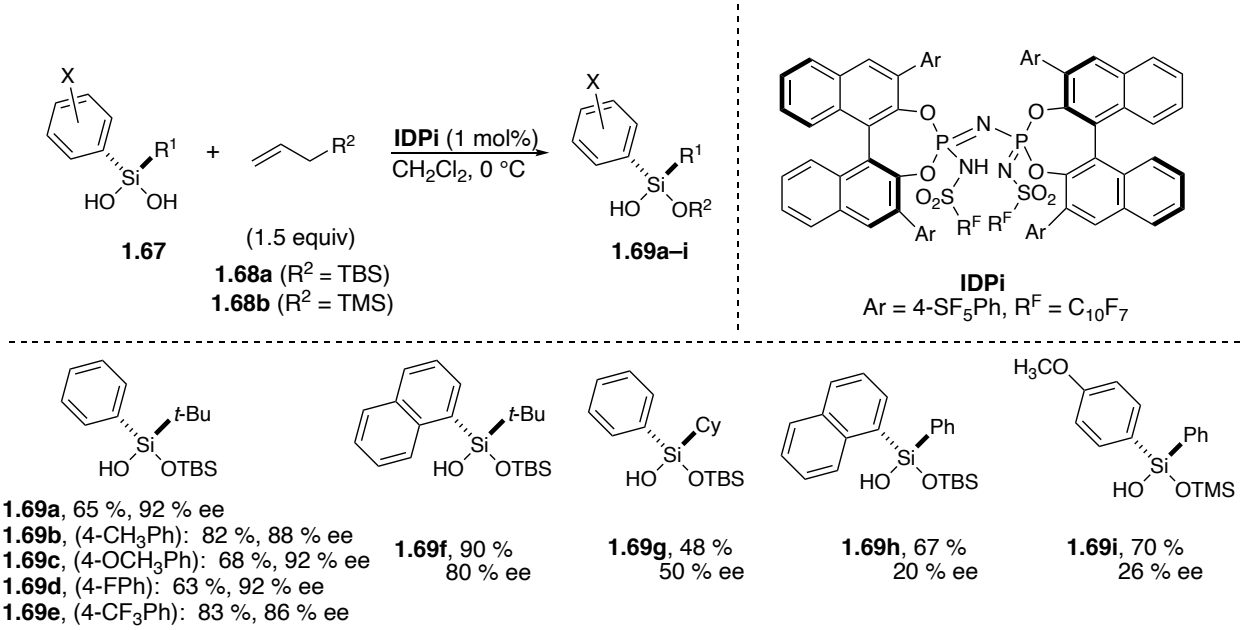

Figure **1.17**. Chiral counteranion-directed desymmetrization of prochiral silanediols.

The introduction has highlighted and discussed the burgeoning field of asymmetric organosilanol synthesis from the landmark discovery of Landenburg to the influences from silica gel catalysis. A brief overview of the development of silanols as catalysts in the Franz group was

presented. Strategies for accessing silicon-stereogenic silanols were highlighted. The recent development of two methodologies for the desymmetrization of prochiral silanediols was introduced. The influence of the all the above studies will be elaborated in subsequent chapters.

1.6 Overview of Dissertation

My research is focused on the theme of accessing silicon-stereogenic centers and will be presented in two chapters (Figure **1.18**). The asymmetric synthesis of silicon-stereogenic siloxanols from prochiral silanediols created a space for the design and synthesis of novel silanediol substrates. Silanediols with aryl-isobutyl groups resulted in higher levels of enantioselectivities and informed the substrate scope. The desymmetrization reaction provided access to chiral 1,3-disiloxanediols for their evaluation as a new class of hydrogen-bonding organocatalysts. A central method used to probe the solution-state hydrogen-bonding interactions of organosilanols were the analyses of ^{1}H NMR binding studies which informed the exciting opportunities for the future design of silanediols.

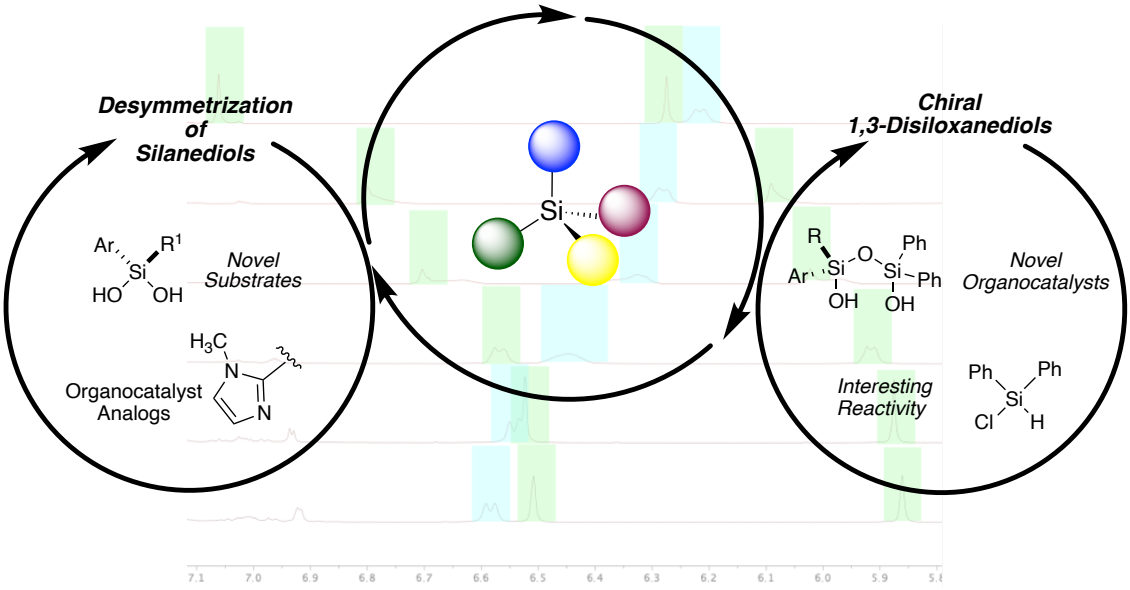

Figure **1.18**. Overview of my research presented in dissertation towards the synthesis of silicon-stereogenic centers.

Chapter 2 will discuss my contributions to the organocatalytic asymmetric synthesis of silicon-stereogenic siloxanols (Figure **1.19A**).[113] The development of an organocatalyst is described. A small collection of organocatalyst analogs were synthesized and tested. The lack of catalytic activity of these analogs proved that the imidazole moiety of the organocatalyst is crucial for catalysis. A delve into the expansion of substrate scope is described. An optimal route was established for future access to novel prochiral silanediols. Verification of the solid-state interaction between the organocatalyst and the silanediols were investigated with binding studies conducted *via* ^{1}H NMR analyses with a correlation between enantioenrichment and catalyst binding described.

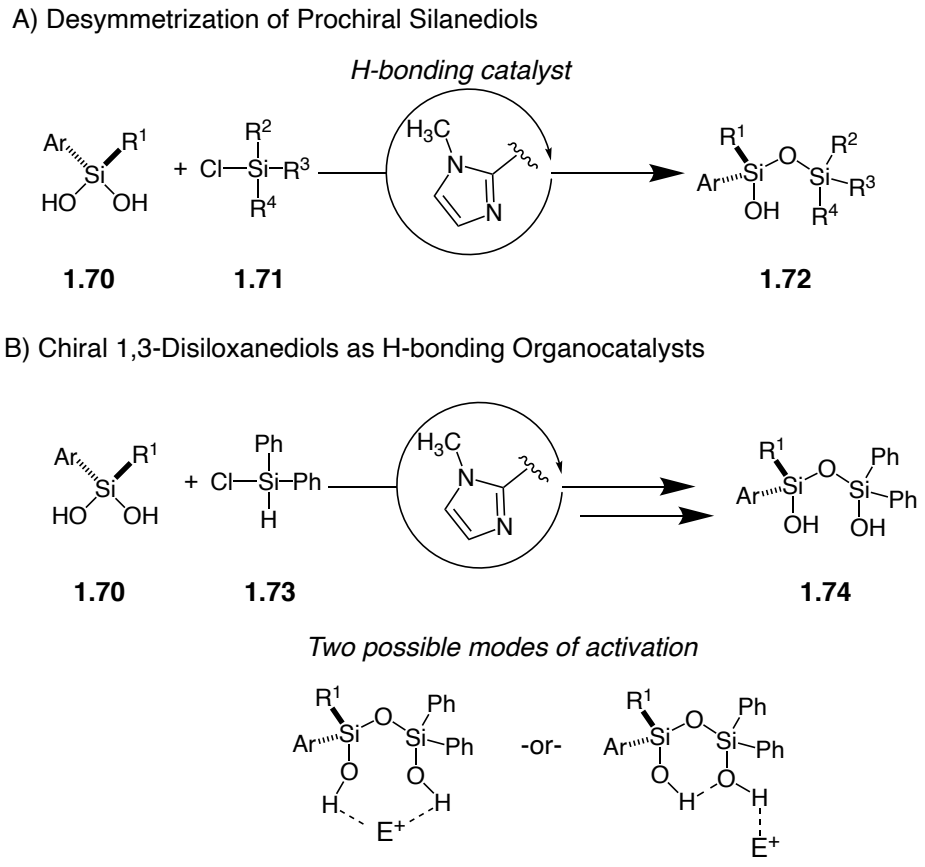

Figure 1.19. A) Desymmetrization of prochiral silanediols and the pursuit of novel substrates. B) Synthesis of chiral 1,3-disiloxanels as a new class of hydrogen–bonding organocatalysts.

Chapter 3 outlines the synthesis of chiral 1,3-disiloxanediols *via* the desymmetrization of prochiral silanediols (Figure **1.19B**). A small collection of chiral 1,3-dsiloxanediols were synthesized. New insights were obtained regarding the relationship between prochiral silanediols and diphenylchlorosilane – the reaction partner necessary for the synthesis of chiral 1,3-disiloxanediols. Chiral 1,3-disiloxanediols were explored as a new class of hydrogen-bonding organocatalysts. With two possible available modes of activation, the acidity of the Si–OH groups in chiral 1,3-disiloxanediols may offer enhanced catalytic activity in asymmetric transformations. Successful syntheses of chiral 1,3-disiloxanediols were found to be concentration dependent. The solution-state hydrogen-bonding interactions of chiral 1,3-disiloxanediols have been explored with pyridine. Disiloxanediols were found to bind weakly to pyridine with neutral Lewis bases expected to exhibit better binding affinity. Preliminary investigations demonstrated that chiral 1,3-disiloxanediols appended with electron-withdrawing groups generally improved the catalytic activity for a Diels–Alder reaction. An understanding of the activation modes will open exciting possibilities for chiral 1,3-disiloxanediol catalysis.

1.7 References

(1) Ladenburg, A. Die Pentachlorbenzole. *Berichte Dtsch. Chem. Ges.* **1872**, *5* (2), 789–790. https://doi.org/10.1002/cber.18720050261.

(2) Frisch, K. C.; Goodwin, P. A.; Scott, R. E. Hydrolysis and Separation of Unsaturated Chlorosilanes. *J. Am. Chem. Soc.* **1952**, *74* (18), 4584–4585. https://doi.org/10.1021/ja01138a040.

(3) Burkhard, C. A. Hydrolysis of Diphenyldichlorosilane. *J. Am. Chem. Soc.* **1945**, *67* (12), 2173–2174. https://doi.org/10.1021/ja01228a034.

(4) Deno, N. C.; Fishbein, R.; Pierson, C. Increasing Terminal (.Omega.) Chlorination of Fatty Acids by Absorbing and Aligning the Reactants on Alumina. *J. Am. Chem. Soc.* **1970**, *92* (5), 1451–1452. https://doi.org/10.1021/ja00708a083.

(5) Takiguchi, T. Preparation of Some Organosilanediols and Phenylsilanetriol by Direct Hydrolysis Using Aniline as Hydrogen Chloride Acceptor1. *J. Am. Chem. Soc.* **1959**, *81* (10), 2359–2361. https://doi.org/10.1021/ja01519a021.

(6) Tripp, C. P.; Hair, M. L. Reaction of Methylsilanols with Hydrated Silica Surfaces: The Hydrolysis of Trichloro-, Dichloro-, and Monochloromethylsilanes and the Effects of Curing. *Langmuir* **1995**, *11* (1), 149–155. https://doi.org/10.1021/la00001a027.

(7) Shaffer, L. H.; Flanigen, E. M. The Hydrolysis of Alkyl and Aryl Chlorosilanes. II. Rates and Mechanism of Hydrolysis in Homogeneous Solution. *J. Phys. Chem.* **1957**, *61* (12), 1595–1600. https://doi.org/10.1021/j150558a005.

(8) Kantor, S. W. The Hydrolysis of Methoxysilanes. Dimethylsilanediol. *J. Am. Chem. Soc.* **1953**, *75* (11), 2712–2714. https://doi.org/10.1021/ja01107a048.

(9) Szabó, G.; Szieberth, D.; Nyulászi, L. Theoretical Study of the Hydrolysis of Chlorosilane. *Struct. Chem.* **2015**, *26* (1), 231–238. https://doi.org/10.1007/s11224-014-0543-y.

(10) Wendler, C.; Reinke, H.; Kelling, H. 2,2-Dihydroxy-Methylcyclosiloxanes and Other 2,2-Difunctional Methylcyclosiloxanes. *J. Organomet. Chem.* **2001**, *626* (1), 53–58. https://doi.org/10.1016/S0022-328X(01)00653-2.

(11) Lickiss, P. D. The Synthesis and Structure of Organosilanols. In *Advances in Inorganic Chemistry*; Sykes, A. G., Ed.; Academic Press, 1995; Vol. 42, pp 147–262. https://doi.org/10.1016/S0898-8838(08)60053-7.

(12) Marciniec, B.; Maciejewski, H. Transition Metal-Siloxide Complexes; Synthesis, Structure and Application to Catalysis. *Coord. Chem. Rev.* **2001**, *223* (1), 301–335. https://doi.org/10.1016/S0010-8545(01)00400-3.

(13) Chandrasekhar, V.; Boomishankar, R.; Nagendran, S. Recent Developments in the Synthesis and Structure of Organosilanols. *Chem. Rev.* **2004**, *104* (12), 5847–5910. https://doi.org/10.1021/cr0306135.

(14) Brook, M. A. *Silicon in Organic, Orgamometallic, and Polymer Chemistry*; 1999.

(15) Sen, S. S. A Stable Silanone with a Three-Coordinate Silicon Atom: A Century-Long Wait Is Over. *Angew. Chem. Int. Ed.* **2014**, *53* (34), 8820–8822. https://doi.org/10.1002/anie.201404793.

(16) Kocienski, P. J. *Protecting Groups*, 3rd ed.; Thieme: Stuggart, Germany, 2005.

(17) Wuts, P. G. M.; Greene, T. W. *Green's Protective Groups in Organic Synthesis*, 4th ed.; John Wiley & Sons: Hoboken, NJ, 2006.

(18) Corey, E. J.; Venkateswarlu, A. Protection of Hydroxyl Groups as Tert-Butyldimethylsilyl Derivatives. *J. Am. Chem. Soc.* **1972**, *94* (17), 6190–6191. https://doi.org/10.1021/ja00772a043.

(19) Damrauer, R.; Simon, R.; Krempp, M. Effect of Substituents on the Gas-Phase Acidity of Silanols. *J. Am. Chem. Soc.* **1991**, *113* (12), 4431–4435. https://doi.org/10.1021/ja00012a009.
(20) Liu, M.; Tran, N. T.; Franz, A. K.; Lee, J. K. Gas-Phase Acidity Studies of Dual Hydrogen-Bonding Organic Silanols and Organocatalysts. *J. Org. Chem.* **2011**, *76* (17), 7186–7194. https://doi.org/10.1021/jo201214x.
(21) Sarkar, D.; Nesterov, V.; Szilvási, T.; Altmann, P. J.; Inoue, S. The Quest for Stable Silaaldehydes: Synthesis and Reactivity of a Masked Silacarbonyl. *Chem. Eur. J.* **2019**, *25* (5), 1198–1202. https://doi.org/10.1002/chem.201805604.
(22) Loh, Y. K.; Aldridge, S. Acid–Base Free Main Group Carbonyl Analogues. *Angew. Chem. Int. Ed.* **2021**, *60* (16), 8626–8648. https://doi.org/10.1002/anie.202008174.
(23) Murugavel, R.; Chandrasekhar, V.; Voigt, A.; Roesky, H. W.; Schmidt, H.-G.; Noltemeyer, M. New Lipophilic Air-Stable Silanetriols: First Example of an X-Ray Crystal Structure of a Silanetriol with Si-N Bonds. *Organometallics* **1995**, *14* (11), 5298–5301. https://doi.org/10.1021/om00011a054.
(24) Tran, N. T. Design, Synthesis, and Study of Silanediols as Homogenous, Hydrogen-Bonding Organocatalysts for Asymmetric Transformation, 2014.
(25) Tran, N. T.; Wilson, S. O.; Franz, A. K. Cooperative Hydrogen-Bonding Effects in Silanediol Catalysis. *Org. Lett.* **2012**, *14* (1), 186–189. https://doi.org/10.1021/ol202971m.
(26) Sugiura, M.; Kotani, S.; Nakajima, M. CHAPTER 11: Catalysis by Silicon Species. In *Catalysis with Earth-abundant Elements*; Royal Society of Chemistry; p 412.
(27) Dijkstra, T. W.; Duchateau, R.; van Santen, R. A.; Meetsma, A.; Yap, G. P. A. Silsesquioxane Models for Geminal Silica Surface Silanol Sites. A Spectroscopic Investigation of Different Types of Silanols. *J. Am. Chem. Soc.* **2002**, *124* (33), 9856–9864. https://doi.org/10.1021/ja0122243.
(28) Zhao, X. S.; Lu, G. Q.; Whittaker, A. K.; Millar, G. J.; Zhu, H. Y. Comprehensive Study of Surface Chemistry of MCM-41 Using 29Si CP/MAS NMR, FTIR, Pyridine-TPD, and TGA. *J. Phys. Chem. B* **1997**, *101* (33), 6525–6531. https://doi.org/10.1021/jp971366+.
(29) Protsak, I. S.; Tertykh, V. A.; Bolbukh, Y. M.; Sternik, D.; Derylo-Marczewska, A. Synthesis and Properties of Fumed Silicas Modified with Mixtures of Poly(Methylphenylsiloxane) and Dimethyl Carbonate. *World J. Nano Sci. Eng.* **2015**, *5* (4), 152–160. https://doi.org/10.4236/wjnse.2015.54017.
(30) Smith, K. *Solid Supports and Catalysts in Organic Synthesis*; New York: Ellis Horwood, 1992.
(31) Villemin, D. Stereoselective Enolization of Methyl Dithiopropanoate by Adsorption on Alumina–Potassium Fluoride. *J. Chem. Soc. Chem. Commun.* **1985**, No. 13, 870–870. https://doi.org/10.1039/C39850000870.
(32) Yamawaki, J.; Ando, T.; Hanafusa, T. N-Alkylation of Amides and N-Heterocycles with Potassium Fluoride on Alumina. *Chem. Lett.* **1981**, *10* (8), 1143–1146. https://doi.org/10.1246/cl.1981.1143.
(33) Kamitori, Y.; Hojo, M.; Masuda, R.; Yoshida, T. Alumina as an Versatile Catalyst for the Selective Acetalization of Aldehydes. *Tetrahedron Lett.* **1985**, *26* (39), 4767–4770. https://doi.org/10.1016/S0040-4039(00)94946-3.
(34) Muzart, J. Self-Condensation of Ketones Catalysed by Basic Aluminium Oxide. *Synthesis* **1982**, *1982* (01), 60–61. https://doi.org/10.1055/s-1982-29700.

(35) Ogawa, H.; Hiraga, N.; Chihara, T.; Teratani, S.; Taya, K. Selective Preferential Esterification of the Dicarboxylic Acids with Longer Carbon Chain by Diazomethane in the Presence of Dicarboxylic Acids with Shorter Carbon Chain by Adsorbing and Aligning the Acids on Alumina. *Bull. Chem. Soc. Jpn.* **1988**, *61* (7), 2383–2386. https://doi.org/10.1246/bcsj.61.2383.
(36) Ogawa, H.; Chihara, T.; Taya, K. Selective Monomethyl Esterification of Dicarboxylic Acids by Use of Monocarboxylate Chemisorption on Alumina. *J. Am. Chem. Soc.* **1985**, *107* (5), 1365–1369. https://doi.org/10.1021/ja00291a042.
(37) Pogrebnoi, S. I.; Kalyan, Y. B.; Krimer, M. Z.; Smit, W. A. Carrol Rearrangement on the Surface of Chromatographic Grade Alumina. *Tetrahedron Lett.* **1987**, *28* (41), 4893–4896. https://doi.org/10.1016/S0040-4039(00)96654-1.
(38) Posner, G. H. Organic Reactions at Alumina Surfaces. *Angew. Chem. Int. Ed. Engl.* **1978**, *17* (7), 487–496. https://doi.org/10.1002/anie.197804871.
(39) Santaniello, E.; Ponti, F.; Manzocchi, A. Reduction of Carbonyl Compounds by Sodium Borohydride Adsorbed on Alumina. *Synthesis* **1978**, *1978* (12), 891–892. https://doi.org/10.1055/s-1978-24927.
(40) Bram, G.; Loupy, A.; Majdoub, M.; Gutierrez, E.; Ruiz-Hitzsky, E. Alkylation of Potassium Acetate in "Dry Media" Thermal Activation in Commercial Microwave Ovens. *Tetrahedron* **1990**, *46* (15), 5167–5176. https://doi.org/10.1016/S0040-4020(01)87823-6.
(41) Bram, G.; Cabaret, D.; Welvart, Z.; Geraghty, N. W. A.; Garvey, J. Surface Enhanced Enantiodifferentiation in Reactions of Chiral Acetoacetates. *Tetrahedron Lett.* **1988**, *29* (36), 4615–4618. https://doi.org/10.1016/S0040-4039(00)80562-6.
(42) Shabtai, J.; Lazar, R.; Biron, E. Catalysis of Organic Reactions by Molecular Sieve Systems: 1. Meerwein-Ponndorf-Verley Reductions. *J. Mol. Catal.* **1984**, *27* (1), 35–43. https://doi.org/10.1016/0304-5102(84)85068-3.
(43) Risbood, P. A.; Ruthven, D. M. Bromine Adsorbed on a Molecular Sieve: A Reagent for Selective Bromination. *J. Am. Chem. Soc.* **1978**, *100* (15), 4919–4921. https://doi.org/10.1021/ja00483a062.
(44) Perot, G.; Guisnet, M. Advantages and Disadvantages of Zeolites as Catalysts in Organic Chemistry. *J. Mol. Catal.* **1990**, *61* (2), 173–196. https://doi.org/10.1016/0304-5102(90)85154-A.
(45) Smith, K. Solids For Catalysis and Control in Organic Synthesis. In *Studies in Surface Science and Catalysis*; Guisnet, M., Barrault, J., Bouchoule, C., Duprez, D., Pérot, G., Maurel, R., Montassier, C., Eds.; Heterogeneous Catalysis and Fine Chemicals II; Elsevier, 1991; Vol. 59, pp 55–71. https://doi.org/10.1016/S0167-2991(08)61107-6.
(46) Hölderich, W. F. New Reactions in Various Fields and Production of Specialty Chemicals. In *Studies in Surface Science and Catalysis*; Guczi, L., Solymosi, F., Tétényi, P., Eds.; New Frontiers in Catalysis - Proceedings of the 10th International Congress on Catalysis, Budapest, 19-24 July 1992; Elsevier, 1993; Vol. 75, pp 127–163. https://doi.org/10.1016/S0167-2991(08)64007-0.
(47) Ernst, S.; Weitkamp, J. Oxidative Coupling of Methane:Activities and Selectivities of Modified Zeolite Catalysts. In *Studies in Surface Science and Catalysis*; Holmen, A., Jens, K.-J., Kolboe, S., Eds.; Natural Gas Conversion; Elsevier, 1991; Vol. 61, pp 25–31. https://doi.org/10.1016/S0167-2991(08)60059-2.

(48) Cornelis, A.; Laszlo, P. Clay-Supported Copper(II) and Iron(III) Nitrates: Novel Multi-Purpose Reagents for Organic Synthesis. *Synthesis* **1985**, *1985* (10), 909–918. https://doi.org/10.1055/s-1985-31382.
(49) Laszlo, P. Chemical Reactions on Clays. *Science* **1987**, *235* (4795), 1473–1477. https://doi.org/10.1126/science.235.4795.1473.
(50) Hojo, M.; and Masuda, R. Electrophilic Chlorination by Sulfuryl Chloride in the Presence of Silica Gel. *Synth. Commun.* **1975**, *5* (3), 169–171. https://doi.org/10.1080/00397917508064104.
(51) Kamitori, Y.; Hojo, M.; Masuda, R.; Izumi, T.; Tsukamoto, S. Silica Gel as an Effective Catalyst for the Alkylation of Phenols and Some Heterocyclic Aromatic Compounds. *J. Org. Chem.* **1984**, *49* (22), 4161–4165. https://doi.org/10.1021/jo00196a012.
(52) Kotsuki, H.; Hayashida, K.; Shimanouchi, T.; Nishizawa, H. High-Pressure Organic Chemistry. 19. High-Pressure-Promoted, Silica Gel-Catalyzed Reaction of Epoxides with Nitrogen Heterocycles1,. *J. Org. Chem.* **1996**, *61* (3), 984–990. https://doi.org/10.1021/jo951106t.
(53) Riego, J. M.; Sedin, Z.; Zaldívar, J.; Marziano, N. C.; Tortato, C. Sulfuric Acid on Silica-Gel: An Inexpensive Catalyst for Aromatic Nitration. *Tetrahedron Lett.* **1996**, *37* (4), 513–516. https://doi.org/10.1016/0040-4039(95)02174-4.
(54) Matsumoto, K.; Oshima, K.; Utimoto, K. Noncatalyzed Stereoselective Allylation of Carbonyl Compounds with Allylsilacyclobutanes. *J. Org. Chem.* **1994**, *59* (23), 7152–7155. https://doi.org/10.1021/jo00102a052.
(55) Mathew, S. M.; Biradar, A. V.; Umbarkar, S. B.; Dongare, M. K. Regioselective Nitration of Cumene to 4-Nitro Cumene Using Nitric Acid over Solid Acid Catalyst. *Catal. Commun.* **2006**, *7* (6), 394–398. https://doi.org/10.1016/j.catcom.2005.12.022.
(56) Patil, V. J.; Mävers, U. Wittig Reactions in the Presence of Silica Gel. *Tetrahedron Lett.* **1996**, *37* (8), 1281–1284. https://doi.org/10.1016/0040-4039(95)02374-7.
(57) Ramazani, A.; Kazemizadeh, A. R.; Ahmadi, E.; Rahnema, M. Silica Gel Powder Catalyzed Intermolecular Wittig Reaction of Fluorine-Containing Stabilized Phosphorus Ylides with Ninhydrin in Solvent-Free Conditions. *Asian J. Chem.* **2006**, *18* (1), 701–703.
(58) Basavaiah, D.; Reddy, R. M. The Baylis-Hillman Reaction: Rate Acceleration in Silica Gel Solid Phase Medium. *Indian J. Chem.* **2001**, *40B*, 985–988.
(59) Shi, M.; Jiang, Y. The Baylis-Hillman Reactions of Aldehydes with Methyl Vinyl Ketone in the Presence of Imidazole, Binol and Silica Gel. *J. Chem. Res.* **2003**. https://doi.org/10.3184/030823403322597324.
(60) Mack, J.; Shumba, M. Rate Enhancement of the Morita–Baylis–Hillman Reaction through Mechanochemistry. *Green Chem.* **2007**, *9* (4), 328–330. https://doi.org/10.1039/B612983H.
(61) Min, T.; Fettinger, J. C.; Franz, A. K. Enantiocontrol with a Hydrogen-Bond Directing Pyrrolidinylsilanol Catalyst. *ACS Catal.* **2012**, *2* (8), 1661–1666. https://doi.org/10.1021/cs300290j.
(62) Huang, Y.; Unni, A. K.; Thadani, A. N.; Rawal, V. H. Single Enantiomers from a Chiral-Alcohol Catalyst. *Nature* **2003**, *424* (6945), 146–146. https://doi.org/10.1038/424146a.
(63) Beemelmanns, C.; Husmann, R.; Whelligan, D. K.; Özçubukçu, S.; Bolm, C. Planar-Chiral Bis-Silanols and Diols as H-Bonding Asymmetric Organocatalysts. *Eur. J. Org. Chem.* **2012**, *2012* (18), 3373–3376. https://doi.org/10.1002/ejoc.201200548.

(64) Shumaila, A. M. A.; and Kusurkar, R. S. Silica Gel, an Effective Catalyst for the Reaction of Electron-Deficient Nitro-Olefins with Nitrogen Heterocycles. *Synth. Commun.* **2010**, *40* (19), 2935–2940. https://doi.org/10.1080/00397910903340694.
(65) Diemoz, K. M.; Hein, J. E.; Wilson, S. O.; Fettinger, J. C.; Franz, A. K. Reaction Progress Kinetics Analysis of 1,3-Disiloxanediols as Hydrogen-Bonding Catalysts. *J. Org. Chem.* **2017**, *82* (13), 6738–6747. https://doi.org/10.1021/acs.joc.7b00875.
(66) Blackmond, D. G. Reaction Progress Kinetic Analysis: A Powerful Methodology for Mechanistic Studies of Complex Catalytic Reactions. *Angew. Chem. Int. Ed.* **2005**, *44* (28), 4302–4320. https://doi.org/10.1002/anie.200462544.
(67) Kondo, S.; Fukuda, A.; Yamamura, T.; Tanaka, R.; Unno, M. Anion Recognition by a Disiloxane-1,3-Diol in Organic Solvents. *Tetrahedron Lett.* **2007**, *48* (45), 7946–7949. https://doi.org/10.1016/j.tetlet.2007.09.067.
(68) Wieting, J. M.; Fisher, T. J.; Schafer, A. G.; Visco, M. D.; Gallucci, J. C.; Mattson, A. E. Preparation and Catalytic Activity of BINOL-Derived Silanediols. *Eur. J. Org. Chem.* **2015**, *2015* (3), 525–533. https://doi.org/10.1002/ejoc.201403441.
(69) Zhou, Q.; Yan, S.; Han, C. C.; Xie, P.; Zhang, R. Promising Functional Materials Based on Ladder Polysiloxanes. *Adv. Mater.* **2008**, *20* (15), 2970–2976. https://doi.org/10.1002/adma.200800580.
(70) Jeon, M.; Han, J.; Park, J. Catalytic Synthesis of Silanols from Hydrosilanes and Applications. *ACS Catal.* **2012**, *2* (8), 1539–1549. https://doi.org/10.1021/cs300296x.
(71) Sieburth, S. McN.; Nittoli, T.; Mutahi, A. M.; Guo, L. Silanediols: A New Class of Potent Protease Inhibitors. *Angew. Chem. Int. Ed.* **1998**, *37* (6), 812–814. https://doi.org/10.1002/(SICI)1521-3773(19980403)37:6<812::AID-ANIE812>3.0.CO;2-I.
(72) Singh, S.; Sieburth, S. McN. Serine Protease Inhibition by a Silanediol Peptidomimetic. *Org. Lett.* **2012**, *14* (17), 4422–4425. https://doi.org/10.1021/ol301933n.
(73) Franz, A. K.; Wilson, S. O. Organosilicon Molecules with Medicinal Applications. *J. Med. Chem.* **2013**, *56* (2), 388–405. https://doi.org/10.1021/jm3010114.
(74) Min, G. K.; Hernández, D.; Skrydstrup, T. Efficient Routes to Carbon–Silicon Bond Formation for the Synthesis of Silicon-Containing Peptides and Azasilaheterocycles. *Acc. Chem. Res.* **2013**, *46* (2), 457–470. https://doi.org/10.1021/ar300200h.
(75) Ramesh, R.; Reddy, D. S. Quest for Novel Chemical Entities through Incorporation of Silicon in Drug Scaffolds. *J. Med. Chem.* **2018**, *61* (9), 3779–3798. https://doi.org/10.1021/acs.jmedchem.7b00718.
(76) Denmark, S. E.; Regens, C. S. Palladium-Catalyzed Cross-Coupling Reactions of Organosilanols and Their Salts: Practical Alternatives to Boron- and Tin-Based Methods. *Acc. Chem. Res.* **2008**, *41* (11), 1486–1499. https://doi.org/10.1021/ar800037p.
(77) Denmark, S. E. The Interplay of Invention, Discovery, Development, and Application in Organic Synthetic Methodology: A Case Study. *J. Org. Chem.* **2009**, *74* (8), 2915–2927. https://doi.org/10.1021/jo900032x.
(78) Schafer, A. G.; Wieting, J. M.; Mattson, A. E. Silanediols: A New Class of Hydrogen Bond Donor Catalysts. *Org. Lett.* **2011**, *13* (19), 5228–5231. https://doi.org/10.1021/ol2021115.
(79) Schafer, A. G.; Wieting, J. M.; Fisher, T. J.; Mattson, A. E. Chiral Silanediols in Anion-Binding Catalysis. *Angew. Chem. Int. Ed.* **2013**, *52* (43), 11321–11324. https://doi.org/10.1002/anie.201305496.

(80) Tran, N. T.; Min, T.; Franz, A. K. Silanediol Hydrogen Bonding Activation of Carbonyl Compounds. *Chem. Eur. J.* **2011**, *17* (36), 9897–9900. https://doi.org/10.1002/chem.201101492.
(81) Mewald, M.; Schiffner, J. A.; Oestreich, M. A New Direction in C□H Alkenylation: Silanol as a Helping Hand. *Angew. Chem. Int. Ed.* **2012**, *51* (8), 1763–1765. https://doi.org/10.1002/anie.201107859.
(82) Zhang, H.; Zhao, D. Synthesis of Silicon-Stereogenic Silanols Involving Iridium-Catalyzed Enantioselective C–H Silylation Leading to a New Ligand Scaffold. *ACS Catal.* **2021**, *11* (17), 10748–10753. https://doi.org/10.1021/acscatal.1c03112.
(83) Parasram, M.; Gevorgyan, V. Silicon-Tethered Strategies for C–H Functionalization Reactions. *Acc. Chem. Res.* **2017**, *50* (8), 2038–2053. https://doi.org/10.1021/acs.accounts.7b00306.
(84) Diemoz, K. M.; Wilson, S. O.; Franz, A. K. Synthesis of Structurally Varied 1,3-Disiloxanediols and Their Activity as Anion-Binding Catalysts. *Chem. Eur. J.* **2016**, *22* (51), 18349–18353. https://doi.org/10.1002/chem.201604103.
(85) Ohta, T.; Ito, M.; Tsuneto, A.; Takaya, H. Asymmetric Synthesis of Silanes with a Stereogenic Centre at Silicon via Hydrosilylation of Symmetric Ketones with Prochiral Diaryl Silanes Catalysed by Binap–RhI Complexes. *J. Chem. Soc. Chem. Commun.* **1994**, No. 21, 2525–2526. https://doi.org/10.1039/C39940002525.
(86) Zhu, J.; Chen, S.; He, C. Catalytic Enantioselective Dehydrogenative Si–O Coupling to Access Chiroptical Silicon-Stereogenic Siloxanes and Alkoxysilanes. *J. Am. Chem. Soc.* **2021**, *143* (14), 5301–5307. https://doi.org/10.1021/jacs.1c01106.
(87) Wen, H.; Wan, X.; Huang, Z. Asymmetric Synthesis of Silicon-Stereogenic Vinylhydrosilanes by Cobalt-Catalyzed Regio- and Enantioselective Alkyne Hydrosilylation with Dihydrosilanes. *Angew. Chem. Int. Ed.* **2018**, *57* (21), 6319–6323. https://doi.org/10.1002/anie.201802806.
(88) Jagannathan, J. R.; Diemoz, K. M.; Targos, K.; Fettinger, J. C.; Franz, A. K. Kinetic and Binding Studies Reveal Cooperativity and Off-Cycle Competition for H-Bonding Catalysis with Silsesquioxane Silanols. *Chem. Eur. J.* **2019**, *25* (65), 14953–14958. https://doi.org/10.1002/chem.201903693.
(89) Wang, L.; Lu, W.; Zhang, J.; Chong, Q.; Meng, F. Cobalt-Catalyzed Regio-, Diastereo- and Enantioselective Intermolecular Hydrosilylation of 1,3-Dienes with Prochiral Silanes. *Angew. Chem.* **2022**, *134* (30), e202205624. https://doi.org/10.1002/ange.202205624.
(90) Yuan, W.; Zhu, X.; Xu, Y.; He, C. Synthesis of Si-Stereogenic Silanols by Catalytic Asymmetric Hydrolytic Oxidation. *Angew. Chem. Int. Ed.* **2022**, *61* (31), e202204912. https://doi.org/10.1002/anie.202204912.
(91) Yamamoto, K.; Kawanami, Y.; Miyazawa, M. Kinetic Resolution of (±)-Cyclohex-1-Enylsilanols by the Sharpless Asymmetric Epoxidation. *J. Chem. Soc. Chem. Commun.* **1993**, No. 5, 436–437. https://doi.org/10.1039/C39930000436.
(92) Weickgenannt, A.; Mewald, M.; Oestreich, M. Asymmetric Si–O Coupling of Alcohols. *Org. Biomol. Chem.* **2010**, *8* (7), 1497–1504. https://doi.org/10.1039/B925722E.
(93) Mori, A.; Toriyama, F.; Kajiro, H.; Hirabayashi, K.; Nishihara, Y.; Hiyama, T. Synthesis and Optical Resolution of Novel Chiral Silanols. *Chem. Lett.* **1999**, *28* (7), 549–550. https://doi.org/10.1246/cl.1999.549.

(94) Bi, X.; Feng, J.; Xue, X.; Gu, Z. Construction of Axial Chirality and Silicon-Stereogenic Center via Rh-Catalyzed Asymmetric Ring-Opening of Silafluorenes. *Org. Lett.* **2021**, *23* (8), 3201–3206. https://doi.org/10.1021/acs.orglett.1c00935.
(95) Sommer, L. H.; Ulland, L. A.; Parker, G. A. Stereochemistry of Asymmetric Silicon. XX. Hydroxylation and Carbene Insertion Reactions of R3SiH. *J. Am. Chem. Soc.* **1972**, *94* (10), 3469–3471. https://doi.org/10.1021/ja00765a036.
(96) Tomooka, K.; Nakazaki, A.; Nakai, T. A Novel Aryl Migration from Silicon to Carbon: An Efficient Approach to Asymmetric Synthesis of α-Aryl β-Hydroxy Cyclic Amines and Silanols. *J. Am. Chem. Soc.* **2000**, *122* (2), 408–409. https://doi.org/10.1021/ja993295t.
(97) Igawa, K.; Yoshihiro, D.; Ichikawa, N.; Kokan, N.; Tomooka, K. Catalytic Enantioselective Synthesis of Alkenylhydrosilanes. *Angew. Chem. Int. Ed.* **2012**, *51* (51), 12745–12748. https://doi.org/10.1002/anie.201207361.
(98) Igawa, K.; Takada, J.; Shimono, T.; Tomooka, K. Enantioselective Synthesis of Silanol. *J. Am. Chem. Soc.* **2008**, *130* (48), 16132–16133. https://doi.org/10.1021/ja805848z.
(99) Wu, Y.; Wang, P. Silicon-Stereogenic Monohydrosilane: Synthesis and Applications. *Angew. Chem.* **2022**, *134* (36), e202205382. https://doi.org/10.1002/ange.202205382.
(100) Adam, W.; Mello, R.; Curci, R. O-Atom-Insertion in Si-H-Bindungen Mit Hilfe von Dioxiranen: Eine Stereospezifische Und Direkte Umwandlung von Silanen in Silanole. *Angew. Chem.* **1990**, *102* (8), 916–917. https://doi.org/10.1002/ange.19901020812.
(101) Cavicchioli, M.; Montanari, V.; Resnati, G. Oxyfunctionalization Reactions by Perfluoro *Cis*-2,3-Dialkyloxaziridines. Enantioselective Conversion of Silanes into Silanols. *Tetrahedron Lett.* **1994**, *35* (34), 6329–6330. https://doi.org/10.1016/S0040-4039(00)73424-1.
(102) Adam, W.; Mitchell, C. M.; Saha-Möller, C. R.; Weichold, O. Host−Guest Chemistry in a Urea Matrix: Catalytic and Selective Oxidation of Triorganosilanes to the Corresponding Silanols by Methyltrioxorhenium and the Urea/Hydrogen Peroxide Adduct. *J. Am. Chem. Soc.* **1999**, *121* (10), 2097–2103. https://doi.org/10.1021/ja9826542.
(103) Okada, Y.; Oba, M.; Arai, A.; Tanaka, K.; Nishiyama, K.; Ando, W. Diorganotelluride-Catalyzed Oxidation of Silanes to Silanols under Atmospheric Oxygen. *Inorg. Chem.* **2010**, *49* (2), 383–385. https://doi.org/10.1021/ic9022745.
(104) Ishimoto, R.; Kamata, K.; Mizuno, N. Highly Selective Oxidation of Organosilanes to Silanols with Hydrogen Peroxide Catalyzed by a Lacunary Polyoxotungstate. *Angew. Chem.* **2009**, *121* (47), 9062–9066. https://doi.org/10.1002/ange.200904694.
(105) Lee, M.; Ko, S.; Chang, S. Highly Selective and Practical Hydrolytic Oxidation of Organosilanes to Silanols Catalyzed by a Ruthenium Complex. *J. Am. Chem. Soc.* **2000**, *122* (48), 12011–12012. https://doi.org/10.1021/ja003079g.
(106) Sommer, L. H.; Lyons, J. E. Stereochemistry of Asymmetric Silicon. XVI. Transition Metal Catalyzed Substitution Reactions of Optically Active Organosilicon Hydrides. *J. Am. Chem. Soc.* **1969**, *91* (25), 7061–7067. https://doi.org/10.1021/ja01053a028.
(107) Mori, K.; Tano, M.; Mizugaki, T.; Ebitani, K.; Kaneda, K. Efficient Heterogeneous Oxidation of Organosilanes to Silanols Catalysed by a Hydroxyapatite-Bound Ru Complex in the Presence of Water and Molecular Oxygen. *New J. Chem.* **2002**, *26* (11), 1536–1538. https://doi.org/10.1039/B205498C.
(108) Igawa, K.; Takada, J.; Shimono, T.; Tomooka, K. Enantioselective Synthesis of Silanol. *J. Am. Chem. Soc.* **2008**, *130* (48), 16132–16133. https://doi.org/10.1021/ja805848z.

(109) Zhang, H.; Zhao, D. Synthesis of Silicon-Stereogenic Silanols Involving Iridium-Catalyzed Enantioselective C–H Silylation Leading to a New Ligand Scaffold. *ACS Catal.* **2021**, *11* (17), 10748–10753. https://doi.org/10.1021/acscatal.1c03112.
(110) Yuan, W.; Zhu, X.; Xu, Y.; He, C. Synthesis of Si-Stereogenic Silanols by Catalytic Asymmetric Hydrolytic Oxidation. *Angew. Chem. Int. Ed.* **2022**, *61* (31), e202204912. https://doi.org/10.1002/anie.202204912.
(111) Gao, J.; Mai, P.-L.; Ge, Y.; Yuan, W.; Li, Y.; He, C. Copper-Catalyzed Desymmetrization of Prochiral Silanediols to Silicon-Stereogenic Silanols. *ACS Catal.* **2022**, *12* (14), 8476–8483. https://doi.org/10.1021/acscatal.2c02482.
(112) Zhu, M.; Oestreich, M. Generation of Silicon-Centered Stereogenicity by Chiral Counteranion-Directed Desymmetrization of Silanediols. *ACS Catal.* **2023**, *13* (15), 10244–10247. https://doi.org/10.1021/acscatal.3c02682.
(113) Dalton, J. J.; Bernal Sánchez, A.; Kelly, A. T.; Fettinger, J. C.; Franz, A. K. Organocatalytic Asymmetric Synthesis of Si-Stereogenic Siloxanols. *ACS Catal.* **2024**, *14* (2), 1005–1012. https://doi.org/10.1021/acscatal.3c03932.
(114) Schreyer, L.; Properzi, R.; List, B. IDPi Catalysis. *Angew. Chem. Int. Ed.* **2019**, *58* (37), 12761–12777. https://doi.org/10.1002/anie.201900932.

Chapter 2: Studies Towards Understanding the Enantioselective Synthesis of Siloxanols *via* Hydrogen-Bonding Organocatalysis*

2.1 Introduction and Background

This chapter presents my contributions to the organocatalytic asymmetric synthesis of silicon-stereogenic siloxanols *via* the desymmetrization of prochiral silanediols.[1] The design, synthesis, and evaluation of organocatalyst analogs is described. The screening for organocatalyst analogs demonstrated that the imidazole is a key structural feature necessary for the desymmetrization reaction. Efforts towards the synthesis of novel prochiral silanediols have been evaluated, and a successful route for future access was established. The solution-state hydrogen-bonding interactions were investigated and a correlation between enantioselectivity and catalyst binding was determined.

The silylation of alcohols is a landmark protecting group strategy in organic synthesis.[2,3] In 1972, Venkateswarlu and Corey first reported the protection of secondary alcohols using *tert*-butyldimethylsilyl chloride (TBSCl) and imidazole. The silyl group was cleaved under mild conditions using fluoride reagents (Equation **2.1**).[4] While this seminal work ushered in the use of a silyl group as an advantageous protecting group, the use of imidazole prompted the development of exciting methodologies towards the enantioselective silylation of alcohols.[5–7] The role of the Lewis base activation of Lewis acids became apparent in transformations involving silylated nucleophiles.[8–12] These results provided fundamental knowledge for the role of different chiral agents: 1) chiral transition metal complex activation of a silane, 2) chiral Lewis base activation of a silyl chloride, and 3) chiral Brønsted or Lewis acid activation of a silyl amine (Figure **2.1A**).[13–15] The desymmetrization of *meso* diols proceed through a chiral Lewis base activation of a silyl chloride followed by enantioselective silylation of the alcohol (Figure **2.1B).**

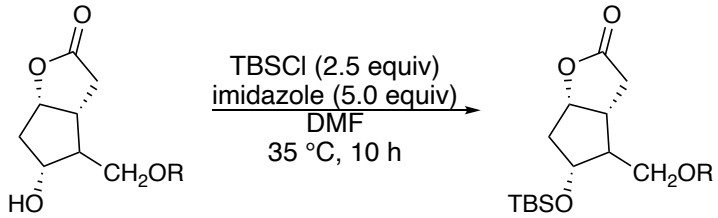

2.1 **2.2**, 96%

Equation 2.1 Secondary alcohol protection developed by Corey.

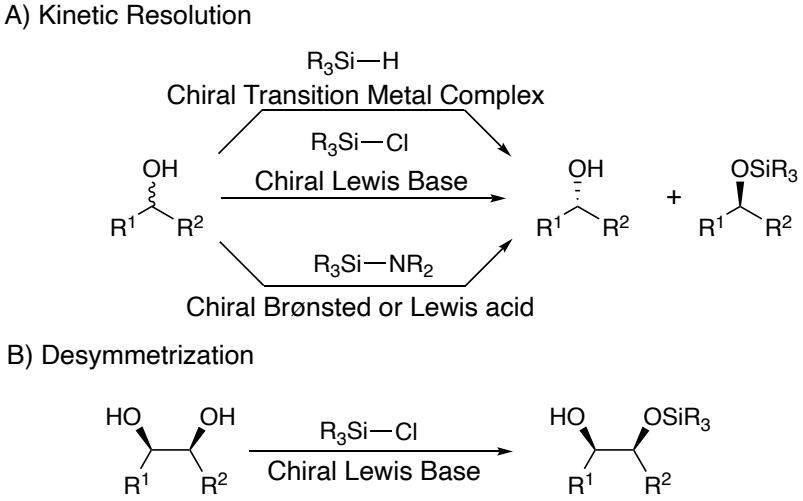

Figure 2.1 Methodologies for the enantioselective silylation of alcohols.

The earliest report of a Lewis base-mediated catalytic enantioselective silylation of a secondary alcohol was reported by Ishikawa and coworkers in 2001.[16] The Ishikawa group surveyed a collection of chiral guanidines for the resolution of indan-1-ol **2.3** to **2.6** and **2.7** (Scheme **2.1**). The modest selectivity for the formation of **2.6** was achieved with chiral guanidine **2.4** and exhibited a slow reaction rate. Chiral bicyclic guanidine **2.5** improved selectivity for the formation of **2.7** using TIPSCl with an increased rate of reaction rate. Notably, the chiral guanidines could be recovered. The Ishikawa group hypothesized that the mechanism proceeds through formation of a chiral silylguanidinium salt, which was supported using preliminary ^{1}H NMR studies. This work supported the development of future catalytic enantioselective silylation reactions of alcohols.

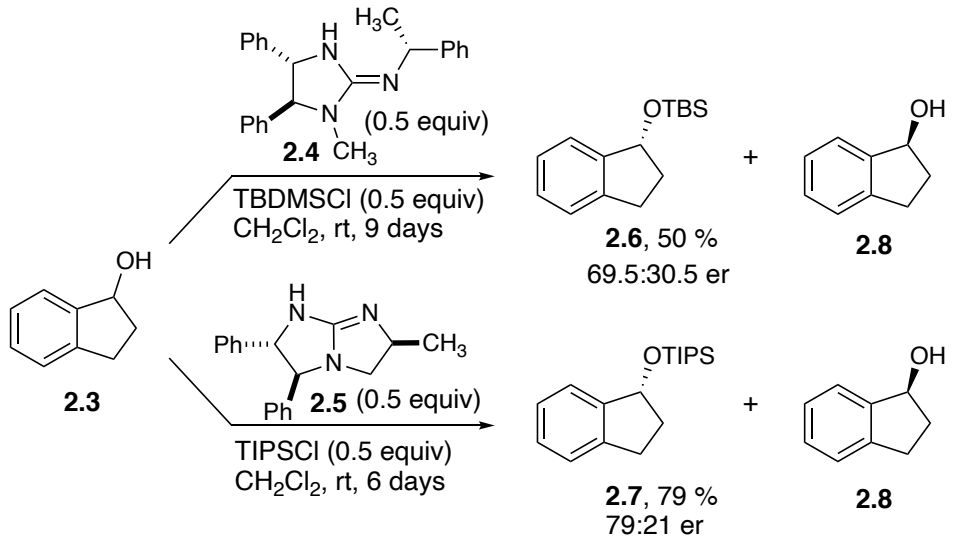

Scheme 2.1 Ishikawa chiral guanidines for early Lewis base-mediated enantioselective silylations of alcohols.

In 2008, the Wiskur group first developed an enantioselective Mukaiyama aldol process and noted the chiral ammonium salt was responsible for promoting the kinetic resolution of the alkoxide enantiomers and laid the groundwork for the subsequent studies described.[17] Later in 2011, Wiskur identified (-)-tetramisole **2.10**, an isothiourea Lewis basic heterocyclic catalyst, capable for the silylative kinetic resolution of secondary alcohols (Scheme **2.2**A).[18] Isothiourea **2.10** was shown to be an effective catalyst for benzylic alcohols at 25 mol %, with unhindered bicyclic benzylic alcohols selective for this method. Hindered and acyclic benzylic alcohols were not selective.

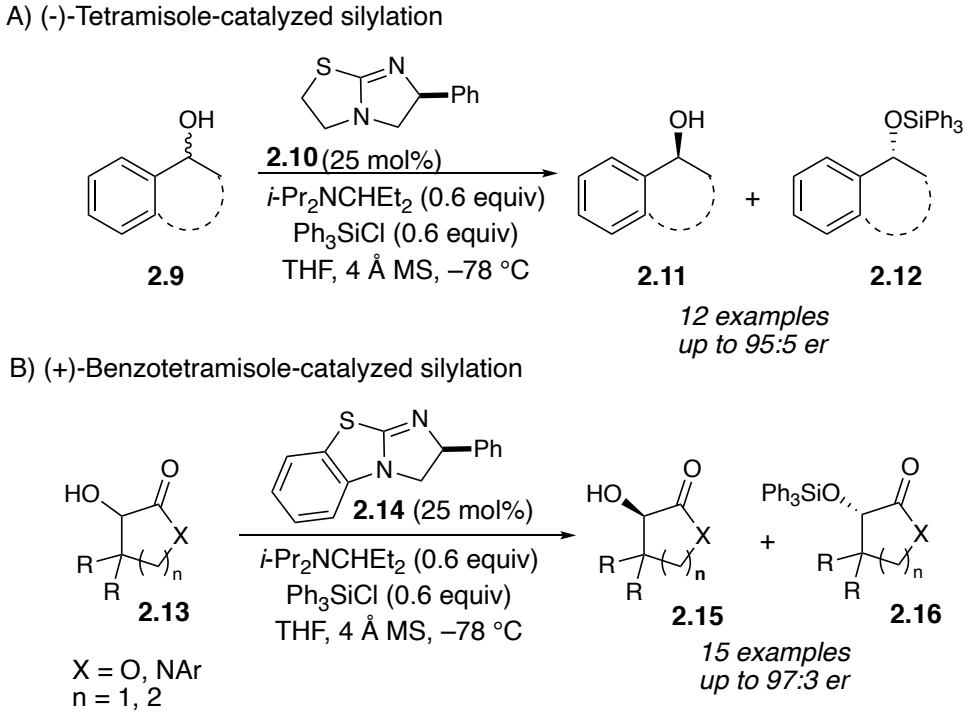

Scheme 2.2 Contributions by Wiskur and co-workers to the silylative kinetic resolution of alcohols.

The Wiskur group expanded their methodology to include the kinetic resolution of α-hydroxy lactones and lactams **2.13** (Scheme **2.2**B).[19] In this study, (+)-benzotetramisole **2.14** served as an effective catalyst at 25 mol % with an expanded substrate scope compared to their initial methodology. Under these conditions, the selectivity of the resolution was significantly increased with the presence of additional steric bulk near the reactive alcohol group (i.e., *β* position). This efficient method represented the first reported nonenzymatic resolution for this class of compounds. Although impressive work was investigated using kinetic resolution, desymmetrization methods were needed to increase theoretical yields for wider applicability in organic synthesis.

In 2006, Hoveyda and Snapper reported the enantioselective silyl protection of *meso*-1,2-diols promoted by an imidazole catalyst **2.18** (Scheme **2.3**).[20] Although the methodology required long reaction times and 20–30 mol % catalyst loadings, yields and selectivities were

good to excellent. The substrate scope features cyclic *meso*-1,2-diols and one acyclic example that performed with excellent selectivity (95:5 er). Extensive catalyst analog studies allowed for understanding of the structural features that promoted the enantioselective silylation. Changes to the Lewis base and chiral amino acid were made to the catalyst analogs. From these studies, an activation model emerged (Scheme **2.3**). Hoveyda and Snapper proposed that the imidazole coordinates to the silyl group *via* a Lewis base activation of the silyl chloride to favor nucleophilic attack by the oxygen of the diol. The proposed transition state model also invokes a two-point binding mode with the carbonyl of **2.18** and amine both acting as a hydrogen-bond acceptors. The Hoveyda-Snapper methodology with **2.18** has also been extended to the kinetic resolution of vicinal *syn*-diols,[21] the enantioselective silylation of terminal 1,2-diols,[22] the regiodivergent resolution of 1,2-diols,[23] and the catalytic desymmetrization of *meso* triols.[24]

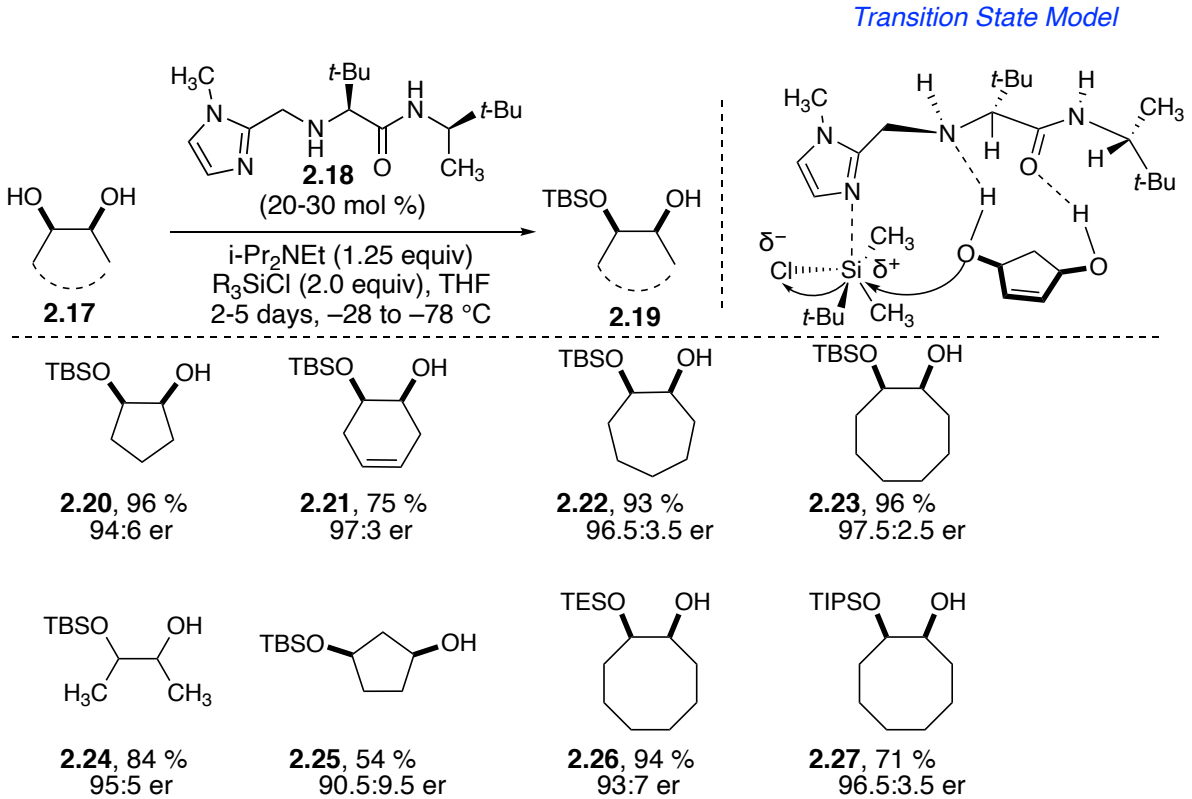

Scheme 2.3 Hoveyda and Snapper catalytic desymmetrization of *meso*-diols and proposed transition state model.

In 2011, the Tan group developed a desymmetrization of a small collection of *meso*-1,2-diols using TBSCl with catalyst **2.29** (Scheme **2.4**).[25,26] Chiral imidazole **2.29** at 20 mol % is an effective catalyst with high selectivities for acyclic and cyclic substrates. In contrast to the work of Hoveyda and Snapper, the Tan group used a strategy that allows for the reversible formation of a covalent bond with the diol substrates. Tan and co-workers incorporated the methoxyoxazolidine in catalyst **2.29** as a key structural feature that binds the alcohol moiety. When the diol is bound to the catalyst, a free hydroxyl group is found to be in proximity and primed for silylation by the activated imidazole (Scheme **2.4**). This unique catalytic system required acidic buffer additives to promote catalyst-substrate formation. The Tan group applied this methodology for the regiodivergent resolution of 1,2-diols[27] and the kinetic resolution of 1,2-diols.[28]

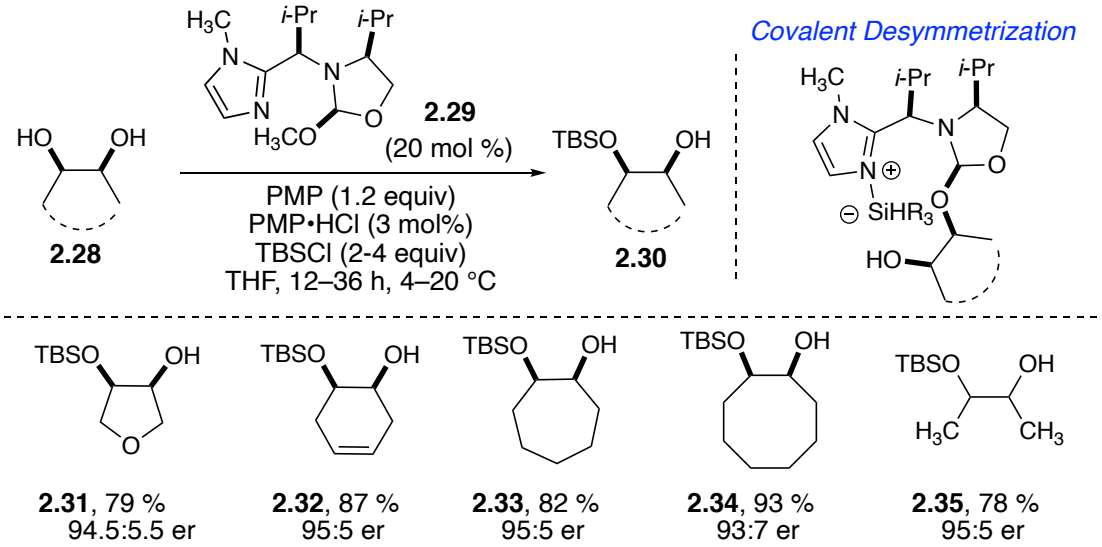

Scheme 2.4 Tan desymmetrization of *meso*-diols.

Inspired by the desymmetrization of *meso*-diols, the Franz Lab has developed the first Lewis base-catalyzed silylation of prochiral silanediols to produce silicon-stereogenic siloxanols (Scheme **2.5**).[1] Silanediols were hypothesized to be capable for selective silylation of one enantiotopic hydroxyl group by a Lewis base. Remarkably, the Hoveyda-Snapper catalyst **2.18** is

an effective catalyst at 5 mol % for the silylation of prochiral silanediols. A wide range of prochiral substrates were synthesized. Desymmetrization methodologies were developed by the He and Oestreich groups and were published contemporaneously with our work.[29,30] Nonetheless, these contributions informed our substrate scope. Each of these methodologies required using a *tert*butyl(phenyl)silanediol to achieve high selectivities, which will be discussed in more detail later in this chapter. Notably, the *tert*-butyl substituent on the parent silanediols was not required using our methodology. Our organocatalytic method features isobutyl, isopropyl, and *n*-butyl groups among a diverse class of aryl groups. The contributions by the He and Oestreich groups allowed us to explore the synthesis of novel substrates which answered questions about the unique aryl-alkyl system necessary around the silicon atom that led to high levels of enantioenrichment. Additionally, we showcased a diverse scope of chlorosilanes with structural features capable of further transformations. To understand the mechanism of silylation for our methodology, I synthesized analogs and investigated the structural features of the Hoveyda-Snapper catalyst followed by a venture into the substrate scope unknown that generated many hypotheses for future exploration.

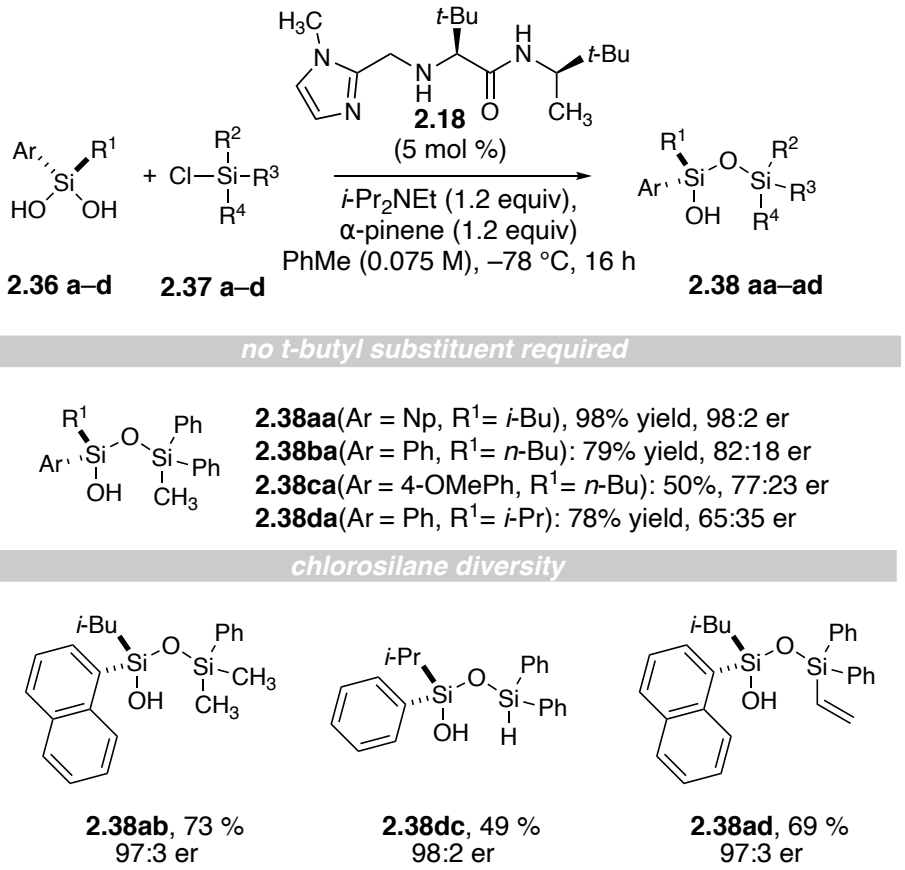

Scheme 2.5 Franz lab desymmetrization of prochiral silanediols using the Hoveyda-Snapper catalyst **2.18**.

2.2 Importance of Hoveyda-Snapper Catalyst

To probe catalyst-substrate interactions in the solid state, Jacob J. Dalton, Ph.D. performed crystallization studies and obtained a crystal structure of the complex between **2.18** and naphthalen-1-yl(phenyl)silanediol **2.39** (Figure **2.2**, X-ray solved by James C. Fettinger, Ph.D.).[1] This structure gave insight into the potential binding mode and mechanism of the desymmetrization of prochiral silanediols with catalyst **2.18** The solid-state study revealed a dual-binding mode in the catalyst-substrate complex with a two-point hydrogen-bonding interaction. Here, the imidazole serves as a hydrogen-bond acceptor, with a distance of 1.74 Å between

the nitrogen of the imidazole and the hydrogen of the silanol (O-NH1.74 Å). The amide NH serves as a hydrogen-bond donor, with a distance of 2.14 Å between the hydrogen of the amide and the oxygen of the silanol (NH-O 2.14 Å) (Figure **2.2**). The enantiopure co-crystal suggests that binding to a single hydroxyl group of **2.39** is responsible for generating the chiral environment. Initial ^{1}H NMR binding studies supported these interactions in solution.

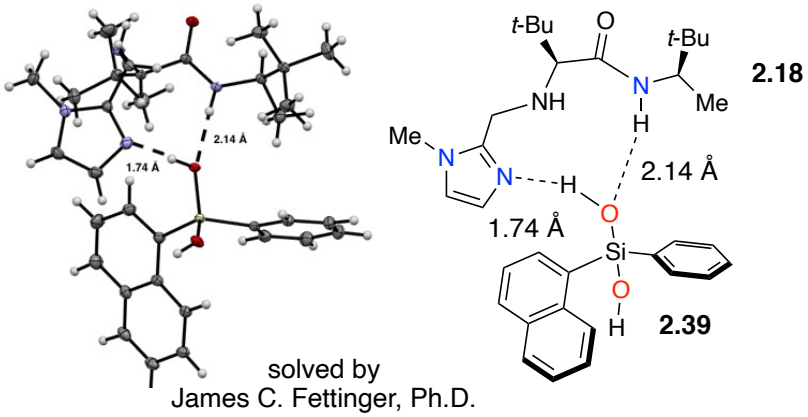

Figure 2.2 Crystal structure of the complex of the Hoveyda-Snapper catalyst **2.18** binding to naphthalen-1-yl(phenyl)silanediol **2.39**.

2.3 Design of Hoveyda-Snapper Catalyst Analogs

With the initial analysis of the organocatalyst-substrate complex, we sought to evaluate the activation/binding mode that promotes the enantioselectivity for the desymmetrization reaction. The enantioselectivity of the desymmetrization reaction could be influenced through structural changes in the organocatalyst. To accomplish this, we recognized four structural components **2.18** that can be modified: the Lewis base, the hydrogen-bond acceptor, the chiral amino acid, and the hydrogen-bond donor (Figure **2.3**). We then set out to design organocatalyst analogs of interest.

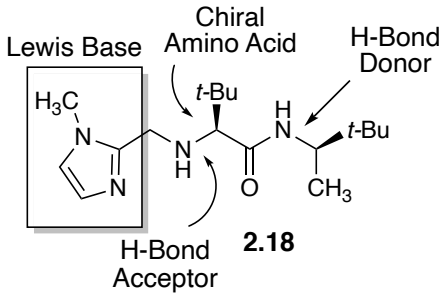

Figure 2.3 Structural components of **2.18**.

Initial designs of organocatalyst analogs were based off the co-crystal (Figure **2.4**). The first design of catalyst analogs focused on substitution of the chiral amino acid and the chiral center alpha to the hydrogen-bond donor. Targets **2.40**–**2.41** were designed based off of initial studies by Hoveyda and Snapper indicating catalysts derived from valine with C-terminus substituents phenyl and *tert*-butyl gave enantiomeric ratios as high as 91:9 er (Figure **2.4**A).[20] The second design of catalyst analogs focused on replacing the Lewis base. The co-crystal structure and ^{1}H NMR binding data revealed the imidazole has a key hydrogen-bonding interaction. We envisioned that organocatalyst analogs that replace (or lack) the imidazole component would allow us to investigate the role of the Lewis base during silylation (Figure **2.4**B). In addition, Hoveyda and Sapper proposed an activation model for the catalytic enantioselective silylation of (1*R*,3*S*)-cyclopent-4-ene-1,3-diol where the imidazole served to promote silylation providing meaningful precedent.[20] Specifically, targets **2.42**–**2.44** were designed to investigate the effect of the aryl group. Pyridine derivatives have previously been employed to promote silylation.[5,6] Targets **2.44**–**2.47** propose to evaluate various pyridine analogs with enhanced nucleophilicity. Lastly, targets **2.48**–**2.49** were designed to evaluate the effect of the pyridine with different *C*-terminus substituents, i.e., phenyl and *tert*-butyl (Figure **2.4**C).

A) Chiral Amino Acid & Hydrogen-bond donor

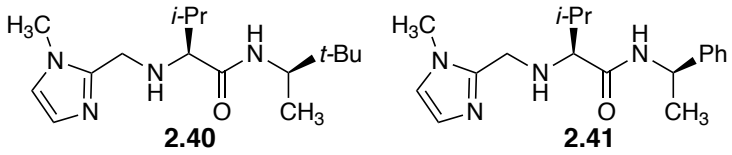

B) Lewis Base

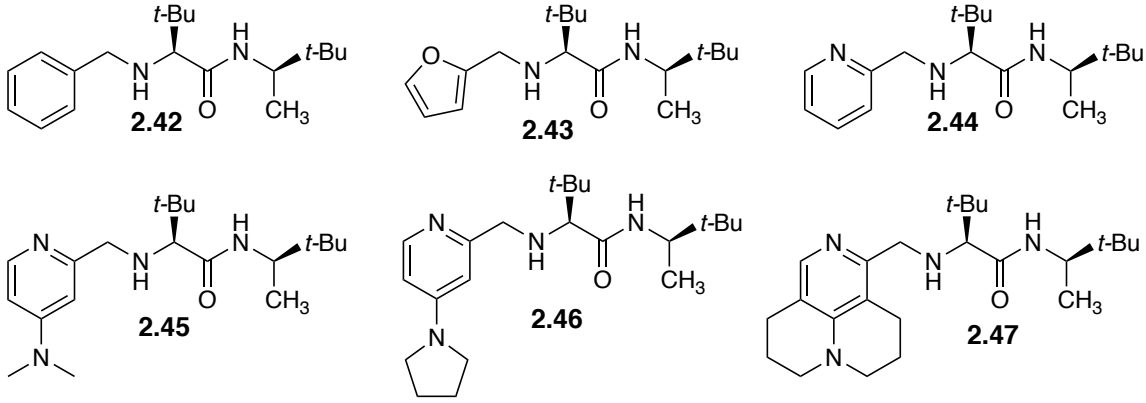

C) Simultaneous Variation of Multiple Components

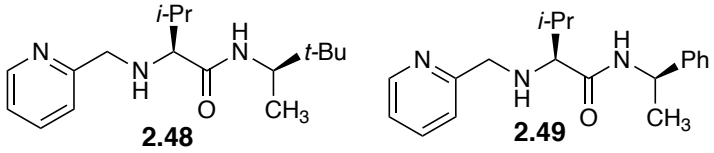

Figure 2.4 Initial designs of organocatalyst analogs.

We refined the organocatalyst analogs of interest to a narrower focus (Scheme **2.5**). It was clear that the imidazole moiety was important to promote silylation in the system we developed and, in the system developed by Hoveyda and Snapper. Therefore, the synthesis and evaluation of targets **2.42**, **2.44, 2.48**–**2.49** would accomplish our goal to test this hypothesis while also exploring the importance of *C*-terminus substituents.

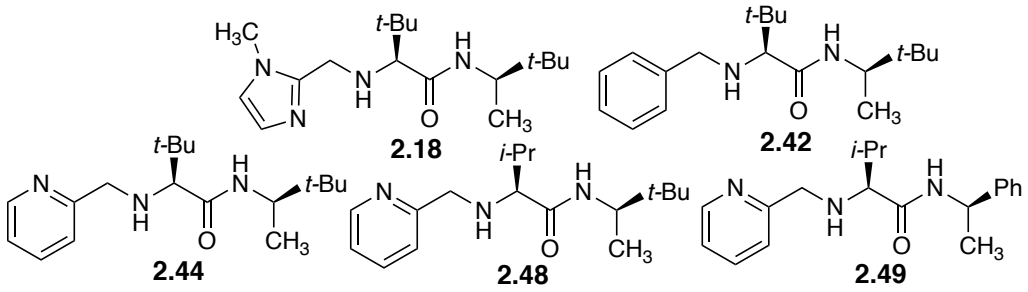

Figure 2.5 Hoveyda-Snapper catalyst **2.18** and refined catalyst targets.

2.4 Synthesis of Hoveyda-Snapper Catalyst Analogs

The first syntheses performed were for organocatalyst targets **2.42** and **2.44** which most closely resembled **2.18** (Scheme **2.6**). First, Boc-*tert*-leucine **2.50** underwent an amide coupling with EDC and HOBt using chiral amine **2.51** resulting in the formation of *N*-Boc amide **2.52** in excellent yield (90%). Compound **2.52** was then deprotected with 3.0 equivalents of 4.0 M HCl • dioxane at 0 °C for 1 hour and yielded quantitative conversion to amino amide **2.53**. Rapid derivatization of **2.53** using reductive amination would allow access to targets **2.42** and **2.44**. The benzyl target **2.42**, synthesized by Jacob J. Dalton, was accessible in moderate yield (55%), while **2.44** required optimization.

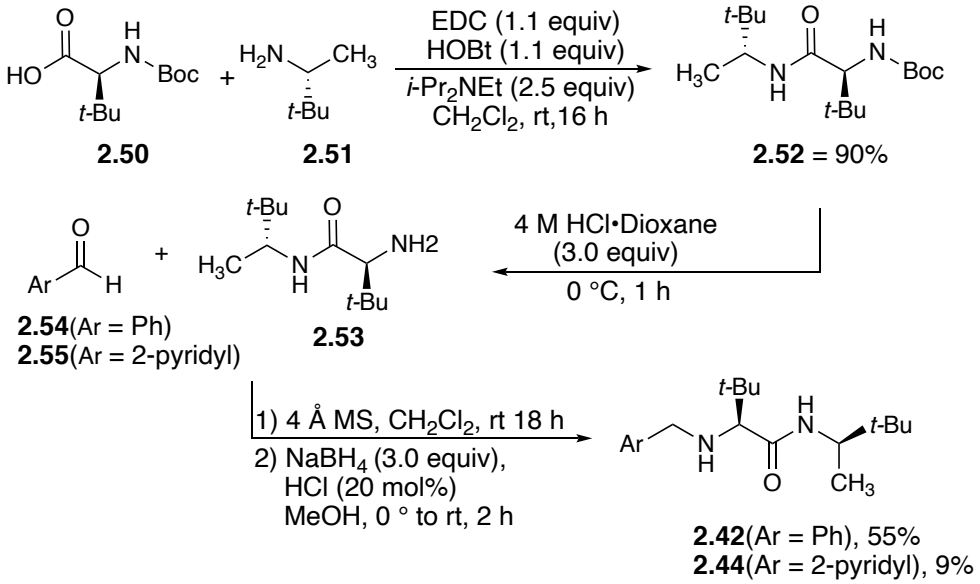

Scheme 2.6 Synthesis of analogs **2.42** and **2.44**.

The reductive amination of amino amide **2.53** was evaluated with various reducing agents to optimize formation of target **2.44** (Table **2.1**). Amino amide **2.53** was subjected to imine forming conditions with 4 Å molecular sieves (or $MgSO_4$ where indicated) to give imine products, which were not purified after workup and exhibited 50% conversion *via* ^{1}H NMR analysis. Reduction of pyridyl imines formed using $MgSO_4$ was evaluated with various reducing agents at a constant time of 1 hour, where each reaction resulted in less than 5% conversion to product (Table **2.1**, entries 1–3). To improve conversion, the scale of the test reactions was increased to 0.5 mmol with 4 Å molecular sieves which afforded an increased conversion to imines of 60% (Table **2.1**, entries 4–6). Molecular sieves were then utilized in the subsequent test conditions to form imines for the reductive amination.

Table 2.1 Reductive amination conditions tested for analog **2.44**.

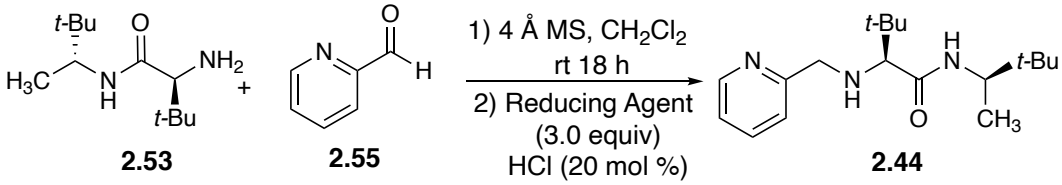

2.53 **2.55** **2.44**

entry	scale (mmol)	reducing agent	time (h)	conversion [a]
1 [b]	0.20	$NaBH_4$	1	< 5
2 [b]	0.20	$NaBH(OAc)_3$	1	< 5
3 [b]	0.20	$NaBH_3CN$	1	< 5
4	0.50	$NaBH_4$	3	< 5
5	0.50	$NaBH(OAc)_3$	3	< 5
6	0.50	$NaBH_3CN$	3	< 5
7	0.50	$NaBH_4$	6	< 5
8	0.50	$NaBH(OAc)_3$	6	< 5
9	0.50	$NaBH_3CN$	6	< 5
10 [c]	0.50	$NaBH(OAc)_3$ (1.5 equiv), AcOH, THF	18	< 5
11	2.30	$NaBH_4$	1	10
12	4.70	$NaBH_4$	1	10 (9) [d]

[a]Observed using ^{1}H NMR spectroscopy. [b]$MgSO_4$ utilized in place of 4 Å MS for imine formation. [c]One-pot procedure. [d] Isolated yield.

The subsequent screening used 4 Å molecular sieves and extended reaction times. It was determined that the use of molecular sieves provided imines in higher conversions. The conversion of imines increased slightly, from 50% to 60%, indicating that the use of the molecular sieves suppressed imine hydrolysis which was deemed a contributing factor for the less than 5% conversion to **2.44**. With this understanding, longer reaction times were employed for the reduction to improve conversion. Extended reduction times ranging from 3–6 hours resulted in less than 5% conversion to **2.44** which was attributed to the imine hydrolyzing faster than the rate of reduction (Table **2.1**, entries 4–9). To reduce the rate of imine hydrolysis and potentially improve conversion to **2.44**, a one-pot procedure using $NaBH(OAc)_3$ was tested, also resulting in less than 5% conversion (Table **2.1**, entries 10). Encouragingly, there was a noticeable difference seen with larger scale reactions which resulted in 9% yield of **2.44** (Table **2.1**, entries 11–12). Finally, the optimization for the synthesis of **2.44** was completed using 4 Å molecular sieves and $NaBH_4$ and **2.44** could then be tested in the desymmetrization reaction (Scheme **2.7**).

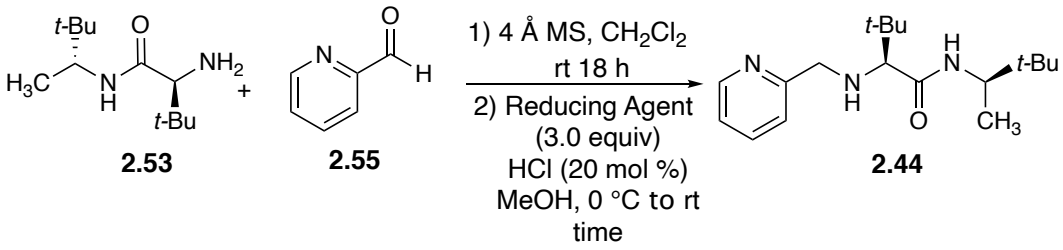

Scheme 2.7 Optimized conditions for the synthesis of organocatalyst analog **2.44**.

The general synthesis for valine-containing targets follows the synthetic route of previous targets discussed (Scheme **2.8**). Boc-*L*-valine was subjected to amide coupling conditions in the presence of DCC and chiral amines **2.51** and **2.57** to yield *N*-Boc amides **2.58**–**2.59** in low conversion requiring optimization**.** Compounds **2.58**–**2.59** would be deprotected with 10

equivalents of TFA to give amino amides **2.60**–**2.61** that can readily be utilized in the optimized reductive amination conditions identified for the synthesis of leucine-containing targets.

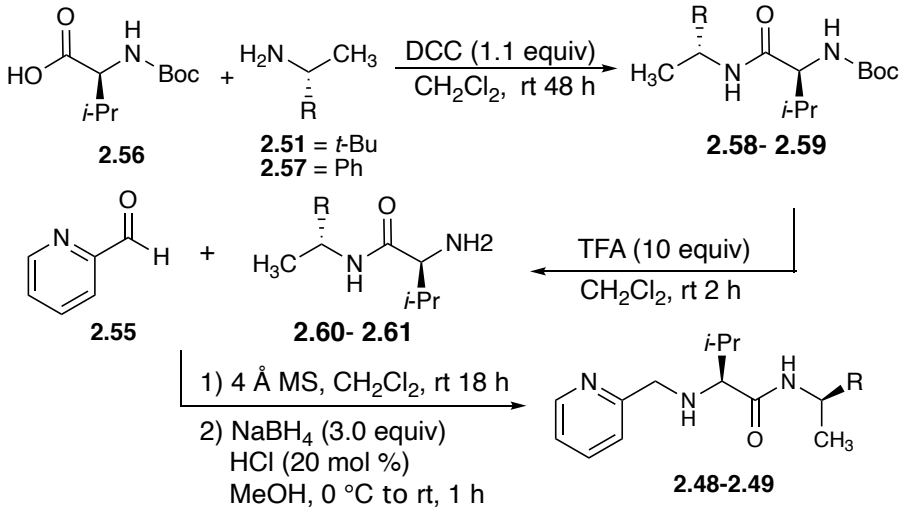

Scheme 2.8 Synthesis of analogs **2.48**– **2.49**.

The optimization for the amidation conditions with **2.59** was investigated with various coupling agents (Table **2.2**). Overnight amidation conditions with DCC and without base resulted in low 25% conversion to product **2.59** (Table **2.2**, entry 1). Notably, the same was true for EDC/HOBt and ethyl chloroformate conditions in the presence of base (Table **2.2**, entries 2–3). To improve conversion to product **2.59**, longer reaction times allowed for an increased conversion using DCC (Table **2.2**, entries 4–6). A combination of *N*,*N*,*N*,*N*-tetramethylchloroformamidinium (TCFH) and *N*-methylimidazole conditions have been used for challenging couplings of hindered carboxylic acids.[31] To reduce the reaction time, the TCFH/NMI conditions were tested, resulting in less than 5% conversion to **2.59**. The optimized protocol for the synthesis of **2.59** involved using DCC at extended reactions time and was ready for subsequent steps in the synthesis.

Table 2.2 Amidation conditions tested to access **2.59**.

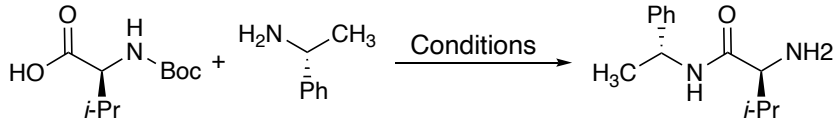

2.56 **2.57** **2.59**

entry	coupling agents	base	solvent	time (h)	temp	conversion [a]
1	DCC	N/A	DCM	18	rt	23
2	EDC, HOBt	DIPEA	DCM	18	rt	25
3	$Cl(CO)CH_2CH_3$	TEA	THF	18	rt	20
4	DCC	N/A	DCM	48	rt	70
5	EDC, HOBt	DIPEA	DCM	48	rt	33
6	$Cl(CO)CH_2CH_3$	TEA	THF	48	rt	37
7	TCFH, NMI	N/A	CH_3CN	24	rt	<5

[a]Observed using ^{1}H NMR spectroscopy.

2.5 Discussion of Hoveyda-Snapper Catalyst Analogs for Desymmetrization of Prochiral Silanediols

With catalyst analogs **2.42** and **2.44** in hand, we evaluated their efficacy in the desymmetrization reaction (Scheme **2.10**). Catalyst **2.42**, which features a phenyl ring, did not catalyze the reaction leaving only unreacted starting material **2.36a**. Replacement of the imidazole ring with pyridine for catalyst **2.44** resulted in no reaction and only recovered starting material. The results of catalysts **2.42** and **2.44** support that the imidazole plays a key role to promote silylation in the desymmetrization reaction. In tandem with my design of organocatalyst analogs, my colleague Jacob J. Dalton, Ph.D. synthesized and tested valine-derived imidazole analogs **2.62**–**2.64**. Amino alcohol **2.62** resulted in no reaction. Targets **2.63**–**2.64** exhibited slight reactivity with no selectivity. From these results, it is concluded that the imidazole was the only Lewis base capable, among those screened thus far, of promoting silylation in the desymmetrization reaction. Given these results, the remaining organocatalyst analog targets were no longer synthesized and tested.

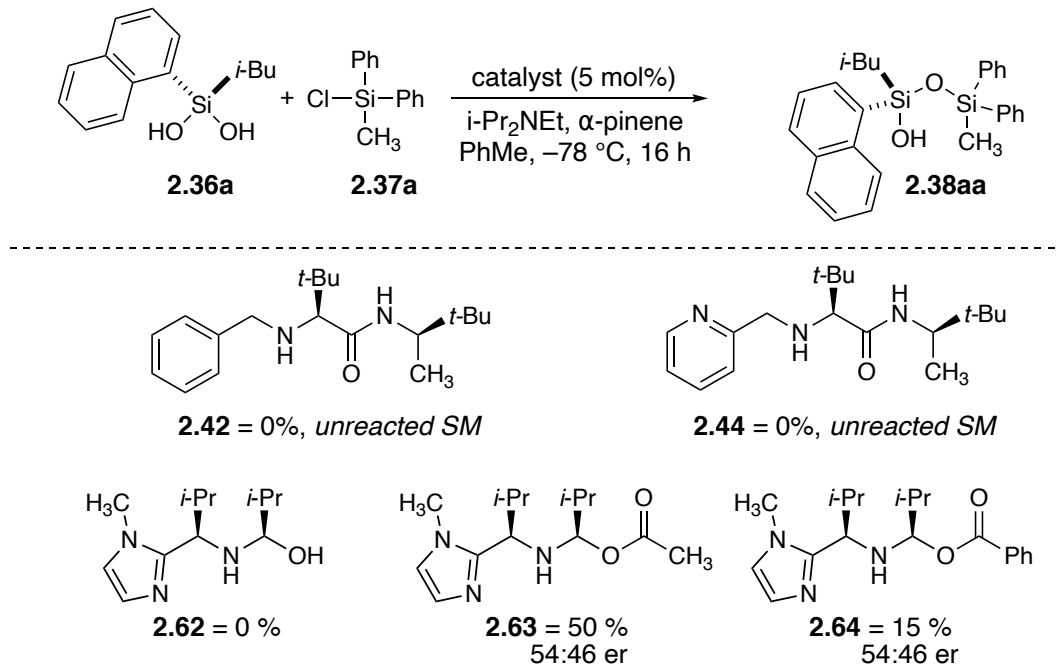

Scheme 2.9 Organocatalyst analogs results for the desymmetrization of isobutyl(naphthalen-1-yl)silanediol **2.36a**.

2.6 Discussion of Interest in New Prochiral Silanediol Substrates

Concurrent with our work to develop the desymmetrization of prochiral silanediols, two asymmetric methods were recently reported for the desymmetrization of prochiral silanediols to access enantioenriched siloxanols (Figure **2.5**).[29,30] He and co-workers reported a Cu-catalyzed intermolecular dehydrogenative coupling of silanediols with hydrosilanes. The He group methodology was optimized with *tert*-butyl(phenyl)silanediol and diphenylsilane. In their methodology, the silane reaction partner was limited to diphenylsilane. Silanediols decorated with isopropyl, cyclohexyl, naphthyl and 2,6-dimethylphenyl and lacking the *tert*-butyl substituent (4 out of 25 substrates) exhibited up to 83% yield and 91:9 e.r. Zhu and Oestreich utilized a counteranion-directed silylation methodology[32] for the desymmetrization of *tert*-butyl(phenyl)silanediol with allyl(*tert*-butyl)dimethylsilane and allyltrimethylsilane as a limitation.[30] Silanediols decorated with isopropyl, cyclohexyl, naphthyl and 2,6-dimethylphenyl

and lacking the *tert*-butyl substituent (4 out of 18 substrates) exhibited up to 88% yield and 75:25 e.r. Both methods required the *tert*-butyl group as a key design feature responsible for high levels of enantioenrichment. Interestingly, the desymmetrization of *tert*-butyl(phenyl)silanediol in the Franz Lab resulted in complete loss of reactivity with unreacted starting material for **2.65** and a lack of enantioselectivity (51:49 er) for **2.66**. From these results, we determined that expanding the scope of the desymmetrization reaction, primarily substrates containing mixed alkyl-aryl groups with some aryl-aryl substrates, would provide valuable insight into the variation around the silicon atom that leads to enantioinduction.

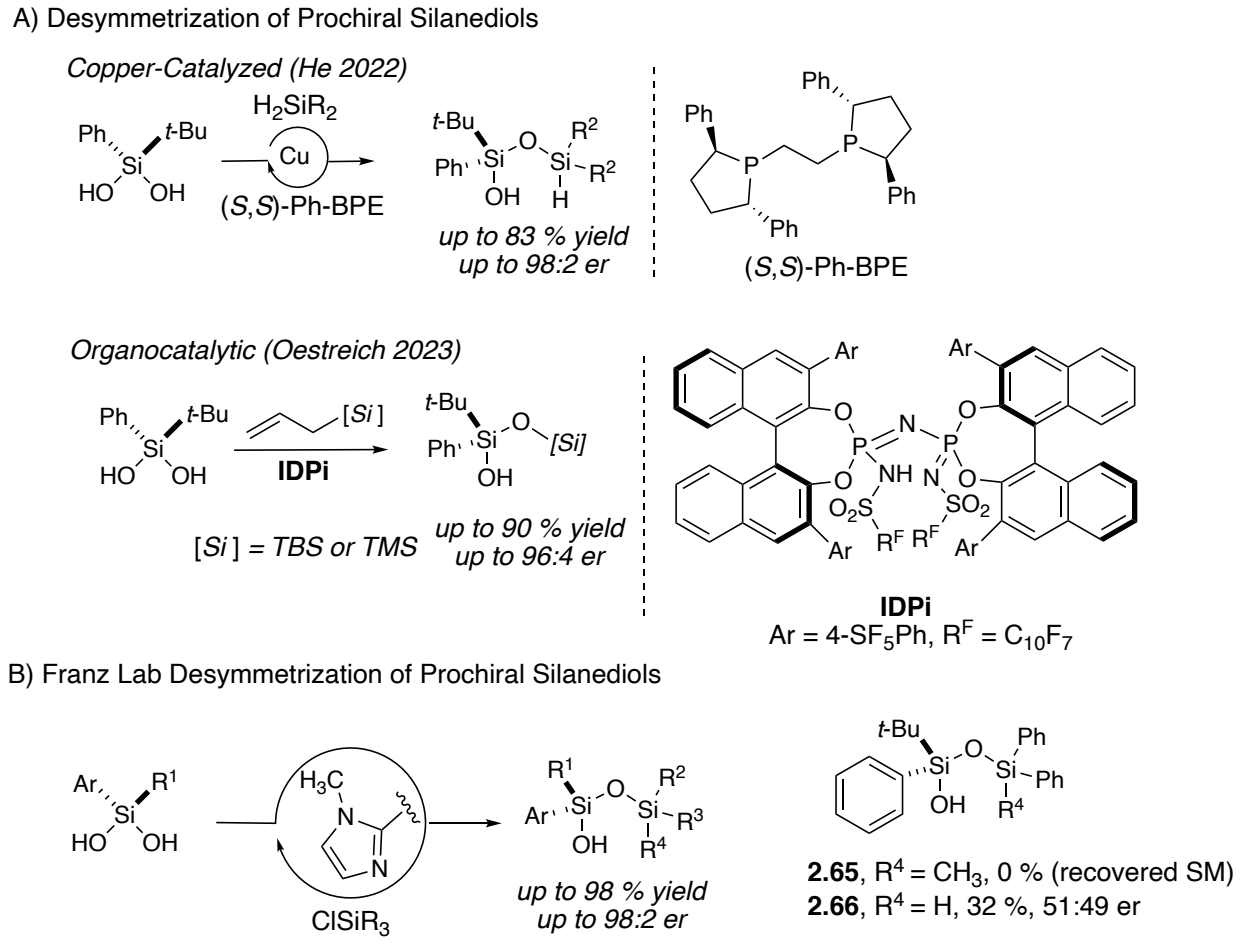

Figure 2.5 A) Methodologies reported for the desymmetrization of prochiral silanediols concurrent with this work. B) Franz Lab methodology indicating lack of selectivity for prochiral substrate necessary for previous methodologies.

2.7 Synthesis of Prochiral Silanediols

With initial understanding of the activation mode for the desymmetrization reaction through catalyst analogs, I turned my attention to expanding the scope of prochiral silanediols. A small collection of aryl-isopropyl and aryl-isobutyl silanediols were synthesized to explore the scope of the desymmetrization reaction.

Silanediols were first reported by Kipping in 1901[33] and have since been historically challenging to access. Industrial processes to prepare siloxane polymers take advantage of the instability of sterically small silanediols (i.e., dimethylsilanediol) to promote self-condensation.[34–36] Previous work in the Franz Lab has employed two general strategies to synthesize soluble, stable, and isolable silanediols that could avoid the propensity towards self-condensation.[37–40] First, increasing the steric environment around the silicon atom (i.e., with mesityl or naphthyl) and, second, the incorporation of electron-withdrawing groups allowed for increased acidity and hydrogen-bonding.[40]

In addition to employing the above strategy, the Franz Lab has optimized a procedure with a silane hydrolysis step for access to modular silanol structures. Self-condensation and acid impurities (i.e.,HCl) are commonly observed with the direct hydrolysis of chlorosilanes.[41,42] Thus, a Pd/C hydrolysis of silanes was valuable for access to pure silanediols. Chlorosilanes **2.67a–b** was added quickly to aryl Grignards, made from commercially available aryl bromide reagents (Scheme **2.10**). The remaining Si–Cl bond is reduced *in situ* with LAH to yield silanes **2.68a–e** that are purified by flash column chromatography or Kugelrhor distillation. Silanes **2.68a–e** are carried forward to silanediols **2.69a–f** *via* a Pd/C-catalyzed hydrolysis.

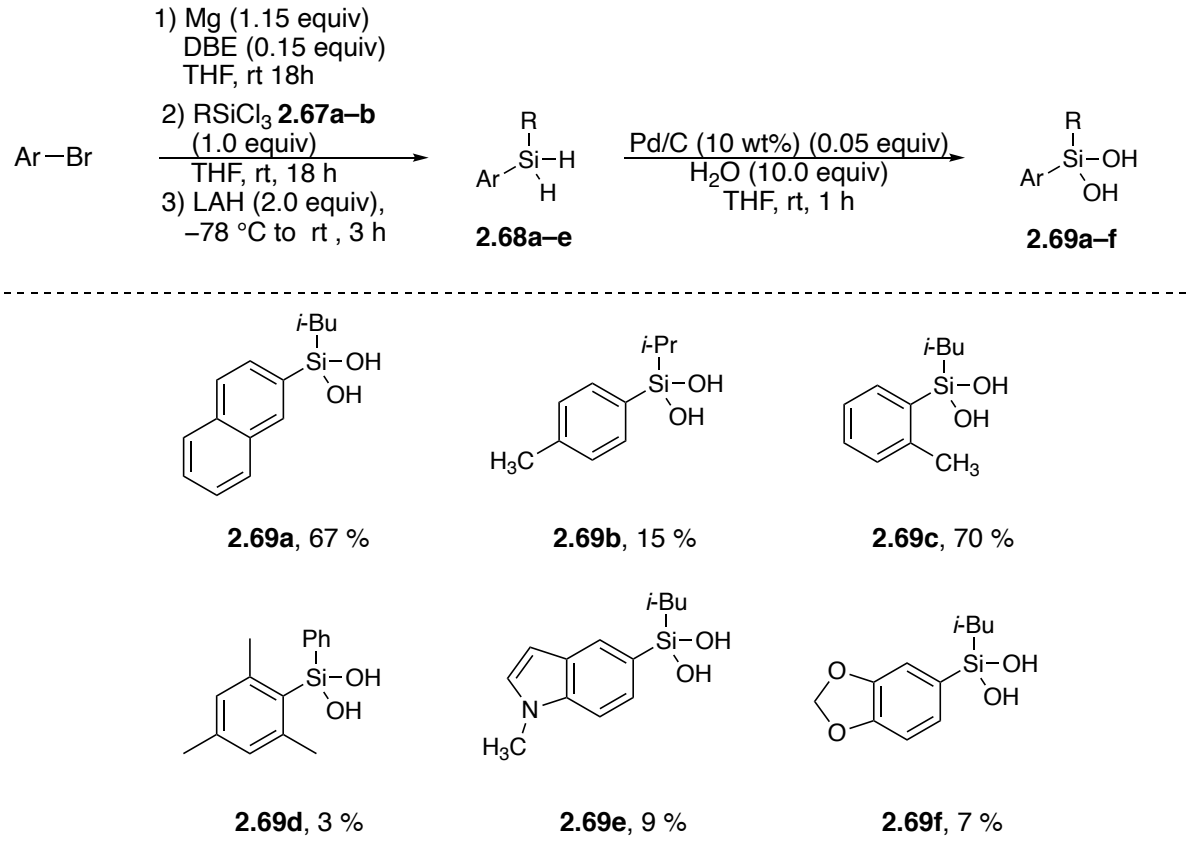

Scheme 2.10 Synthesis of prochiral silanediols **2.69a**–**f**.

2.8 Efforts Toward Substrate Scope Expansion

The synthesis of compounds with aryl variations on the silicon atom was attempted applying nucleophilic substitution reactions (Scheme **2.11**). Starting from Grignard or organolithium reagents and the corresponding trichlorosilanes as electrophiles in THF, followed by reduction with lithium aluminum hydride provided access silanes **2.70a**–**i.** Interestingly, chiral silicon centers have been shown to influence chiroptical materials yielding moderate quantum yields and exceptional emission efficiency.[43,44] Silanes **2.70a**–**c** were of interest for promising potential in OLED technology. Heterocycle-containing silanes **2.70d**–**i** were of interest as novel substrates and utilized in our desymmetrization methodology. If successful, the desymmetrization of the corresponding silanediols of **2.70g**–**h** were potential candidates as chiral ligands for transition metal complexes.

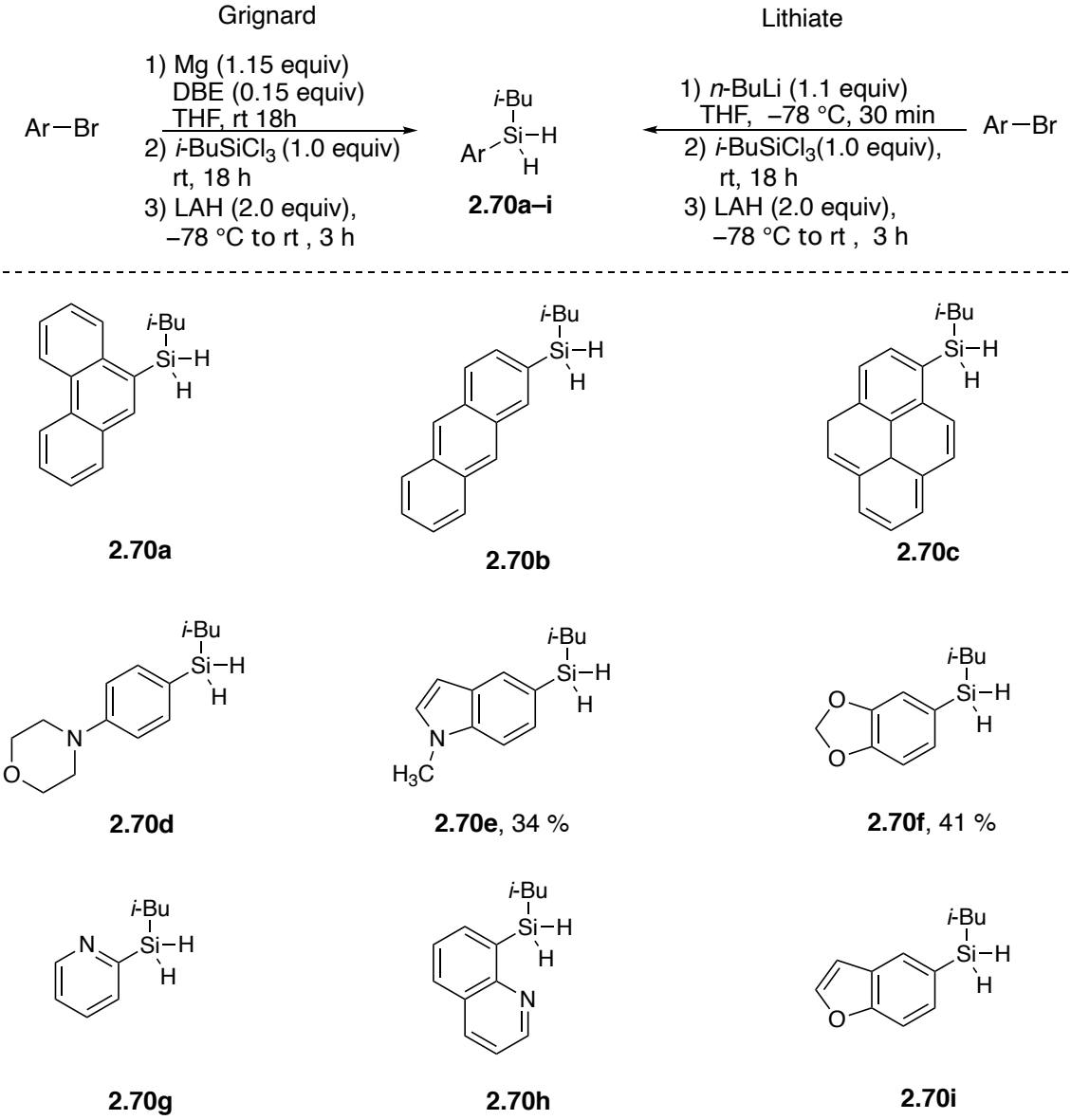

Scheme 2.11 Attempted synthesis of isobutyl-containing silanes **2.70a–i**.

The results of the synthesis of silanes **2.70a–i** are summarized (Table **2.3**). Analyses of the ^{1}H NMR spectra of the unpurified mixtures of **2.70a–c** revealed no silanes peaks present for Grignard and lithiation reactions (Table **2.3**, entry 1–3). For **2.70d**, lithiation resulted in less than 5% conversion (Table **2.3**, entry 4). Silanes **2.70e–f** were accessed using the Grignard method

(Table **2.3**, entry 5–6). Silanes **2.70g–i** were inaccessible from Grignard or lithiation reactions with no visible silane peaks in the ^{1}H NMR spectra of the unpurified mixtures (Table **2.3**, entry 7–9). Silanes **2.70e–f** were upscaled and isolated in acceptable yields (34% and 41%, respectively) and carried forward to the next step.

Table 2.3 Grignard and lithiation results for the synthesis of silanes **2.70a–i**.

entry [a]	silane	Grignard result [b]	Lithiation result [b]
1	**2.70a**	no silane	no silane
2	**2.70b**	no silane	no silane
3	**2.70c**	no silane	no silane
4	**2.70d**	no silane	< 5 % conversion
5	**2.70e**	silane	no silane
6	**2.70f**	silane	no silane
7	**2.70g**	no silane	no silane
8	**2.70h**	no silane	no silane
9	**2.70i**	no silane	no silane

[a]0.5 mmol scale. [b]Observed by ^{1}H NMR spectroscopy.

Silanes **2.70e–f** containing heterocycles and isobutyl groups were synthesized and obtained in acceptable yields and carried forward to Pd/C hydrolysis. A series of conditions were tested for the synthesis of silanediol **2.69e** (Table **2.4**). The initial small scale test reaction at the standard 10 mol% of Pd/C produced **2.69e** in 9% isolated yield (Table **2.4**, entry 1). Encouraged by this initial lead result for a novel compound, a large-scale (5.16 mmol) reaction was attempted, but unsuccessful, resulting in protodesilylation (Table **2.4**, entry 2). Additionally, a small-scale test reaction (0.2 M) was unsuccessful and resulted in protodesilylation (Table **2.4**, entry 3). Protodesilylation was independent of concentration and reaction scale. A stoichiometric loading of Pd/C at 0.73 mmol scale produced **2.69e** in 9% yield (Table **2.4**, entry 4). Attempts to verify this result with 10 mol% of Pd/C at small scales resulted in protodesilylation (Table **2.4**, entry 5–6). When Pd/C was sourced from Strem, the synthesis of **2.69e** was successful and resulted in 8% isolated yield (Table **2.4**, entry 7). To test if the Pd/C source was the contributing factor to protodesilylation, a reaction at a 1.66 mmol scale was investigated using Pd/C sourced

from Sigma-Aldrich (Table **2.4**, entry 8). TLC reaction progress monitoring for a 1.66 mmol scale at 0.2 M (entry 8) resulted in no consumption of starting material after 18 hours. When the temperature was increased to 40 °C for 1 hour, TLC reaction progress monitoring indicated consumption of starting material but resulted in protodesilylation. Pd/C sourced from Strem and was complete at 2 hours (entry 7), a 1.42 mmol scale reaction with Pd/C sourced from Sigma-Aldrich was investigated as a comparison point (Table **2.4**, entry 9). Using conditions with Pd/C from Sigma-Aldrich were unsuccessful and resulted in protodesilylation. From these results, it was concluded that the Pd/C sourced from Sigma-Aldrich from our lab was no longer sufficiently active at catalytic levels. The Pd/C sourced from Strem was observed to perform better at larger scales and was deemed a more reliable reagent.[45]

Table 2.4 Pd/C-catalyzed hydrolysis conditions tested for **2.70e**

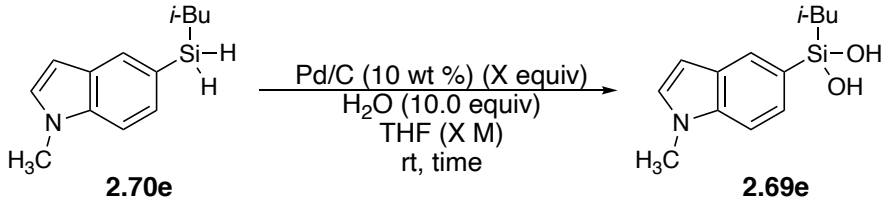

2.70e **2.69e**

entry [a]	scale (mmol)	Pd/C (equiv)	concent. (M)	time (h)	result
1	0.39	0.10	0.1	18	9%
2	5.16	0.10	0.1	18	protodesilylation
3	0.65	0.10	0.2	19	protodesilylation
4	0.73	1.0	0.2	18	9%
5	0.76	0.10	0.2	18	protodesilylation
6	0.61	0.10	0.2	19	protodesilylation
7 [b]	1.99	0.10	0.2	2	8%
8 [c]	1.66	0.10	0.2	18	protodesilylation
9	1.42	0.10	0.2	3	protodesilylation

[a]Franz group Sigma Pd/C bottle utilized. [b] Shaw group Strem Pd/C bottle utilized. [c]Reaction ran at 40 °C for 1 h after TLC reaction progress indicated no consumption of starting material at 18 h; result indicated in entry.

In tandem with the optimization for silanediol **2.70e**, a series of hydrolysis conditions were tested for the synthesis of silanediol **2.69f** (Table **2.5**). A small-scale test reaction verified consumption of starting material and the presence of **2.69f** by ^{1}H NMR analysis (Table **2.5**, entry

1). A scaled-up 4.89 mmol reaction produced **2.69f** in 7% isolated yield (Table **2.5**, entry 2). This result was reproduceable and resulted in 4% isolated yield **(**Table **2.5**, entry 3). At 0.2M, a small-scale test reaction resulted in protodesilylation (Table **2.5**, entry 4). Pd/C sourced from Strem at 1.68 mmol scale at 0.2 M resulted in 13% isolated yield. Pd/C sourced from Sigma-Aldrich at 3.51 mmol resulted in protodesilylation. Silanediol **2.69f** was synthesized with increased yields using Pd/C sourced from Strem.

Table 2.5 Pd/C-catalyzed hydrolysis conditions tested for **2.70f**

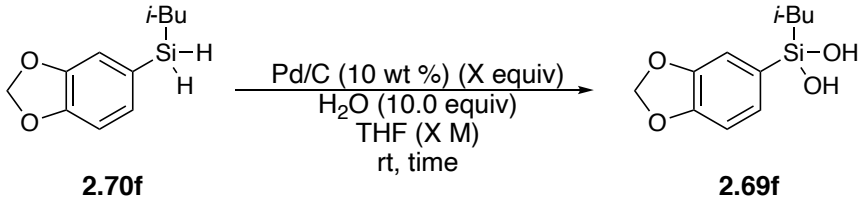

2.70f **2.69f**

entry [a]	scale (mmol)	Pd/C (equiv)	concentration (M)	time (h)	result
1	0.81	0.10	0.1	15	SM consumed
2	4.89	0.10	0.1	21	7%
3	2.72	0.10	0.1	19	4%
4	0.89	0.10	0.2	18	protodesilylation
5[b]	1.68	0.10	0.2	18	13%
6	3.51	0.10	0.2	2	protodesilylation

[a]Franz group Sigma Pd/C bottle utilized. [b] Shaw group Strem Pd/C bottle utilized.

Overall, silanediols with heterocycles and isobutyl groups were synthesized and isolated in low yields with the opportunity for further optimization (Scheme **2.12**). Protodesilylation is a contributing factor in the challenge of synthetic accessibility of these compounds and lended to the understanding that the competing protodesilylation process occurs independent of reaction scale, concentration, or time. Rather, accessibility to silanediols with heterocyclic-isobutyl groups is improved using Pd/C catalysts ideally sourced from Strem.

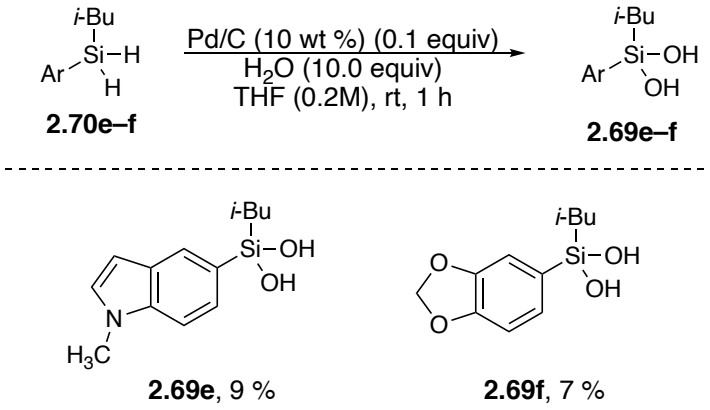

Scheme 2.12 Synthesis of isobutyl-containing silanediols **2.69e–f**.

To avoid protodesilylation seen in previous syntheses, a one-pot synthesis of silanediols was attempted *via* chlorosilanes to access silanediols containing aryl-isopropyl groups **2.71a–g** (Scheme **2.13**). One-pot ammonium bicarbonate syntheses *via* the chlorosilane have previously been utilized for the syntheses of (poly)aromatic substitution patterns at the silicon atom.[46] With the synthetic success of silanes **2.70e–f** using Grignard reagents over lithiations, it was deemed the most reliable starting point for this method. Preparation of aryl-alkyl silanediols **2.71a–g** started from the respective Grignard reagents and the appropriate trichlorosilanes as electrophiles in THF. The corresponding dichlorosilanes formed *in situ* were not isolated. Subsequent addition of NH_4HCO_3 at (2.3 equiv) suppressed residual HCl produced in the formation of dichlorosilanes and prevented possible self-condensation.

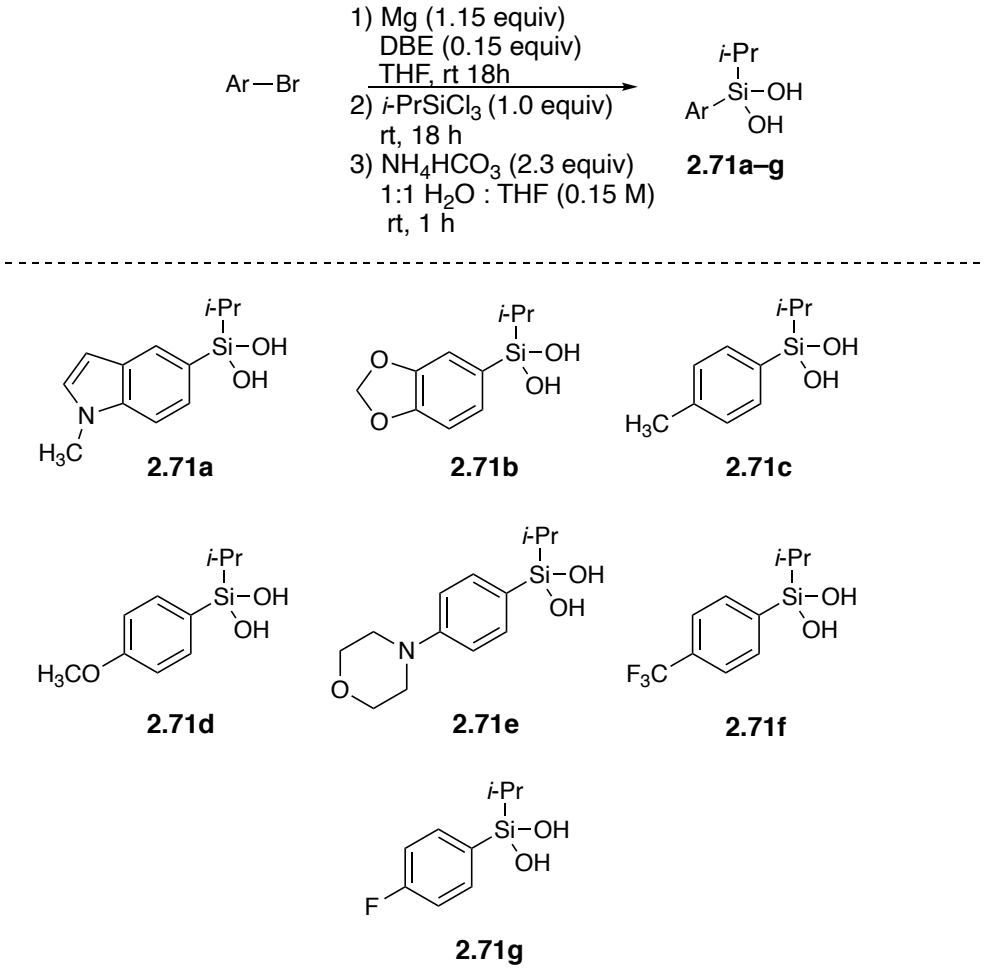

Scheme 2.13. Attempted one-pot ammonium bicarbonate synthesis of **2.71a–g**.

Analysis of ^{1}H NMR spectra of the unpurified mixtures of silanediols **2.71a**–**g** continued to show a trend for protodesilylation (Table **2.6**). Notably, a one-pot procedure to synthesize heterocyclic-containing silanediols **2.71a–b** resulted in protodesilylation. Isopropyl(*p*-tolyl)silanediol **2.71c** produced an unidentifiable side product. Silanediols **2.71d–e** resulted in decomposition. For **2.71d–e**, full consumption of starting material was observed with neither protodesilylation nor condensation products visible using ^{1}H NMR spectroscopy. Silanediols **2.71f–g**, appended with electron-withdrawing groups, resulted in protodesilylation. For the synthesis of aryl-alkyl silanediols the one-pot ammonium bicarbonate method employing *in situ* Grignard formation was not a reliable route to expand substrate scope.

Table 2.6 One-pot ammonium bicarbonate conditions tested for **2.71a–g**.

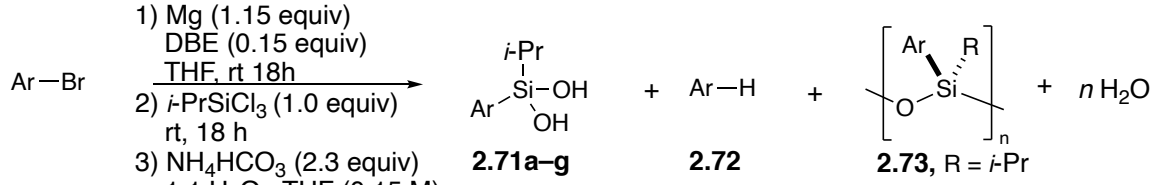

entry	silanediol	scale (mmol)	concentration (M)	**2.71a–g: 2.72: 2.73** [a]
1	**2.71a**	0.75	0.2	0: 1: 0
2	**2.71b**	0.75	0.2	0: 1: 0
3	**2.71c**	0.75	0.2	unidentifiable product
4	**2.71d**	0.75	0.2	decomp
5	**2.71e**	0.75	0.2	decomp
6	**2.71f**	0.75	0.2	0: 1: 0
7	**2.71g**	0.75	0.2	0: 1: 0

[a]Observed via ^{1}H NMR analysis of crude reaction mixture.

With acceptable yields for silanes **2.70e–f** containing heterocyclic-isobutyl groups using the Grignard method, access to isopropyl-containing silanes **2.74a**–**d** was investigated (Scheme **2.14**). Grignard and lithiation methods were utilized for the synthesis of **2.74a–d** results are summarized in Table **2.7.** The analysis of the ^{1}H NMR spectra of the unpurified mixtures for para-substituted phenyl silanes **2.74aa–ad** resulted in no silane peaks present (Table **2.7**, entry 1–4). Interestingly, the Grignard method resulted in ≤5% conversion to silane **2.74b** (Table **2.7**, entry 5). Neither Grignard nor lithiation methods produced silanes **2.74c–d** containing heterocyclic-isopropyl groups (Table **2.7**, entry 6–7). These approaches were unsuccessful for the synthesis of isopropyl containing silanes **2.74a**–**d**.

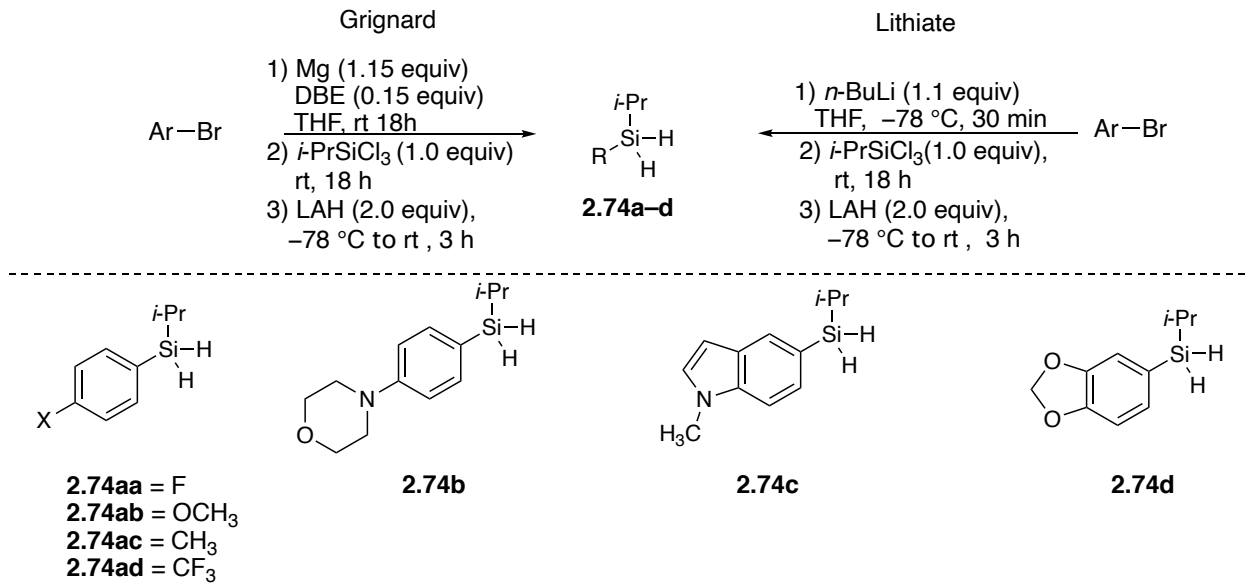

Scheme 2.14 Attempted synthesis of isopropyl-containing silanes **2.74a–d**.

Table 2.7 Grignard and lithiation results for the synthesis of silanes **2.74a–d**.

entry [a]	silane	Grignard result [b]	Lithiation result [b]
1	**2.74aa**	no silane	no silane
2	**2.74ab**	no silane	no silane
3	**2.74ac**	no silane	no silane
4	**2.74ad**	no silane	no silane
5	**2.74b**	≤5 % conversion	no silane
6	**2.74c**	no silane	no silane
7	**2.74d**	no silane	no silane

[a]0.5 mmol scale. [b]Observed by ^{1}H NMR spectroscopy.

To address the possible incomplete formation of Grignard, solutions of arylMgBr purchased from Sigma-Aldrich were investigated and the one-pot ammonium bicarbonate method was revisited (Scheme **2.15**). Method 1 resulted in protodesilylation for **2.75aa**–**ab** upon analysis of the ^{1}H NMR spectra. Surprisingly, method 2 resulted in no formation of **2.74ab**–**ac**. No silane peak was visible in the analysis of the ^{1}H NMR of the unpurified mixtures. Also present in these spectra were unidentifiable products. Since protodesilylation was observed with Method 1, the electrophilicity of isopropyltrichlorosilane is eliminated as the determining factor for the lack of formation of **2.74ab**–**ac**. Methods 1-2 were eliminated as reliable routes for access to isopropyl-containing silanes **2.74ab–ac** and silanediols **2.75aa–ab**.

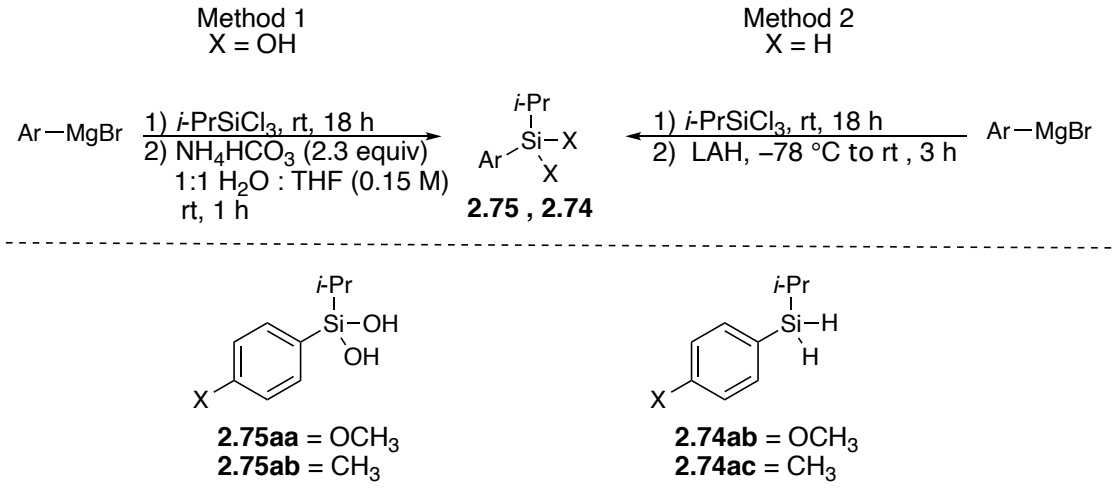

Scheme 2.15 Synthesis of isopropyl-containing silanediols **2.75aa–ab** and silanes **2.74ab–ac** using Grignard solutions.

The alternative strategy to synthesize isopropyl-containing silanes and silanediols utilized *i*-PrMgCl, purchased from Sigma-Aldrich, added directly to aryltrichlorosilanes (Scheme **2.16**). Method 1 investigated a new one-pot method for access to **2.76a–c**. Here, direct hydrolysis of the chlorosilanes to the silanediols was performed using previously reported KOH conditions.[47] **2.76a** resulted in an unidentifiable product, while both **2.77b**–**c** resulted in protodesilylation. Method 2 allowed access to **2.77a**–**c** with silane peaks present in the analysis of the ^{1}H NMR of the unpurified mixtures. Given the volatility of **2.77b**–**c**, the compounds were filtered through a silica plug and concentrated *in vacuo* at a rotovap bath of 33 °C and increased pressure of 190 torr to remove solvent. Silanes **2.77a** was found to be unstable on silica. Silane **2.77b** was presumed to also be unstable on silica and was not isolated. With these results, the synthesis of silanediols via a reliable one-pot method was unsuccessful. Ultimately, Method 2 resulted in a reliable synthesis of isopropyl-containing substrates *via i*-PrMgCl solution.

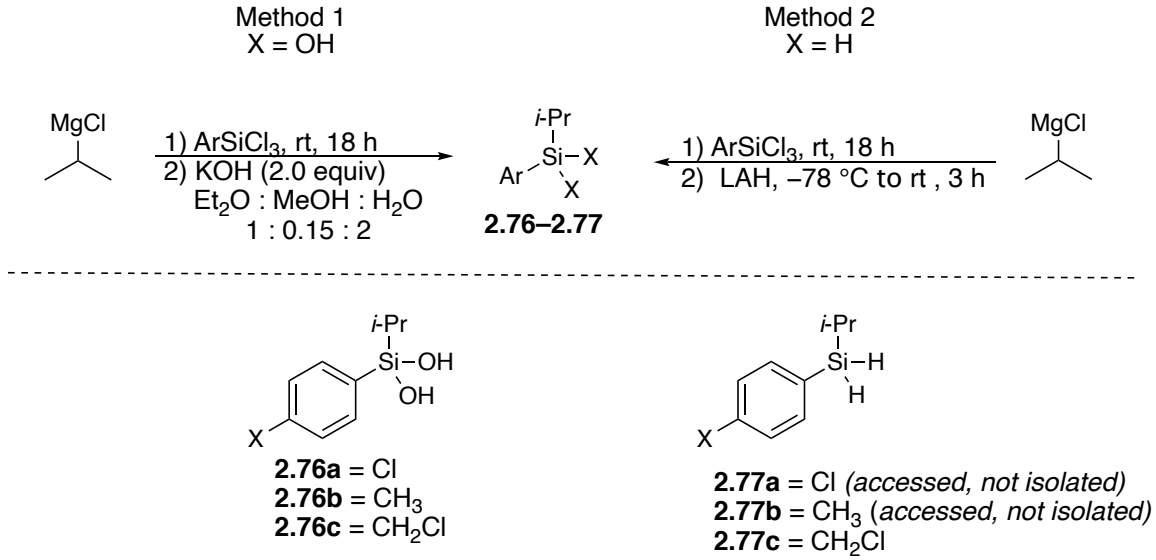

Scheme 2.16 Synthesis of isopropyl-containing substrates with isopropyl magnesium chloride solution for silanediols **2.76a–c** and silanes **2.77a–c**.

Silanes **2.77a**–**b** were carried forward to Pd/C hydrolysis using Pd/C sourced from Strem (Scheme **2.17**). Upon ^{1}H NMR analysis of the crude reaction mixture containing **2.78a** no protodesilylation or self-condensation was observed. With this promising analysis, **2.78a** was carried forward with purification and was unstable on silica**.** The analysis of the ^{1}H NMR of the unpurified mixture for **2.78b** indicated no protodesilylation or self-condensation was observed. **2.78b** was isolated in low yield of 15%. Since no side products were observed *via* analysis of the ^{1}H NMR of the unpurified mixture, the low yield observed for **2.78b** was attributed to partial instability on silica.

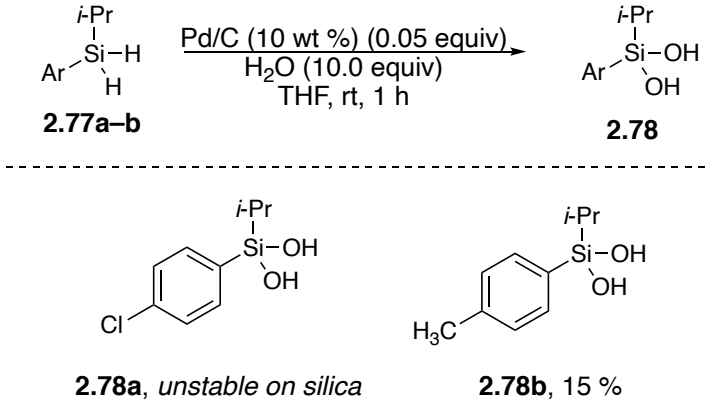

Scheme 2.17 Synthesis of isopropyl-containing silanediols **2.78a–b**.

To verify the reproducibility of the synthesis of **2.78b**, conditions were tested with Pd/C sourced from Strem (Table **2.8**). The initial small scale test reaction using the standard 5 mol% of Pd/C produced **2.78b** with no protodesilylation or condensation products present *via* the ^{1}H NMR analysis of the crude reaction mixture (Table **2.8**, entry 1). Reactions performed at a larger scale with varying concentrations also resulted in formation of **2.78b** with no protodesilylation or condensation products present in the ^{1}H NMR analysis of the crude reaction mixtures (Table **2.8**, entry 2–3). A large-scale reaction resulted in 14% isolated yield (Table **2.8**, entry 4). The low yield of **2.78b** was once again attributed to partial instability on silica with no side products observed *via* analysis of the ^{1}H NMR of the unpurified mixture.

Table 2.8 Pd/C-catalyzed hydrolysis conditions tested for **2.78b**

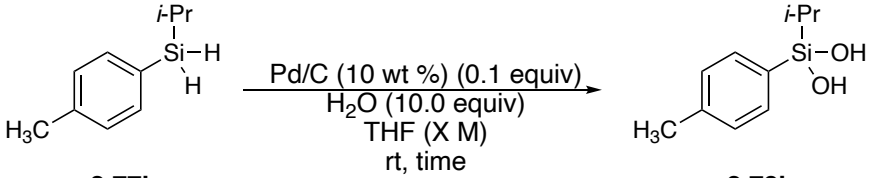

entry [a]	scale (mmol)	concentration (M)	time (h)	result
1 [b]	0.65	0.2	1	SM consumed; **2.78b** present
2	1.0	0.2	1	SM consumed; **2.78b** present
3	2.0	0.1	3	SM consumed; **2.78b** present
4	5.0	0.2	2	14%

[a]Shaw group Strem Pd/C bottle utilized. [b] Reaction ran with Pd/C (0.5 equiv)

Silanediols **2.69e–f** containing heterocyclic-isobutyl groups were subjected to the racemic desymmetrization reaction (Scheme **2.18**). The low yields of **2.69e–f** (9% and 7%, respectively) indicated not much material was available for the enantioselective reaction. The racemic reaction using stoichiometric amounts of *N*-methylimidazole **2.79** was deemed a feasible starting point. Chlorosilane **2.37a** was selected as the reaction partner for the desymmetrization of **2.69e–f**. Chlorosilane **2.37a** was used in the optimization of the desymmetrization of lead substrate isobutyl(naphthalen-1-yl)silanediol **2.36a** and was hypothesized to have similar reactivity with the heterocyclic-isobutyl groups present in **2.69e–f**. The desymmetrization of **2.69e** resulted in product degradation with full consumption of starting material. Notably, the desymmetrization of **2.69e** did not result in the bis-silylated product **2.81**. The desymmetrization of **2.69f** resulted in no product with unreacted starting material. Given the synthetic inaccessibility of **2.69e–f** and their performance in the desymmetrization reaction, **2.69e–f** was abandoned as viable substrates for continued exploration.

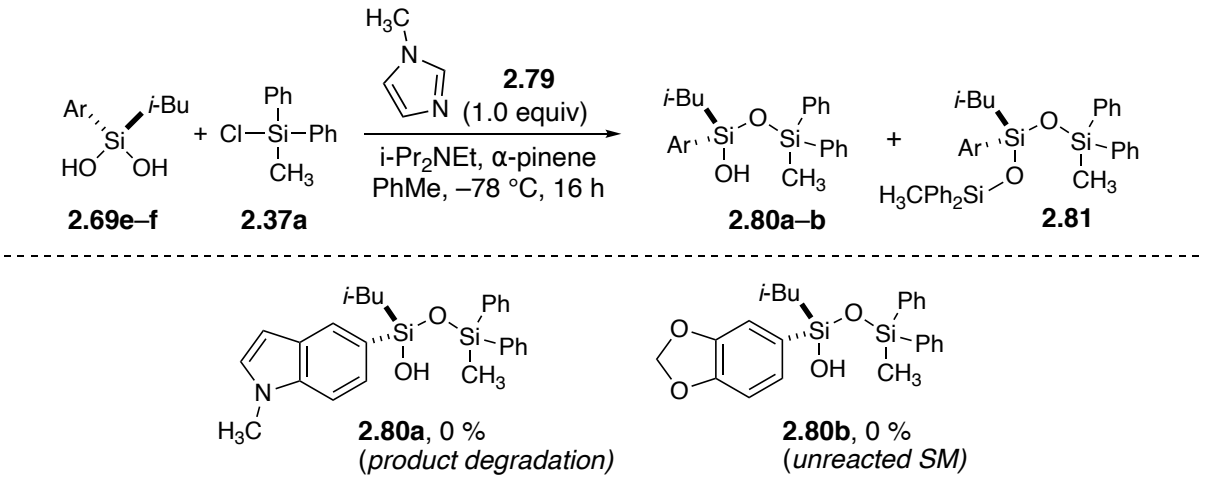

Scheme 2.18 Racemic desymmetrization of lead heterocycle-containing prochiral silanediols **2.69e**–**f**.

The desymmetrization of isopropyl(phenyl)silanediol to produce **2.38dc** in moderate yield and excellent selectivity (49%, 98:2 er) guided the desymmetrization of **2.78b** (Scheme **2.19**). Chlorosilane **2.37d** was utilized in the desymmetrization of isopropyl(phenyl)silanediol

and was hypothesized to have similar reactivity with **2.78b**. The ^{1}H NMR analysis of the unpurified mixture for the desymmetrization of **2.78b** indicated product present with no bis-silylated product. However, upon purification, the reaction mixture for **2.82** was observed to be an inseparable mixture with some product. Given the low yields for **2.78b** and the subsequent desymmetrization results, **2.78b** was no longer pursued as a substrate of interest. However, the desymmetrization of **2.78b** with standard chlorosilane **2.37a** can still be an opportunity for **2.78b** to be explored as a substrate of interest.

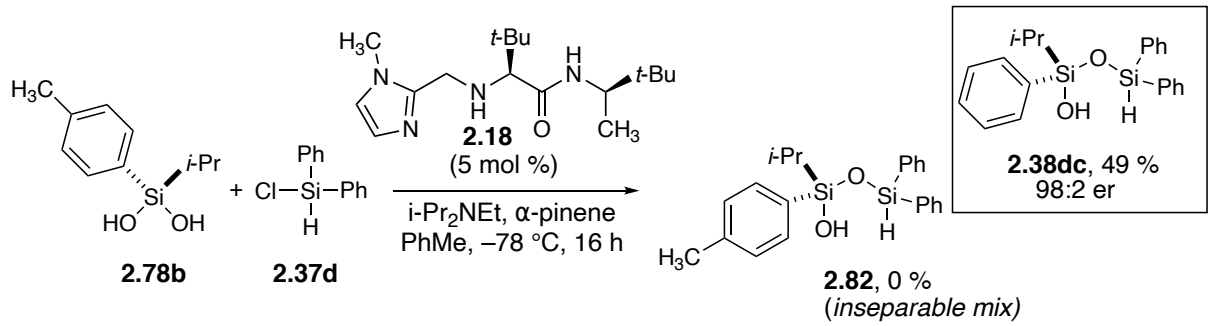

Scheme 2.19 Desymmetrization of isopropyl containing silanediol **2.78b**.

2.9 Discussion of Substrate Scope Expansion

Building on lessons learned from all unsuccessful experiments, the final route to silanediols decorated with isopropyl and isobutyl groups was established (Figure **2.6**). To incorporate isopropyl groups successfully, *i*-PrMgCl solution outcompeted aryl-MgBr solutions and was the best strategy. This method was both time and cost effective. Additionally, the challenges encountered with moisture-sensitive Grignard formations was avoided. To incorporate isobutyl groups, the Grignard method followed by Pd/C-catalyzed hydrolysis was successful over lithiation. One-pot methods using NH_4HCO_3 (or KOH with specific examples) were unsuccessful. My experiments showcased the synthetic accessibility of aryl-alkyl silanediols and serve as a foundation for future studies.

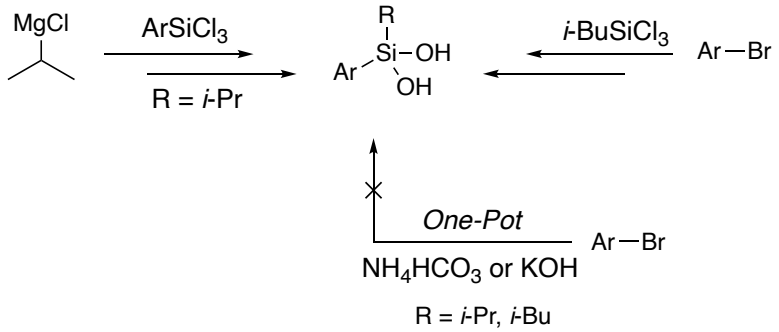

Figure 2.6 Summary of access to silanediols containing isopropyl and isobutyl groups.

2.10 ^{1}H NMR Binding Studies of Catalyst 2.18 with Silanediols 2.83-2.86

^{1}H NMR binding studies were performed as a collaborative effort with Jacob J. Dalton, Ph.D. and were utilized to further understand the hydrogen-bonding interactions between the silanediols and organocatalyst. NMR titration studies were performed to verify the interactions in the solid-state co-crystal are also present in solution. The binding affinities (K_a) were expected to range from low ($K_a \approx 30$) to high ($K_a \approx 200$).[48] ^{1}H NMR titration experiments in C_6D_6 were performed with 10 equivalents of **2.83** in the presence of organocatalyst **2.18**. Dr. Austin T. Kelly began the initial reaction discovery of the desymmetrization project in the Franz Lab with **2.83**, so this substrate was selected for a binding study for this reason. A downfield amide chemical shift of $\Delta\delta^{NH} = 0.53$ ppm was observed. Upfield chemical shifts were seen for the imidazole protons, $\Delta\delta^{Ha} = 0.43$ ppm and $\Delta\delta^{Hb} = 0.69$ ppm, consistent with a hydrogen-bond interaction (Figure **2.7** A).[49] The binding constant (K_a) was calculated for the imidazole C-H^b peak to be $K_a = 90 \pm 3$ indicative of a slightly weak interaction.

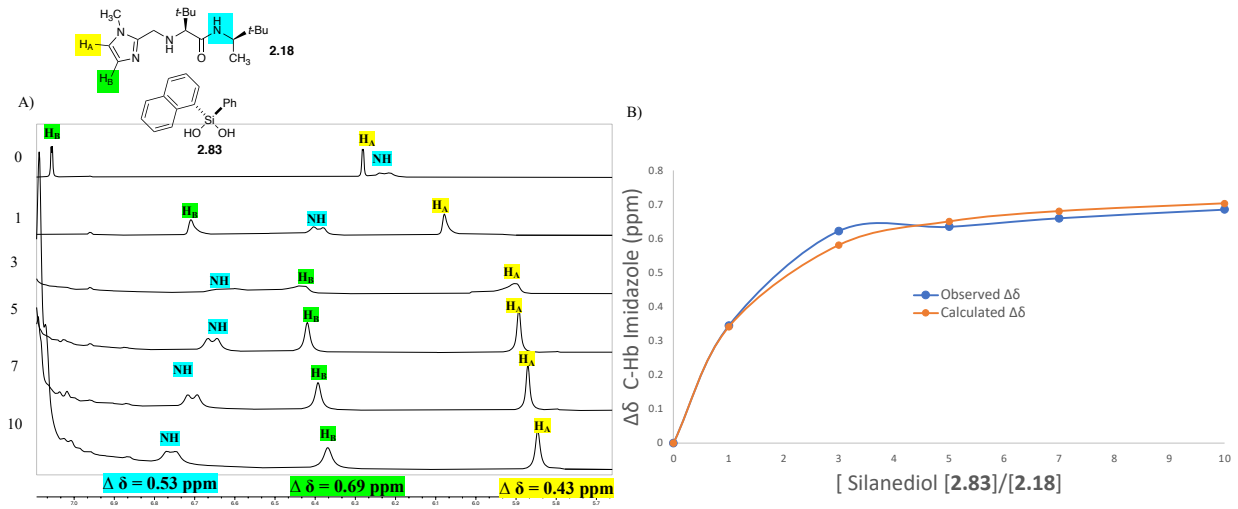

Figure 2.7 A) ^{1}H NMR binding study of chiral imidazole **2.18** (2 mM inC_6D_6) in the presence of silanediol **2.83** at 0 = 0 equiv, 1 = 1 equiv, 3 = 3 equiv, 5 = 5 equiv, 7 = 7 equiv, 10 = 10 equiv. Δδ = 0.69 ppm is observed for the C-H^{b} peak in the presence of 10 equivalents of **2.83**. b) Binding constant was calculated using ^{1}H NMR titration data for the imidazole C-H^{b} peak; $K_a = 90 \pm 3$.

To explore the effect of *ortho* substitution on the binding interaction, isobutyl(*o*-tolyl)silanediol **2.84** was selected. When 10 equivalents of **2.84** were titrated in the presence of organocatalyst **2.18**, a downfield amide chemical shift of $\Delta\delta^{NH} = 0.47$ ppm was observed. Upfield chemical shifts were continued to be seen for the imidazole protons, $\Delta\delta^{Ha} = 0.23$ ppm and $\Delta\delta^{Hb} = 0.38$ ppm (Figure **2.8**A). From the ^{1}H NMR data, the binding constant using imidazole C-H^{b} peak was calculated to be $K_a = 151 \pm 2$ indicative of a strong interaction (Figure **2.8**B).[49]

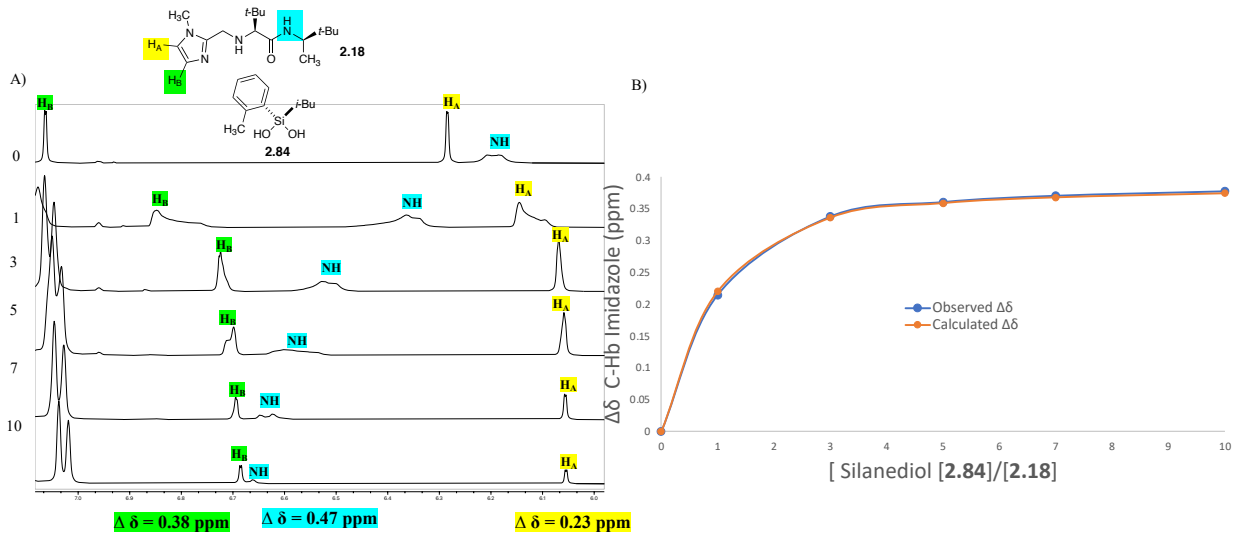

Figure 2.8 A) ^{1}H NMR binding study of chiral imidazole **2.18** (2 mM inC_6D_6) in the presence of silanediol **2.84** at 0 = 0 equiv, 1 = 1 equiv, 3 = 3 equiv, 5 = 5 equiv, 7 = 7 equiv, 10 = 10 equiv. Δδ = 0.38 ppm is observed for the C-H^{b} peak in the presence of 10 equivalents of **2.84**. b) Binding constant was calculated using ^{1}H NMR titration data for the imidazole C-H^{b} peak; K_a = 151 ± 2.

The desymmetrization of prochiral silanediols investigated He and Oestreich groups[29,30] saw great performance with *tert*-butyl(phenyl)silanediol **2.85**, and thus was chosen as a valuable binding partner to probe the interactions in our reaction. This substrate was investigated by Jacob J. Dalton, Ph.D. (Figure **2.9**). When organocatalyst **2.18** was titrated with 10 equivalents of silanediol **2.85**, a downfield amide chemical shift of $\Delta\delta^{NH}$ = 0.21 ppm was observed. Similar to the results observed for previous silanediols, upfield chemical shifts were seen for the imidazole protons, $\Delta\delta^{Ha}$ = 0.23 ppm and $\Delta\delta^{Hb}$ = 0.29 ppm (Figure **2.9**A). The binding constant using imidazole C-H^{b} peak was calculated to be K_a = 35 ± 1 indicative of a very weak interaction (Figure **2.9**B). The NMR shifts and low binding constant was the lowest seen of all silanediols investigated.

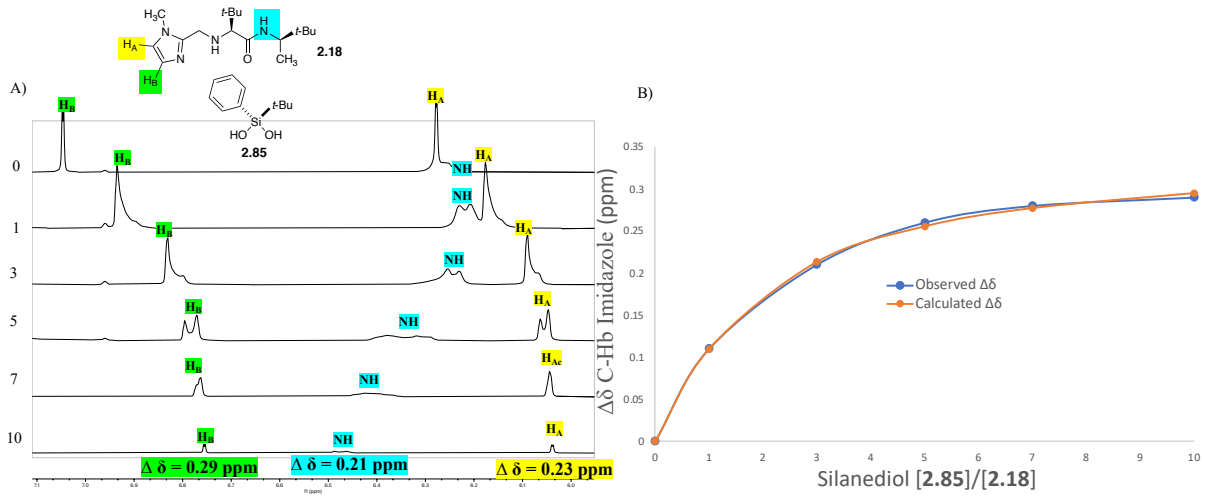

Figure 2.9. Data collected by Jacob J. Dalton, Ph.D. a) ^{1}H NMR binding study of chiral imidazole **2.18** (2 mM in C_6D_6) in the presence of silanediol **2.85** at 0 = 0 equiv, 1 = 1 equiv, 3 = 3 equiv, 5 = 5 equiv, 7 = 7 equiv, 10 = 10 equiv. $\Delta\delta$ = 0.29 ppm is observed for the C-H^b peak in the presence of 10 equivalents of **2.85**. b) Binding constant was calculated using ^{1}H NMR titration data for the C-H^b peak; K_a = 35 ± 1.

The desymmetrization reaction was optimized with isobutyl(naphthalen-1-yl)silanediol **2.86** as the lead substrate based on relative synthetic accessibility. Silanediol **2.86** was hypothesized to have the strongest binding interaction and was investigated in a binding study performed by Jacob J. Dalton, Ph.D. (Figure **2.10**). In the presence of 10 equivalents of **2.86**, **2.18** exhibited a downfield amide chemical shift of $\Delta\delta^{NH}$ = 0.37 ppm. Similar to the results observed for previous silanediols, upfield chemical shifts were seen for the imidazole protons, $\Delta\delta^{Ha}$ = 0.42 ppm and $\Delta\delta^{Hb}$ = 0.55 ppm (Figure **2.10**A). From the ^{1}H NMR data, a binding constant of K_a = 191 ± 25 was calculated for the imidazole C-H^b peak indicative of the strongest binding interaction (Figure **2.10**B).

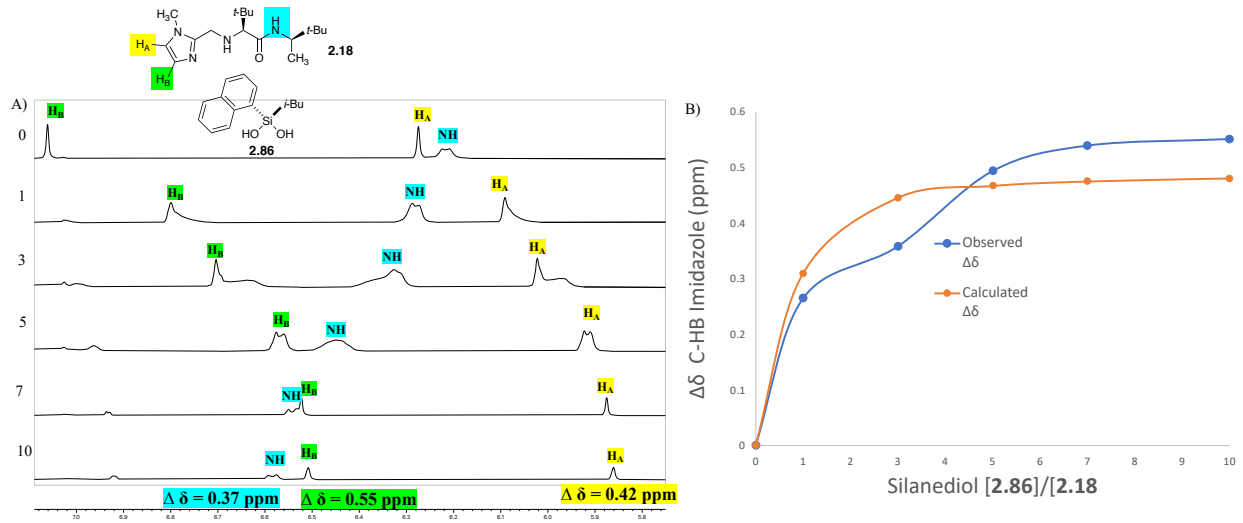

Figure 2.10 performed by Jacob J. Dalton, Ph.D. a) ^{1}H NMR binding study of chiral imidazole **2.18** (2 mM in C_6D_6) in the presence of silanediol **2.86** at 0 = 0 equiv, 1 = 1 equiv, 3 = 3 equiv, 5 = 5 equiv, 7 = 7 equiv, 10 = 10 equiv. $\Delta\delta$ = 0.55 ppm is observed for the C-H^b peak in the presence of 10 equivalents of **2.86**. b) Binding constant was calculated using ^{1}H NMR titration data for the C-H^b peak; K_a = 191 ± 25.

2.11 Discussion of ^{1}H NMR Binding Studies

After quantifying the ability of silanediols **2.83**–**2.86** to bind **2.38**, it was determined the ^{1}H NMR binding data exhibited trends in binding affinities that correlate to structural features (Table **2.9**). Diaryl silanediol **2.83** was the second weakest to bind the catalyst but exhibited the largest chemical shifts for the imidazole protons. In contrast, aryl-alkyl silanediols **2.84**–**2.86** exhibited lower chemical shifts for all protons monitored. Specifically, silanediol **2.84**, chosen to study ortho substitution, exhibited the second to lowest imidazole chemical shift for C-H^b resulting in a strong binding constant of 151 ± 2. This trend is attributed to decreased steric bulk that allows for a better binding interaction not seen with diaryl silanediol **2.83**. Silanediol **2.85** exhibited the lowest chemical shifts of all protons monitored; this resulted in the lowest binding constant of 35 ± 1. These trends implied the bulkiness of the *tert*-butyl group interfered with binding. Lastly, silanediol **2.86** exhibited the second largest chemical shift for the imidazole C-H^b proton and

resulted in a binding constant of 191 ± 25. This value was indicative of a very strong binding interaction as we had expected. These data suggested that aryl-alkyl silanediols can bind relatively strongly to organocatalyst **2.18** depending on the rate of saturation which can affect the chemical shifts of the protons.

Table 2.9 Summary of binding data with **2.38** host and **2.36a**, **2.40**, **2.84**–**2.85** guests.

Host	Guest	NH (amide) Δδ (ppm)	H_b (imidazole) Δδ (ppm)	H_a (imidazole) Δδ (ppm)	K_a (M^{-1}) [a]
2.38	**2.83**	0.53	−0.69	−0.43	90 ± 3
2.38	**2.84**	0.47	−0.38	−0.23	151 ± 2
2.38	**2.85**	0.21	−0.29	−0.23	35 ± 1
2.38	**2.86**	0.37	−0.55	−0.42	191 ± 25

[a] K_a calculated using Δδ for imidazole peak H_b.

To visualize the correlation between binding affinities (K_a) and enantioselectivity of the desymmetrization reaction, the siloxanol product ee was plotted as a function of silanediol binding affinity (K_a) with organocatalyst **2.18** (Figure **2.11**). The graph illustrated a strong correlation (R^2 = 0.997) between binding affinity and enantioenrichment based on the initial substrates evaluate. An additional data point with isobutyl(phenyl)silanediol was collected (K_a = 74 ± 3) and did not match the predicted enantioselectivity. The structure of the silanediols, specifically the substitution patterns around silicon, greatly influenced the formation of a strong hydrogen-bonding complex; ostensibly, this is strongly correlated to the observed enantioselectivity. Overall, the selectivity of the desymmetrization reaction was also dependent on the steric interactions between silanediols and the organocatalyst.

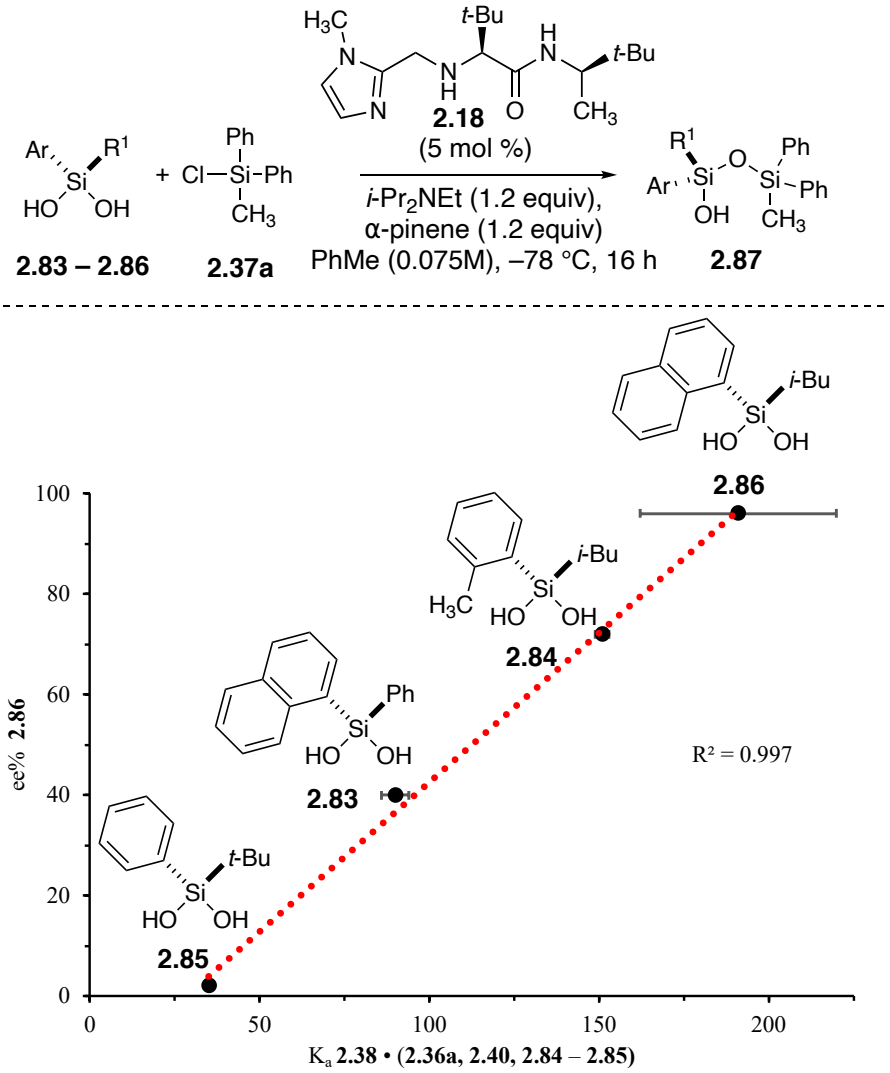

Figure 2.11 Siloxanols **2.87** ee% as a function of **2.18** binding with silanediols **2.83**–**2.86**.

2.12 Conclusion

To conclude, this chapter highlights my contributions to the organocatalytic asymmetric synthesis of Si-stereogenic siloxanols. Specifically, organocatalyst analogs were designed, synthesized, and evaluated in the desymmetrization reaction which demonstrated that the imidazole was crucial to promote silylation. Silanediols were accessed through a two-step synthesis. Two key challenges were possible for successful access to silanediols: 1) proto-

desilylation and 2) the possible self-condensation to produce **2.89** (Figure **2.12A**). Access to silanediols with isopropyl and isobutyl groups was most reliable through Grignard additions to chlorosilanes followed by subsequent Pd/C hydrolysis (Figure **2.12B**). It was hypothesized that the Grignard formation for access to aryl-isopropyl silanes was unreliable. Therefore, silanes with aryl-isopropyl substituents were successfully synthesized using *i*-PrMgCl solution. Protodesilylation of silanediol **2.78b** was partially prevented with the use of Pd/C sourced from Strem Chemicals. The synthesis of **2.78b** using Pd/C sourced from Sigma-Aldrich resulted in higher instances of protodesilylation. Steric bulk around the silicon center fully prevented self-condensation for all aryl-isobutyl silanediols synthesized. Heterocycle-containing silanediols **2.69e–f** were showcased as novel substrates for the desymmetrization reaction and serve as important design features for future scope. Overall, Pd sourced from Strem chemicals prevented protodesilylation for all silanediols.

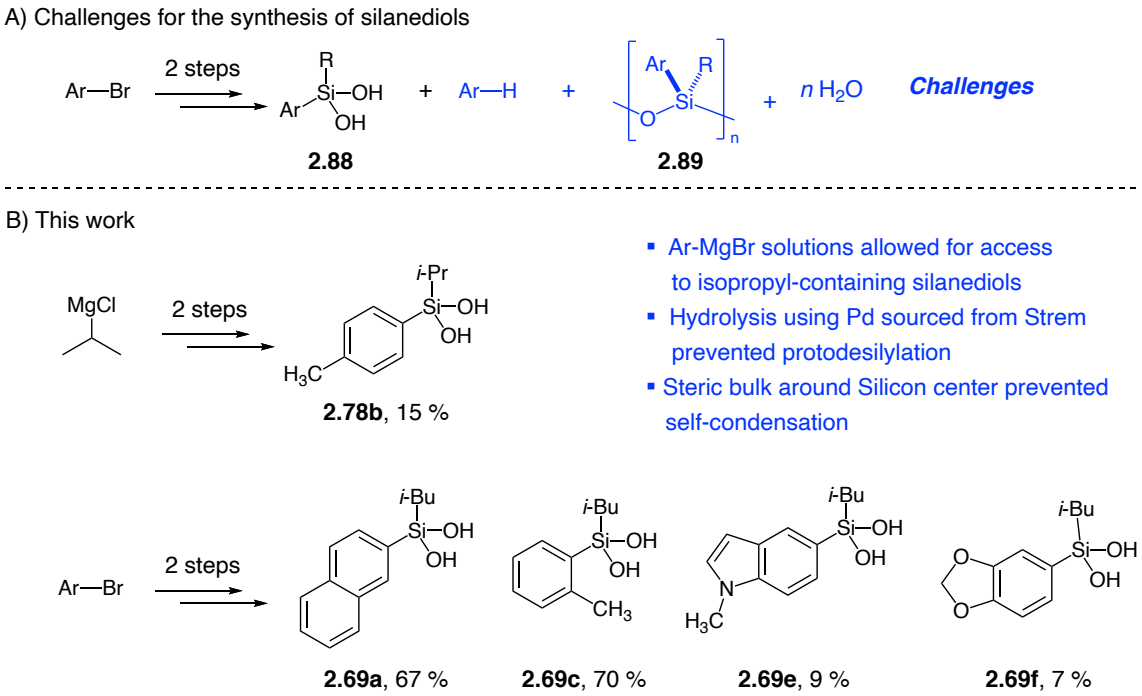

Figure 2.12 A) Challenges for the synthesis of silanediols. B) Key strategies to address challenges for the synthesis of silanediols.

The importance of the hydrogen-bonding interactions present in the solid state were verified using ^{1}H NMR binding studies. From these results, a correlation of binding affinities and enantioselectivity of the desymmetrization reaction was determined. Herein was presented the first Lewis base-catalyzed silylation of prochiral silanediols. This work reported the H-bonding activation method was highly influenced by secondary alkyl groups (i.e., isobutyl and isopropyl). Silanediols with steric bulk and isobutyl groups are expected to result in the highly enantioselective substrates for the desymmetrization reaction.

2.13 Experimental Procedures

General Information

Synthesis, Purification, and Analysis: Dry THF, Et_2O and PhMe were dispensed from a solvent purification system that passes solvent through two columns of dry neutral alumina prior to use. All other reagents, unless otherwise noted were purchased from commercial sources. Chlorosilanes were purchased from Gelest; magnesium turnings, dibromoethane, diisopropylethylamine, HCl•dioxane, aryl bromides, 4 Å spherical molecular sieves were purchased from Sigma-Aldrich; *N*-methylimidazole (Sure/Seal bottles) was purchased from Sigma-Aldrich. α-Pinene was purchased from Acros and used without purification. All deuterated solvents were dried under 4 Å spherical molecular sieves for at least 24 hours prior to use in binding and dilution studies. Boc-*tert*-leucine was purchased from Chem Impex. Pd/C (10 wt%, dry support) used for the synthesis of prochiral silanediols was purchased from Strem; 4.0 M solution of lithium aluminum hydride in THF was purchased from Fisher Chemicals.
All reactions were performed in flame-dried and argon-purged glassware. Reactions were analyzed by thin layer chromatography (TLC) on EMD glass plates that were pre-coated with

silica gel 60 F254. The reactions were purified by column chromatography using Acros silica gel 60 Å (0.035–0.070 mm).

Nuclear magnetic resonance (NMR) spectra obtained on Bruker Avance III equipped with Bruker CPTCI Cryoprobe (800 MHz for ^{1}H, 200 MHz for ^{13}C), 600 MHz Bruker Avance III equipped with Bruker CPTCI Cryoprobe (600 MHz for ^{1}H, 151 for ^{13}C), Bruker Avance IIIHD Nanobay Spectrometer(400 MHz for ^{1}H; 101 MHz for ^{13}C; 376, 79 MHz for ^{29}Si), 300 MHz Bruker Avance-NEO Spectrometer (300 MHz for ^{1}H; 76 MHz for ^{13}C), and/or Varian VNMRS (600 MHz for ^{1}H; 151 MHz for ^{13}C). The ^{1}H spectral data are reported as follows: chemical shifts were reported in parts per million downfield from tetramethylsilane internal standard on the δ scale, multiplicity (s, singlet; d, doublet; t, triplet; q, quartet; m, multiplet; dd, doublet of doublets and br, broadened), coupling constant (Hz), and integration. Apparent signals are indicated and are used when signals with multiple couplings appear to form a certain peak type. Carbon NMR chemical shifts are reported in ppm from tetramethylsilane (TMS at 0.0 ppm) with solvent reference employed as the internal standard (deuterochloroform ($CDCl_3$) at. 77.2 ppm or deuterobenzene (C_6D_6) at 128.06 ppm). High-resolution mass spectra (HRMS) were acquired on Thermo Fischer Scientific Electron LTQ-Orbitrap XL Hybrid mass spectrometer on positive ESI mode. High performance liquid chromatography (HPLC) data were obtained on Shimadzu LC-20AB system with CHIRALPAK® AD-H column (4.6 x 250 mm, 5 μm), CHIRALPAK® OD-H column (4.6 x 250 mm, 5 μm) or CHIRALPAK® AS column (4.6 x 250 mm, 5 μm) and Shimadzu SPD-M20A photodiode array detector. Each HPLC sample was eluted at a constant flow rate with isocratic hexanes/isopropanol system and 40 or 30 °C column oven temperature. Nestlab CB 80 Cryocool was utilized to maintain reaction temperature for the desymmetrization reactions which required cryogenic temperatures for 16 h.

General Procedure

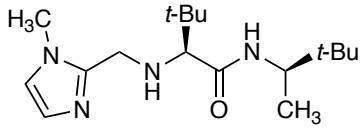

(*S*)-*N*-((*R*)-3,3-dimethylbutan-2-yl)-3,3-dimethyl-2-(((1-methyl-1*H*-imidazol-2-yl)methyl)amino)butanamide (2.18)

Compound **2.38** was synthesized according to literature procedure and found to match NMR signals of previously reported compounds.[20]

^{1}H NMR (600 MHz, $CDCl_3$) δ 6.94 (d, *J* = 1.0 Hz, 1H), 6.82 (d, *J* = 1.0 Hz, 1H), 6.56 (d, *J* = 9.6 Hz, 1H), 3.92 (dq, *J* = 9.8, 6.8 Hz, 1H), 3.80 (d, *J* = 14.0 Hz, 1H), 3.63 (s, 3H), 3.62 (dd obscured, 1H), 2.69 (s, 1H), 1.77 (s, br, 1H), 1.07 (d, *J* = 6.8 Hz, 3H), 0.97 (s, 9H), 0.93 (s, 9H).

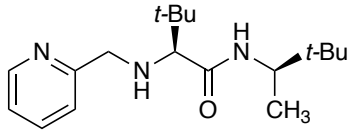

(*S*)-*N*-((*R*)-3,3-dimethylbutan-2-yl)-3,3-dimethyl-2-((pyridin-2-ylmethyl)amino)butanamide (2.44)

Compound **2.44** was synthesized by adapting the previously reported synthesis of **2.18**.[20] A flame-dried round-bottom flask was charged with a stir bar followed by (*S*)-2-amino-*N*-((*R*)-3,3-dimethylbutan-2-yl)-3,3-dimethylbutanamide (0.62g, 4.72 mmol, 1.0 equiv) which was synthesized over 2 steps and carried forward without purification. Then $MgSO_4$ (0.57g, 4.72 mmol, 1.0 equiv), CH_2Cl_2 (2.4 mL) followed by 2-pyridinecarboxaldehyde (0.45 mL, 4.72 mmol, 1.0 equiv) were added. The reaction was stirred at room temperature (23 °C) for 18 h. The reaction mixture was filtered and concentrated *in vacuo* to yield an orange oil. The oil was then dissolved in MeOH (2 mL) followed by addition of $NaBH_4$ (0.54 g, 14.16 mmol, 3.0 equiv), and

concentrated HCl (9.50 μL, 0.31 mmol, 0.07 equiv). The reaction mixture was stirred at 0 °C for 5 min then at room temperature for 1.5 h. The reaction mixture was quenched with 5 mL $NaHCO_3$ (5mL). The resulting mixture was washed with CH_2Cl_2 (3 x 10 mL) and brine (1 x 10 mL) and then dried over $MgSO_4$ and concentrated *in vacuo*. The reaction mixture was purified using flash column chromatography (SiO_2, hexanes/EtOAc, 98:2 DCM/MeOH to 96:4:0.2 DCM/MeOH/ TEA *v/v*) to yield corresponding catalyst as a brown oil (0.14 g, 9% over 4 steps).

^{1}H NMR (400 MHz, $CDCl_3$) δ 8.56 (ddd, *J* = 4.9, 1.8, 0.9 Hz, 1H), 7.63 (dd, *J* = 7.7, 1.8 Hz, 1H), 7.19 (m, 2H), 3.89 (m, 1H), 3.85 (d, *J* = 13.7 Hz, 2H), 3.66 (d, *J* = 14.1 Hz, 1H), 2.80 (s, 1H), 1.06 (d, *J* = 6.7 Hz, 4H), 1.01 (s, 10H), 0.91 (s, 9H). ^{13}C NMR (100 MHz, CDCl3) δ 171.9, 136.7, 122.6, 122.4, 72.6, 53.9, 53.2, 34.1, 33.9, 27.5, 26.6, 16.4. HRMS (ESI) m/z: calc for $C_{18}H_{32}N_3O$ $[M + H]^+$ 306.2540, found 306.2547.

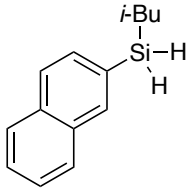

isobutyl(naphthalen-2-yl)silane (2.68a)

To a 250-mL round-bottom flask were added magnesium turnings (0.42 g, 17.3 mmol, 1.15 equiv) and flame-dried under high vacuum (< 2 torr) and allowed to cool to room temperature. Once the flask was cooled to room temperature, it was purged three times with argon. THF (0.2 M) and 1,2-dibromoethane (2.25 mmol, 0.2 mL, 0.15 equiv) were then added. The reaction mixture temperature (23 °C) for 18 h or until the reaction mixture was a pitch-black color, which is indicative of activated magnesium turnings. Note: In some cases, an off-gray color is also indicative of proper activation of magnesium turnings. Then 2-bromonaphthalene (3.11 g, 15.0

mmol, 1.0 equiv) was added and left to stir at room temperature (23 °C) for 5-6 h followed by fast addition of isobutyltrichlorosilane (2.49 mL, 15.0 mmol, 1.0 equiv). Note: 5-6 hours is the optimal time range to allow for Grignard formation; 1-4 hours and ≥ 6 hours this will result in lower yields. Upon addition of isobutyltrichlorosilane a yellow color is a good indicator that the reaction is proceeding accordingly. The reaction was left to stir at room temperature (23 °C) for 18 h. The reaction mixture was then cooled to –78 °C and lithium aluminum hydride (4.0 M, 7.5 mL, 2.0 equiv) was added dropwise. The solution was then allowed to cool to room temperature (23 °C) over 3 h. The solution was quenched with Rochelle salt (8 mL) and filtered through Celite. The aqueous phase was extracted with diethyl ether (3 × 25 mL). The combined organic phase was dried over $MgSO_4$, filtered, and concentrated *in vacuo*. The reaction mixture was purified using bulb-to-bulb distillation, followed by sublimation (80 °C at 1 atm) to yield **2.68a** as a clear oil (1.74 g, 54%)

^{1}H NMR (400 MHz, $CDCl_3$) δ 8.13 (s, 1H), 7.90 – 7.82 (m, 3H), 7.55 – 7.48 (dd, J = 8.1, 1.2 Hz, 1H), 7.52 (m, 2H), 4.47 (m, J = 3.9 Hz, 2H), 1.92 (m, 1H), 1.09 – 1.01 (m, 8H).^{13}C NMR (101 MHz, $CDCl_3$) δ 136.33, 134.00, 133.13, 131.20, 130.58, 128.11, 127.91, 127.31, 126.70, 126.19, 25.82, 25.65, 20.72. ^{29}Si NMR (79 MHz, $CDCl_3$, $Cr(acac)_3$) δ –33.30.

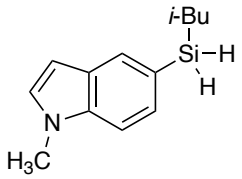

5-(isobutylsilyl)-1-methyl-1*H*-indole (2.68e)

To a 250-mL round bottom flask were added magnesium turnings (0.42 g, 17.3 mmol, 1.15 equiv) and flame-dried under high vacuum (< 2 torr) and allowed to cool to room temperature.

Once the flask was cooled to room temperature, it was purged three times with argon. THF (0.2 M) and 1,2-dibromoethane (2.25 mmol, 0.2 mL, 0.15 equiv) were then added. The reaction mixture was left to stir at room temperature (23 °C) for 18 h or until the reaction mixture was a pitch-black color, which is indicative of activated magnesium turnings. Note: In some cases, an off-gray color is also indicative of proper activation of magnesium turnings. Then 5-bromo-1-methyl-1*H*-indole (3.15 g, 15.0 mmol, 1.0 equiv) was added and left to stir at room temperature (23 °C) for 5-6 h followed by fast addition of isobutyltrichlorosilane (2.49 mL, 15.0 mmol, 1.0 equiv). Note: 5-6 hours is the optimal time range to allow for Grignard formation; 1-4 hours and ≥ 6 hours this will result in lower yields. Upon addition of isobutyltrichlorosilane a yellow color is a good indicator that the reaction is proceeding accordingly. The reaction was left to stir at room temperature (23 °C) for 18 h. The reaction mixture was then cooled to –78 °C and lithium aluminum hydride (4.0 M, 7.5 mL, 2.0 equiv) was added dropwise. The solution was then allowed to cool to room temperature (23 °C) over 3 h. The solution was quenched with Rochelle salt (8 mL) and filtered through Celite. The aqueous phase was extracted with diethyl ether (3 × 25 mL). The combined organic phase was dried over $MgSO_4$, filtered, and concentrated *in vacuo*. The reaction mixture was purified using flash column chromatography (SiO_2, hexanes/EtOAc, 97:3 to 95:5 *v/v*) to yield corresponding silanes **2.68e** as a yellow oil (1.21 g, 34 %).

Note: Characterization data revealed an unidentifiable impurity is present in the mixture via ^{13}C NMR spectroscopy. Confirmation of the product was achieved through ^{1}H NMR and ^{29}Si NMR spectroscopy and carried through to the next step.

^{1}H NMR (400 MHz, $CDCl_3$) δ 7.04 (d, *J* = 1.1 Hz, 2H), 6.99 (s, 1H), 6.83 (d, *J* = 7.6 Hz, 1H), 5.93 (s, 3H), 4.27 (s, 1H), 0.98 (d, *J* = 6.6 Hz, 6H), 0.90 (dt, *J* = 7.2, 3.8 Hz, 2H).^{13}C NMR (101

MHz, $CDCl_3$) δ 148.99, 147.60, 129.50, 125.60, 124.44, 112.43, 109.70, 108.91, 101.72, 100.74, 25.69, 25.60, 20.97.$^{29}Si\{^1H\}$ NMR (79 MHz, $CDCl_3$) δ 146.03, –33.04.

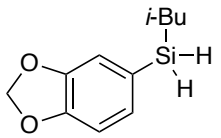

benzo[*d*][1,3]dioxol-5-yl(isobutyl)silane (2.68f)

To a 250-mL round bottom flask were added magnesium turnings (0.42 g, 17.3 mmol, 1.15 equiv) and flame-dried under high vacuum (< 2 torr) and allowed to cool to room temperature. Once the flask was cooled to room temperature, it was purged three times with argon. THF (0.2 M) and 1,2-dibromoethane (2.25 mmol, 0.2 mL, 0.15 equiv) were then added. The reaction mixture was left to stir at room temperature (23 °C) for 18 h or until the reaction mixture was a pitch-black color, which is indicative of activated magnesium turnings. Note: In some cases, an off-gray color is also indicative of proper activation of magnesium turnings. Then 5-bromobenzo[*d*][1,3]dioxole (1.80 mL, 15.0 mmol,1.0 equiv) was added and left to stir at room temperature (23 °C) for 5-6 h followed by fast addition of isobutyltrichlorosilane (2.49 mL, 15.0 mmol, 1.0 equiv). Note: 5-6 hours is the optimal time range to allow for Grignard formation; 1-4 hours and ≥ 6 hours this will result in lower yields. Upon addition of isobutyltrichlorosilane a yellow color is a good indicator that the reaction is proceeding accordingly. The reaction was left to stir at room temperature (23 °C) for 18 h. The reaction mixture was then cooled to –78 °C and lithium aluminum hydride (4.0 M, 7.5 mL, 2.0 equiv) was added dropwise. The solution was then allowed to cool to room temperature (23 °C) over 3 h. The solution was quenched with Rochelle salt (8 mL) and filtered through Celite. The aqueous phase was extracted with diethyl ether (3 × 25 mL). The combined organic phase was dried over $MgSO_4$, filtered, and

concentrated *in vacuo*. The reaction mixture was purified using flash column chromatography (SiO_2, hexanes/EtOAc, 99:1 *v/v*) to yield corresponding silanes **2.68f** as a yellow oil (1.10 g, 35%).

^{1}H NMR (400 MHz, $CDCl_3$) δ 7.04 (dd, *J* = 7.6, 1.1 Hz, 1H), 6.99 (d, *J* = 1.1 Hz, 1H), 6.83 (d, *J* = 7.7 Hz, 1H), 5.93 (s, 2H), 4.27 (m, 2H), 0.98 (d, *J* = 6.6 Hz, 6H), 0.90 (dt, *J* = 7.0, 3.9 Hz, 2H). ^{13}C NMR (101 MHz, $CDCl_3$) δ 148.98, 147.55 (d, *J* = 5.9 Hz), 129.43, 125.45, 114.35, 108.83, 100.65, 100.62, 25.54, 20.91. ^{29}Si NMR (79 MHz, $CDCl_3$ $Cr(acac)_3$) δ –32.97.

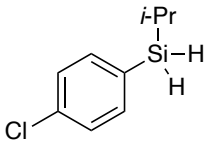

(4-chlorophenyl)(isopropyl)silane (2.77a)

To a 250-mL round bottom flask purged with argon was added isopropylmagnesium chloride (0.2 M in THF, 7.5 mL, 15.0 mmol, 1.0 equiv) and dissolved in THF (0.2 M). Trichloro(4-chlorophenyl)silane (2.58 mL, 15.0 mmol, 1.0 equiv) was then added. The reaction mixture was allowed to stir at room temperature (23 °C) for 20 h. The reaction mixture was then cooled to –78 °C and lithium aluminum hydride (4.0 M, 7.5 mL, 2.0 equiv) was added dropwise. The solution was then allowed to cool to room temperature (23 °C) over 3 h. The solution was quenched with Rochelle salt (8 mL) and filtered through Celite. The aqueous phase was extracted with diethyl ether (3 × 25 mL). The combined organic phase was dried over $MgSO_4$, filtered, and concentrated *in vacuo* at 190 torr and 33 °C due to volatility of the product. The reaction mixture was purified using flash column chromatography (SiO_2, hexanes/EtOAc, 9:1 *v/v*) but was found to be unstable on silica. Therefore, subsequent syntheses of this compound

were no longer isolated. The reaction mixture was run through a silica plug after concentration *in vacuo* and carried through to the next step.

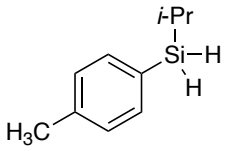

isopropyl(*p*-tolyl)silane (2.77b)

To a 250-mL round bottom flask purged with argon was added isopropylmagnesium chloride (0.2 M in THF, 7.5 mL, 15.0 mmol, 1.0 equiv) and dissolved in THF (0.2 M). Trichloro(4-methylphenyl)silane (2.66 mL, 15.0 mmol, 1.0 equiv) was then added. The reaction mixture was allowed to stir at room temperature (23 °C) for 20 h. The reaction mixture was then cooled to –78 °C and lithium aluminum hydride (4.0 M, 7.5 mL, 2.0 equiv) was added dropwise. The solution was then allowed to cool to room temperature (23 °C) over 3 h. The solution was quenched with Rochelle salt (8 mL) and filtered through Celite. The aqueous phase was extracted with diethyl ether (3 × 25 mL). The combined organic phase was dried over $MgSO_4$, filtered, and concentrated *in vacuo* at 190 torr and 33 °C due to volatility of the compound and carried through to the next step. The reaction mixture was run through a silica plug after concentration *in vacuo*.

Note: Confirmation of the product was achieved through ^1H NMR and carried through to the next step.

^{1}H NMR (300 MHz, $CDCl_3$) δ 7.46 (d, 2H), 7.18 (d, J = 0.8 Hz, 2H), 4.16 (d, J = 2.8 Hz, 2H), 2.35 (s, 3H), 1.25–1.14 (m, 1H), 1.07–1.03 (m, 6H).

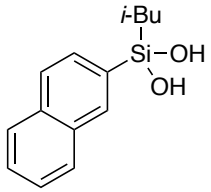

isobutyl(naphthalen-2-yl)silanediol (2.69a)

To a flame-dried round-bottom flask purged with argon were added Pd/C (10 wt %, 0.05 g, 0.25 mmol, 0.10 equiv) and was dissolved in THF (0.2 M). Silane (0.54 g, 2.50 mmol, 1.0 equiv) was added after being dissolved in a minimum amount of THF followed by the addition of deionized water (0.45 mL, 25 mmol, 10 equiv). (Caution: H_2 gas evolves as the reaction proceeds). The reaction was capped with a septum and allowed to stir at room temperature (23 °C). The reaction was monitored using TLC for the consumption of starting material silane. TLC conditions: hexanes/EtOAc, 4:1 *v/v*. Once silane was fully consumed, the reaction was filtered through Celite to remove Pd/C. The filtrate was dried over $MgSO_4$ filtered and concentrated *in vacuo*. The reaction mixture was purified using flash chromatography (SiO_2, hexanes/EtOAc, 4:1 *v/v or* DCM/Et_2O, 4:1 *v/v*) to yield corresponding silanediol **2.69a** as a white solid (0.62 g, 67%).

^{1}H NMR (400 MHz, C_6D_6) δ 8.27 (m, 1H), 7.75 (dd, J = 8.1, 1.1 Hz, 1H), 7.70–7.58 (m, 3H), 7.29–7.21 (m, 2H), 3.80 (b, 2H), 1.90 (m, 1H), 0.94 (d, J = 6.6 Hz, 6H), 0.89 (d, J = 7.0 Hz, 2H). ^{13}C NMR (101 MHz, C_6D_6) δ 135.53, 134.81, 134.39, 133.46, 130.26, 128.77, 127.58, 126.97, 126.25, 26.27, 25.88, 24.28. ^{29}Si NMR (79 MHz, C_6D_6 $Cr(acac)_3$) δ –16.53. HRMS (ESI) m/z: calc for $C_{14}H_{18}O_2Si$+$HCOO^-$ [M + $HCOO^-$] 291.1058, found 291.1051.

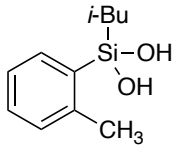

isobutyl(*o*-tolyl)silanediol (2.69c)

To a flame-dried round-bottom flask purged with argon were added Pd/C (10 wt%, 0.03 g, 0.30 mmol, 0.10 equiv) and was dissolved in THF (0.2 M). Silane (0.61 g, 3.40 mmol, 1.0 equiv) was added after being dissolved in a minimum amount of THF followed by the addition of deionized water (0.61 mL, 34 mmol, 10 equiv). (Caution: H_2 gas evolves as the reaction proceeds). The reaction was capped with a septum and allowed to stir at room temperature (23 °C). The reaction was monitored using TLC for the consumption of starting material silane. TLC conditions: hexanes/EtOAc, 4:1 *v/v*. Once silane was fully consumed, the reaction was filtered through Celite to remove Pd/C. The filtrate was dried over $MgSO_4$ filtered and concentrated *in vacuo*. The reaction mixture was purified using flash chromatography (SiO_2, hexanes/EtOAc, 4:1 *v/v*) to yield corresponding silanediol **2.69c** as a white solid (0.43 g, 70%).

^{1}H NMR (400 MHz, C_6D_6) 7.77 (dd, J = 7.3, 1.7 Hz, 1H), 7.19 (m, 2H), 7.14 (t, J = 7.3 1H), 7.04 (d, J = 7.5 Hz, 1H), 2.44 (s, 3H), 1.83 (m, 1H), 0.93 (d, J = 6.6 Hz, 6H), 0.78 (d, J = 7.1 Hz, 2H). ^{13}C NMR (101 MHz, C_6D_6) δ 143.76, 135.73, 135.58, 130.45, 130.16, 125.24, 26.67, 26.23, 24.33, 22.97. ^{29}Si NMR (79 MHz, C_6D_6, $Cr(acac)_3$) δ –16.09. HRMS (ESI) m/z: calc for $C_{11}H_{18}O_2Si$+$HCOO^-$ $[M + HCOO]^-$ 255.1058 found 255.1052.

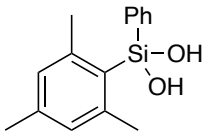

mesityl(phenyl)silanediol (2.69d)

To a flame-dried round-bottom flask purged with argon were added Pd/C (10 wt %, 0.07 g, 0.35 mmol, 0.10 equiv) and was dissolved in THF (0.5 M). Silane (0.74 g, 3.50 mmol, 1.0 equiv) was added after being dissolved in a minimum amount of THF followed by the addition of deionized water (0.15 mL, 7.00 mmol, 2.0 equiv). (Caution: H_2 gas evolves as the reaction proceeds). The reaction was capped with a septum and allowed to stir at room temperature (23 °C). The reaction was monitored using TLC for the consumption of starting material silane. TLC conditions: hexanes/EtOAc, 9:1 *v/v*. Once silane was fully consumed, the reaction was filtered through Celite to remove Pd/C. The filtrate was dried over $MgSO_4$ filtered and concentrated *in vacuo*. The reaction mixture was purified using flash chromatography (SiO_2, hexanes/EtOAc, 4:1 *v/v*) to yield corresponding silanediol **2.69d** as a white solid (0.03 g, 3%).

^{1}H NMR (300 MHz, C_6D_6) δ 7.16–7.14 (m, 5H), 6.74 (d, J = 6.9 Hz, 2H), 2.52 (d, J = 7.8 Hz, 6H), 2.10 (d, J = 5.4 Hz, 3H), 0.44 (s, 2H). ^{13}C NMR (101 MHz, C_6D_6) δ 145.58, 139.91, 138.03, 136.31, 134.14, 130.09, 129.48, 128.74, 24.59, 23.76. ^{29}Si NMR (79 MHz, C_6D_6) δ 22.41. HRMS (ESI) m/z: calc for $C_{15}H_{17}O_2Si^-$ $[M - H]^-$ 257.0998 found 257.0997.

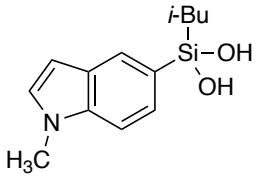

isobutyl(1-methyl-1*H*-indol-5-yl)silanediol (2.69e)

To a flame-dried round-bottom flask purged with argon were added Pd/C (10 wt %, 0.78 g, 0.73 mmol, 0.10 equiv) and was dissolved in THF (0.2 M). Silane (0.16 g, 0.73 mmol, 1.0 equiv) was added after being dissolved in a minimum amount of THF followed by the addition of deionized water (0.14 mL, 7.30 mmol, 10 equiv). (Caution: H_2 gas evolves as the reaction proceeds). The reaction was capped with a septum and allowed to stir at room temperature (23 °C). The reaction was monitored using TLC for the consumption of starting material silane. TLC conditions: DCM/Et_2O, 4:1 *v/v*. Once silane was fully consumed, the reaction was filtered through Celite to remove Pd/C. The filtrate was dried over $MgSO_4$ filtered and concentrated *in vacuo*. The reaction mixture was purified using flash chromatography (SiO_2, DCM/Et_2O, 7:3 *v/v*) to yield corresponding silanediol **2.69e** as an oil (0.17 g, 9%).

^{1}H NMR (400 MHz, $CDCl_3$) δ 7.94 (s, 1H), 7.47 (dd, *J* = 8.2, 1.1 Hz, 1H), 7.33 (d, *J* = 8.2 Hz, 1H), 7.05 (d, *J* = 3.1 Hz, 1H), 6.50 (dd, *J* = 3.1, 0.9 Hz, 1H), 3.78 (s, 3H), 2.79 (s, 2H), 1.87 (m, 1H), 0.94 (d, *J* = 6.6 Hz, 6H), 0.88 (d, *J* = 7.1 Hz, 2H).^{13}C NMR (101 MHz, $CDCl_3$) δ 137.97, 129.16, 128.45, 127.47, 126.47, 125.25, 109.17, 101.51, 32.90, 29.85, 26.22, 25.72, 24.17. ^{29}Si NMR (79 MHz, $CDCl_3$ $Cr(acac)_3$) δ –13.77.

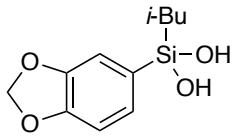

benzo[*d*][1,3]dioxol-5-yl(isobutyl)silanediol (2.69f)

To a flame-dried round-bottom flask purged with argon were added Pd/C (10 wt%, 0.02 g, 0.17 mmol, 0.10 equiv) and was dissolved in THF (0.2M). Silane (0.35 g, 1.68 mmol, 1.0 equiv) was added after being dissolved in a minimum amount of THF followed by the addition of deionized water (0.30 mL, 17 mmol, 10 equiv). (Caution: H_2 gas evolves as the reaction proceeds). The reaction was capped with a septum and allowed to stir at room temperature (23 °C). The reaction was monitored using TLC for the consumption of starting material silane. TLC conditions: DCM/Et_2O, 4:1 *v/v*. Once silane was fully consumed, the reaction was filtered through Celite to remove Pd/C. The filtrate was dried over $MgSO_4$ filtered and concentrated *in vacuo*. The reaction mixture was purified using flash chromatography (SiO_2, DCM/Et_2O, 4:1 *v/v*) to yield corresponding silanediol **2.69f** as a white solid (0.05 g, 7%, average of 3 runs).

Note: *Note: Confirmation of the product was achieved through ^1H NMR and carried through to the next step.*

^1H NMR (300 MHz, C_6D_6) δ 7.34 (s, 1H), 7.29–1.88 (m, 2H), 6.76 (dd, *J* = 10.0, 7.6 Hz, 1H), 5.29 (d, *J* = 3.3 Hz, 2H), 3.27 (s, 2H), 2.03–1.88 (m, 1H), 1.03–0.84 (m, 7H)

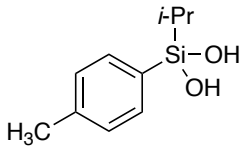

isopropyl(*p*-tolyl)silanediol (2.78b)

To a flame-dried round-bottom flask purged with argon were added Pd/C (10 wt %, 0.03 g, 0.25 mmol, 0.05 equiv) and was dissolved in THF (0.2 M). Silane (0.2 M in THF, 25 mL, 5.0 mmol, 1.0 equiv) was added after being dissolved in a minimum amount of THF followed by the addition of deionized water (0.90 mL, 50 mmol, 10 equiv). (Caution: H_2 gas evolves as the reaction proceeds). The reaction was capped with a septum and allowed to stir at room temperature (23 °C). The reaction was monitored using TLC for the consumption of starting material silane. TLC conditions: hexanes/EtOAc, 7:3 *v/v*. Once silane was fully consumed, the reaction was filtered through Celite to remove Pd/C. The filtrate was dried over $MgSO_4$ filtered and concentrated *in vacuo*. The reaction mixture was purified using flash chromatography (SiO_2, hexanes/EtOAc, 7:3 *v/v*) to yield corresponding silanediol **2.78b** as an oil (0.15g, 15% over 2 steps).

^{1}H NMR (400 MHz, C_6D_6) δ 7.65 (d, J = 7.7 Hz, 2H), 7.05 (d, J = 7.6 Hz, 2H), 4.26 (s, 2H), 2.12 (s, 3H), 1.11 (m, 1H).^{13}C NMR (101 MHz, C_6D_6) δ 140.02, 134.95, 131.47, 128.92, 21.54, 17.07, 14.27. ^{29}Si NMR (79 MHz, C_6D_6, $Cr(acac)_3$) δ –16.27.

General Procedure: ^{1}H NMR Spectroscopy Binding Studies

Two 20-mL scintillation vials were flame dried and back purged with argon. Each scintillation vial was fitted with a septa and argon balloon. An unused bottle of deuterated solvent (C_6D_6) equipped with activated 4 Å molecular sieves was used. Note: The deuterated solvent (C_6D_6) was left to sit with activated 4 Å molecular sieves for a minimum of 18 h prior to

use. NMR tubes were placed in the oven for 1 h prior to use. Two stock solutions were made, (1) with the silanediol, and (2) the organocatalyst. The first stock solution was made by dissolving the disiloxanediol in 4 mL of deuterate solvent (C_6D_6). The organocatalyst (10.0 equiv) was added to the other scintillation vial. To further eliminate any moisture, the deuterated solvent (C_6D_6) was fitted with a septum and argon balloon when being used. A 2 mL aliquot was taken from the stock solution containing the disiloxanediol and transferred to the stock solution containing the Lewis base. Then different volumes of each stock solution were mixed into the corresponding NMR tubes with the desired equivalents of organocatalyst (Table **2.10**).

Table **2.10** Volumes needed for binding studies.

NMR tube	Silanediol (equiv)	Volume from (SD solution)	Volume from (Organocatalyst solution)
A	0	0.50	0
B	1	0.45	0.05
C	3	0.35	0.15
D	5	0.25	0.25
E	7	0.15	0.35
F	10	0	0.50

Each NMR tube was capped with a rubber septum. Then, each NMR tube was purged with argon. The ^{1}H NMR spectrum of each solution was recorded using the 400 MHz NMR spectrometer after 16 scans at room temperature. Binding constants were calculated using Microsoft Excel Solver to fit a nonlinear curve with the model equation below.[50] The binding affinity (K_a) was the only variable optimized and no constraints were used. The error was calculated at a 95% confidence interval based on the NMR data to the model.

$$\Delta\delta_i = \delta_{obs,i} - \delta_{free} = \frac{C}{R_o} \qquad \text{eq. } \mathbf{2.2}$$

$$C = \frac{(K_aR_o+1+K_aS_i) \pm \sqrt{(K_aR_o+1+K_aS_i)^2-4K_a{}^2R_oS_i}}{2K_a} \qquad \text{eq. } \mathbf{2.3}$$

The chemical shift (ppm) of the SiOH proton in the bound Lewis base complex is equal to $\delta_{complex}$, and thus $\Delta\delta = \delta_{complex} - \delta_{free}$ where $\delta_{free} =$ chemical shift (ppm) of the SiOH proton when no Lewis base is present (i.e., NMR tube A). This value ($\Delta\delta$) is estimated from extrapolation of where the binding curve levels off. The remaining values are as follows: $\delta_{obs,i} =$ chemical shift (ppm) of SiOH proton at *i* equivalents of Lewis base, $R_o =$ initial concentration of disiloxanediols, and $S_i =$ concentration of Lewis base at *i* equivalents in M, and $K_a =$ binding constant in M^{-1}.

2.14 References

(1) Dalton, J. J.; Bernal Sánchez, A.; Kelly, A. T.; Fettinger, J. C.; Franz, A. K. Organocatalytic Asymmetric Synthesis of Si-Stereogenic Siloxanols. *ACS Catal.* **2024**, *14* (2), 1005–1012. https://doi.org/10.1021/acscatal.3c03932.

(2) Kocienski, P. J. *Protecting Groups*, 3rd ed.; Thieme: Stuggart, Germany, 2005.

(3) Wuts, P. G. M.; Greene, T. W. *Green's Protective Groups in Organic Synthesis*, 4th ed.; John Wiley & Sons: Hoboken, NJ, 2006.

(4) Corey, E. J.; Venkateswarlu, A. Protection of Hydroxyl Groups as Tert-Butyldimethylsilyl Derivatives. *J. Am. Chem. Soc.* **1972**, *94* (17), 6190–6191. https://doi.org/10.1021/ja00772a043.

(5) Chaudhary, S. K.; Hernandez, O. 4-DIMETHYLAMINOPYRIDINE: AN EFFICIENT AND SELECTIVE CATALYST FOR THE SILYLATION OF ALCOHOLS. *Tetrahedron Lett.* **1979**, No. 2, 99–102.

(6) Patschinski, P.; Zhang, C.; Zipse, H. The Lewis Base-Catalyzed Silylation of Alcohols—A Mechanistic Analysis. *J. Org. Chem.* **2014**, *79* (17), 8348–8357. https://doi.org/10.1021/jo5016568.

(7) Seliger, J.; Oestreich, M. Making the Silylation of Alcohols Chiral: Asymmetric Protection of Hydroxy Groups. *Chem. – Eur. J.* **2019**, *25* (40), 9358–9365. https://doi.org/10.1002/chem.201900792.

(8) Denmark, S. E.; Jacobs, R. T.; Dai-Ho, G.; Wilson, S. Synthesis, Structure, and Reactivity of an Organogermanium Lewis Acid. *Organometallics* **1990**, *9* (12), 3015–3019. https://doi.org/10.1021/om00162a006.

(9) Myers, A. G.; Kephart, S. E.; Chen, H. Silicon-Directed Aldol Reactions. Rate Acceleration by Small Rings. *J. Am. Chem. Soc.* **1992**, *114* (20), 7922–7923. https://doi.org/10.1021/ja00046a054.

(10) Denmark, S. E.; Griedel, B. D.; Coe, D. M. The Chemistry of Enoxysilacyclobutanes: Highly Selective, Uncatalyzed Aldol Additions. *J. Org. Chem.* **1993**, *58* (5), 988–990. https://doi.org/10.1021/jo00057a002.

(11) Matsumoto, K.; Oshima, K.; Utimoto, K. Noncatalyzed Stereoselective Allylation of Carbonyl Compounds with Allylsilacyclobutanes. *J. Org. Chem.* **1994**, *59* (23), 7152–7155. https://doi.org/10.1021/jo00102a052.

(12) Zhang, X.; Houk, K. N.; Leighton, J. L. Origins of Stereoselectivity in Strain-Release Allylations. *Angew. Chem. Int. Ed.* **2005**, *44* (6), 938–941. https://doi.org/10.1002/anie.200462130.

(13) Xu, L.-W.; Chen, Y.; Lu, Y. Catalytic Silylations of Alcohols: Turning Simple Protecting-Group Strategies into Powerful Enantioselective Synthetic Methods. *Angew. Chem. Int. Ed.* **2015**, *54* (33), 9456–9466. https://doi.org/10.1002/anie.201504127.

(14) Weickgenannt, A.; Mewald, M.; Oestreich, M. Asymmetric Si–O Coupling of Alcohols. *Org. Biomol. Chem.* **2010**, *8* (7), 1497–1504. https://doi.org/10.1039/B925722E.

(15) Rendler, S.; Oestreich, M. Kinetic Resolution and Desymmetrization by Stereoselective Silylation of Alcohols. *Angew. Chem. Int. Ed.* **2008**, *47* (2), 248–250. https://doi.org/10.1002/anie.200704210.

(16) Isobe, T.; Fukuda, K.; Araki, Y.; Ishikawa, T. Modified Guanidines as Chiral Superbases: The First Example of Asymmetric Silylation of Secondary Alcohols. *Chem. Commun.* **2001**, No. 3, 243–244. https://doi.org/10.1039/B009173L.

(17) Patel, S. G.; Wiskur, S. L. Mechanistic Investigations of the Mukaiyama Aldol Reaction as a Two Part Enantioselective Reaction. *Tetrahedron Lett.* **2009**, *50* (11), 1164–1166. https://doi.org/10.1016/j.tetlet.2008.12.083.
(18) Sheppard, C. I.; Taylor, J. L.; Wiskur, S. L. Silylation-Based Kinetic Resolution of Monofunctional Secondary Alcohols. *Org. Lett.* **2011**, *13* (15), 3794–3797. https://doi.org/10.1021/ol2012617.
(19) Clark, R. W.; Deaton, T. M.; Zhang, Y.; Moore, M. I.; Wiskur, S. L. Silylation-Based Kinetic Resolution of α-Hydroxy Lactones and Lactams. *Org. Lett.* **2013**, *15* (24), 6132–6135. https://doi.org/10.1021/ol402982w.
(20) Zhao, Y.; Rodrigo, J.; Hoveyda, A. H.; Snapper, M. L. Enantioselective Silyl Protection of Alcohols Catalysed by an Amino-Acid-Based Small Molecule. *Nature* **2006**, *443* (7107), 67–70. https://doi.org/10.1038/nature05102.
(21) Zhao, Y.; Mitra, A. W.; Hoveyda, A. H.; Snapper, M. L. Kinetic Resolution of 1,2-Diols through Highly Site- and Enantioselective Catalytic Silylation. *Angew. Chem. Int. Ed.* **2007**, *46* (44), 8471–8474. https://doi.org/10.1002/anie.200703650.
(22) Rodrigo, J. M.; Zhao, Y.; Hoveyda, A. H.; Snapper, M. L. Regiodivergent Reactions through Catalytic Enantioselective Silylation of Chiral Diols. Synthesis of Sapinofuranone A. *Org. Lett.* **2011**, *13* (15), 3778–3781. https://doi.org/10.1021/ol2010819.
(23) You, Z.; Hoveyda, A. H.; Snapper, M. L. Catalytic Enantioselective Silylation of Acyclic and Cyclic Triols: Application to Total Syntheses of Cleroindicins D, F, and C. *Angew. Chem. Int. Ed.* **2009**, *48* (3), 547–550. https://doi.org/10.1002/anie.200805338.
(24) You, Z.; Hoveyda, A. H.; Snapper, M. L. Catalytic Enantioselective Silylation of Acyclic and Cyclic Triols: Application to Total Syntheses of Cleroindicins D, F, and C. *Angew. Chem. Int. Ed.* **2009**, *48* (3), 547–550. https://doi.org/10.1002/anie.200805338.
(25) Tan, K. L.; Sun, X.; Worthy, A. D. Scaffolding Catalysis: Expanding the Repertoire of Bifunctional Catalysts. *Synlett* **2012**, *2012* (3), 321–325. https://doi.org/10.1055/s-0031-1290321.
(26) *Scaffolding Catalysts: Highly Enantioselective Desymmetrization Reactions - Sun - 2011 - Angewandte Chemie International Edition - Wiley Online Library*. https://onlinelibrary.wiley.com/doi/full/10.1002/anie.201103470 (accessed 2025-04-04).
(27) Worthy, A. D.; Sun, X.; Tan, K. L. Site-Selective Catalysis: Toward a Regiodivergent Resolution of 1,2-Diols. *J. Am. Chem. Soc.* **2012**, *134* (17), 7321–7324. https://doi.org/10.1021/ja3027086.
(28) Sun, X.; Worthy, A. D.; Tan, K. L. Resolution of Terminal 1,2-Diols via Silyl Transfer. *J. Org. Chem.* **2013**, *78* (20), 10494–10499. https://doi.org/10.1021/jo4012909.
(29) Gao, J.; Mai, P.-L.; Ge, Y.; Yuan, W.; Li, Y.; He, C. Copper-Catalyzed Desymmetrization of Prochiral Silanediols to Silicon-Stereogenic Silanols. *ACS Catal.* **2022**, *12* (14), 8476–8483. https://doi.org/10.1021/acscatal.2c02482.
(30) Zhu, M.; Oestreich, M. Generation of Silicon-Centered Stereogenicity by Chiral Counteranion-Directed Desymmetrization of Silanediols. *ACS Catal.* **2023**, *13* (15), 10244–10247. https://doi.org/10.1021/acscatal.3c02682.
(31) Beutner, G. L.; Young, I. S.; Davies, M. L.; Hickey, M. R.; Park, H.; Stevens, J. M.; Ye, Q. TCFH–NMI: Direct Access to N-Acyl Imidazoliums for Challenging Amide Bond Formations. *Org. Lett.* **2018**, *20* (14), 4218–4222. https://doi.org/10.1021/acs.orglett.8b01591.

(32) Schreyer, L.; Properzi, R.; List, B. IDPi Catalysis. *Angew. Chem. Int. Ed.* **2019**, *58* (37), 12761–12777. https://doi.org/10.1002/anie.201900932.
(33) Kipping, F. S.; Lloyd, L. L. XLVII.—Organic Derivatives of Silicon. Triphenylsilicol and Alkyloxysilicon Chlorides. *J. Chem. Soc. Trans.* **1901**, *79* (0), 449–459. https://doi.org/10.1039/CT9017900449.
(34) Lickiss, P. D. The Synthesis and Structure of Organosilanols. In *Advances in Inorganic Chemistry*; Sykes, A. G., Ed.; Academic Press, 1995; Vol. 42, pp 147–262. https://doi.org/10.1016/S0898-8838(08)60053-7.
(35) Chandrasekhar, V.; Boomishankar, R.; Nagendran, S. Recent Developments in the Synthesis and Structure of Organosilanols. *Chem. Rev.* **2004**, *104* (12), 5847–5910. https://doi.org/10.1021/cr0306135.
(36) Cella, J. A.; Carpenter, J. C. Procedures for the Preparation of Silanols. *J. Organomet. Chem.* **1994**, *480* (1), 23–26. https://doi.org/10.1016/0022-328X(94)87098-5.
(37) Tran, N. T.; Wilson, S. O.; Franz, A. K. Cooperative Hydrogen-Bonding Effects in Silanediol Catalysis. *Org. Lett.* **2012**, *14* (1), 186–189. https://doi.org/10.1021/ol202971m.
(38) Tran, N. T.; Wilson, S. O.; Franz, A. K. Supramolecular Hydrogen-Bonding Assembly of Silanediols with Bifunctional Heterocycles. *Chem. Commun.* **2014**, *50* (28), 3738–3740. https://doi.org/10.1039/C4CC00672K.
(39) Wilson, S. O.; Tran, N. T.; Franz, A. K. NMR and X-Ray Studies of Hydrogen Bonding for Amide-Containing Silanediols. *Organometallics* **2012**, *31* (19), 6715–6718. https://doi.org/10.1021/om300736n.
(40) Tran, N. T.; Min, T.; Franz, A. K. Silanediol Hydrogen Bonding Activation of Carbonyl Compounds. *Chem. – Eur. J.* **2011**, *17* (36), 9897–9900. https://doi.org/10.1002/chem.201101492.
(41) Schafer, A. G.; Wieting, J. M.; Mattson, A. E. Silanediols: A New Class of Hydrogen Bond Donor Catalysts. *Org. Lett.* **2011**, *13* (19), 5228–5231. https://doi.org/10.1021/ol2021115.
(42) Tran, N. T. Design, Synthesis, and Study of Silanediols as Homogenous, Hydrogen-Bonding Organocatalysts for Asymmetric Transformation, 2014.
(43) Koga, S.; Ueki, S.; Shimada, M.; Ishii, R.; Kurihara, Y.; Yamanoi, Y.; Yuasa, J.; Kawai, T.; Uchida, T.; Iwamura, M.; Nozaki, K.; Nishihara, H. Access to Chiral Silicon Centers for Application to Circularly Polarized Luminescence Materials. *J. Org. Chem.* **2017**, *82* (12), 6108–6117. https://doi.org/10.1021/acs.joc.7b00583.
(44) Zhu, J.; Chen, S.; He, C. Catalytic Enantioselective Dehydrogenative Si–O Coupling to Access Chiroptical Silicon-Stereogenic Siloxanes and Alkoxysilanes. *J. Am. Chem. Soc.* **2021**, *143* (14), 5301–5307. https://doi.org/10.1021/jacs.1c01106.
(45) Crawford, C. J.; Qiao, Y.; Liu, Y.; Huang, D.; Yan, W.; Seeberger, P. H.; Oscarson, S.; Chen, S. Defining the Qualities of High-Quality Palladium on Carbon Catalysts for Hydrogenolysis. *Org. Process Res. Dev.* **2021**, *25* (7), 1573–1578. https://doi.org/10.1021/acs.oprd.0c00536.
(46) Kannengießer, J.-F.; Briesenick, M.; Meier, D.; Huch, V.; Morgenstern, B.; Kickelbick, G. Synthesis and Hydrogen-Bond Patterns of Aryl-Group Substituted Silanediols and -Triols from Alkoxy- and Chlorosilanes. *Chem. – Eur. J.* **2021**, *27* (66), 16461–16476. https://doi.org/10.1002/chem.202102729.
(47) Sommer, L. H.; Tyler, L. J. Steric Effects of the T-Butyl Group in Organosilicon Compounds1. *J. Am. Chem. Soc.* **1954**, *76* (4), 1030–1033. https://doi.org/10.1021/ja01633a032.

(48) Diemoz, K. M. Design, Synthesis and Investigation of Siloxanol Hydrogen-Bonding Catalysts and Chiral Silanol Ligands, 2011.
(49) Kondo, S.; Fukuda, A.; Yamamura, T.; Tanaka, R.; Unno, M. Anion Recognition by a Disiloxane-1,3-Diol in Organic Solvents. *Tetrahedron Lett.* **2007**, *48* (45), 7946–7949. https://doi.org/10.1016/j.tetlet.2007.09.067.
(50) Thordarson, P. Determining Association Constants from Titration Experiments in Supramolecular Chemistry. *Chem. Soc. Rev.* **2011**, *40* (3), 1305–1323. https://doi.org/10.1039/C0CS00062K.

Chapter 3: Synthesis of Chiral 1,3-Disiloxanediols and Exploration as Hydrogen-bonding Organocatalysts

3.1 Introduction and Background

This chapter presents the efforts towards the synthesis of chiral 1,3-disiloxanediols using the desymmetrization of prochiral silanediols. The synthesis of novel prochiral silanediols have been investigated, and new insight was gained regarding the synergistic selectivity interplay between the silanediols and chlorosilanes. Silanediol and chlorosilanes were observed to perform with great (86:14 er) to excellent selectivity (96:4 er) with two new aryl-aryl silanediols in the desymmetrization reaction. The design, synthesis, and preliminary evaluation of chiral 1,3-disiloxanediols as hydrogen-bonding organocatalysts were also explored. The solution-state hydrogen-bonding interactions were investigated and an interesting role of the chlorosilane in dictating the selectivity of the desymmetrization reaction was explained. The hydrogen-bonding interactions were initially related to observed selectivities for the test reactions explored. More studies will be required to understand the active binding mode.

The power of hydrogen bonding was first described by Pauling: "..it will be found that the significance of the hydrogen bond for physiology is greater than that of any other structural feature."[1] Hydrogen bonds play an integral role in biological systems and are arguably fundamental to life. Hydrogen bonds have risen in popularity in the field of asymmetric organocatalysis.[2–9] Early beginnings of hydrogen-bonding catalysis was inspired by work from Yates and Eaton for the Lewis acid accelerated Diels-Alder reaction between anthracene **3.1** and furan-2,5-dione **3.2**.[10] In the presence of aluminum trichloride, the Diels-Alder reaction between **3.1** and **3.2** was complete in two minutes for the formation of **3.3**, while the absence of the Lewis

acid required approximately three days and afforded less pure product. This work signaled the power of metal-centered Lewis acid catalysts.[10–19]

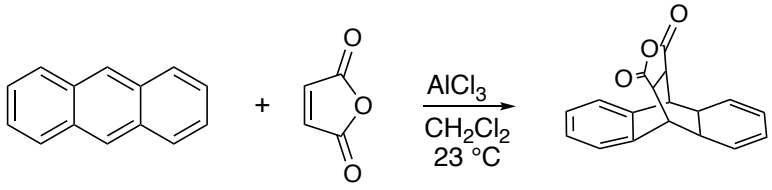

3.1 **3.2** **3.3**

Scheme **3.1.** Diels-Alder cycloaddition accelerated by aluminum trichloride.

Metal-centered Lewis acid catalysts have well defined and highly tunable Lewis acid/base interactions leading to enhanced stereochemical outcomes.[20] Brønsted acid activation of generic electrophiles have loosely defined and somewhat tunable interactions with careful consideration needed for pK_a.[21] Nonetheless, many factors are to be considered in the development of metal-centered Lewis acids such as cost, toxicity, isolation, and stability. The discovery that distinct hydrogen-bond donor motifs can catalyze an array of organic transformations was pioneered by Hine and co-workers (Scheme **3.2**).[22] Enhanced activity was observed with **3.5** relative to phenol (k_{rel} 12.5 vs 1.0). A solid-state structure of **3.5** and **3.4** supported a two-point binding mode that supports that the activation mode is also two-point binding.

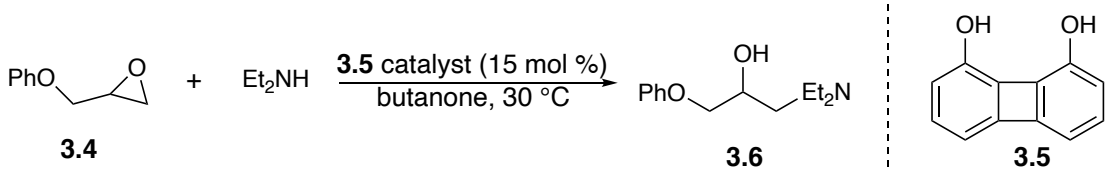

3.4 **3.6** **3.5**

Scheme **3.2.** Epoxide-ring opening catalyzed by 1,8-biphenylenediol **3.5**.

3.2 Early Hydrogen-bonding Organocatalysts

Since Friedel and Crafts' electrophilic aromatic substitution with aluminum trichloride[23] and Eaton's venture with aluminum trichloride,[10] many hydrogen-bonding organocatalysts were developed – selected examples are shown below (Figure **3.1**). These organocatalysts are flanked by a single or dual hydrogen-bond donor [24] site with structural differences allowing for secondary interactions. The Michael addition is arguably one of the most important carbon–carbon bond forming reactions in organic chemistry[25–28] and served as a model reaction for the early development of thiourea-based organocatalysts. Nitroolefins are excellent Michael acceptors with enhanced reactivity. Takemoto and co-workers harnessed this reactivity for the development of bifunctional thiourea catalyst **3.7** that promoted the Michael reaction of malonates with high enantioselectivities.[29] Thereafter, a surge in thiourea-based catalysts flooded the exciting new field of hydrogen-bonding organocatalysis. Ricci and co-workers developed the first catalytic, enantioselective Friedel–Crafts alkylation of indoles with nitroalkenes catalyzed by **3.8**, which is easily accessed in both enantiomeric forms from commercially available materials.[30] In 2006, Tsogoeva and co-workers demonstrated the first example of an asymmetric nitro Michael addition catalyzed by a primary amine derived thiourea-catalyzed **3.9**.[31] Noteworthy, Terada and co-workers developed an axially chiral guanidine **3.10** that facilitated the 1,4-addition of 1,3-dicarbonyl in high enantioselectivities.[32] Concurrent with Tsogoeva, Jacobsen and co-workers designed primary amine-thiourea **3.11** that underwent an enamine mechanism which allowed for cooperative activation of the electrophile by the thiourea and primary amine.[33]

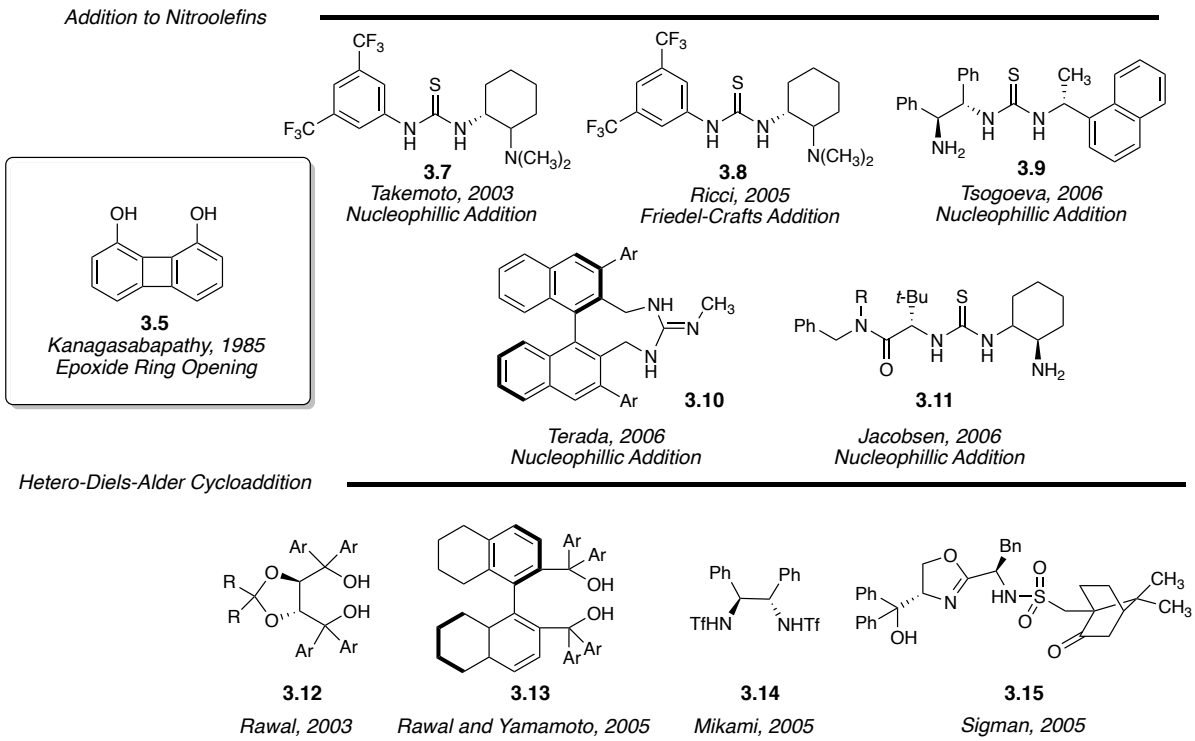

Figure **3.1**. Early hydrogen-bonding organocatalysts in asymmetric catalysis.

The Diels–Alder cycloaddition reaction is one of the most powerful C–C bond-forming reactions in organic chemistry, allowing construction of six-membered rings with high regio- and stereocontrol.[34] Rawal and co-workers developed a highly reactive diene (Rawal's diene) for the asymmetric Hetero-Diels-Alder (HDA) reaction with methacrolein, which was discovered to be catalyzed by α,α,α',α'-tetrataryl-2,2-disubstituted-1,3-dioxalane-4,5-dimethanol (TADDOL) **3.12** as the first example of a "simple chiral alcohol" promoted transformation.[35] Expanding the initial success with **3.12**, Rawal and Yamamoto demonstrated BAMOL **3.13** to catalyze the HDA reaction of Rawal's diene with unactivated aldehydes.[36] Structurally different catalyst **3.14** was discovered as an active catalysts for the HDA reaction of TIPS-substituted Danishefsky's diene[37] with glyoxylates.[38] Sigman and co-workers developed a new class of modular oxazoline catalysts that facilitated the HDA reaction of Rawal's diene with a series of activated aldehydes in high enantioselectivities.[39] Chiral diol-based organocatalysts such as TADDOL **3.12**, and many other

well-known catalysts (including VAPOL, VANOL, and BINOL) have been designed to promote notable transformations of the asymmetric Petasis reaction,[40] enantioselective protonation of silyl enol ethers[41], and asymmetric allylboration of ketones,[42] respectively.

Silanols are highly acidic and exhibit unique hydrogen bonding patterns with other proton donors or acceptors,[43] making them an attractive option for incorporation into chiral catalysts. Bolm and coworkers designed the first planar-chiral bis-silanol **3.13** to demonstrate for asymmetric organocatalysis, also in the HDA reaction of Rawal's diene with **3.13**.[44] Silanol catalyst **3.13** promoted the HDA reaction in moderate yield and enantioselectivity (45% yield and 64:36 er), with the carbinol derivative performing similarly (45% yield and 70:30 er).

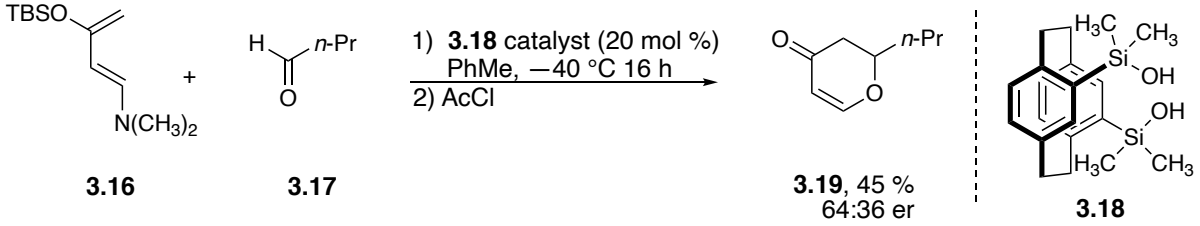

3.16 **3.17** **3.19**, 45 % 64:36 er **3.18**

Scheme **3.3**. Bolm and coworkers' chiral bis-silanol-catalyzed hetero-Diels–Alder reaction.

The potential for chiral organosilanols as hydrogen-bonding organocatalysts remains largely underexplored. To date, only one report exists in the literature for the synthesis of chiral 1,3-disiloxanediol (Scheme **3.4**).[45] Kawakami developed a highly stereoselective cleavage reaction of the carbon–silicon bond of an (4-methoxyl-1-naphthyl)silane in **3.24** over a three step synthesis with low yields. Kawakami employed the typical ways to functionalize organosilicon compounds by introducing a reaction functional group such as Br and Cl which facilitated the cleavage of the silicon-naphthyl bond. However, the development of more stereoselective methods was required for access to chiral 1,3-disiloxanediols.

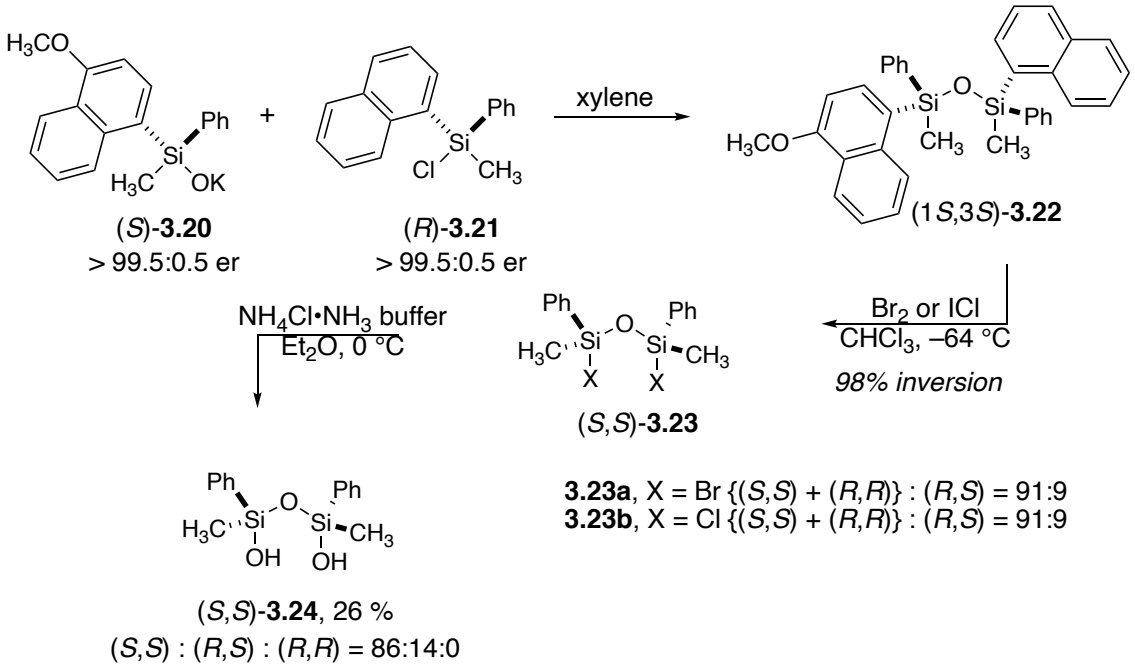

Scheme **3.4.** Synthesis of chiral 1,3-disiloxanediol reported by Kawakami.

3.3 Synthesis of Chiral 1,3-disiloxanediols

The Franz group has developed the first Lewis base-catalyzed silylation of prochiral silanediols for the synthesis of silicon-stereogenic siloxanols (Scheme **3.5**).[46] A co-crystal was obtained of the organocatalyst and naphthyl(phenyl)silanediol. The role of the Lewis base during silylation was evaluated by synthesizing and testing analogs of organocatalyst **3.22**. The hydrogen-bonding interactions in the reaction were investigated *via* analyses of ^{1}H NMR binding studies. The scope of the chlorosilane partner resulted in the successful synthesis of several siloxanols featuring the Si–H handle necessary for the synthesis of chiral 1,3-disiloxanediols. The Franz group has developed great knowledge about 1,3-disiloxanediols[47–49] and it remained a goal to synthesize chiral 1,3-dsiloxanediols for their application as catalysts in asymmetric transformations.

The desymmetrization reaction provided a route to synthesize chiral 1,3-disiloxanediols with unique selectivities observed with chlorosilane **3.26b** (Scheme **3.5**). High levels of enanti-

oenrichment in the desymmetrization reaction were attributed to the need for aryl-alkyl silanediols, more specifically, an isobutyl group. When (4-fluoronaphthalen 1yl)(isobutyl)silanediol was subjected to the desymmetrization reaction with chlorosilane **3.26a** excellent yield and selectivity for siloxanol **3.28aa** were observed (98% yield and 98:2 er). The desymmetrization reaction was optimized with isobutyl(naphthalen-1-yl)silanediol and chlorosilane **3.26a** which excellent yield and selectivity. When (4-fluoronaphthalen-1yl)(isobutyl)silanediol was paired with chlorosilane **3.26b** a loss of reactivity and selectivity was observed for siloxanol **3.28ab** (73% yield and 85:15 er). When paired with chlorosilane **3.26a**, isopropyl(phenyl)silanediol resulted in good reactivity and some selectivity for siloxanol **3.28ba** (78% yield and 65:35 er). Surprisingly, with chlorosilane **3.26b** isopropyl(phenyl)silanediol resulted in excellent yield and selectivity for siloxanol **3.28bb** (49% yield and 98:2 er). Interestingly, diaryl silanediol naphthalen-1-yl(phenyl)silanediol resulted in no change in selectivity with either chlorosilane **3.26a** or **3.26b**. These results demonstrated the uniqueness of chlorosilane **3.26b** in the desymmetrization reaction.

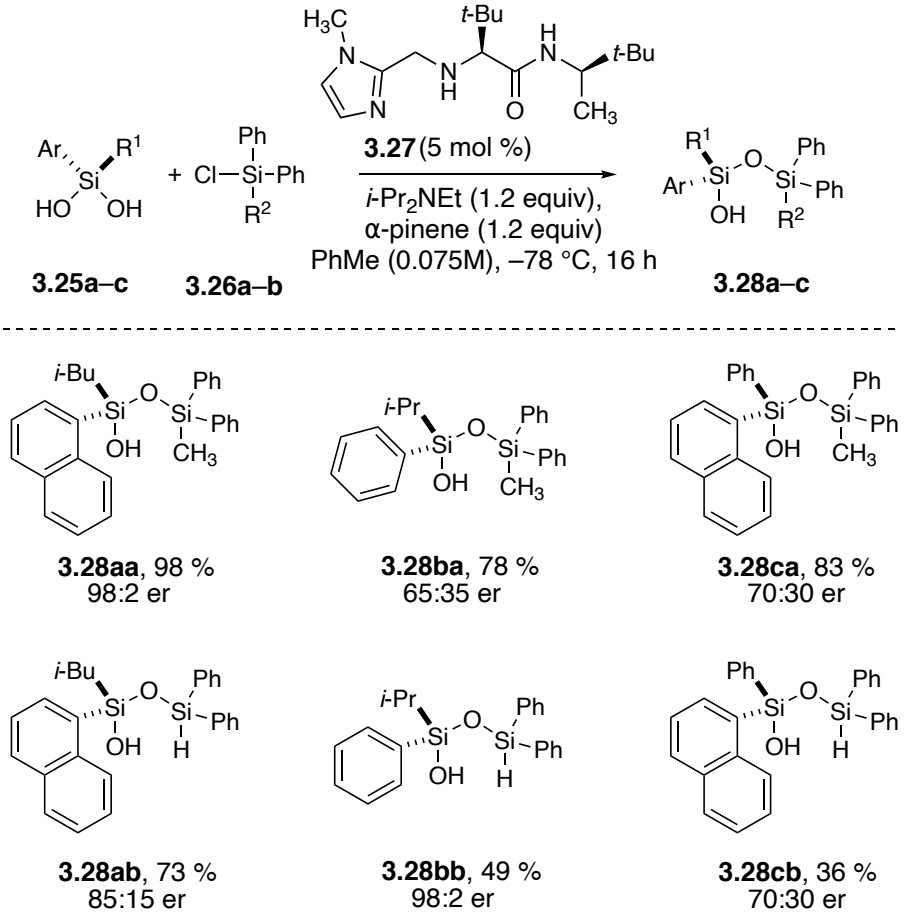

Scheme **3.5.** Effect of silanediol and chlorosilane on enantioselectivity.

The synthesis of chiral 1,3-dsiloxanediols now has an established route in the Franz group (Scheme **3.6**). The efforts towards the synthesis of novel prochiral substrates detailed in Chapter 2 of my dissertation illustrated the Grignard as the best route for access aryl-alkyl silanes **3.29**. Access to pure silanediols **3.30** is achieved through a Pd/C-catalyzed hydrolysis of silanes and avoids HCl impurities commonly observed with the direct hydrolysis of chlorosilanes.[50,51] In Chapter 2 of my dissertation, efforts towards a one-pot procedure for the synthesis of silanediols proved to be unreliable and highly dependent on the desired substitution pattern around the silicon center.[52] Silanediols **3.30** are subjected to the desymmetrization reaction with chlorosilane **3.26b** catalyzed at 5 mol% by **3.27** to give silicon-stereogenic siloxanols **3.31**. Chiral 1,3-dsiloxanediols **3.32** are synthesized upon Pd/C hydrolysis of siloxanols **3.31**.

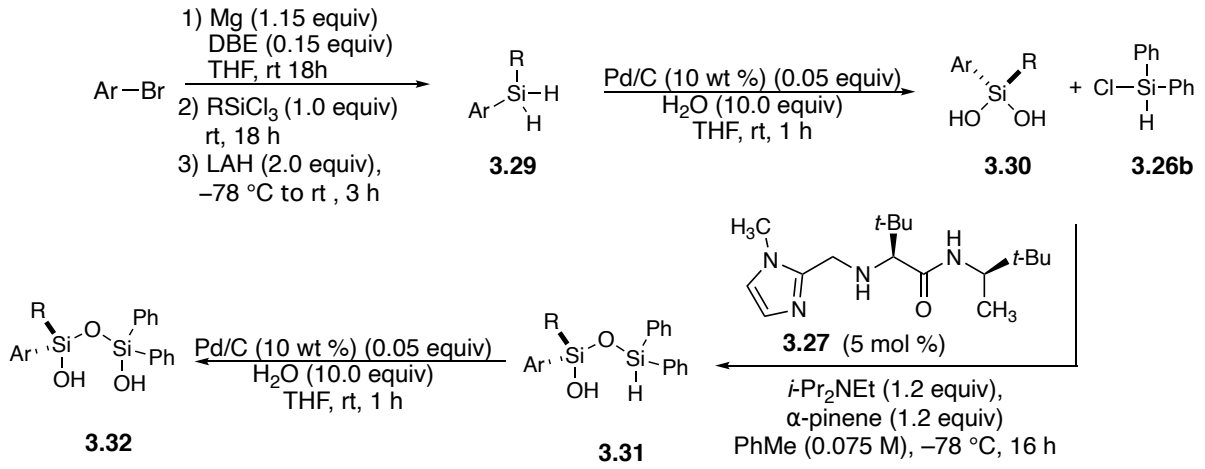

Scheme **3.6.** Synthesis of chiral 1,3-disiloxanediols.

A small collection of chiral 1,3-disiloxanediols were synthesized with yields reported over two steps (Scheme **3.7**). When (4-fluoronaphthalen-1yl)(isobutyl)silanediol was subjected to the desymmetrization reaction low yield and moderate selectivity for siloxanol **3.34a** was observed (11% yield and 86:14 er). Very interestingly, when diaryl mesityl(phenyl)silanediol was subjected to the desymmetrization reaction low yield, but excellent selectivity for siloxanol **3.34b** was observed (9% yield and 96:4 er). Mesityl(methyl)silanediol was tested as a comparison point to this result. Attempts to synthesize isobutyl(mesityl)silanediol were unsuccessful with mesityl(methyl)silanediol the only accessible substrate. Increased reactivity and a huge loss of selectivity was observed for siloxanol **3.34c** (38% yield and 57:43 er). This result suggested an interesting chemical relationship taking place between mesityl(methyl)silanediol and chlorosilane **3.26b**. Diaryl silanediols decorated with electron-withdrawing groups resulted in low reactivity for siloxanols **3.34d-e**. However, moderate selectivity was observed for siloxanol **3.34d** (86:14 er) while mesityl-containing siloxanol **3.34e** resulted in a complete loss of selectivity. These results suggested an interaction between prochiral silanediols and chlorosilane **3.26b**.

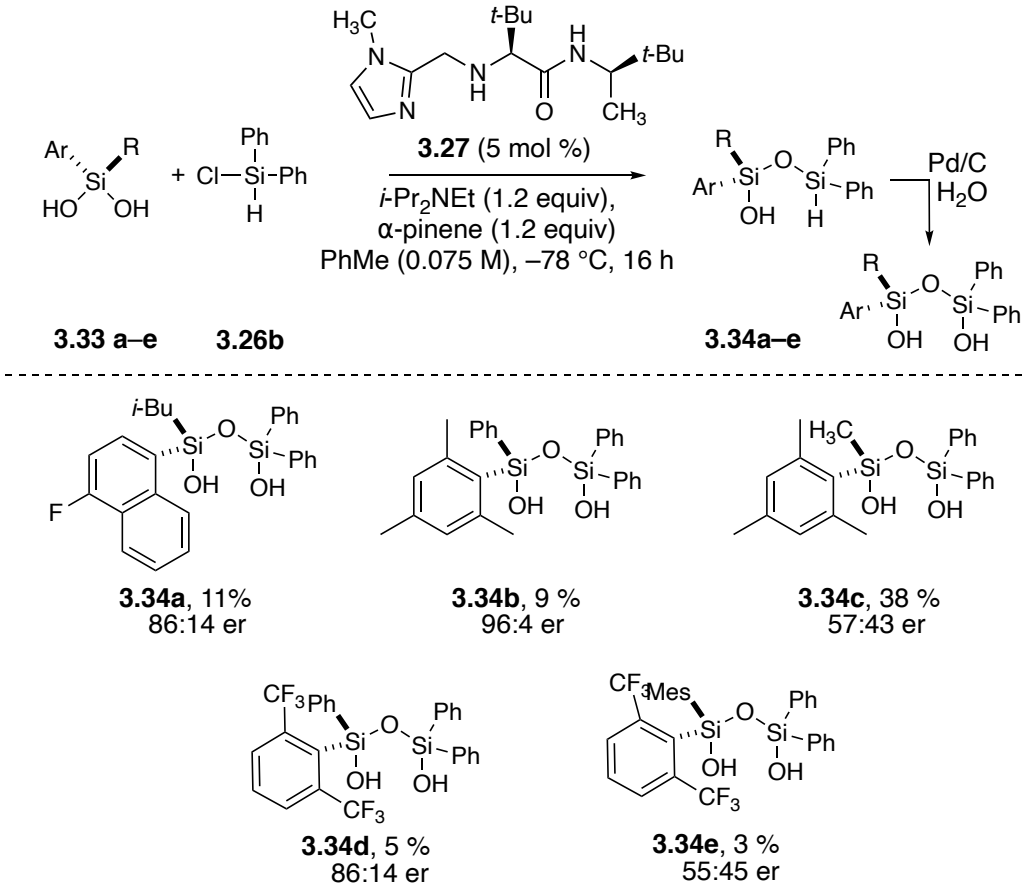

Scheme **3.7.** Chiral 1,3-disiloxanediols accessed *via* the desymmetrization reaction.

3.4 Synthesis of Prochiral Silanediols for Chiral 1,3-Disiloxanediols

The synthesis of silanediols followed the established route in the Franz group.[51,53] The synthesis of **3.37a** resulted in a 6% yield over two steps. Silanediol (4-fluoronaphthalen-1-yl)(isobutyl)silane **3.36a** was purified using flash column chromatography to yield a 3:1 mixture of 4-fluoronaphthalene to corresponding **3.36a**. Attempts to further purify **3.36a** were unsuccessful, and it was carried through to the next step. Encouragingly, mesityl(phenyl)silanediol **3.37b** was synthesized in higher yield (18%). Batch syntheses of a scale of 1.0 mmol for **3.37b** resulted in higher yield (i.e.,12% vs 18%). Large scale (18 mmol) Pd/C-catalyzed reactions for the synthesis of **3.37b** resulted in protodesilylation. Pd/C sourced from Strem was used for large- and small-scale reactions. In Chapter 2 of my dissertation, Pd/C sourced from Strem proved to be

most reliable for the synthesis of aryl-alkyl silanediols.[54] Trichlorosilanes **3.35a-b** (i.e., isobutyl and phenyl) were used for the synthesis of silanediols **3.37a-b**. Silanediol **3.37c** was accessed using dichloromethylsilane **3.35c** and resulted in 29% yield for silane **3.36c** and 23% for silanediol **3.37c**.

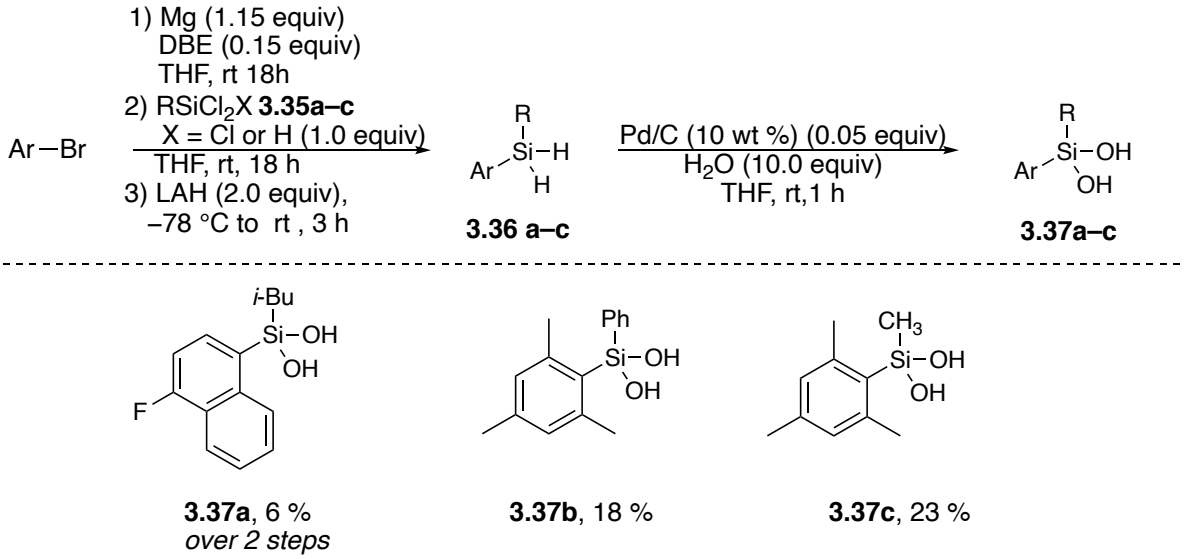

Scheme **3.8.** Synthesis of prochiral silanediols **3.32a–c**.

The synthesis of silanediols decorated with 1,3-bis(trifluoromethyl)phenyl **3.41** were attempted using an established route developed by Ngon T. Tran, Ph.D. (Scheme **3.8**A).[55] Early investigations in the Franz group allowed for mesityl-containing silanediols to be highly soluble, crystalline and isolable.[24] The incorporation of the mesityl group was influenced by strategies used for the synthesis of disilylenes and terphenylsilanes and chlorosilanes.[56,57] The addition of 2-mesitylmagnesiumbromide **3.38** to trichlorosilane followed by reduction with lithium aluminum hydride. Schmidbaur and coworkers have reported a shorter reaction time with moderate yields (68%) for the lithium aluminum hydride reduction of alkoxysilane, triethoxylmesitylsilane,[58] but results from Ngon T. Tran Ph.D. proved this method to be unreliable and led to low yields.[24] Chloromesitylsilane **3.40** was chlorinated efficiently with boron trichloride and

matched literature precedent.[58] Silanediols with 1,3-bis(trifluoromethyl)phenyl **3.41** and mesityl groups were designed to be highly lipophilic and soluble. Sterically encumbered chlorosilane **3.40** or commercially available chlorophenylsilane is then added slowly to a solution of Ar^FLi (Scheme **3.8**B). Silanes **3.42a–b** were hydrolyzed with Pd/C resulted in highly acidic silanediols **3.43a–b**. Chlorophenylsilane was not commercially available at the time I worked on this project. Attempts to synthesize chlorophenylsilane upon reduction of phenyltrichlorosilane were unsuccessful. Therefore, silanediol **3.43a** was recovered from the archive left by Ngon T. Tran, Ph.D. and subjected to desymmetrization reaction. Attempts to synthesize silane **3.42b** with were also unsuccessful. Silanediol **3.43b** was also recovered from the archive left by Ngon T. Tran, Ph.D. and subjected to desymmetrization reaction.

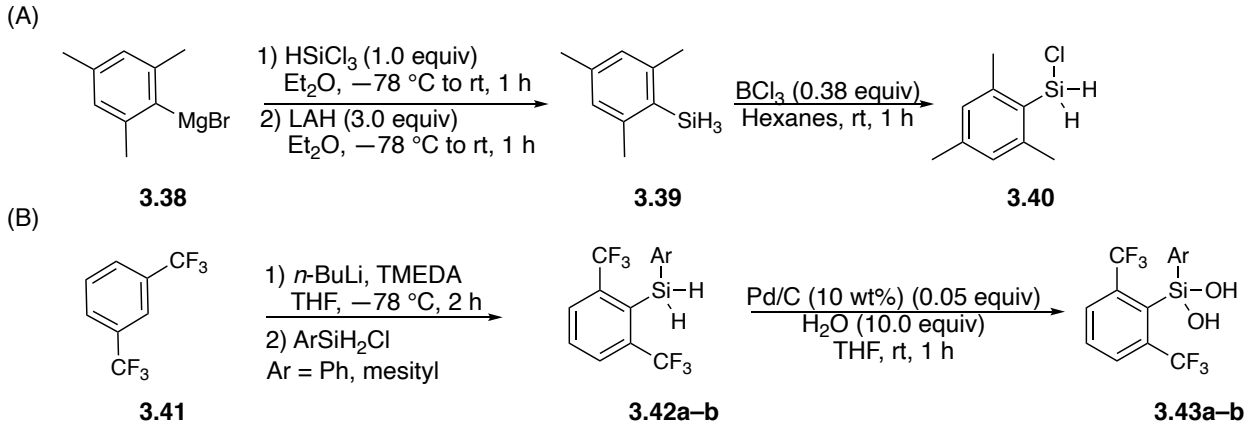

Scheme **3.8.** A) Synthesis of **3.40** B) Synthesis of prochiral silanediols **3.43a–b**.

A series of conditions were tested for the synthesis of silanediol **3.37a** from a 3:1 ratio of **3.44**:**3.36a** (Table **3.1**). Ruthenium based catalysts have been used for the highly selective and practical oxidation of organosilanes to silanols.[59,60] Encouraged by these results, small scale test reactions were unsuccessful and resulted in protodesilylation (Table **3.1**, entry 1–2). Additionally, a small-scale test reaction using an established method by the Franz group for the synthesis of 1.3-disiloxsnediols[61] was unsuccessful and resulted in unreacted starting material (Table **3.1**,

entry 3). Oxidation using potassium permanganate[43] resulted in protodesilylation (Table **3.1**, entry 4). An iridium-catalyzed hydrolysis[62] resulted in 26% isolated yield (Table **3.1**, entry 5).

Table 3.1 Conditions tested for the synthesis of **3.37a**.

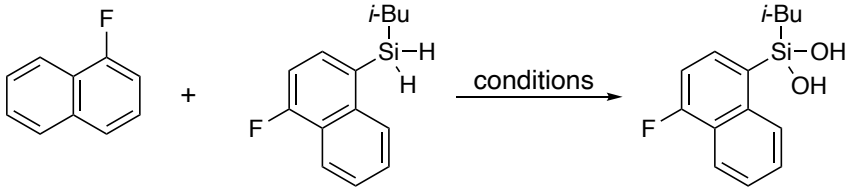

3.44 **3.36a** **3.37a**

entry	scale (mmol)	conditions	result[a]
1	0.08	$[Ru(benzene)Cl_2]_2$ (2 mol%), H_2O (4.0 equiv) CH_3CN (0.33 M), rt 2 h then 40 °C 2 h	protodesilylation
2	0.14	$[Ru(p\text{-cymene})Cl_2]_2$ (2 mol%), H_2O (4.0 equiv), CH_3CN (0.33 M), rt 2 h then 40 °C 2 h	protodesilylation
3	0.10	$BzCF_3$[b] (1 mol%), EDTA buffer pH = 11, CH_3CN (4.0 equiv), H_2O_2 (3.0 equiv/ SiH), THF (1.0 M), rt 24 h	unreacted SM
4	0.05	$KMnO_4$ (3.5 equiv), THF (0.2 M), rt 24 h	protodesilylation
5	0.075	$[Ir(COD)Cl]_2$ (5 mol%), H_2O (5.0 equiv), Et_2O (0.02 M), rt 3 h	26 %[c]

[a]Observed by ^1H NMR spectroscopy. [b]$BzCF_3$ = 2,2,2-trifluoroacetophenone. [c]Isolated yield.

A Pd-base catalyst screen was investigated to reduce overall costs associated with using Ir-based catalyst systems (Table **3.2**). Given the success for the synthesis for aryl-isopropyl and aryl-isobutyl containing silanediols in Chapter 2 with Pd/C sourced from Strem vs Sigma-Aldrich, I observed similar results for the synthesis of **3.37a**. Small scale test reactions in 1,4-di-oxane at room temperature resulted in a 1:1 mixture of **3.44**:**3.37a** (Table **3.1**, entry 1). Interestingly, a test reaction of the same scale at 0 °C resulted in exclusive formation of silanediol **3.37a** (Table **3.1**, entry 2). This result was replicated and confirmed (Table **3.1**, entry 3—4). Lindlar's catalyst was unsuccessful for the synthesis of **3.37a**. A large-scale test reaction

of 1.0 mmol using Pd/C (17 mol%) in THF at 0 °C resulted in protodesilylation. Iridium was deemed a more reliable metal for the oxidation of **3.36a**.

Table 3.2 Pd-based catalyst screen for the synthesis of **3.37a**.

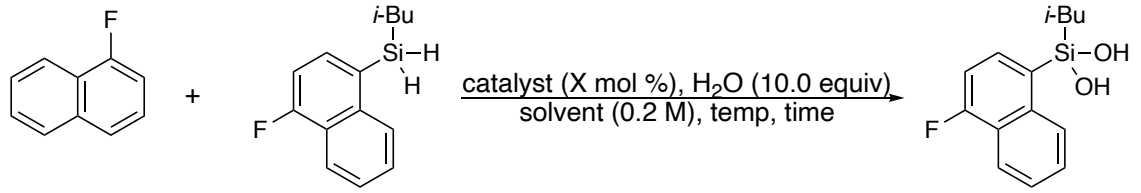

3.44 **3.36a** **3.37a**

entry	scale (mmol)	catalyst [a]	mol %	solvent	temp (°C)	time (min)	result (**3.44**:**3.37a**)[b]
1	0.11	Pd/C	17	1,4-dioxane	23	27	1: 1
2	0.10	Pd/C	17	Et_2O	0	23	0: 1
3	0.23	Pd/C	17	THF	0	15	0: 1
4	0.19	Pd/C	17	THF	0	29	0: 1
5	0.12	$Pd/CaCO_3$	5	THF	23	22	0: 0

[a]Franz group Pd/C sourced from Strem. [b]Observed by ^1H NMR spectroscopy.

Pd/C sourced from Strem was tested to ensure the catalytic activity of Pd/C sourced from Sigma-Aldrich was not the contributing factor for the large-scale synthesis of **3.37a** that resulted in protodesilylation (Table **3.3**). For this investigation, a series of concentrations were investigated influenced by silanediol concentration studies performed by Ngon T. Tran, Ph.D. Concentrations of 0.08 M and 0.06 M resulted in exclusive formation of **3.37a** (Table **3.3**, entry 1–2). However, concentrations of 0.03 M and 0.01 M resulted in a 1:1 formation of **3.44** :**3.37a** (Table **3.3**, entry 3–4). This data suggested that the optimal concentrations for the synthesis of **3.37a** were 0.08 M and 0.06 M, and Pd/C sourced from Strem from the Shaw group and Franz group was catalytically active.

Table **3.3** Concentration conditions tested for the synthesis of **3.37a**.

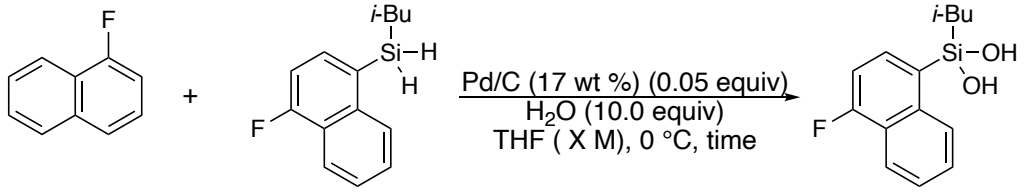

3.44 **3.36a** **3.37a**

entry	scale (mmol)	time (min)	concentration (M)	result (**3**:**44**:**3.37a**)[a]
1	0.09	15	0.08	0: 1
2	0.09	16	0.06	0: 1
3	0.09	12	0.03	1: 1
4	0.09	15	0.01	1: 1

[a]Observed by ^{1}H NMR spectroscopy.

Overall, silanediol **3.37a** was synthesized and isolated in low yield using th combined temperature and concentration results with the opportunity for further optimization (Scheme **3.9**). Pd/C-catalyzed hydrolysis at large scale resulted in protodesilylation. An iridium-catalyzed hydrolysis at a concentration of 0.06 M were the best conditions for access to silanediol **3.37a**.

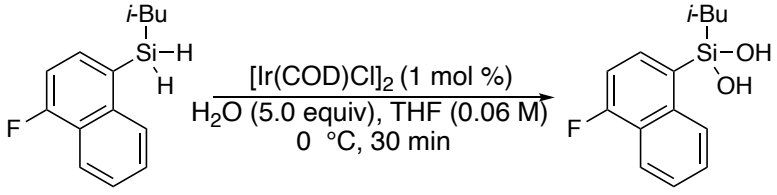

3.36a **3.37a**, 26 %

Scheme **3.9**. Optimized conditions for the synthesis of silanediol **3.37a**.

3.5 Attempts to Improve Synthesis of Chiral 1,3-Disiloxanediols

Given the concentration dependence of silanediols**,** a series of conditions were tested for the synthesis of siloxanol **3.34b** with Pd/C sourced from Strem from the Franz group (Table **3.4**) A small scale test reaction at a concentration 0.08 M and stoichiometric Pd/C resulted in unreacted starting material (Table **3.4**, entry 1). Longer reaction time using 30 mol % Pd/C and a concentration of 0.08 M also resulted in unreacted starting material (Table **3.4**, entry 2). At a con-

centration of 0.03 M using 30 mol % Pd/C, TLC reaction progress monitoring indicated consumption of starting material at 120 min. However, ^{1}H NMR spectroscopy resulted proved unreacted starting material remained (Table **3.4**, entry 3). Pd/C sourced from Strem from the Shaw group was tested at 30 mol% at a concentration of 0.03 M and resulted in unreacted starting material using ^{1}H NMR spectroscopy but TLC reaction progress monitoring indicated otherwise (Table **3.4**, entry 4). When the temperature was increased to 40 °C for 1 hour followed by 60 °C for 1 hour at stoichiometric loading of Pd/C, TLC reaction progress and ^{1}H NMR spectroscopy indicated no consumption of material (Table **3.4**, entry 5). With the success of Iridium-catalyzed hydrolysis for silanediol **3.37a**, Iridium was investigated at a concentration of 0.08 M for the synthesis of **3.34b** and found to result in product formation (Table **3.4**, entry 6).

Table **3.4** Hydrolysis conditions tested for the synthesis of **3.34b**.

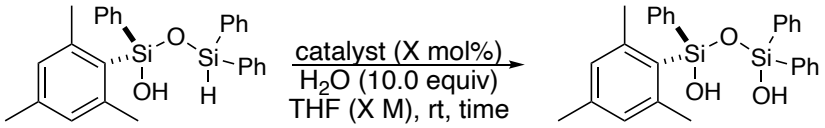

3.44 **3.34b**

entry	scale (mmol)	catalyst[b]	mol %	concent. (M)	time (min)	result[d]
1	0.02	Pd/C	100	0.08	90	unreacted SM
2	0.02	Pd/C	30	0.08	133	unreacted SM
3	0.03	Pd/C	30	0.03	120	unreacted SM
4	0.03	Pd/C[c]	30	0.03	20	unreacted SM
5[a]	0.03	Pd/C	100	0.08	40	unreacted SM
6	0.02	$[Ir(COD)Cl]_2$	3	0.08	15	SM consumed

[a] Reaction ran at 40 °C for 1 h followed by 60 °C for 1 h; TLC reaction progress indicated no consumption of starting material at rt for 40 min; result indicated in entry. [b] Strem Pd/C sourced from Franz Lab. [c] Strem Pd/C sourced from Shaw Lab. [d]Observed using 1H NMR spectroscopy.

Siloxanol **3.34b** was synthesized and isolated in very low yields (Scheme **3.10**) The optimal concentration was determined to be 0.08 M in the presence of $[Ir(COD)Cl]_2$. Pd/C-catalyzed hydrolysis was determined as an inefficient method to access **3.34b** at stoichiometric levels, dif-

ferent concentrations, and temperatures. Further optimization is needed for the synthesis of **3.34b**.

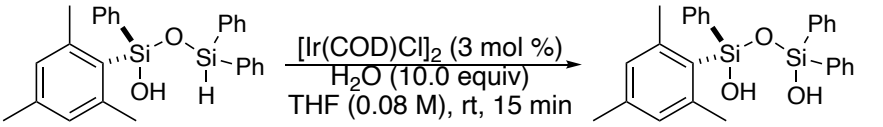

3.44 **3.34b**, 9 %

Scheme **3.10.** Optimized conditions for the synthesis of **3.34b**.

Since the synthesis of chiral 1,3-disiloxanediol required further optimization, solvent and temperature conditions were investigated for the synthesis of precursor **3.44** (Table **3.5**). In the optimization performed by Jacob J. Dalton, Ph.D. for the desymmetrization reaction, chlorobenzene at 20 mol% of **3.27** was found to retain reactivity and lose selectivity (95% yield and 88:12 er) with isobutyl(naphthalen-1-yl)silanediol and chlorosilane **3.26a** at –78 °C.[46] These conditions were applied to silanediol **3.37b** and resulted in complete loss of reactivity and selectivity (18% yield and 66:34 er; Table **3.5**, entry 1). In our preliminary solvent optimization at –40 °C and 20 mol% of **3.27** for the desymmetrization with isobutyl(naphthalen-1-yl)silanediol, chlorosilane **3.26a** was presumed to be a viable parameter and was applied to the synthesis of **3.44**. These conditions resulted in a complete loss of reactivity and selectivity (6% yield and 66:34 er; Table **3.5**, entry 2). Changes in temperature and solvent resulted in no increase in yield for the synthesis of **3.44**.

Table **3.5** Conditions tested for the synthesis of **3.44**.

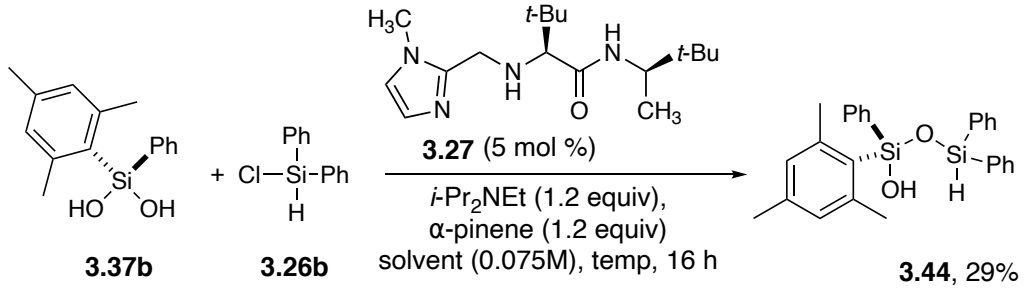

3.37b **3.26b** **3.44**, 29%

entry	solvent	temperature (°C)	yield (%)[a]	er
1	PhCl	–78 °C	18	66:34[b]
2	PhMe	–40 °C	6	66:34[c]

[a]Isolated yield. [b]Determined using HPLC CHIRALPAK AD-H column. [c]Determined using HPLC CHIRALPAK OD-H column.

3.6 Exploration of Chiral 1,3-Disiloxanediols as Hydrogen-bonding Organocatalysts

The Franz group established the first example of a silanediol catalysis for the addition of heteroarenes to *trans-β*-nitrostyrene.[63] Silanediols decorated with mesityl and electron-withdrawing groups exhibited excellent yields (92%). It was also proposed that silanediols engage in self-recognition that allow for silanol acidification to promote effective catalysis, outcompeting a concurrent report.[50] This model reaction is an important carbon–carbon bond forming reaction known to be catalyzed by silica gel[64] and served as an important test reaction. The Franz group has reported a sodium tetrakis[3,5-bis(trifluoromethyl)phenyl]borate (NaBArF)-catalyzed Friedel–Crafts reaction that proceeded in high yields with various phenolic and amino nucleophiles.[65] A catalyst screen was investigated for the synthesis of **3.47** that included catalysts and solvents established from literature precedent (Table **3.6**). With NaBArF at 20 mol% loading resulted in good reactivity (71% yield; Table **3.6**, entry 1). Silica-gel promoted synthesis of **3.47** demonstrated similar reactivity as entry 1 (75% yield; Table **3.6**, entry 2). 1,1,3,3-tetraphenyldisiloxanediol **3.48** resulted in good reactivity (71% yield; Table **3.6**, entry 3). Chiral disiloxanediol **3.34a** at 20 and 10 mol% catalyst loadings exhibited poor reactivity and no selectivity (Table **3.6**, entry 4–5). These results suggested that increased catalyst loadings for chiral

disiloxanediol **3.34a** had no effect on selectivity. The indole addition to *trans-β*-nitrostyrene was deemed not a sufficient test reaction for exploration of chiral 1,3-disiloxanediols.

Table **3.6** Catalysts screen for the synthesis of **3.47**.

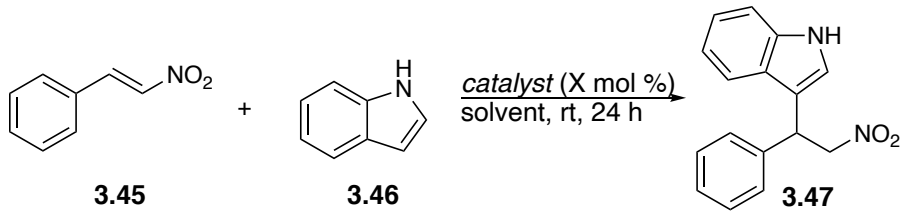

3.45 **3.46** **3.47**

entry	catalyst	mol %	solvent (M)	yield (%)[a]	er[b]
1	$NaBAr^F$	20	PhMe (0.67)	71	N/A
2	silica gel	20	DCM (2.0)	75	N/A
3	**3.48**	20	DCB (1.9)	71	N/A
4	**3.34a**	20	DCB (1.9)	11	55:45
5	**3.34a**	10	DCB (1.9)	6[c](5)	51:49

[a]Isolated yield. [b]Determined using HPLC with Diacel CHIRALPAK AD-H column. [c]Yield determined using ^{1}H NMR spectroscopy using $PhSi(CH_3)_3$ as an internal standard.

The Diels-Alder reaction was chosen as a reference reaction and was catalyzed by TADDOL **3.12** as previously discussed in this chapter. Titration studies using ^{1}H NMR performed by Ngon T. Tran, Ph.D. of organosilanols, ranging from mono- to disiloxanediols, with DMF showcased organosilanols had a higher binding affinity than TADDOL **3.12**.[51] Specifically, 1,1,3,3-tetraphenyldisiloxanediol **3.43** resulted in the highest binding affinity to DMF. The acidity of achiral disiloxanediol **3.48** was calculated to be 5.9;[66] moreover **3.48** catalyzed the Diels-Alder reaction more efficiently than silanediols (72% vs. 56%). These results suggested that chiral 1,3-disiloxanediols were suitable catalysts for exploration as hydrogen-bonding catalysts in the Diels-Alder reaction (Table **3.7**). Chiral disiloxanediol **3.34a** at 20 mol% loading resulted in low reactivity and little to no selectivity (33% yield and 63:37 er) (Table **3.7**, entry 1). Electron-rich chiral disiloxanediol **3.34b** at 20 mol% loading resulted in no selectivity (50:50 er) (Table **3.7**, entry 2). Electron-deficient chiral siloxanol **3.51** at 33 mol % loading resulted in no low reactivity and no selectivity (13% yield and 55:45 er; Table **3.7**, entry 3).

Interestingly, chiral siloxanol **3.51** was hypothesized to activate the diene through single-point activation and not impart selectivity. The slight increase in selectivity observed with chiral disiloxanediol **3.34a** suggested an enhanced binding mode for further exploration. However, chiral disiloxanediol **3.34a** was deemed not a suitable catalyst for further exploration due to synthetic inaccessibility.

Table **3.7** Catalysts screen for the synthesis of **3.55**.

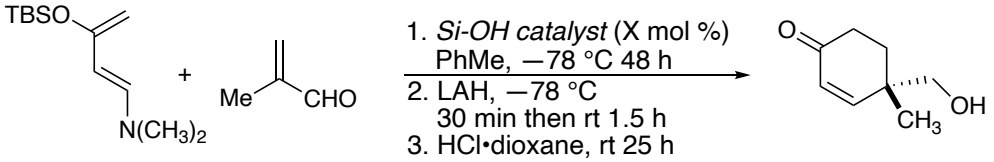

3.48 **3.49** **3.50**

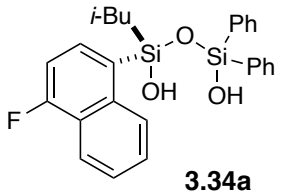

3.34a

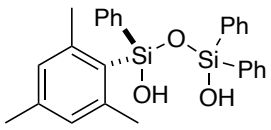

3.34b

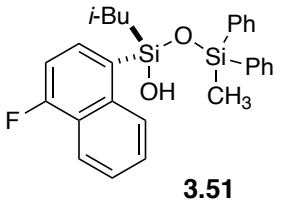

3.51

entry	catalyst	mol%	yield (%) [a]	er
1	**3.34a**	20	33	63:37[c]
2	**3.34b**	20	N/A [b]	50:50 [c]
3	**3.51**	33	13	55:45[d]

[a]Isolated yield. [b] TLC purification taken; see Experimental General Procedure C. [c]Determined using HPLC with Diacel CHIRALPAK OD-H column. [d]Determined using HPLC CHIRALPAK AS-H column.

3.7 ^{1}H NMR Binding Studies of Catalyst 3.27 with Silanediols 3.32a, 3.57a–b, 3.60

The Franz group has been vested in utilizing ^{1}H NMR titrations to quantify hydrogen-bonding strength for its versatility with organosilicon compounds.[46,47,51,55,55] Quantification of hydrogen-bonding has interested the Franz group for its ease with quick data collection suitable for any student while alluding to important information about molecular assembly,[67] anion binding,[47,68] and self-association.[43] Specifically, NMR titration has reigned a powerful tool to understand self-association in 1,3-disiloxanediols as noted through silanol shifts.

With the success of ^{1}H NMR binding studies for the desymmetrization paper,[46] I investigated the hydrogen-bonding interactions between the silanediols and organocatalyst. I was intrigued by the synergistic selectivity "sweet spot" that was taking place utilizing chlorodiphenylsilane **3.21b** to access the precursor necessary for the synthesis of chiral 1,3-disiloxanediols. A notable example of the selectivity "sweet spot" was discussed in Chapter 2 of this dissertation with *tert*-butyl(phenyl)silanediol where this prochiral substrate was necessary for concurrent desymmetrization methodologies being developed at the same time as the Franz group (Scheme **3.11**). When *tert*-butyl(phenyl)silanediol **3.52a** was subjected to the desymmetrization reaction with chloromethyldiphenylsilane **3.53a** reaction partner no reactivity was observed with recovered starting material. When **3.57a** was subjected to the desymmetrization reaction with chlorodiphenylsilane **3.26b** reaction partner some reactivity and negligible selectivity was observed. Notably, isopropyl(phenyl)silanediol **3.52b** when paired with chlorosilanes **3.53a** and **3.26a**, elicited excellent selectivity for **3.54bb** (98:2 er) and partial selectivity for **3.54ba** (65:35 er) (Scheme **3.11**).

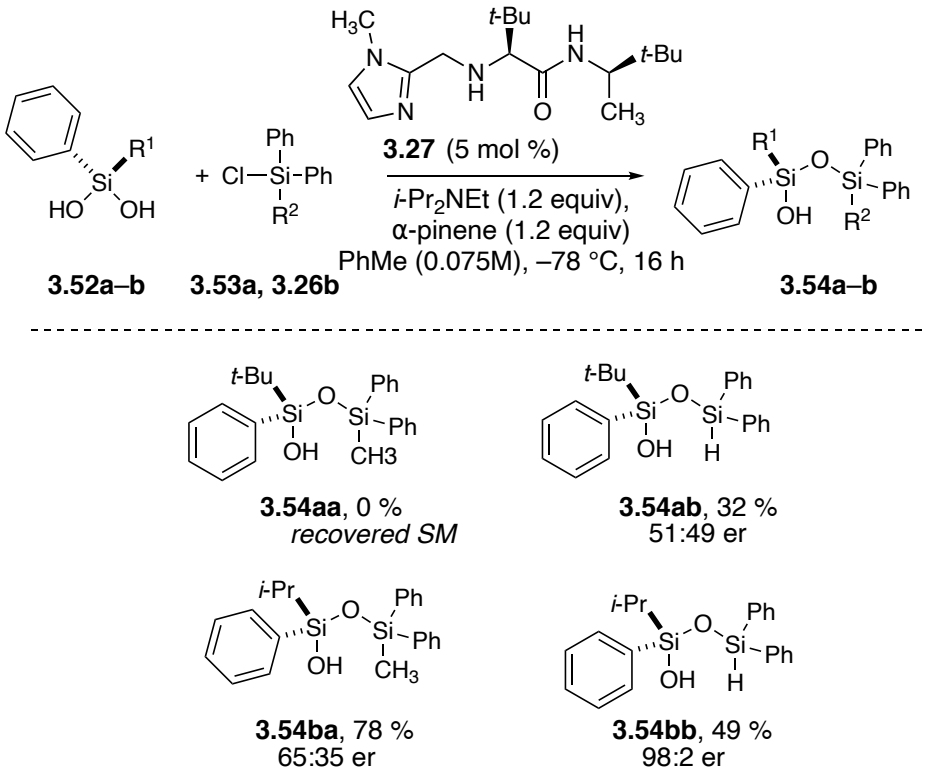

Scheme **3.11.** Desymmetrization of silanediol **3.52a–b** indicating interesting chlorosilane effect on selectivity.

To date, no solid-state co-crystal has been obtained for the desymmetrization products. Attempts to crystallize the products of the desymmetrization reaction, performed by Jacob J. Dalton and myself, were unsuccessful.[69] Therefore, I performed NMR titration studies to probe the hydrogen-bonding interactions of the intermediates necessary for the synthesis of chiral 1,3-disiloxanediols. ^{1}H NMR titration experiments in C_6D_6 were performed with 10 equivalents of **3.37b** in the presence of organocatalysts **3.27**. Silanediol **3.37b** was selected for a binding study as the first example of an aryl-aryl silanediol with high enantioselectivity (96:4 er) using chloro-diphenylsilane **3.26b**. As was the case for *tert*-butyl(phenyl)silanediol **3.52a**, with chloromethyldiphenylsilane **3.53a**, neither reactivity nor selectivity was observed (i.e., unreacted starting material was recovered). This could suggest that chlorodiphenylsilane **3.26b** may be playing a role in the desymmetrization reaction. A downfield amide chemical shift of $\Delta\delta^{NH}$ =

0.15 ppm was observed. Upfield chemical shifts were seen for the imidazole protons, $\Delta\delta^{Ha}$ = 0.12 ppm and $\Delta\delta^{Hb}$ = 0.12 ppm, consistent with a hydrogen-bond interaction (Figure **3.2**A). The binding constant (K_a) was calculated for the imidazole NH peak to be K_a = 26 ± 5 indicative of an apparent weak interaction (Figure **3.2**B).

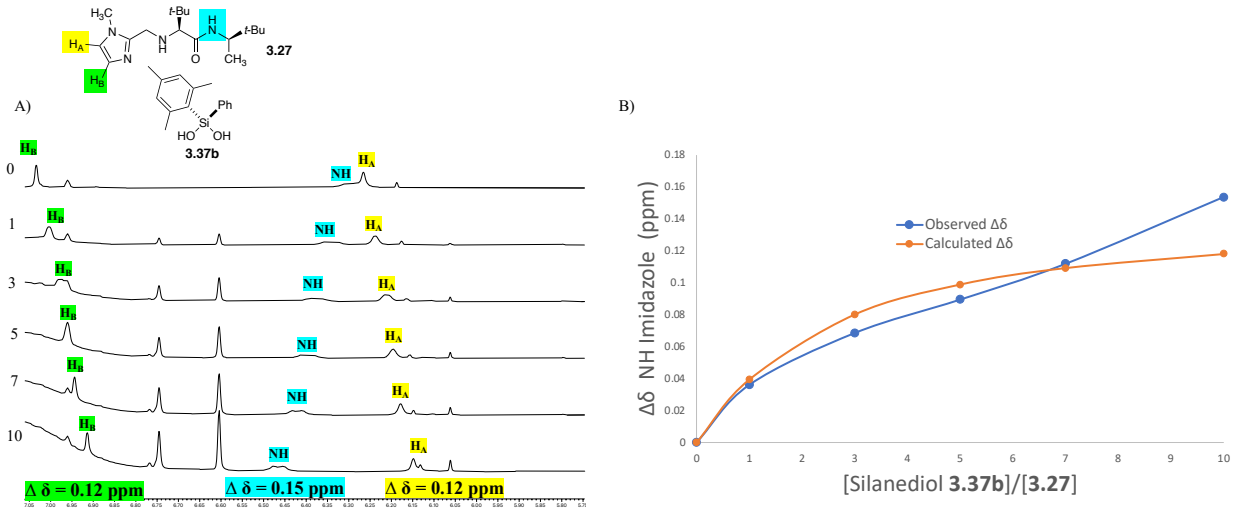

Figure **3.2**. A) ^{1}H NMR binding study of chiral imidazole **3.27** (2 mM in C_6D_6) in the presence of silanediol **3.37b** at 0 = 0 equiv, 1 = 1 equiv, 3 = 3 equiv, 5 = 5 equiv, 7 = 7 equiv, 10 = 10 equiv. Δδ = 0.15 ppm is observed for the NH peak in the presence of 10 equivalents of **3.37b**. b) Binding constant was calculated using ^{1}H NMR titration data for the NH peak; K_a = 26 ± 5.

The desymmetrization reaction was optimized with lead substrate isobutyl(naphthalen-1-yl)silanediol **3.55** and exhibited excellent yield and selectivity with chloromethyldiphenylsilane **3.26b (**98% yield and 98:2 er) and good yield with moderate selectivity with chloromethyl-diphenylsilane **3.53a** (73% yield and 85:15 er) (Scheme **3.5**). In addition to these reasons, **3.55** was selected as a comparison to the additional aryl-alkyl containing silanediols chosen for the subsequent NMR titration studies. When 10 equivalents of **3.55** were titrated in the presence of organocatalyst **3.27**, a downfield amide chemical shift of $\Delta\delta^{NH}$ = 0.21 ppm was observed. Upfield chemical shifts were continued to be seen for the imidazole protons, $\Delta\delta^{Ha}$ = 0.29 ppm and $\Delta\delta^{Hb}$ = 0.40 ppm (Figure **3.3**A). From the ^{1}H NMR data, the binding constant using

imidazole C–H^b peak was calculated to be K_a = 100 ± 11 indicative of a strong interaction (Figure **3.3**B).

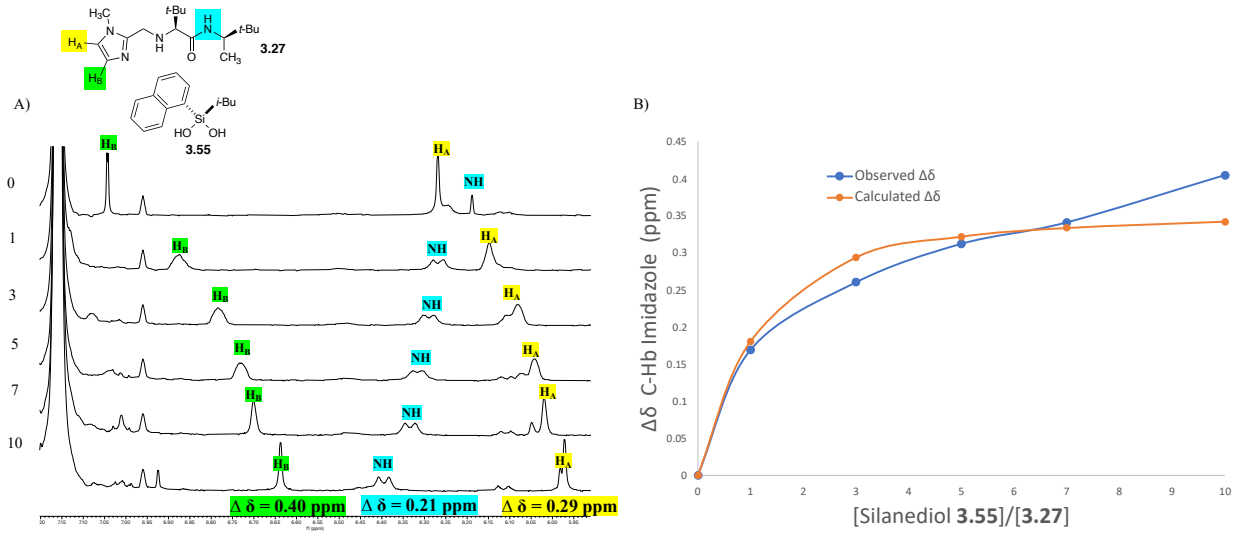

Figure **3.3**. A) ^{1}H NMR binding study of chiral imidazole **3.27** (2 mM in C_6D_6) in the presence of silanediol **3.55** at 0 = 0 equiv, 1 = 1 equiv, 3 = 3 equiv, 5 = 5 equiv, 7 = 7 equiv, 10 = 10 equiv. Δδ = 0.40 ppm is observed for the NH peak in the presence of 10 equivalents of **3.55**. b) Binding constant was calculated using ^{1}H NMR titration data for the imidazole C–H^b peak; K_a = 100 ± 11.

To probe the effects of the *tert*-butyl substituent on the binding interaction *tert*-butyl(phenyl)silanediol **3.54a** was selected. When 10 equivalents of **3.54a** were titrated in the presence of organocatalyst **3.27**, a downfield amide chemical shift of $\Delta\delta^{NH}$ = 0.28 ppm was observed. Upfield chemical shifts were continued to be seen for the imidazole protons, $\Delta\delta^{Ha}$ = 0.23 ppm and $\Delta\delta^{Hb}$ = 0.29 ppm (Figure **3.4**A). From the ^{1}H NMR data, the binding constant using imidazole C–H^a peak was calculated to be K_a = 81 ± 30 indicative of a strong interaction (Figure **3.4**B).

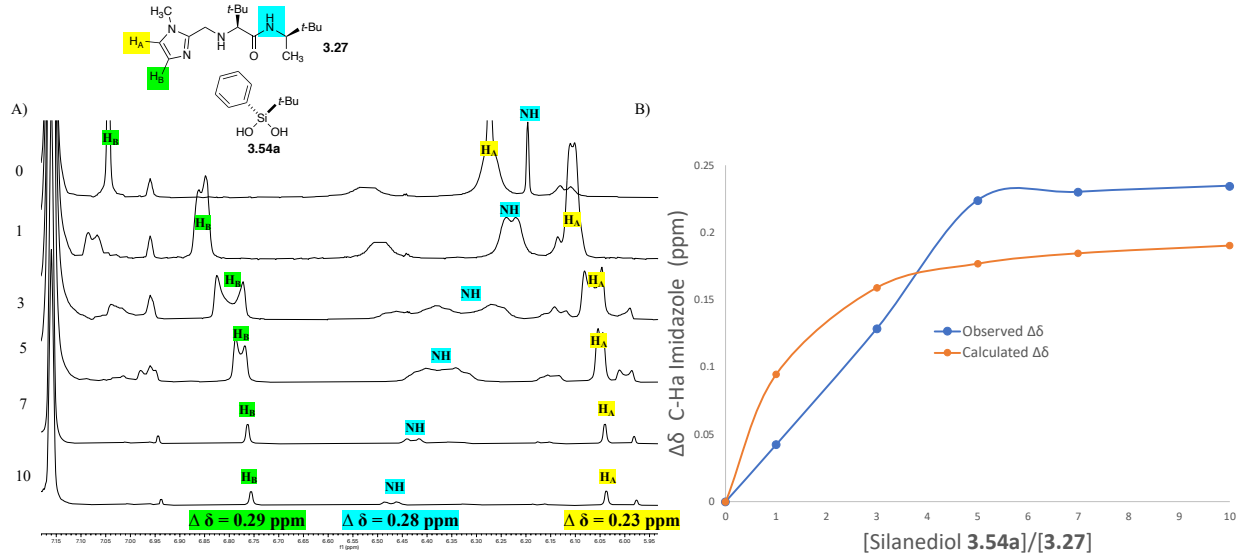

Figure **3.4.** A) ^{1}H NMR binding study of chiral imidazole **3.27** (2 mM in C_6D_6) in the presence of silanediol **3.54a** at 0 = 0 equiv, 1 = 1 equiv, 3 = 3 equiv, 5 = 5 equiv, 7 = 7 equiv, 10 = 10 equiv. Δδ = 0.23 ppm is observed for the NH peak in the presence of 10 equivalents of **3.54a**. b) Binding constant was calculated using ^{1}H NMR titration data for the imidazole C–H^{a} peak ; K_a = 81 ± 30.

Given the performance of isopropyl(phenyl)silanediol **3.54b** in the desymmetrization reaction with chlorosilane **3.21b** (i.e., 98:2 er) it was chosen as an extremely valuable binding partner as a direct comparison point for *tert*-butyl(phenyl)silanediol **3.57a**, which exhibited no selectivity using chlorosilane **3.26b** (i.e., 51:49 er). When 10 equivalents of **3.54b** were titrated in the presence of organocatalyst **3.22**, a downfield amide chemical shift of $\Delta\delta^{NH}$ = 0.25 ppm was observed. Upfield chemical shifts were continued to be seen for the imidazole protons, $\Delta\delta^{Ha}$ = 0.23 ppm and $\Delta\delta^{Hb}$ = 0.11 ppm (Figure **3.5**A). From the ^{1}H NMR data, the binding constant using imidazole C–H^{a} peak was calculated to be K_a = 24 ± 2 indicative of a weak interaction (Figure **3.5**B).

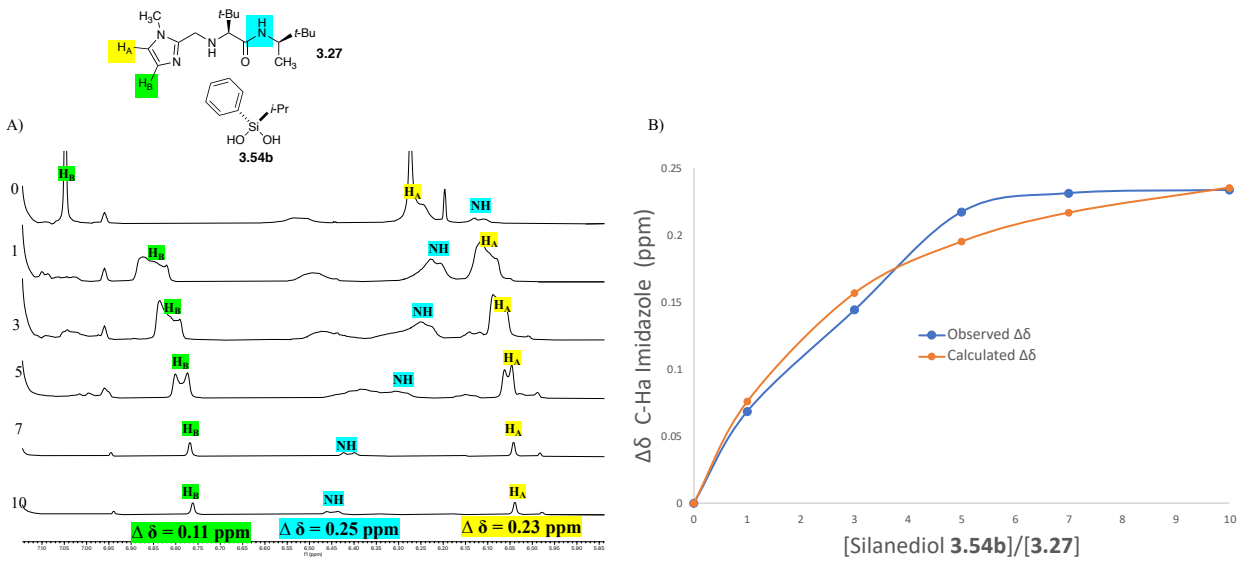

Figure **3.5**. A) ^{1}H NMR binding study of chiral imidazole **3.27** (2 mM in C_6D_6) in the presence of silanediol **3.54b** at 0 = 0 equiv, 1 = 1 equiv, 3 = 3 equiv, 5 = 5 equiv, 7 = 7 equiv, 10 = 10 equiv**.** Δδ = 0.23 ppm is observed for the NH peak in the presence of 10 equivalents of **3.54b**. b) Binding constant was calculated using ^{1}H NMR titration data for the imidazole C–H^{a} peak ; $K_a = 24 \pm 2$.

In Hoveyda and Snapper's seminal paper for *meso*-diol desymmetrization, the authors proposed a transition state model whereby the imidazole of organocatalyst **3.27** enhanced the electrophilicity of the silicon center which allowed for nucleophilic attack from the oxygen of the *meso*-diol that was bound through a two-point binding motif to the amine and carbonyl of the organocatalyst.[70] The Lewis base activation of silicon center allowed for a unique substrate-catalyst association which promoted silylation.[71,72] We have investigated the possible activation of chlorosilane **3.26b** by organocatalysts **3.27.**[46,69] It was determined through this study performed by Jacob J. Dalton, Ph.D. that additional experiments were required to probe the interaction between methyldiphenylchlorosilane **3.53a** and organocatalyst **3.27**. Therefore, I investigated the nature of the interaction between chlorosilane **3.26b** and organocatalyst **3.27.** When 10 equivalents of chlorosilane **3.26b** were titrated in the presence of organocatalyst **3.27**, a dramatic downfield amide chemical shift of $\Delta\delta^{NH} = 2.26$ ppm was observed. Upfield chemical

shifts were continued to be seen for the imidazole protons, $\Delta\delta^{Ha}$ = 0.60 ppm and $\Delta\delta^{Hb}$ = 0.11 ppm (Figure **3.6**A). In contrast to Jacob J. Dalton, Ph.D.'s results, there was no reverse direction of shifts for H^a and H^b. From the ^{1}H NMR data, the binding constant using imidazole NH peak was calculated to be K_a = 246 ± 4 indicative of a very strong interaction (Figure **3.6**B).

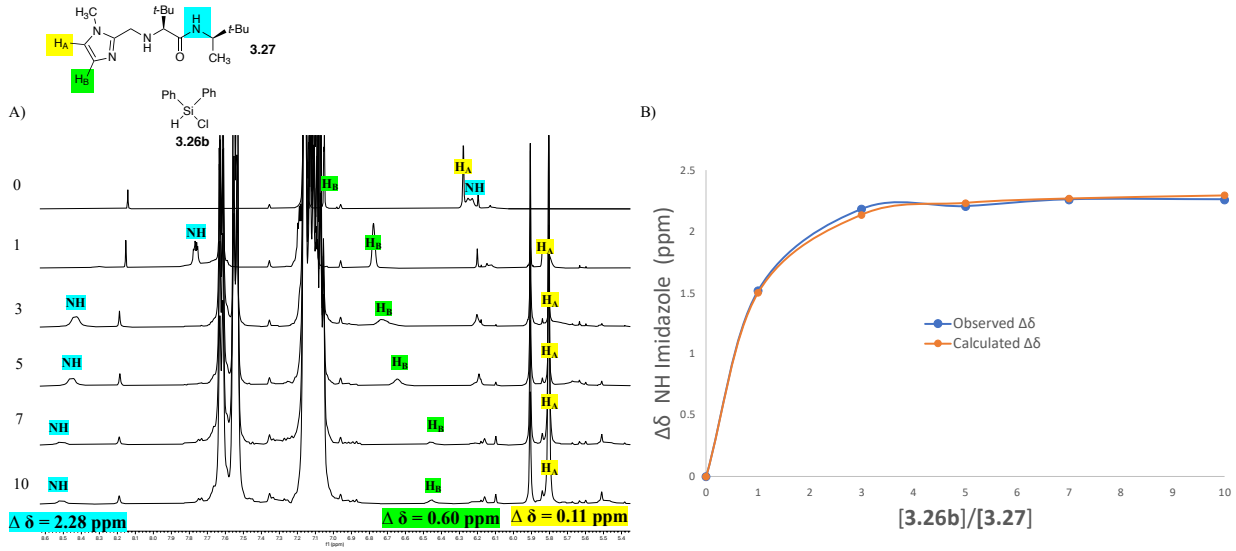

Figure **3.6**. A) ^{1}H NMR binding study of chiral imidazole **3.27** (2 mM in C_6D_6) in the presence of silanediol **3.26b** at 0 = 0 equiv, 1 = 1 equiv, 3 = 3 equiv, 5 = 5 equiv, 7 = 7 equiv, 10 = 10 equiv. Δδ = 2.26 ppm is observed for the NH peak in the presence of 10 equivalents of **3.26b**. b) Binding constant was calculated using ^{1}H NMR titration data for the imidazole NH peak; K_a = 246 ± 4.

In contrast to previous ^{1}H NMR binding data that was related to structural features (i.e. see Chapter 2 of this dissertation), the ^{1}H NMR binding data here exhibited interesting results (Table **3.8**). Diaryl silanediol **3.37b** resulted in a small chemical shift for the imidazole peak H_a (0.12 ppm) with a K_a = 26 ± 5. Surprisingly, diaryl silanediol **3.37b** was selected as a lead diaryl substrate that demonstrated excellent selectivity (96:4 er) for the desymmetrization reaction but exhibited a weak interaction. In contrast, isopropyl(phenyl)silanediol **3.54b** resulted in a larger chemical shift for the imidazole peak H_a (0.23 ppm). Similar to diaryl silanediol **3.37b**, isopropyl(phenyl)silanediol **3.54b** resulted in K_a = 24 ± 2. Here, no trend was attributed to structural features with phenyl rings as the only similarity. However, silanediol **3.37b** and **3.54b**

both exhibited excellent selectivities in the desymmetrization reaction, which alluded to the role of the chlorosilane **3.26b** as a key binding partner.

Table **3.8** Summary of binding data with **3.27** host, and **3.37b**, **3.26b**, **3.54a-b**, and **3.55** guests.

Host	Guest	NH (amide) Δδ (ppm)	H_b (imidazole) Δδ (ppm)	H_a (imidazole) Δδ (ppm)	K_a (M^{-1}) [a]
3.27	**3.37b**	0.15	−0.12	−0.12	26 ± 5
3.27	**3.55**	0.21	−0.40	−0.29	100 ± 11 [b]
3.27	**3.54a**	0.28	−0.29	−0.28	81 ± 30
3.27	**3.54b**	0.25	−0.11	−0.23	24 ± 2
3.27	**3.26b**	2.26	−0.11	−0.60	246 ± 4 [c]

[a] K_a calculated using Δδ for imidazole peak H_a. [b] K_a calculated using Δδ for imidazole peak H_b. [c] K_a calculated using Δδ for imidazole peak NH.

Isobutyl(naphthalen-1-yl)silanediol **3.55** resulted in the largest chemical shift for the imidazole peak H_b (0.40 ppm) with a $K_a = 100 \pm 11$. This result is attributed to the excellent selectivities observed with both chlorosilane **3.26b** and **3.53a** indicative of a strong interaction with organocatalysts **3.27**. Notably, *tert*-butyl(phenyl)silanediol **3.54a** resulted in a large chemical shift for the imidazole peak H_a (0.29 ppm) with a $K_a = 81 \pm 30$. This value is indicative that the bulkiness of the *tert*-butyl group did not interfere with binding when paired with chlorosilane **3.26b** in the desymmetrization reaction and illustrated the lack of reactivity with chlorosilane **3.53a** (i.e., unreacted starting material was recovered). This data suggested that the high selectivity observed with chlorosilane **3.26b** may be related to the potential effect chlorosilane **3.26b** may play as a binding partner in the desymmetrization reaction. This preliminary hypothesis is supported through the ^{1}H NMR binding study of chlorosilane **3.26b** with organocatalysts **3.27**.

3.8 ^{1}H NMR Binding Studies of Pyridine with Chiral 1,3-Disiloxanediol 3.29b

In addition to the investigation of the effect of chlorosilane **3.26b** on the hydrogen-bonding interactions in the desymmetrization reaction, ^{1}H NMR binding studies were utilized to understand the hydrogen-bonding ability of chiral 1,3-disiloxanediols. The Franz group has quantified the ability of 1,3-disiloxanediols to bind anionic Lewis bases[47,49] and neutral Lewis bases. [49] The Franz group has demonstrated the effect of intramolecular hydrogen-bonding on molecular conformation of silanediols using pyridine.[73] Pyridine has been previously used to quantify the proton-donating ability of silanols on silica gel surfaces,[74–76] and was determined to be a good neutral Lewis base for probing hydrogen-bonding interactions of chiral 1,3-disilox-anediols

Achiral disiloxanediols, 1,1,3,3-Tetraphenyldisiloxanediol **3.48**, was investigated for binding to pyridine at a concentration of 0.1 M. When five equivalents of pyridine were titrated in the presence of **3.48**, a downfield chemical shift of the silanol peak ($\Delta\delta$ = 1.55 ppm) was observed (Figure **3.7**A). A binding constant of K_a = 30399 ± 20417 was initially calculated using the ^{1}H NMR titration data for the silanol binding affinity to pyridine (Figure **3.7**B). Due to the large error, the binding constant was determined to not be meaningful. Previous reports in the Franz group have indicated DMF to be an efficient hydrogen-bond acceptor for silanediols[55,63] and disiloxanediols.[49] In these previous experiments at a concentration of 0.01 M with DMF, 1,1,3,3-tetraphenyldisiloxanediol **3.48** exhibited a silanol shift of 2.52 ppm, and 3.44 ppm at a concentration of 0.2 M. In the case of **3.48** with pyridine at 0.1 M, the observed smaller silanol shift suggested that there may be an interference that prevents pyridine hydrogen-bonding with this substrate evident in the large error for the calculated binding affinity.

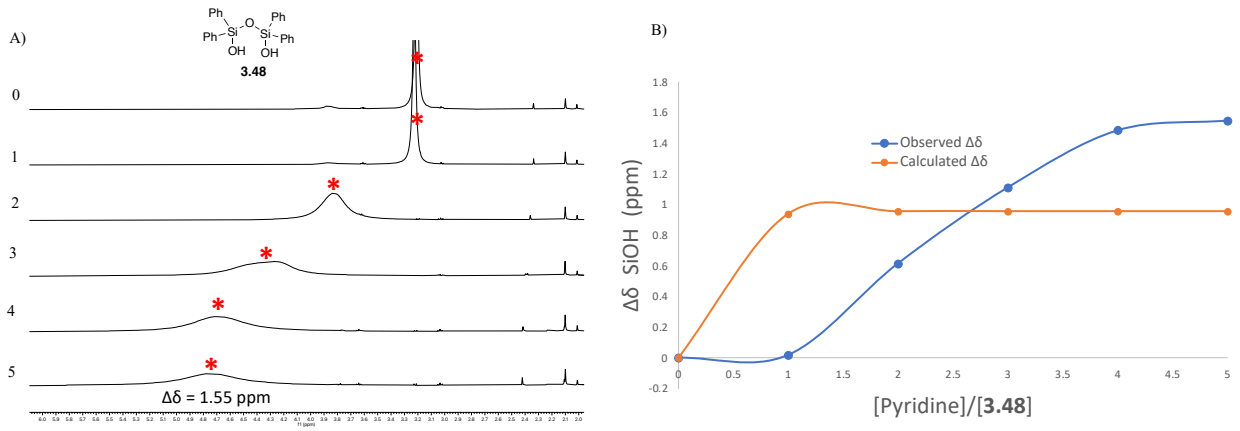

Figure **3.7**. A) ^{1}H NMR binding study of 1,3-disiloxanediol **3.48** (100 mM in C_6D_6) in the presence of pyridine at 0 = 0 equiv, 1 = 1 equiv, 2 = 2 equiv, 3 = 3 equiv, 4 = 4 equiv, 5 = 5 equiv. Δδ = 1.55 ppm is observed for the silanol peak in the presence of 5 equivalents of pyridine B) Attempts to calculate a binding constant calculated using ^{1}H NMR titration data; K_a = 30399 ± 20417.

Chiral disiloxanediol **3.34b** was investigated for binding to pyridine at a concentration of 0.01 M. Previously, at a concentration of 0.01 M with DMF, 1,1,3,3-tetraphenyldisiloxanediol **3.48** exhibited a silanol shift of 2.52 ppm. A similar silanol shift was hypothesized to be observed for chiral disiloxanediol **3.34b**. When five equivalents of pyridine were titrated in the presence of **3.34b**, a small downfield chemical shift of the silanol peak (Δδ = 0.45 ppm) was observed (Figure **3.8**A). Initially, based on this data, a binding constant of K_a = 677 ± 347 was calculated using the ^{1}H NMR titration data (Figure **3.8**B). Due to the large error, the binding constant was determined to not be meaningful, but this data suggested that pyridine only weakly binds to **3.34b**.

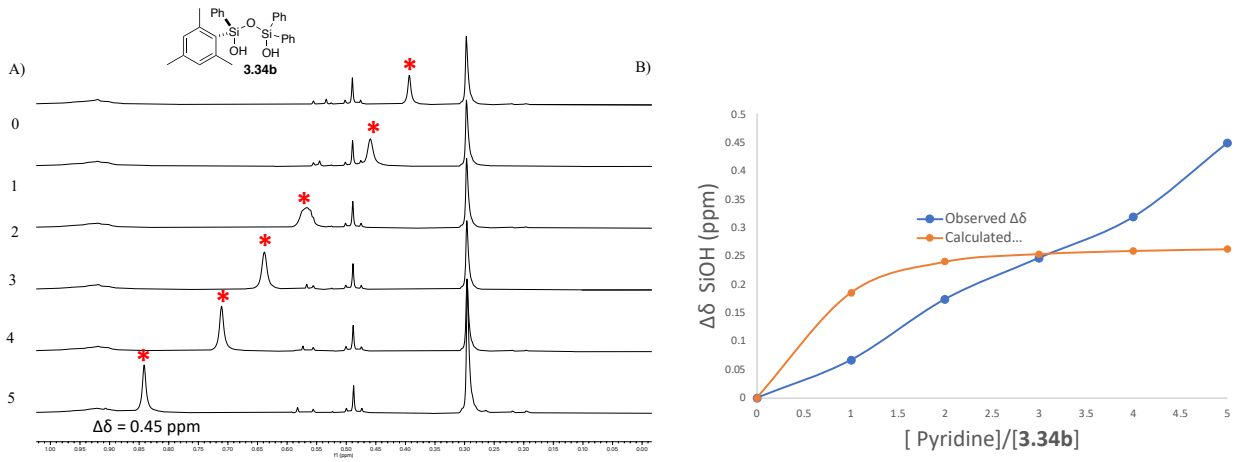

Figure **3.8**. A) ^{1}H NMR binding study of 1,3-disiloxanediol **3.34b** (10 mM in C_6D_6) in the presence of pyridine at 0 = 0 equiv, 1 = 1 equiv, 2 = 2 equiv, 3 = 3 equiv, 4 = 4 equiv, 5 = 5 equiv. Δδ = 0.45 ppm is observed for the silanol peak in the presence of 5 equivalents of pyridine B) Attempts to calculate a binding constant was calculated using ^{1}H NMR titration data; K_a = 677 ± 347.

To probe the effects of the hydrogen-boning ability of **3.34b** with pyridine, an additional data point was added to the previous binding study. With the addition of higher equivalents of pyridine, the silanol OH protons of **3.34b** was hypothesized to form a 2:1 complex with pyridine and thus result in a larger chemical shift. When 10 equivalents of pyridine were titrated in the presence of **3.34b**, a downfield chemical shift of the silanol peak (Δδ = 2.48 ppm) was observed (Figure **3.9**A). Initially, based on this data, a large binding constant of K_a = 11300000 ± 1760000 was calculated using the ^{1}H NMR titration data (Figure **3.9**B). Using 10 equivalents of pyridine had no observed effect on the binding affinity. Due to the large error, the binding constant was determined to not be a reliable result. This experiment further suggested that pyridine may have the ability to bind **3.34b** at higher equivalents.

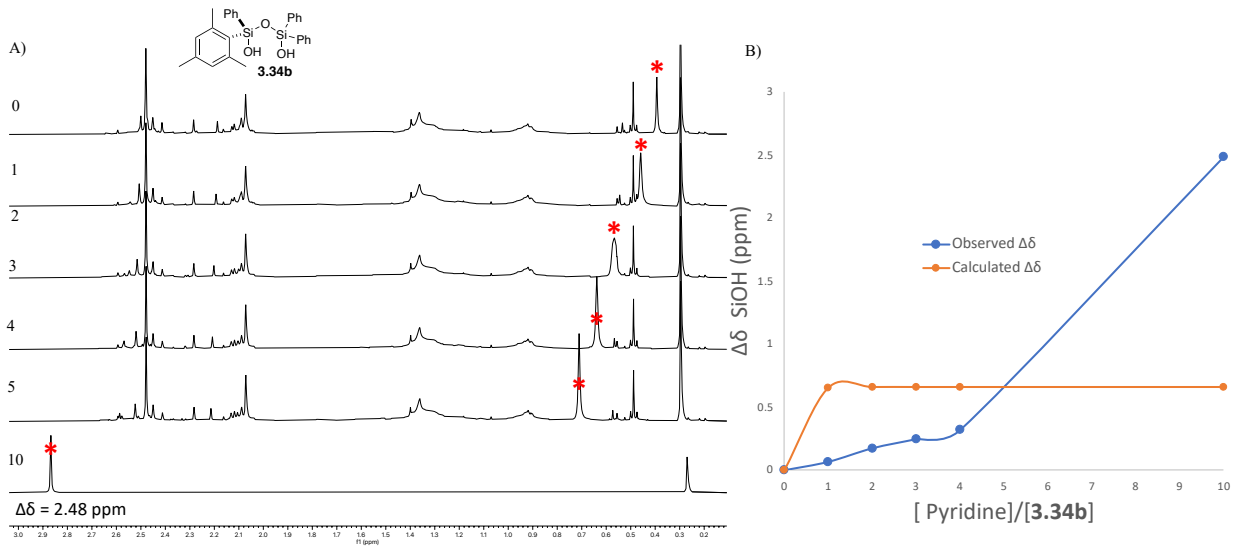

Figure **3.9**. A) ^{1}H NMR binding study of 1,3-disiloxanediol **3.34b** (10 mM in C_6D_6) in the presence of pyridine at 0 = 0 equiv, 1 = 1 equiv, 2 = 2 equiv, 3 = 3 equiv, 4 = 4 equiv, 5 = 5 equiv, 10 = 10 equiv. Δδ = 2.48 ppm is observed for the silanol peak in the presence of 10 equivalents of pyridine B) Attempts to calculate a binding constant was calculated using ^{1}H NMR titration data; K_a = 11300000 ± 1760000.

Chiral disiloxanediol **3.34b** was further purified through a small silica plug with diethyl ether to ensure no impurities were affecting the binding data. When 5 equivalents of pyridine were titrated in the presence of **3.34b**, a small downfield chemical shift of the silanol peak (Δδ = 0.34 ppm) was observed (Figure **3.10**A). A binding constant of $K_a = 9 \pm 3$ was calculated using the ^{1}H NMR titration data for the silanol binding affinity to pyridine (Figure **3.10**B). This data suggested that pyridine very weakly binds to **3.34b** making it a weak hydrogen-bond acceptor for ^{1}H NMR binding studies with chiral 1,3-disiloxanediols at a concentration of 0.003 M. Additionally, this data suggested that the purity of the sample affected previous binding studies.

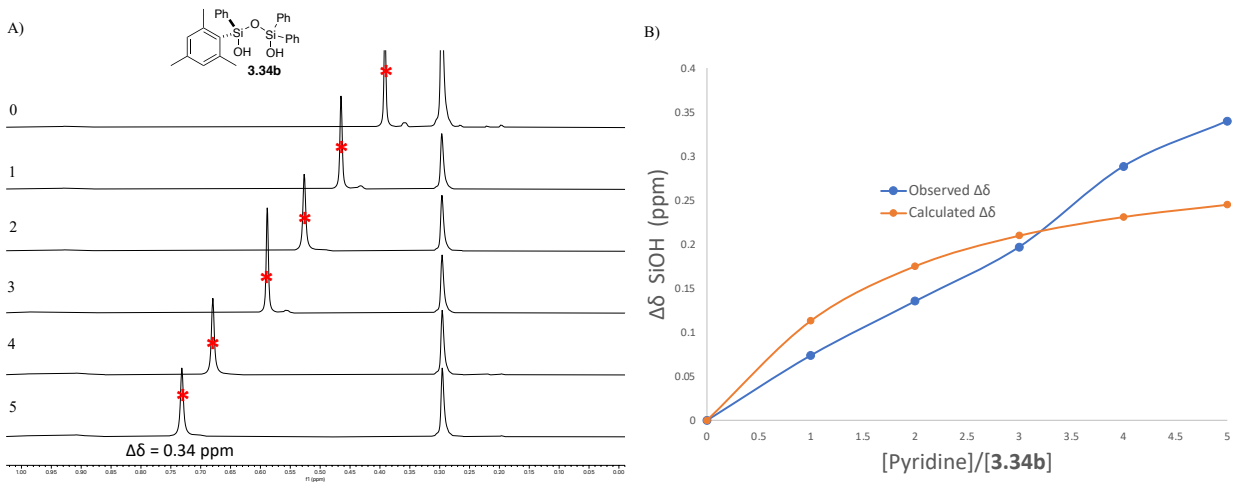

Figure **3.10**. A) ^{1}H NMR binding study of 1,3-disiloxanediol **3.29b** (3 mM in C_6D_6) in the presence of pyridine at 0 = 0 equiv, 1 = 1 equiv, 2 = 2 equiv, 3 = 3 equiv, 4 = 4 equiv, 5 = 5 equiv. Δδ = 0.34 ppm is observed for the silanol peak in the presence of 5 equivalents of pyridine B) Binding constant was calculated using ^{1}H NMR titration data; $K_a = 9 \pm 3$.

The ^{1}H NMR binding data exhibited no trends in binding affinity that are related to structural features. In fact, the bulkiness of the mesityl group was determined to be a possible factor in the apparent weak binding. However, the binding of pyridine to **3.34b** was determined to be the biggest contributing factor in addition to the purity of the sample. The observed ^{1}H NMR chemical shift of silanol peak for **3.34b** is a range that most closely resembles the silanol surface of zeolites (ranges from 1.8 ppm to 5.8 ppm).[77] Overall, this data suggested that pyridine is a weak hydrogen-bond acceptor with **3.34b**. A future redesign of this study should include a few considerations. First, synthesis of chiral 1,3-disiloxanediol in high yields and purity will allow for adequate material. Thereafter, a binding study at a concentration of 100 mM will be a direct comparison to the binding study between achiral disiloxanediol **3.48** and pyridine. The concentration of the binding study is important for accurate calculation of binding affinity. A reinvestigation of pyridine and DMF with chiral 1,3-disiloxanediols will be an ideal starting point.

3.9 Relating Binding Studies with Possible Activation Mode

From my preliminary binding experiments, it was and is inaccurate to predict the active binding mode for (1) indole addition to *trans-β*-nitrostyrene, and (2) Diels–Alder cycloaddition between Rawal's diene and methacrolein. A solid-state co-crystal of an unsymmetrical disiloxanediol, collected by Kayla M. Diemoz, Ph.D.[48,49] and solved by James C. Fettinger, Ph.D. allowed for an extrapolation to be made about a potential binding mode. In the solid-state, the unsymmetrical disiloxanediol decorated with alkyl and electron-withdrawing groups formed a dimeric cluster (Figure **3.11**A). For this solid-state structure, a discrete intermolecular hydrogen-bonded dimeric cluster was observed rather than an intermolecular polymeric hydrogen-bond network. In the solid-state, it was observed that the hydrogen of the silanol in close contact with the fluorine atom on the naphthyl substituent in the adjacent dimeric cluster. It is extrapolated that chiral 1,3-disiloxanediols are possibly exhibiting a similar association in the solution-state (Figure **3.11**). The co-crystal collected by Kayla M. Diemoz, Ph.D. provided insight into the mode of hydrogen-bonding for catalysis using chiral 1,3-disiloxanediol **3.34b** (Figure **3.11**B). Therefore, a dual H-bonding activation or an intramolecular hydrogen-bonding activation may not be favored for catalysis under these conditions. The dual activation mode may be the predominant form required for catalysis. The possibility for cooperative hydrogen-bonding and subsequent single-point activation of electrophiles is also proposed but remains to be investigated. It is imperative for me to communicate in this dissertation that the experiments to determine the active binding modes for the test reactions presented here are still to be performed. Further solution-state studies are needed.

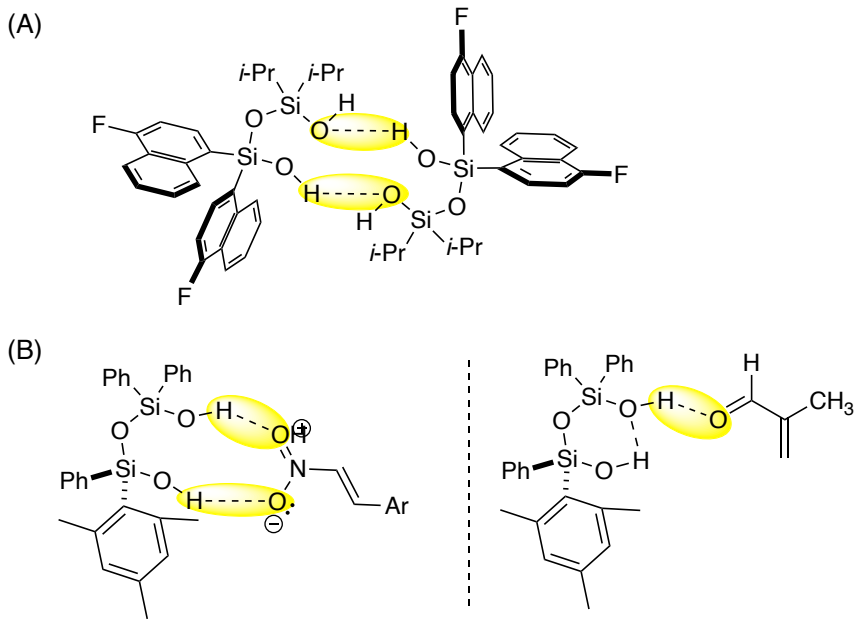

Figure **3.11**.A) Solid-state dimeric cluster of unsymmetrical disiloxanediol performed by. Kayla M. Diemoz, Ph.D. B) Possible dual hydrogen-bond activation mode proposed for the electrophile activation in test reactions.

3.10 Conclusion

In summary, this chapter highlighted the synthesis of chiral 1,3-dsiloxanediols *via* the desymmetrization reaction. Insights for the synthesis of silanediols **3.37a–c** are highlighted below (Figure **3.12**A). The yield for the synthesis of **3.37a** was increased using $[Ir(COD)Cl]_2$. The use of $[Ir(COD)Cl]_2$ reduced protodesilylation. Silanediols containing mesityl groups **3.37b–c** resulted in low yields (ie., ≤10 %) when synthesized at scales above 1.0 mmol. In these specific instances, the yields for **3.37b–c** were increased using a combination of 1) batch scales of 1.0 mmol, and 2) Pd/C sourced from Strem. These results were consistent throughout multiple trials.

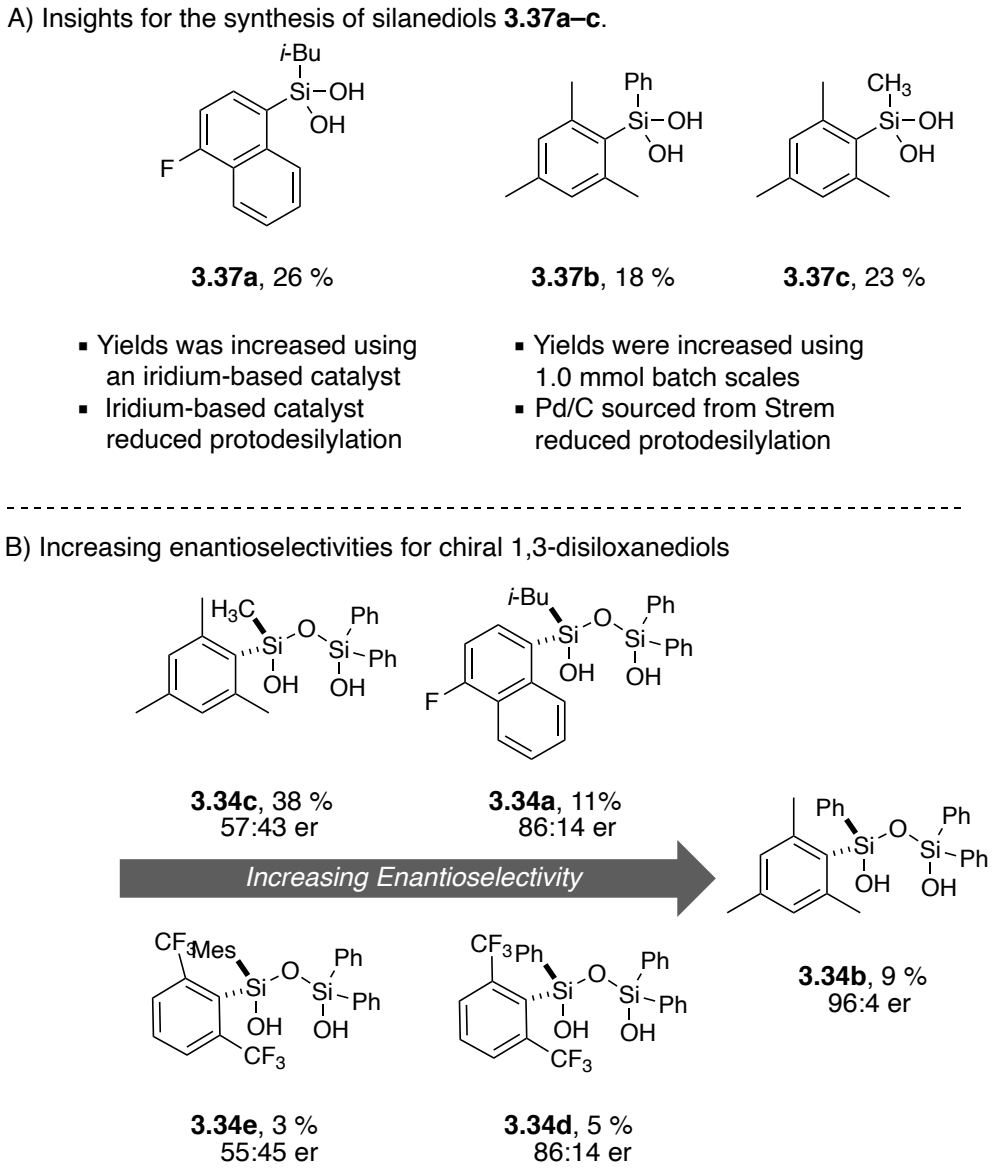

Figure **3.12**. A) Highlights for the synthesis of silanediols **3.37a–c**. B) Effect of substitution pattern around the silicon center on enantioselectivity.

Next, a small collection of chiral 1,3-disiloxanediols were synthesized and resulted in interesting enantioselectivities (Figure **3.12B**). Disiloxanediols containing mesityl groups were found to be either racemic (55:45 er) or highly selective (96:4 er). Chiral disiloxanediols decorated with electron-withdrawing groups demonstrated good enantioselectivity (86:14 er). Chiral disiloxanediol **3.34b** is the first successful desymmetrization of a diaryl silanediol. In

contrast to our initial hypothesis requiring alkyl groups (i.e., isobutyl or isopropyl) for high enantioselectivities, the successful desymmetrization of diaryl silanediol **3.37b** is an exciting result with possible incorporation of axially chiral aryl groups to be incorporated.

After examining chiral disiloxanediol **3.34a** as a hydrogen-bonding organocatalyst, new insights were developed about catalyst design (Figure **3.13**). Chiral disiloxanediol **3.34a** was explored in a hetero Diels–Alder reaction and was found to be slightly reactive and enantioselective (33 % yield and 63:37 er; Figure **3.13**A). In contrast, for the same reaction, fully aryl substituted chiral disiloxanediol **3.34b** was not enantioselective (50:50 er; see Table 3.7 of this chapter). These results suggested that an electron–withdrawing group could serve as a potential design feature for the synthesis of **3.50**. Downstream design of chiral 1,3-disiloxanediols should reflect two key design elements that will greatly influence the enantioselectivity observed in the desymmetrization reaction (Figure **3.13**B). First, prochiral silanediols bearing a combination of aryl–alkyl groups are expected to be selective. Careful attention must be taken when designing diaryl silanediols– since only mesityl(phenyl)silanediol is currently enantioselective for the desymmetrization reaction. Next, chlorosilanes bearing aryl and vinyl groups are expected to exhibit higher levels of enantioselectivity vs. dimethyl(phenyl)– and methyldiphenylchlorosilanes. Ideally, chiral disiloxanediols bearing electron–withdrawing groups are desirable but may not be necessary. The silanediol–chlorosilane pairing is also important for ease of synthetic accessibility. Illustrated below are a few chiral disiloxanediols (**3.63–3.67**) expected to be enantioselective for the desymmetrization and can serve as unique organocatalysts for asymmetric transformations.

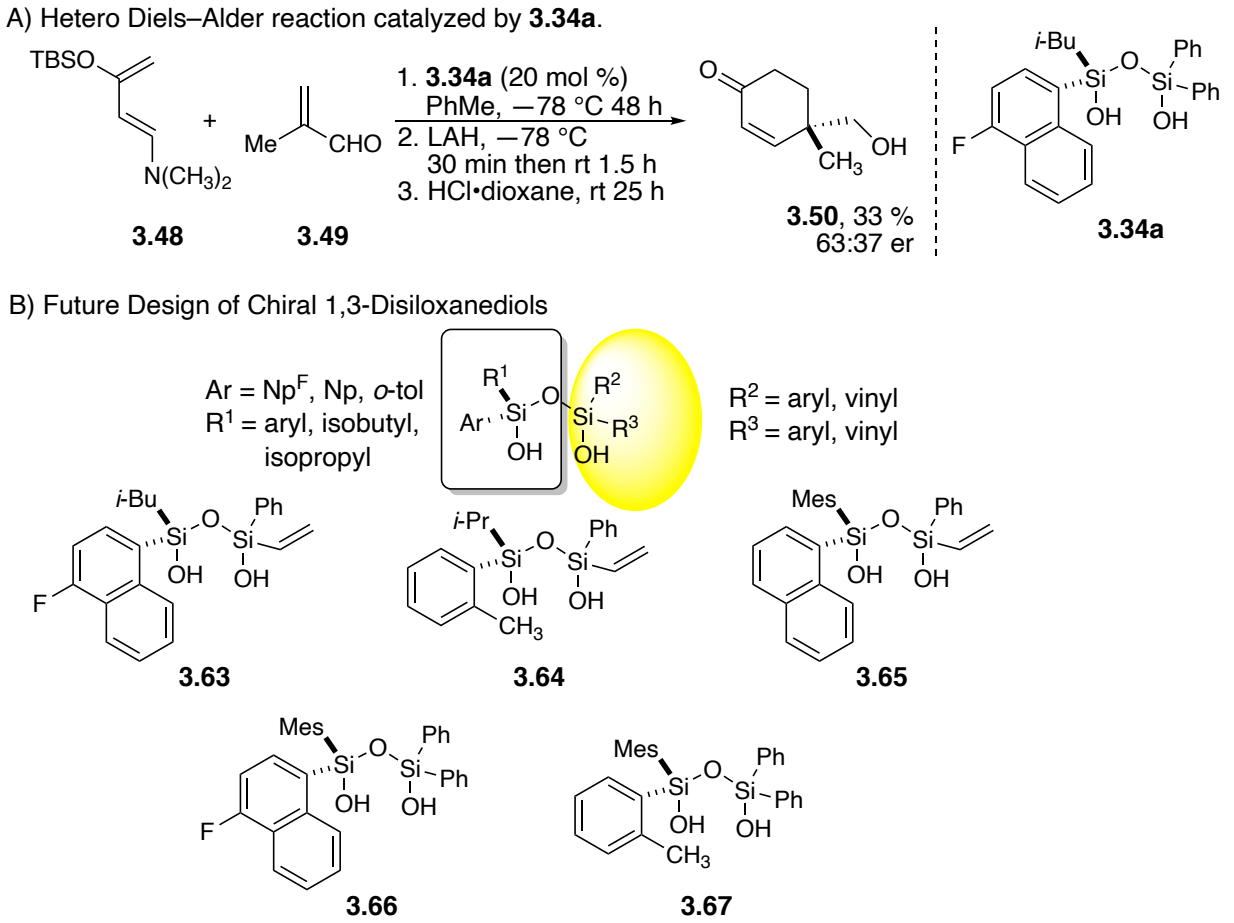

Figure **3.13**. A) Exploration of chiral disiloxanediol **3.34a** as a hydrogen-bonding organocatalyst. B) Key structural features for future design of chiral disiloxanediols.

Lastly, with no solid-state co-crystal of chiral 1,3-disiloxanediols accessed to date, ^{1}H NMR binding studies were used to probe the hydrogen-bonding interactions. The titration studies alluded to the possible role the chlorosilane binding partner may play in the desymmetrization reaction. Additional ^{1}H NMR binding studies of chiral disiloxanediol **3.34b** with pyridine suggested a weak binding interaction (i.e., $K_a = 9 \pm 3$). Varying the Lewis base will provide future insight into the hydrogen-bonding patterns of chiral 1,3-disiloxanediols for their use as a new class of hydrogen-bonding organocatalysts.

3.11 Experimental Procedures

General Information

Synthesis, Purification, and Analysis: Dry THF, Et_2O and PhMe were dispensed from a solvent purification system that passes solvent through two columns of dry neutral alumina prior to use. All other reagents, unless otherwise noted were purchased from commercial sources. Chlorosilanes were purchased from Gelest; magnesium turnings, dibromoethane, diisopropylethylamine, HCl•dioxane, aryl bromides, 4 Å spherical molecular sieves were purchased from Sigma-Aldrich; *N*-methylimidazole (anhydrous bottles) was purchased from Sigma-Aldrich. α-Pinene was purchased from Acros and used without purification. All deuterated solvents were dried under 4 Å spherical molecular sieves for at least 24 hours prior to use in binding and dilution studies. Boc-*tert*-leucine was purchased from Chem Impex. The Pd/C (10 wt %, dry support) used for the synthesis of prochiral silanediols was purchased from Strem; 4.0 M solution of lithium aluminum hydride in THF was purchased from Fisher Chemicals.
All reactions were performed in flame-dried and argon-purged glassware. Reactions were analyzed using thin layer chromatography (TLC) on EMD glass plates that were pre-coated with silica gel 60 F254. The reactions were purified by column chromatography using Acros silica gel 60 Å (0.035–0.070 mm).

Nuclear magnetic resonance (NMR) spectra obtained on Bruker Avance III equipped with Bruker CPTCI Cryoprobe (800 MHz for ^{1}H, 200 MHz for ^{13}C), 600 MHz Bruker Avance III equipped with Bruker CPTCI Cryoprobe (600 MHz for ^{1}H, 151 for ^{13}C), Bruker Avance IIIHD Nanobay Spectrometer(400 MHz for ^{1}H; 101 MHz for ^{13}C; 376, 79MHz for ^{29}Si), 300 MHz Bruker Avance-NEO Spectrometer (300 MHz for 1H; 76 MHz for ^{13}C), and/or Varian VNMRS (600 MHz for ^{1}H; 151 MHz for ^{13}C). The ^{1}H spectral data are reported as follows: chemical

shifts were reported in parts per million downfield from tetramethylsilane internal standard on the δ scale, multiplicity (s, singlet; d, doublet; t, triplet; q, quartet; m, multiplet; dd, doublet of doublets and br, broadened), coupling constant (Hz), and integration. Apparent signals are indicated and are used when signals with multiple couplings appear to form a certain peak type. Carbon NMR chemical shifts are reported in ppm from tetramethylsilane (TMS at 0.0 ppm) with solvent reference employed as the internal standard (deuterochloroform ($CDCl_3$) at. 77.2 ppm or deuterobenzene (C_6D_6) at 128.06 ppm). High-resolution mass spectra (HRMS) were acquired on Thermo Fischer Scientific Electron LTQ-Orbitrap XL Hybrid mass spectrometer on positive ESI mode. High performance liquid chromatography (HPLC) data were obtained on Shimadzu LC-20AB system with CHIRALPAK® AD-H column (4.6 x 250 mm, 5 μm), CHIRALPAK® OD-H column (4.6 x 250 mm, 5 μm) or CHIRALPAK® AS column (4.6 x 250 mm, 5 μm) and Shimadzu SPD-M20A photodiode array detector. Each HPLC sample was eluted at a constant flow rate with isocratic hexanes/isopropanol system and 40 or 30 °C column oven temperature. Nestlab CB 80 Cryocool was utilized to maintain reaction temperature for the desymmetrization reactions which required cryogenic temperatures for 16 h.

General Procedure

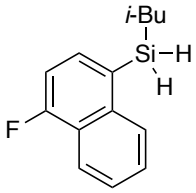

(4-Fluoronaphthalen-1-yl)(isobutyl)silane (3.36a)

To a 250-mL round bottom flask were added magnesium turnings (0.42 g, 17.25 mmol, 1.15 equiv) and flame-dried under high vacuum (< 2 torr) and allowed to cool to room temperature

(23 °C). Once the flask was cooled to room temperature, it was purged three times with argon. THF (0.2 M) and 1,2-dibromoethane (0.19 mL, 2.25 mmol, 0.15 equiv) were then added. The reaction mixture was allowed to stir at room temperature (23 °C) for 21 h or until the reaction mixture was a pitch-black color which is indicative of activated magnesium turnings. Note: In some cases, an off-gray color is also indicative of proper activation of magnesium turnings. Then 1-bromo-4-fluoronaphthalene (3.37 g, 15.0 mmol, 1.0 equiv) was added and left to stir at room temperature (23 °C) for 5-6 h followed by fast addition of isobutyltrichlorosilane (2.49 mL, 15.0 mmol, 1.0 equiv). Note: 5-6 h is the optimal time range to allow for Grignard formation; 1-4 hours and ≥ 6 hours will result in lower yields. Upon addition of isobutyltrichlorosilane a yellow color is a good indicator that the reaction is proceeding accordingly. The reaction was left to stir at room temperature (23 °C) for 19 h. The reaction mixture was then cooled to –78 °C and lithium aluminum hydride (4.0 M, 7.50 mL, 30.0 mmol, 2.0 equiv) was added dropwise. The solution was then allowed to cool to room temperature (23 °C) over a timespan of 3 h. The solution was quenched with Rochelle salt (8 mL) and filtered through Celite. The aqueous phase was extracted with diethyl ether (3 × 25 mL). The combined organic phase was dried over $MgSO_4$, filtered, and concentrated *in vacuo*. The reaction mixture was purified using flash column chromatography (SiO_2, hexanes/EtOAc, 4:1 *v/v*) to yield a 3:1 mixture of 4-fluoronaphthalene **3.44** to silane **3.36a**.

Note: ^{1}H NMR of **3.36a** matches *literature precedent*[46] *and was carried forward to Pd/C hydrolysis.*

^{1}H NMR (400 MHz, $CDCl_3$) δ 8.20 – 8.16 (m, 1H), 7.74 (dd, J = 7.6, 6.1 Hz, 1H), 7.59 (ddd, J = 8.0, 5.6, 1.6 Hz, 2H), 7.41 (td, J = 8.0, 5.4 Hz, 2H), 7.20 – 7.10 (m, 1H, obscured), 4.62 (t, J = 4.0 Hz, 2H), 1.87 (m, 1H), 1.06 (dt, J = 7.0, 4.0 Hz, 2H), 1.01 (d, J = 6.6 Hz, 6H).

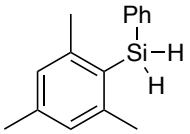

Mesityl(phenyl)silane (3.36b)

To a 250-mL round bottom flask were added magnesium turnings (0.42 g, 17.25 mmol, 1.15 equiv) and flame-dried under high vacuum (< 2 torr) and allowed to cool to room temperature (23 °C). Once the flask was cooled to room temperature, it was purged three times with argon. THF (0.2 M) and 1,2-dibromoethane (0.19 mL, 2.25 mmol 0.15 equiv) were then added. The reaction mixture was left to stir at room temperature (23 °C) for 48 h or until the reaction mixture was a pitch-black color which is indicative of activated magnesium turnings. Note: In some cases, an off-gray color is also indicative of proper activation of magnesium turnings. Then 2-bromomesitylene (2.30 mL, 15.0 mmol,1.0 equiv) was added and left to stir at room temperature (23 °C) for 5-6 h followed by fast addition of phenyltrichlorosilane (2.40 mL, 15.0 mmol, 1.0 equiv). Note: 5-6 h is the optimal time range to allow for Grignard formation; 1-4 hours and ≥ 6 hours will result in lower yields. The reaction was left to stir at room temperature (23 °C) for 18 h. The reaction mixture was then cooled to –78 °C and lithium aluminum hydride (4.0 M, 7.50 mL, 30.0 mmol 2.0 equiv) was added dropwise. The solution was then allowed to cool to room temperature (23 °C) over a timespan of 3 h. The solution was quenched with Rochelle salt (8 mL) and filtered through Celite. The aqueous phase was extracted with diethyl ether (3 × 25 mL). The combined organic phase was dried over $MgSO_4$, filtered, and concentrated *in vacuo*. .

The reaction mixture was purified using flash column chromatography (SiO_2, hexanes/EtOAc, 4:1 *v/v*) to yield silane **3.36b** as an oil with an inseparable impurity.

Note: Silane was passed through a short silica plug with hexanes after purification. Confirmation of the product was achieved using ^{13}C NMR spectroscopy and carried through to the next step.

^{13}C NMR (101 MHz, $CDCl_3$) δ 145.28, 140.22, 138.05, 137.88, 136.42, 135.37, 132.18, 129.65, 129.19, 128.23, 127.08, 23.86, 21.37, 20.81.

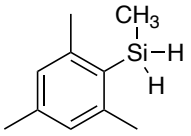

Mesityl(methyl)silane (3.36c)

To a 250-mL round bottom flask were added magnesium turnings (0.42 g, 17.25 mmol, 1.15 equiv) and flame-dried under high vacuum (< 2 torr) and allowed to cool to room temperature (23 °C). Once the flask was cooled to room temperature, it was purged three times with argon. THF (0.2 M) and 1,2-dibromoethane (0.19 mL, 2.25 mmol 0.15 equiv) were then added. The reaction mixture was left to stir at room temperature (23 °C) for 18 h or until the reaction mixture was a pitch-black color which is indicative of activated magnesium turnings. Note: In some cases, an off-gray color is also indicative of proper activation of magnesium turnings. Then 2-mesitylene (2.30 mL, 15.0 mmol,1.0 equiv) was added and left to stir at room temperature (23 °C) for 5-6 h followed by fast addition of methyldichlorosilane (1.60 mL, 15.0 mmol, 1.0 equiv). Note: 5-6 hours is the optimal time range to allow for Grignard formation; 1-4 hours and ≥ 6 hours will result in lower yields. The reaction was left to stir at room temperature (23 °C) for 18

h. The reaction mixture was then cooled to –78 °C and lithium aluminum hydride (4.0 M, 7.50 mL, 30.0 mmol, 2.0 equiv) was added dropwise. The solution was then allowed to cool to room temperature (23 °C) over a timespan of 3 h. The solution was quenched with Rochelle salt (8 mL) and filtered through Celite. The aqueous phase was extracted with diethyl ether (3 × 25 mL). The combined organic phase was dried over $MgSO_4$, filtered, and concentrated *in vacuo*. The reaction mixture was purified using flash column chromatography (SiO_2, hexanes/EtOAc, 4:1 *v/v*) to yield silane **3.31c** as an oil with an oil (1.43 g, 29%). *Note: For reported yield, the reaction mixtures for two 15.0 mmol scale reactions were combined for purification.*

^{1}H NMR (300 MHz, $CDCl_3$) δ 6.87 (s, 2H), 4.44 (q, J = 4.3 Hz, 2H), 2.46 (s, 6H), 2.27 (s, 3H), 0.35 (t, J = 0.7 Hz, 3H). ^{13}C NMR (101 MHz, $CDCl_3$) δ 144.51, 139.57, 129.16, 128.47, 128.30, 127.05, 23.81, 23.55, 21.26, -7.14. ^{29}Si NMR (79 MHz, $CDCl_3$) δ -50.05. HRMS (ESI) m/z: calc for $C_{10}H_{15}Si$ $[M - H]^-$ 163.0943 found 163.0868.

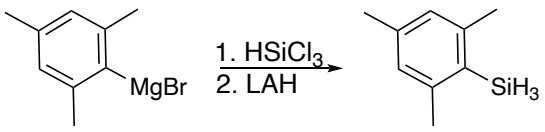

Mesitylsilane (3.39)

Trichlorosilane (0.10 mL, 1.04 mmol, 1.04 equiv) and diethyl ether (0.69 M) were added directly into a flame-dried round-bottom flask with argon. The solution was cooled to –78 °C and 2-mesitylmagnesium bromide (1.0 M in Et_2O, 1.0 mL, 1.0 mmol, 1.0 equiv) and was allowed to cool to room temperature (23 °C) over 2 h. The solution was cooled again to –78 °C and lithium aluminum hydride (4.0 M, 0.75 mL, 3.0 mmol, 3.0 equiv) was added dropwise over a 10 min period. (Caution: Avoid exposing reaction to air since SiH_4, SiH_3Cl, and SiH_2Cl_2 are potential

byproducts and are explosive in the presence of oxygen). The solution was then allowed to cool to room temperature (23 °C) over a timespan of 3 h. The solution was quenched with Rochelle salt (2 mL). The reaction mixture was filtered through Celite and the aqueous phase was extracted with diethyl ether (3 × 5 mL). The combined organic phase was dried over $MgSO_4$, filtered, and concentrated *in vacuo*. The reaction mixture was purified by distillation to yield corresponding silane **3.34** as a colorless oil and matches literature precedent.[56,78]

^{1}H NMR (400 MHz, $CDCl_3$) δ 6.85 (d, J = 26.8 Hz, 2H), 4.16 (d, J = 1.3 Hz, 3H), 2.43 (s, 6H), 2.29 (s, 3H). ^{13}C NMR (101 MHz, $CDCl_3$) δ 145.46, 140.31, 128.56, 127.36, 24.02, 21.62. ^{29}Si NMR (79 MHz, $CDCl_3$) δ -61.47.

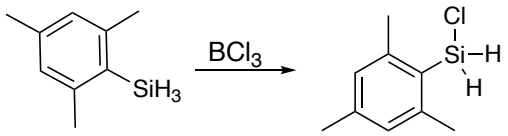

Chloromesitylsilane (3.40)

Mesitylsilane (0.21 g, 1.37 mmol, 1.0 equiv) was dissolved in HPLC-grade hexanes (1.756 M) followed by dropwise-addition of BCl_3 (1.0 M in DCM, 0.52 mL, 0.52 mmol, 0.39 equiv). The reaction was allowed to stir at room temperature (23 °C) over 1 h. The reaction mixture was concentrated *in vacuo* followed by passing through a celite plug to afford chloromesitylsilane **3.35** and matched literature precedent.[78]

^{1}H NMR (400 MHz, $CDCl_3$) δ 6.87 (s, 2H), 5.34 (m, 2H), 2.51 (m, 3H), 2.34 (s, 6H). ^{29}Si NMR (79 MHz, $CDCl_3$) δ -29.253

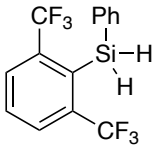

(2,6-bis(trifluoromethyl)phenyl)(phenyl)silane (3.42a)

To a flame-dried round-bottom flask was added 1,3-bis(trifluoromethyl)benzene (78.0 µL, 0.50 mmol, 1.0 equiv) in THF (0.78 M). The reaction mixture was then cooled to –78 °C and TMEDA (80.4 µL, 0.54 mmol, 1.1 equiv) followed by *n*-BuLi (2.32 M in Hexanes, 0.23 mL, 0.53 mmol, 1.05 equiv) were added and allowed to stir at –78 °C for 2 h. To the solution was added chlorophenylsilane (0.14 g,0.55mmol, 1.1 equiv) dropwise. The reaction mixture was then allowed to cool to room temperature (23 °C). The reaction mixture was quenched with $NaHCO_3$ (5 mL). The aqueous phase was extracted with diethyl ether (3 × 5 mL), washed with brine (5 mL), dried over $MgSO_4$, filtered, concentrated in vacuo. *Note: chlorophenylsilane was not commercially available at the time I worked on this project. Attempts to synthesize chlorophenylsilane through reduction of trichlorophenylsilane were unsuccessful resulting in no formation of silane. Selectivity data obtained for the corresponding silanediol* ***3.43a*** *from this substrate for the subsequent desymmetrization reaction was obtained through an archived sample left by Ngon. T. Tran, Ph.D.*[51]

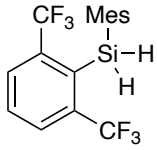

(2,6-bis(trifluoromethyl)phenyl)(mesityl)silane (3.42b)

To a flame-dried round-bottom flask were added 1,3-bis(trifluoromethyl)benzene (30.0 µL, 0.19 mmol, 1.0 equiv) in THF (0.21 M). The reaction mixture was then cooled to –78 °C and

TMEDA (34.7 μL, 0.23 mmol, 1.2 equiv) followed by *n*-BuLi (2.32 M in Hexanes, 0.10 mL, 0.23 mmol, 1.20 equiv) were added and allowed to stir at –78 °C for 2 h. To the solution was added chloromesitylsilane **3.40** (0.92 mL, 0.25 mmol, 1.30 equiv) dropwise. The reaction mixture was then allowed to cool to room temperature (23 °C). The reaction mixture was quenched with $NaHCO_3$ (8 mL). The aqueous phase was extracted with diethyl ether (3 × 5 mL), washed with brine (5 mL), dried over $MgSO_4$, filtered, concentrated in vacuo. *Note: Attempts to synthesize this silane were unsuccessful (see discussion in this chapter pertaining to these reactions). Reported yields here are from Ngon T. Tran Ph.D. dissertation.*[51] *Selectivity data obtained from the corresponding silanediol **3.43b** from this substrate for the subsequent desymmetrization reaction was obtained through an archived sample left by Ngon. T. Tran, Ph.D.*

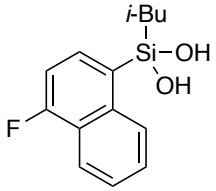

(4-Fluoronaphthalen-1-yl)(isobutyl)silanediol (3.37a)

To a flame-dried round-bottom flask purged with argon were added $[Ir(COD)Cl]_2$ (5.3 mg, 0.01 mmol, 0.24 equiv). Silane (0.06 M in THF, 13.0 mL, 1.0 mmol, 1.0 equiv) was added after being dissolved in THF followed by the addition of deionized water (71.7 μL, 3.98 mmol, 5.0 equiv). (Caution: H_2 gas evolves as the reaction proceeds). The reaction was capped with a septum and allowed to stir at room temperature (23 °C). The reaction was monitored using TLC for the consumption of starting material silane (TLC conditions: hexanes/EtOAc, 4:1 *v/v*). Once silane was fully consumed at. 30 min, the reaction was filtered through Celite to remove $[Ir(COD)Cl]_2$.

The filtrate was dried over $MgSO_4$ filtered and concentrated *in vacuo*. The reaction mixture was purified using flash chromatography (SiO_2, hexanes/EtOAc, 4:1 *v/v* hexanes: EtOAc) to yield corresponding silanediol **3.32a** as a white solid (13.8 mg, 26%) and matches literature precedent.[46]

^{1}H NMR (300 MHz, C_6D_6) δ 8.44 (d, 0H), 8.17 (m, 1H), 7.77 (dd, 1H), 7.26 (m, 2H), 6.94 (ddd, *J* = 10.6, 7.6, 5.7 Hz, 1H), 3.08 (s, 2H), 1.10 (td, *J* = 7.0, 3.8 Hz, 2H), 0.89 (m, 6H).

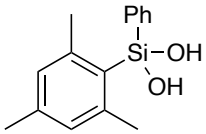

Mesityl(phenyl)silanediol (3.37b)

To a flame-dried round-bottom flask purged with argon were added Pd/C (Strem 10 wt %, 7.0 mg, 0.05 mmol, 0.05 equiv) and was dissolved. Then, silane (0.0 8M in THF, 12.5 mL, 1.0 mmol, 1.0 equiv) was added followed by the addition of deionized water (0.18 mL, 10.00 mmol, 10.0 equiv). (Caution: H_2 gas evolves as the reaction proceeds). The reaction was capped with a septum and allowed to stir at room temperature (23 °C). The reaction was monitored using TLC for the consumption of starting material silane (TLC conditions: hexanes/EtOAc, 4:1 *v/v*). Once silane was fully consumed in 30 min, the reaction was filtered through Celite to remove Pd/C. The filtrate was dried over $MgSO_4$ filtered and concentrated *in vacuo*. The reaction mixture was purified by trituration with hexanes to yield corresponding silanediol **3.37b** as a white solid (0.51 g, 18%).

Note: Reported yield above is for a batch synthesis of eleven 1.0 mmol reactions ran individually and combined for purification. Batch syntheses were found to improve yields significantly with less observed protodesilylation that is more prominent in one large scale reaction.

^{1}H NMR (300 MHz, C_6D_6) δ 7.16–7.14 (m, 5H), 6.74 (d, *J* = 6.9 Hz, 2H), 2.52 (d, *J* = 7.8 Hz, 6H), 2.10 (d, *J* = 5.4 Hz, 3H), 0.44 (s, 2H). ^{13}C NMR (101 MHz, C_6D_6) δ 145.58, 139.91, 138.03, 136.31, 134.14, 130.09, 129.48, 128.74, 24.59, 23.76. ^{29}Si NMR (79 MHz, C_6D_6) δ -22.41. HRMS (ESI) m/z: calc for $C_{15}H_{16}O_2Si$ $[M - H]^-$ 257.0998 found 257.0997.

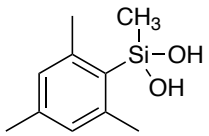

Mesityl(methyl)silanediol (3.37c)

To a flame-dried round-bottom flask purged with argon were added Pd/C (Strem 10 wt %, 5.3 mg, 0.05 mmol, 0.05 equiv). Then, silane (0.08 M, 12.5 mL, 1.0 mmol, 1.0 equiv) was added followed by the addition of deionized water (0.18 mL, 10.0 mmol, 10.0 equiv). (Caution: H_2 gas evolves as the reaction proceeds). The reaction was capped with a septum and allowed to stir at room temperature (23 °C). The reaction was monitored using TLC for the consumption of starting material silane (TLC conditions: hexanes/EtOAc, 4:1 *v/v*). Once silane was fully consumed at 15 min, the reaction was filtered through Celite to remove Pd/C. The filtrate was dried over $MgSO_4$ filtered and concentrated *in vacuo*. The reaction mixture was purified *via* trituration with hexanes to yield corresponding silanediol **3.37c** as a white solid (0.40 g, 23%).

*Note: Reported yield above is for a batch synthesis of nine 1.0 mmol reactions ran individually and combined for purification. Batch syntheses were assumed to also work well with **3.37c** given the success of batch yields for silanediol **3.37b**.*

^{1}H NMR (400 MHz, C_6D_6) δ 6.71 (s, 2H), 4.61 (s, 6H), 2.10 (s, 3H), 0.39 (s, 3H). ^{13}C NMR (101 MHz, C_6D_6) δ 144.47, 139.27, 130.16, 129.30, 129.22, 24.19, 24.10, 20.85, 1.29.^{29}Si NMR (79 MHz, C_6D_6) δ -12.24. HRMS (ESI) m/z: calc for $C_{10}H_{15}O_2Si$ $[M\text{-}H]^-$ 195.0842 found 195.0836.

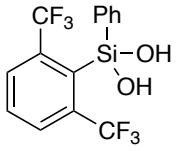

(2,6-bis(trifluoromethyl)phenyl)(phenyl)silanediol (3.43a)

To a flame-dried round-bottom flask purged with argon were added Pd/C (5 wt %, 0.05 equiv) and was dissolved in diethyl ether (0.63 M). Silane **3.42a** (1.0 equiv) was added after being dissolved in a minimum amount of THF followed by the addition of deionized water (5.0 equiv). (Caution: H_2 gas evolves as the reaction proceeds). The reaction was allowed to stir at room temperature (23 °C) for 18 h. Once silane was fully consumed, the reaction was filtered through Celite. The filtrate was dried over $MgSO_4$ filtered and concentrated *in vacuo*. The reaction mixture was purified using flash chromatography (SiO_2, hexanes/Et_2O, 10:1 *v/v*) to yield corresponding silanediol **3.43a** (88%). *Note: Attempts to synthesize the silane precursor were unsuccessful since chlorophenylsilane was not commercially available at the time I worked on this project. Attempts to synthesize chlorophenylsilane through reduction of trichlorophenylsilane were unsuccessful (see discussion in this chapter pertaining to these reactions). Therefore, reported yields here are from Ngon T. Tran Ph.D. dissertation.*[51] *Selectivity data obtained from this substrate for the subsequent desymmetrization reaction was obtained*

through an archived sample left by Ngon. T. Tran, Ph.D. Compound was fully characterized prior to use.

^{1}H NMR (300 MHz, C_6D_6) δ 7.59 (m, 2H), 7.41 (d, J = 7.9 Hz, 2H), 7.14 (s, 3H), 6.75 (t, J = 8.0 Hz, 1H), 2.41 (s, 2H). ^{13}C NMR (101 MHz, C_6D_6) δ 138.18 (q, $^{1}J_{CF}$= 31.2 Hz), 133.99, 130.37 (d, $^{2}J_{CF}$ = 21.9 Hz), 129.66 (q, $^{1}J_{CF}$ = 5.5 Hz), 127.80, 126.04, 123.31.^{19}F NMR (376 MHz, C_6D_6) δ -54.39, -54.57. HRMS (ESI) m/z: calc for $C_{14}H_9F_6O_2Si$ $[M-H]^-$ 351.0376 found 352.0269.

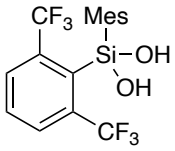

(2,6-bis(trifluoromethyl)phenyl)(mesityl)silanediol (3.43b)

To a flame-dried round-bottom flask purged with argon were added Pd/C (5 wt %, 0.05 equiv) and was dissolved in diethyl ether (0.63 M). Silane (1.0 equiv) was added after being dissolved followed by the addition of deionized water (5.0 equiv). (Caution: H_2 gas evolves as the reaction proceeds). The reaction was allowed to stir at room temperature (23 °C) for 18 h. Once silane was fully consumed, the reaction was filtered through Celite. The filtrate was dried over $MgSO_4$ filtered and concentrated *in vacuo*. The reaction mixture was purified using flash chromatography (SiO_2, hexanes/Et_2O, 10:1 *v/v*) to yield corresponding silanediol **3.43b** (89%). *Note: Attempts to synthesize the silane precursor were unsuccessful. (see discussion in this chapter pertaining to these reactions). Therefore, reported yields here are from Ngon T. Tran Ph.D. dissertation.*[51,55] S*electivity data obtained from this substrate for the subsequent*

desymmetrization reaction was obtained through an archived sample left by Ngon. T. Tran, Ph.D. Compound was fully characterized prior to use.

^{1}H NMR (400 MHz, C_6D_6) δ 7.87 (m, 1H), 7.26 (d, J = 7.9 Hz, 1H), 6.68 (m, 2H), 3.58 (s, 2H), 2.31 (s, 2H), 2.06 (s, 3H). ^{13}C NMR (101 MHz, C_6D_6) δ 144.77, 144.25, 141.11, 140.48, 137.57, 135.31 (q, $^{2}J_{CF}$ = 32.3 Hz), 131.95, 129.43, 125.69, 125.06, 122.65 (t, $^{1}J_{CF}$ = 30.8 Hz), 23.88, 20.82.^{29}Si NMR (79 MHz, C_6D_6) δ -29.76. ^{19}F NMR (376 MHz, C_6D_6) δ -58.93, -63.22. HRMS (ESI) m/z: calc for $C_{17}H_{15}F_6O_2Si_2$ $[M-H]^-$ 393.0746 found 393.0741.

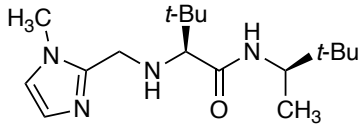

(*S*)-*N*-((*R*)-3,3-dimethylbutan-2-yl)-3,3-dimethyl-2-(((1-methyl-1*H*-imidazol-2-yl)methyl)amino)butanamide (3.27)

Compound **3.27** was synthesized according to literature precedent and found to match ^{1}H NMR signals for previously reported compound.[70]

^{1}H NMR (600 MHz, $CDCl_3$) δ 6.94 (d, J = 1.0 Hz, 1H), 6.82 (d, J = 1.0 Hz, 1H), 6.56 (d, J = 9.6 Hz, 1H), 3.92 (dq, J = 9.8, 6.8 Hz, 1H), 3.80 (d, J = 14.0 Hz, 1H), 3.63 (s, 3H), 3.62 (m, 1H), 2.69 (s, 1H), 1.77 (s, br, 1H), 1.07 (d, J = 6.8 Hz, 3H), 0.97 (s, 9H), 0.93 (s, 9H).

General Procedure A: Desymmetrization of Prochiral Silanediols

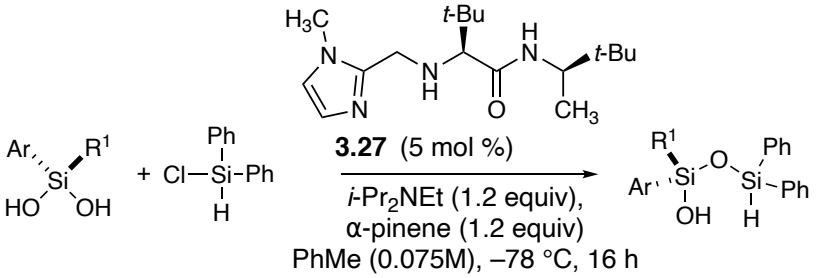

Siloxanols were synthesized utilizing previous reported literature precedent.[46] To a flame-dried round bottom flask purged with argon were added silanediols (0.15 mmol, 1.0 equiv), followed by organocatalyst **3.27** (0.0075 mmol, 0.05 equiv) and dissolved in PhMe (0.075 M). The solution was cooled to –78 °C, followed by addition of *i*-Pr$_2$NEt (0.18 mmol, 1.2 equiv), α–pinene (0.18 mmol, 1.2 equiv), and diphenylchlorosilane **(**0.15 mmol, 1.0 equiv). The reaction was then transferred to the cryocool to maintain the reaction temperature for 16 h. The reaction was monitored using TLC for the consumption of starting material silanediol. TLC conditions: hexanes/EtOAc, 4:1 *v/v*. The solution was quenched with aqueous 10% citric acid (2 mL) and extracted with diethyl ether (3 × 5 mL) washed with brine, dried over $MgSO_4$ filtered and concentrated *in vacuo*. The reaction mixture was purified using flash chromatography (SiO_2, hexanes/EtOAc, (9:1 or 4:1 *v/v* depending on substrate see characterization data below) to yield corresponding siloxanols. HPLC analysis was performed after purification unless otherwise noted. Note: freshly purchased diphenylchlorosilane was utilized for all stereogenic-siloxanols formed. Since there is always residual HCl in chlorosilanes, it is best to prevent any exposure to moisture when handling the bottle. Therefore, each time diphenylchlorosilane was utilized it was capped with a septum and argon balloon.

General Procedure B: Synthesis of racemic standards for use as HPLC standards

For synthesis of racemic siloxanols, the procedure for the desymmetrization of prochiral silanediols was followed with *N*-methylimidazole (NMI) (1.0 equiv) used in place of organocatalyst **3.27**. In some cases, utilizing NMI for the racemic standard will result in undesired side products, including the trisiloxane. These side products could be difficult or impossible to separate from the desired racemic products. To circumvent this difficulty, a 1:3 mixture of organocatalyst: NMI will result in racemic or scalemic products in higher yields and without undesired side products depending on the discrete silanediol and chlorosilane pairing. Siloxanol **3.65** was the only substrate where trisiloxane was exclusively observed. Since synthesizing the prochiral silanediol for this substrate was unsuccessful through many attempts, it may still be possible to use the procedure above for access to a racemic standard.

General Procedure C: Procedure for HPLC Analysis of Non-Purified Products

The silica-filtered reaction mixture was spotted (5 times) as a line on a TLC plate (5 × 5 cm). The plate was allowed to develop (TLC conditions: hexanes/EtOAc, 4:1 *v/v*), and the product band was etched off the TLC plate with a new and not used razor blade. The loose silica gel was washed with hexanes/isopropanol (IPA) (0.5 mL, 9:1 *v/v*) and filtered through a glass fiber to furnish HPLC samples. *Note: For purified products with higher yields, the enantiomeric ratios were not affected by using this procedure.*

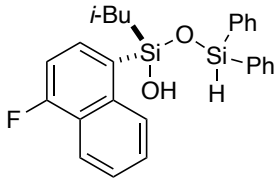

(*S*)-1-(4-Fluoronaphthalen-1-yl)-1-isobutyl-3,3-diphenyldisiloxan-1-ol (3.56)

Synthesized according to General Procedure A using (4-fluoronaphthalen-1yl)(isobutyl)silanediol (0.21 g, 0.80 mmol, 1.0 equiv), organocatalyst **3.27** (12.3 mg, 0.05 mmol, 0.05 equiv), diisopropylethylamine (0.16 mL, 0.95 mmol, 1.2 equiv), α-pinene (0.15 mL, 0.95 mmol, 1.2 equiv) and diphenylchlorosilane (0.16 mL, 0.80 mmol, 1.0 equiv) for the largest upscaled reaction. The reaction was purified using flash column chromatography (SiO_2, hexanes/EtOAc, 9:1 *v/v*) to give siloxanol as an off-white film (0.25 g, 26%) *Note: Reported yield is average of 4 trials.*

^{1}H NMR (300 MHz, C_6D_6) δ 8.41 (m, 1H), 8.16 (dd, *J* = 7.8, 1.9 Hz, 1H), 7.80 (dd, *J* = 7.7, 6.2 Hz, 1H), 7.68 (m, 3H), 7.19 (m, 3H), 6.89 (dd, *J* = 10.6, 7.7 Hz, 1H), 5.91 (s, 1H), 2.10 (s, 1H), 1.87 (m, 1H), 0.98 (m, 2H), 0.88 (m, 6H). ^{29}Si NMR (79 MHz, C_6D_6) δ -21.81, -29.98. ^{13}C NMR (101 MHz, C_6D_6) δ 130.31, 130.28, 128.35, 126.02, 124.17, 121.14, 108.94, 108.75, 31.73, 25.97, 22.82, 14.11. HRMS (ESI) m/z: calc for $C_{26}H_{26}FO_2Si_2$ $[M-H]^-$ 446.1456 found 445.1464.

Racemic standard for **3.56**

<Chromatogram>

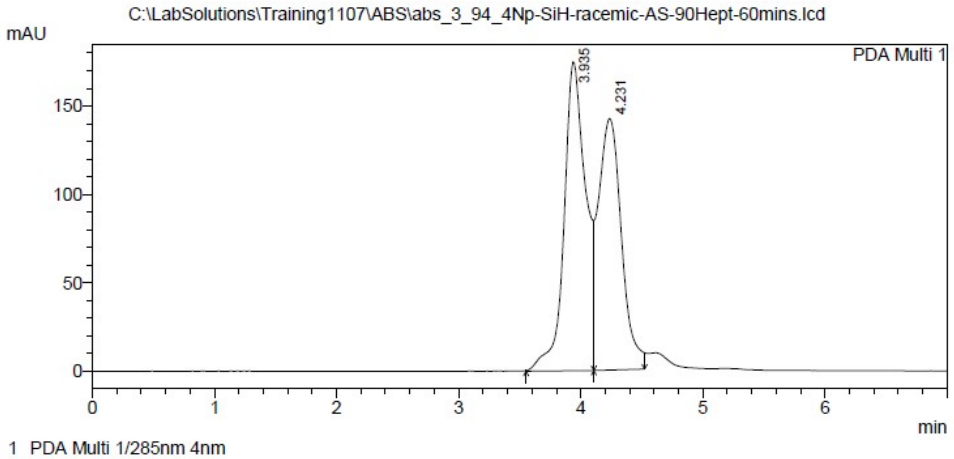

1 PDA Multi 1/285nm 4nm

< Peak Table >

PeakTable C:\LabSolutions\Training1107\ABS\abs_3_94_4Np-SiH-racemic-AS-90Hept-60mins.lcd

PDA Ch1 285nm 4nm

Peak#	Ret. Time	Area	Height	Area %	Height %
1	3.935	2187988	174885	54.240	55.115
2	4.231	1845878	142423	45.760	44.885
Total		4033866	317308	100.000	100.000

Enantiomerically enriched **3.56**, (86:14 er)

Enantiomeric ratios were determined by HPLC Diacel CHIRALPAK AS-H column (10% IPA/heptanes) 1 mL/min **3.56**–1 = 8.2 min, **3.56**–2 = 8.7 min.

<Chromatogram>

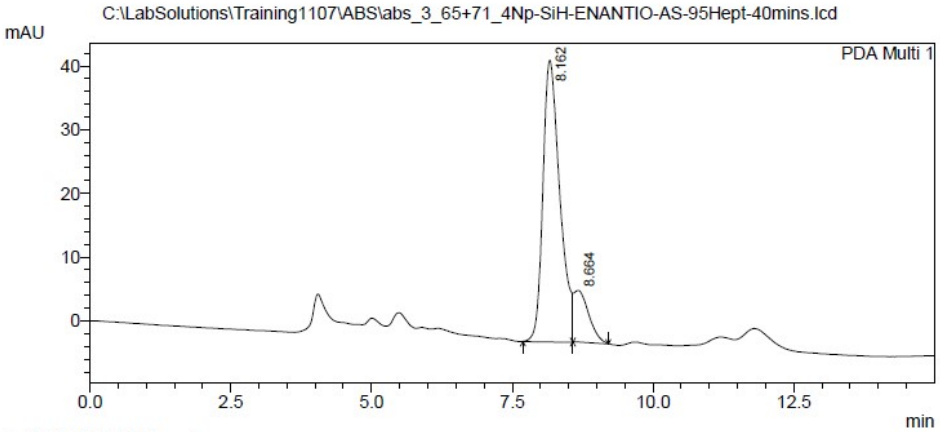

1 PDA Multi 1/285nm 4nm

< Peak Table >

PeakTable C:\LabSolutions\Training1107\ABS\abs_3_65+71_4Np-SiH-ENANTIO-AS-95Hept-40mins.lcd

PDA Ch1 285nm 4nm

Peak#	Ret. Time	Area	Height	Area %	Height %
1	8.162	928565	44218	86.067	84.517
2	8.664	150316	8101	13.933	15.483
Total		1078881	52319	100.000	100.000

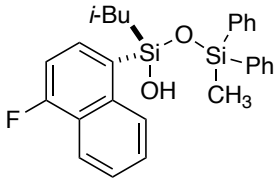

(*S*)-1-(4-Fluoronaphthalen-1-yl)-1-isobutyl-3-methyl-3,3-diphenyldisiloxan-1-ol 3 (3.57)

Synthesized according to the General Procedure A using (4-fluoronaphthalen-1-yl)(isobutyl)silanediol (39.7 mg, 0.15 mmol), organocatalyst **3.27** (2.3 mg, 7.5 x 10^{-3} mmol, 0.05 equiv), diisopropylethylamine (30.7 μL, 0.18 mmol, 1.2 equiv), α-pinene (28.6 μL, 0.18 mmol,1.2 equiv) and diphenylmethylchlorosilane (31.0 μL, 0.39 mmol, 1.0 equiv). The reaction was purified using flash column chromatography (SiO_2, hexanes/EtOAc, 9:1 *v/v*) to give siloxanol as a clear oil (32.7mg, 50%); characterization data are consistent with literature precedent.[46]

^{1}H NMR (400 MHz, C_6D_6) δ 8.16 (m, 1H), 7.57 (m, 6H), 7.19 (dd, *J* = 4.9, 1.9 Hz, 10H), 0.86 (m, 8H), 0.50 (d, *J* = 1.4 Hz, 6H), -0.01 (s, 3H).

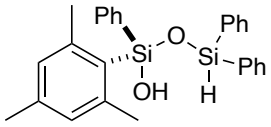

(*S*)-1-Mesityl-1,3,3-triphenyldisiloxan-1-ol (3.58)

Synthesized according to the General Procedure A using mesityl(phenyl)silanediol (0.10 g, 0.39 mmol), organocatalyst **3.27** (6.0 mg, 0.02 mmol, 0.05 equiv), diisopropylethylamine (79.3 μL, 0.46 mmol, 1.2 equiv), α-pinene (73.7 μL, 0.46 mmol,1.2 equiv) and diphenylchlorosilane (75.7 μL, 0.39 mmol, 1.0 equiv). The reaction was purified using flash column chromatography (SiO_2, hexanes/EtOAc, 4:1 *v/v*) to give siloxanol as an off-white film (49.5 mg, 29%).

^{1}H NMR (300 MHz, C_6D_6) δ 7.66 (m, 6H), 7.54 (m, 1H), 7.13 (m, 11H), 6.71 (s, 2H), 5.91 (s, 1H), 2.47 (s, 6H), 2.09 (s, 3H). ^{13}C NMR (101 MHz, C_6D_6) δ 144.17, 139.22, 134.56, 130.22, 129.28, 128.13, 128.10, 24.18, 20.87, 2.86.^{29}Si NMR (79 MHz, C_6D_6) δ -18.87, -21.83. HRMS (ESI) m/z: calc for $C_{27}H_{27}O_2Si_2$ $[M-H]^-$ 439.1550 found 439.1385.

*Note: Compound **3.58** was carried forward to Pd/C hydrolysis to obtain selectivity data.*

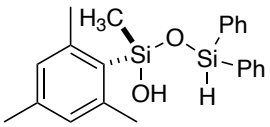

(*S*)-1-Mesityl-1-methyl-3,3-diphenyldisiloxan-1-ol (3.59)

Synthesized according to General Procedure A using mesityl(methyl)silanediol (0.20 g, 1.00 mmol, 1.0 equiv), organocatalyst **3.27** (14.3 mg, 0.05 mmol, 0.05 equiv), diisopropylethylamine (0.20 mL, 1.20 mmol, 1.2 equiv), α-pinene (0.19 mL, 1.20 mmol, 1.2 equiv) and diphenylchlorosilane (0.20 mL, 1.00 mmol, 1.0 equiv) for the largest upscaled reaction. The reaction was purified using flash column chromatography (SiO_2, hexanes/EtOAc, 9:1 *v/v*) to give siloxanol as an off-white film (0.21 g, 56%).

^{1}H NMR (400 MHz, C_6D_6) δ 7.68 (m, 5H), 7.61 (m, 2H), 7.12 (m, 3H), 6.71 (s, 1H), 5.85 (s, 1H), 2.49 (s, 6H), 2.09 (s, 3H), 0.39 (s, 3H). ^{13}C NMR (101 MHz, C_6D_6) δ 144.17, 139.22, 135.65, 134.62, 134.56, 134.52, 130.45, 130.33, 130.22, 129.28, 128.13, 128.10, 24.47, 20.87, 2.86.^{29}Si NMR (79 MHz, C_6D_6) δ -18.87, -22.00. HRMS (ESI) m/z: calc for $C_{22}H_{25}O_2Si_2$ $[M-H]^-$ 377.1393 found 377.1388.

*Note: Compound **3.59** was carried forward to Pd/C hydrolysis to obtain selectivity data.*

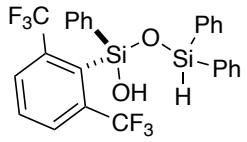

(*S*)-1-(2,6-bis(trifluoromethyl)phenyl)-1,3,3-triphenyldisiloxan-1-ol (3.60)

Synthesized according to General Procedure A using (2,6 bis(trifluoromethyl)phenyl)(phenyl) silanediol, (0.12 g, 0.33 mmol,1.0 equiv), organocatalyst **3.27** (3.9 mg, 0.02 mmol, 0.05 equiv), diisopropylethylamine (68.2 µL, 0.40 mmol, 1.2 equiv), α-pinene (63.4 µL, 0.40 mmol, 1.2 equiv) and diphenylchlorosilane (68.0 µL, 0.33 mmol, 1.0 equiv). The reaction was purified using flash column chromatography (SiO_2, hexanes/EtOAc, 4:1 *v/v*) to give siloxanol as an off-white film (56.9 mg, 32%).

^{1}H NMR (400 MHz, C_6D_6) δ 7.70 (m, 3H), 7.62 (m, 3H), 7.53 (m, 2H), 7.38 (d, *J* = 7.9 Hz, 1H), 7.11 (m, 10H), 6.72 (t, *J* = 8.0 Hz, 1H), 5.92 (d, *J* = 13.3 Hz, 1H), 2.82 (s, 1H).^{13}C NMR (101 MHz, C_6D_6) δ 135.23, 135.13 (d, *J* = 2.3 Hz), 134.72 (d, *J* = 9.9 Hz), 134.53, 133.91, 130.32, 130.18 (d, *J* = 3.0 Hz), 128.09 (d, *J* = 6.8 Hz), 127.98, 127.75.^{19}F NMR (376 MHz, C_6D_6) δ -54.29.^{29}Si NMR (79 MHz, C_6D_6) δ -18.86, -21.81. HRMS (ESI) m/z: calc for $C_{26}H_{19}F_6O_2Si_2$ $[M-H]^-$ 533.0828 found 533.0830.

Racemic standard for **3.60**

<Chromatogram>

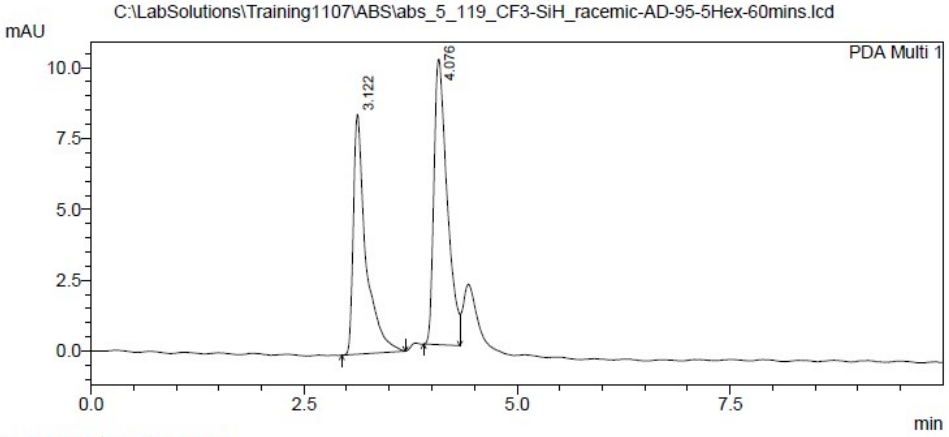

1 PDA Multi 1/220nm 4nm

< Peak Table >

PeakTable C:\LabSolutions\Training1107\ABS\abs_5_119_CF3-SiH_racemic-AD-95-5Hex-60mins.lcd

PDA Ch1 220nm 4nm

Peak#	Ret. Time	Area	Height	Area %	Height %
1	3.122	86647	8478	44.319	45.702
2	4.076	108861	10072	55.681	54.298
Total		195508	18550	100.000	100.000

Enantiomerically enriched **3.60**, (86:14 er)

Enantiomeric ratios were determined by HPLC Diacel CHIRALPAK AD-H column (5% IPA/hexanes) 1 mL/min **3.60**–1 = 3.2 min, **3.60**–2 = 3.8 min.

<Chromatogram>

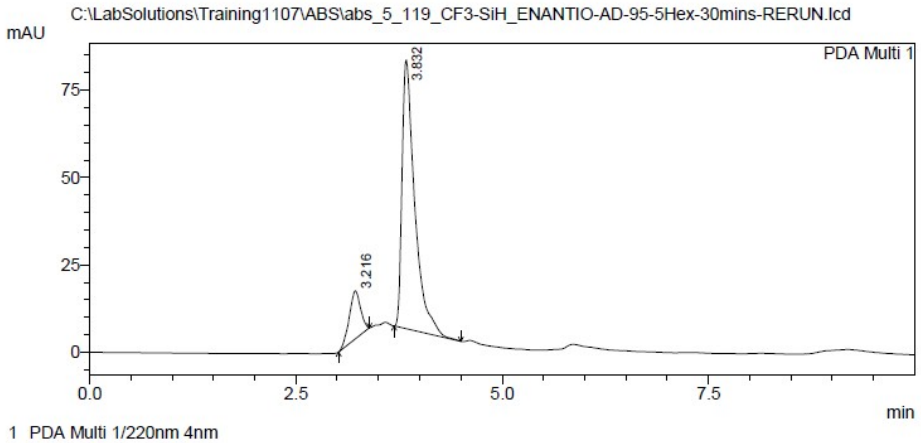

1 PDA Multi 1/220nm 4nm

< Peak Table >

PeakTable C:\LabSolutions\Training1107\ABS\abs_5_119_CF3-SiH_ENANTIO-AD-95-5Hex-30mins-RERUN.lcd

PDA Ch1 220nm 4nm

Peak#	Ret. Time	Area	Height	Area %	Height %
1	3.216	133418	13838	13.985	15.251
2	3.832	820591	76896	86.015	84.749
Total		954009	90733	100.000	100.000

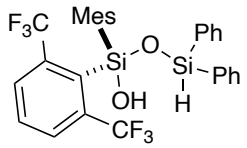

(*S*)-1-(2,6-bis(trifluoromethyl)phenyl)-1-mesityl-3,3-diphenyldisiloxan-1-ol (3.61)

Synthesized according to the General Procedure A using (2,6-bis(trifluoromethyl)phenyl)(mesityl)silanediol (59.2 mg, 0.15 mmol, 1.0 equiv), organocatalyst **3.27** (3.2 mg, 0.0075 mmol, 0.05 equiv), diisopropylethylamine (30.7 μL, 0.18 mmol, 1.2 equiv), α-pinene (28.6 μL, 0.18 mmol,1.2 equiv) and diphenylchlorosilane (29.3 μL, 0.15 mmol, 1.0 equiv). The reaction was purified using flash column chromatography (SiO_2, hexanes/EtOAc, 4:1 *v/v*) to give siloxanol as an oil (2.7 mg, 3%).

^{1}H NMR (400 MHz, C_6D_6) δ 7.97 (d, *J* = 7.9 Hz, 1H), 7.76 (s, 1H), 7.57 (ddt, *J* = 15.8, 6.4, 1.7 Hz, 5H), 7.10 (m, 8H), 6.69 (s, 2H), 5.81 (s, 1H), 2.33 (s, 6H), 2.08 (s, 3H), 1.78 (s, 2H). HRMS (ESI) m/z: calc for $C_{29}H_{26}F_6O_2Si_2$ $[M-H]^-$ 575.1298 found 575.1290

*Note: Racemic Standard for **3.61** resulted in bis-silylated product confirmed using ^{1}H NMR (data below). Attempts to synthesize prochiral material were unsuccessful. This substrate was not further pursued for the following 1) limited amount of material paired with unsuccessful attempts for the synthesis of the prochiral substrate, 2) low reactivity for the desymmetrization reaction, and 3) most importantly a lack of selectivity for the desymmetrization reaction.*

^{1}H NMR (300 MHz, C_6D_6) δ 7.99 (d, *J* = 7.9 Hz, 1H), 7.74 (m, 3H), 7.62 (dd, *J* = 7.5, 2.0 Hz, 4H), 7.48 (m, 4H), 7.09 (m, 13H), 5.91 (s, 1H), 5.77 (s, 1H), 2.31 (s, 6H), 2.08 (s, 3H).

Enantiomerically enriched **3.61**, (55:45 er)

Enantiomeric ratios were determined by HPLC Diacel CHIRALPAK AD-H column (0% IPA/heptanes) 1 mL/min **3.61**–1 = 38.4 min, **3.61**–2 = 44.0 min.

<Chromatogram>

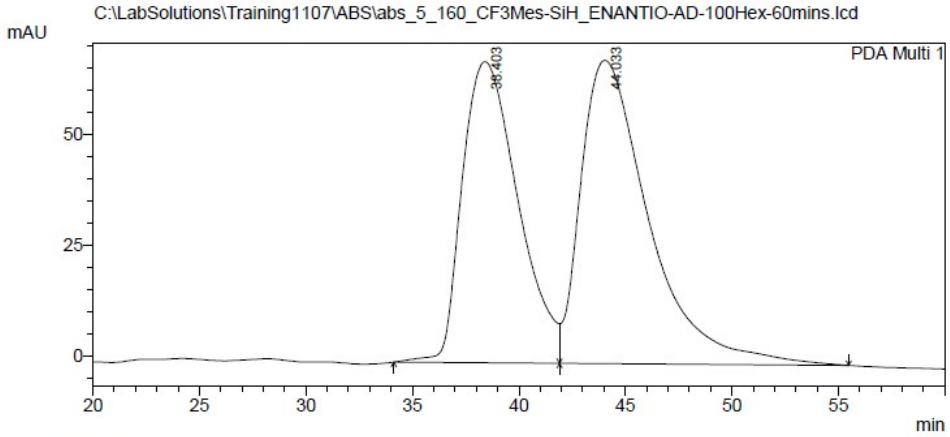

1 PDA Multi 1/225nm 4nm

< Peak Table >

PeakTable C:\LabSolutions\Training1107\ABS\abs_5_160_CF3Mes-SiH_ENANTIO-AD-100Hex-60mins.lcd

PDA Ch1 225nm 4nm

Peak#	Ret. Time	Area	Height	Area %	Height %
1	38.403	12374010	67990	44.850	49.818
2	44.033	15215919	68487	55.150	50.182
Total		27589930	136477	100.000	100.000

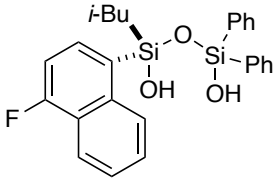

(*S*)-1-(4-Fluoronaphthalen-1-yl)-1-isobutyl-3,3-diphenyldisiloxane-1,3-diol (3.34a)

To a flame-dried argon-purged round-bottom flask was added Pd/C (10 wt%, 1.2 mg, 0.009 mmol, 0.05 equiv) and was dissolved in THF (0.06M). Then (*S*)-1-(4-fluoronaphthalen-1-yl)-1-isobutyl-3,3-diphenyldisiloxan-1-ol (80.7 mg, 0.18 mmol, 1.0 equiv) was added after being dissolved in a minimum amount of THF followed by the addition of deionized water (32.6 µL, 1.80 mmol, 10.0 equiv). Amounts reported were for the largest upscaled reaction. (Caution: H_2 gas evolves as the reaction proceeds.) The reaction was capped with a septum and allowed to stir

at room temperature (23 °C). The reaction was monitored using TLC for the consumption of starting material siloxanol (TLC conditions: hexanes/EtOAc, 4:1 *v/v)*. Once starting material was fully consumed at 18 min, the reaction was filtered through Celite to remove Pd/C. The filtrate was dried over $MgSO_4$ filtered and concentrated *in vacuo*. The reaction mixture was purified using flash column chromatography (SiO_2, hexanes/EtOAc, 4:1 *v/v*) to give **3.34a** as an off-white film (14.4 mg, 17%)

^{1}H NMR (400 MHz, C_6D_6) δ 8.46 (d, *J* = 1.8 Hz, 1H), 8.15 (d, 1H), 7.88 (t, *J* = 6.2 Hz, 1H), 7.78 (m, 3H), 7.72 (m, 2H), 7.19 (m, 4H), 7.11 (m, 4H), 6.89 (ddd, *J* = 10.5, 7.6, 2.1 Hz, 1H), 3.44 (s, 1H), 1.87 (m, 1H), 1.04 (d, *J* = 7.0 Hz, 2H), 0.86 (t, *J* = 1.3 Hz, 6H). HRMS (ESI) m/z: calc for $C_{26}H_{27}FO_2Si_2$ $[M-H]^-$ 461.1405 found 461.1409.

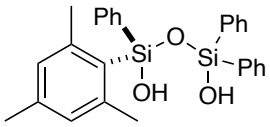

(*S*)-1-mesityl-1,3,3-triphenyldisiloxane-1,3-diol (3.34b)

To a flame-dried argon-purged round-bottom flask was added $[Ir(COD)Cl_2]_2$ (7.4 mg, 0.011 mmol, 0.01 equiv) and was dissolved in THF (0.08M). Then (*S*)-1-mesityl-1,3,3-triphenyldisiloxan-1-ol (0.49 g, 1.11 mmol, 1.0 equiv) was added after being dissolved in a minimum amount of THF followed by the addition of deionized water (0.20 mL, 11.08 mmol, 10.0 equiv). Amounts reported were for the largest upscaled reaction. (Caution: H_2 gas evolves as the reaction proceeds.) The reaction was capped with a septum and allowed to stir at room temperature (23 °C). The reaction was monitored using TLC for the consumption of starting material siloxanol (TLC conditions: hexanes/EtOAc, 4:1 *v/v)*. Once starting material was fully consumed

in 30 min, the reaction was filtered through Celite to remove $[Ir(COD)Cl_2]_2$. The filtrate was dried over $MgSO_4$ filtered and concentrated *in vacuo*. The reaction mixture was purified using flash column chromatography (SiO_2, hexanes/EtOAc, 4:1 *v/v*) to give **3.34b** as an off-white film (75.9 mg, 15%).

^{1}H NMR (400 MHz, C_6D_6) δ 7.61 (m, 4H), 7.13 (m, 11H), 6.70 (m, 2H), 2.49 (s, 6H), 2.08 (s, 3H), 0.93 (s, 2H). ^{13}C NMR (101 MHz, C_6D_6) δ 144.14, 134.63, 130.15, 129.39, 127.95, 127.70, 29.98, 24.47, 20.83.^{29}Si NMR (79 MHz, C_6D_6) δ –27.22, –28.58. HRMS (ESI) m/z: calc for $C_{27}H_{27}O_3Si_2$ $[M-H]^-$ 455.1499 found 455.1491.

Racemic standard for **3.34b**

<Chromatogram>

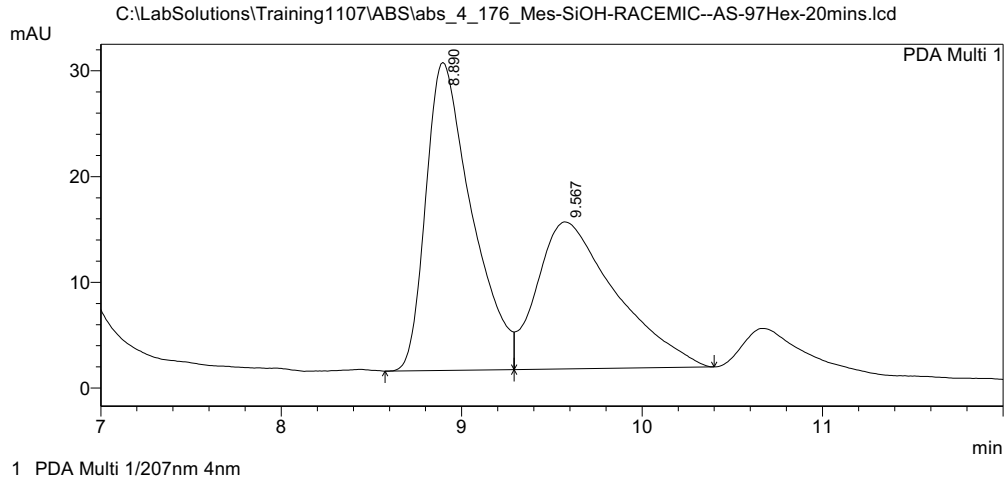

1 PDA Multi 1/207nm 4nm

< Peak Table >

PeakTable C:\LabSolutions\Training1107\ABS\abs_4_176_Mes-SiOH-RACEMIC--AS-97Hex-20mins.lcd

PDA Ch1 207nm 4nm

Peak#	Ret. Time	Area	Height	Area %	Height %
1	8.890	516580	29124	55.028	67.696
2	9.567	422182	13898	44.972	32.304
Total		938762	43022	100.000	100.000

Enantiomerically enriched **3.34b**, (94:6 er)

Enantiomeric ratios were determined by HPLC Diacel CHIRALPAK AS-H column (3% IPA/heptanes) 1 mL/min **3.34b**–1 = 11.5 min, **3.34b**–2 = 13.2 min.

<Chromatogram>

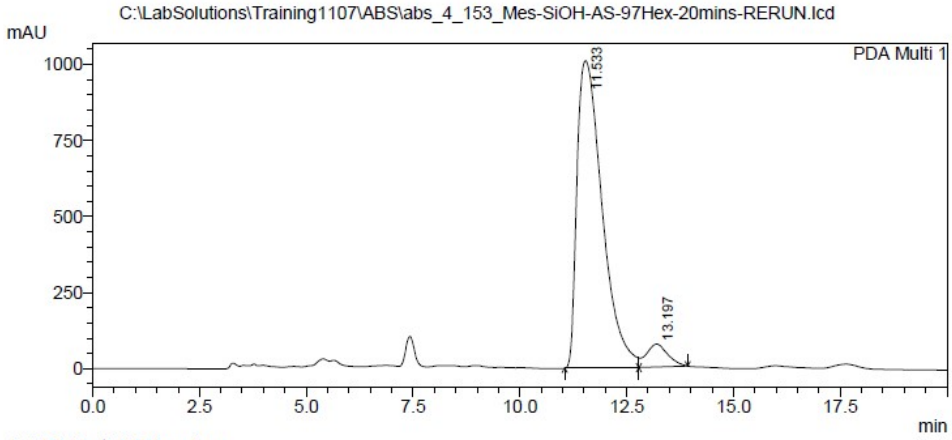

1 PDA Multi 1/224nm 4nm

< Peak Table >

PeakTable C:\LabSolutions\Training1107\ABS\abs_4_153_Mes-SiOH-AS-97Hex-20mins-RERUN.lcd

PDA Ch1 224nm 4nm

Peak#	Ret. Time	Area	Height	Area %	Height %
1	11.533	41507088	1011061	94.065	93.090
2	13.197	2618666	75054	5.935	6.910
Total		44125755	1086115	100.000	100.000

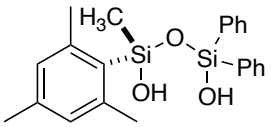

(*S*)-1-Mesityl-1-methyl-3,3-diphenyldisiloxane-1,3-diol (3.34c)

To a flame-dried argon-purged round-bottom flask was added $[Ir(COD)Cl]_2$ (1.3 mg, 0.38 mmol, 0.002 equiv) and was dissolved in THF (0.08M). Then (*S*)-1-mesityl-1-methyl-3,3-diphenyldisiloxan-1-ol (6.0 mg, 0.02 mmol, 1.0 equiv) was added after being dissolved in a minimum amount of THF followed by the addition of deionized water (3.4 µL, 0.18 mmol, 10.0 equiv). (Caution: H_2 gas evolves as the reaction proceeds.) The reaction was capped with a

septum and allowed to stir at room temperature (23 °C). The reaction was monitored using TLC for the consumption of starting material siloxanol (TLC conditions: hexanes/EtOAc, 4:1 *v/v)*. Once starting material was fully consumed at 20 min, the reaction was filtered through Celite to remove $[Ir(COD)Cl]_2$. The reaction was not purified. General Procedure C was followed to obtain selectivity data.

Note: Compound was confirmed with ^1H NMR prior to obtaining selectivity data. ^{1}H NMR (300 MHz, C_6D_6) δ 7.75 (m, 6H), 7.42 (s, 1H), 7.27 (s, 1H), 6.89 (s, 1H), 6.68 (d, J = 8.9 Hz, 1H), 2.45 (s, 6H), 2.07 (d, J = 11.1 Hz, 3H), 1.36 (s, 2H), 0.30 (s, 3H).

Racemic standard for **3.34c**

<Chromatogram>

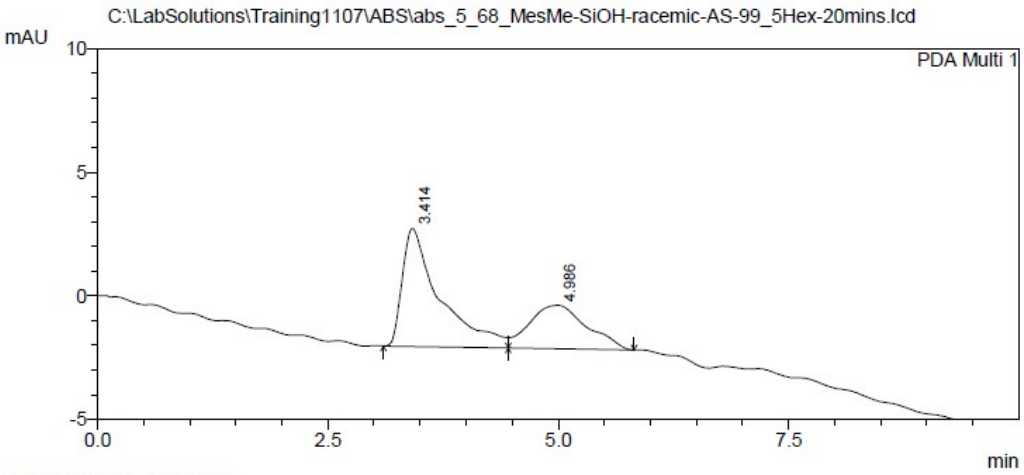

1 PDA Multi 1/235nm 4nm

< Peak Table >

PeakTable C:\LabSolutions\Training1107\ABS\abs_5_68_MesMe-SiOH-racemic-AS-99_5Hex-20mins.lcd

PDA Ch1 235nm 4nm

Peak#	Ret. Time	Area	Height	Area %	Height %
1	3.414	135515	4778	64.008	73.023
2	4.986	76202	1765	35.992	26.977
Total		211716	6543	100.000	100.000

Enantiomerically enriched **3.34c**, (62:38 er)

Enantiomeric ratios were determined by HPLC Diacel CHIRALPAK AS-H column (5% IPA/heptanes) 1 mL/min **3.34c**–1 = 3.4 min, **3.34c**–2 = 4.7 min.

<Chromatogram>

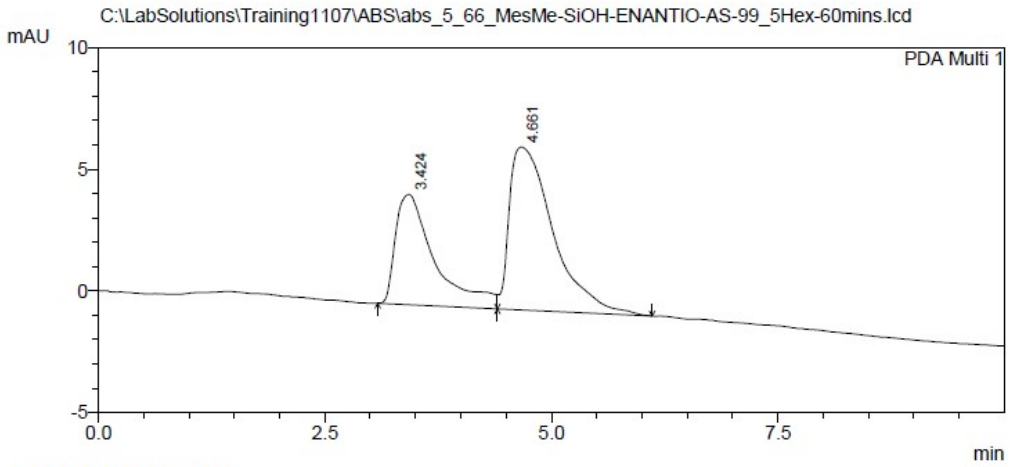

1 PDA Multi 1/235nm 4nm

< Peak Table >

PeakTable C:\LabSolutions\Training1107\ABS\abs_5_66_MesMe-SiOH-ENANTIO-AS-99_5Hex-60mins.lcd

PDA Ch1 235nm 4nm

Peak#	Ret. Time	Area	Height	Area %	Height %
1	3.424	136307	4536	37.719	40.380
2	4.661	225068	6696	62.281	59.620
Total		361374	11232	100.000	100.000

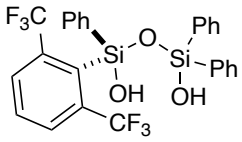

(*S*)-1-(2,6-bis(trifluoromethyl)phenyl)-1,3,3-triphenyldisiloxane-1,3-diol (3.34d)

To a flame-dried argon-purged round-bottom flask was added Pd/C (10 wt%, 1.0 mg, 0.005 mmol, 0.05 equiv) and was dissolved in THF (0.08M). Then (*S*)-1-(2,6-bis(trifluoromethyl)phenyl)-1,3,3-triphenyldisiloxan-1-ol (56.9 mg, 0.11 mmol, 1.0 equiv) was added after being dissolved in a minimum amount of THF followed by the addition of deionized water (19.2

μL, 1.06 mmol, 10.0 equiv). (Caution: H_2 gas evolves as the reaction proceeds.) The reaction was capped with a septum and allowed to stir at room temperature (23 °C). The reaction was monitored using TLC for the consumption of starting material siloxanol (TLC conditions: hexanes/EtOAc, 4:1 *v/v)*. Once starting material was fully consumed at 1 h, the reaction was filtered through Celite to remove Pd/C. The filtrate was dried over $MgSO_4$ filtered and concentrated *in vacuo*. The reaction mixture was purified using preparatory thin-layer chromatography (SiO_2, hexanes/EtOAc, 9:1 *v/v*) to yield **3.34d** as an oil (2.4 mg, 4%).

^{1}H NMR (300 MHz, C_6D_6) δ 7.69 (m, 5H), 7.52 (dd, J = 8.0, 1.6 Hz, 2H), 7.36 (d, J = 8.0 Hz, 2H), 7.10 (m, 12H), 5.93 (s, 1H), 0.29 (s, 1H). HRMS (ESI) m/z: calc for $C_{27}H_{19}F_6O_3Si_2$ $[M\text{-}H]^-$ 549.0777 found 549.0895.

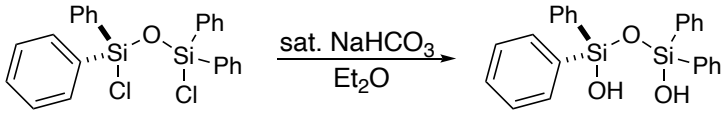

1,1,3,3-tetraphenyldisiloxane-1,3-diol (3.48)

1,3-dichloro-1,1,3,3-tetraphenyldisiloxane (1.71 g, 3.79 mmol) was dissolved in Et_2O (38.0 mL) in a 100 mL round bottom flask and stirred at room temperature for 1 h. A solution of saturated aq. $NaHCO_3$ was added to the reaction mixture dropwise until the solution was neutralized (~10.0 mL), as monitored by pH paper. The organic layer was separated, and the aqueous layer was extracted with Et_2O (3 x 10 mL). The organic layers were combined and washed with brine (15 mL). The organic layer was further dried over anhydrous $MgSO_4$, filtered, and then concentrated in vacuo. The product was recrystallized from a solvent mixture of benzene/petroleum ether to afford **3.48** (0.986 g, 63%) as a white solid. Spectral data was consistent with literature values.[53] ^{1}H NMR (400 MHz, C_6D_6) δ 7.77 (m, 6H), 7.15 (m, 11H), 2.81 (s, 1H), 0.55 (s, 1H).

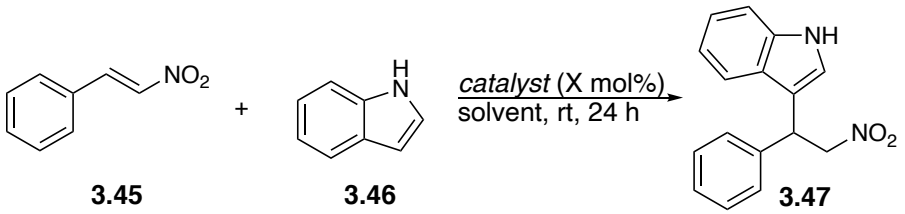

3.45 **3.46** **3.47**

3-(2-nitro-1-phenylethyl)-1*H*-indole (3.47)

To a flame-dried 25 mL round bottom flask purged with argon was added trans-*β*-nitrostyrene **3.45** (1.0 equiv) and catalyst (X mol%) and dissolved in solvent (X M). To the reaction mixture was added indole **3.46** (1.5 equiv), and the resulting solution was stirred for 24 h. Note: see Table **3.6** in this chapter for amounts of each reagent. The reaction mixture was purified using preparatory thin-layer chromatography (SiO_2, hexanes/EtOAc, 95:5 to 4:1 *v/v*) to yield **3.47** as a yellow oil and matched literature precedent.[48,65] *Note: for reported yields, see Table **3.6** in this chapter.*

^{1}H NMR (300 MHz, $CDCl_3$) δ 8.11 (s, 1H), 7.64 (m, 1H), 7.39 (m, 1H), 7.32 (m, 2H), 7.19 (m, 1H), 7.12 (m, 2H), 5.19 (t, J = 0.9 Hz, 1H), 5.05 (d, 1H), 4.95 (d, J = 8.4 Hz, 1H).

Racemic Standard for **3.47**, using disiloxanediol **3.48**

<Chromatogram>

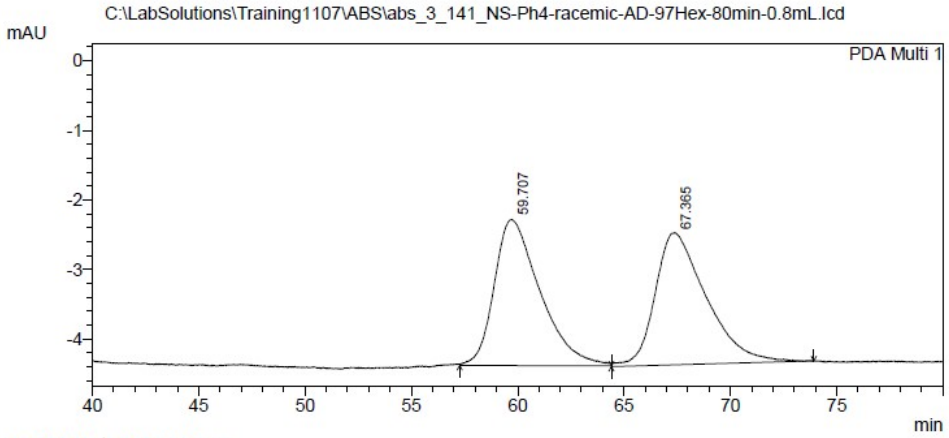

1 PDA Multi 1/254nm 4nm

< Peak Table >

PeakTable C:\LabSolutions\Training1107\ABS\abs_3_141_NS-Ph4-racemic-AD-97Hex-80min-0.8mL.lcd
PDA Ch1 254nm 4nm

Peak#	Ret. Time	Area	Height	Area %	Height %
1	59.707	314138	2101	49.810	52.483
2	67.365	316533	1902	50.190	47.517
Total		630671	4003	100.000	100.000

Enantiomerically enriched, using **3.34a** at 20 mol% (53:47 er)

Enantiomeric ratios were determined by HPLC Diacel CHIRALPAK AD-H column (3% IPA/heptanes) 0.8 mL/min **3.34a**–1 = 59.9 min, **3.34a**–2 = 67.5 min.

<Chromatogram>

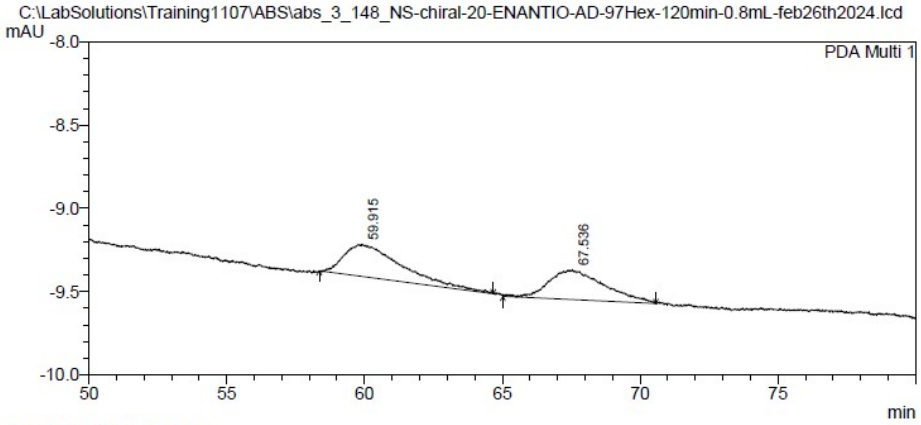

1 PDA Multi 1/254nm 4nm

< Peak Table >

PeakTable C:\LabSolutions\Training1107\ABS\abs_3_148_NS-chiral-20-ENANTIO-AD-97Hex-120min-0.8mL-feb26th2024.lcd
PDA Ch1 254nm 4nm

Peak#	Ret. Time	Area	Height	Area %	Height %
1	59.915	28031	195	53.006	51.731
2	67.536	24851	182	46.994	48.269
Total		52882	377	100.000	100.000

Enantiomerically enriched, using disiloxanediol **3.29a** at 10 mol% (51:49 er)

Enantiomeric ratios were determined by HPLC Diacel CHIRALPAK AD-H column (3% IPA/heptanes) 0.8 mL/min **3.47**–1 = 62.3 min, **3.47**–2 = 70.2 min.

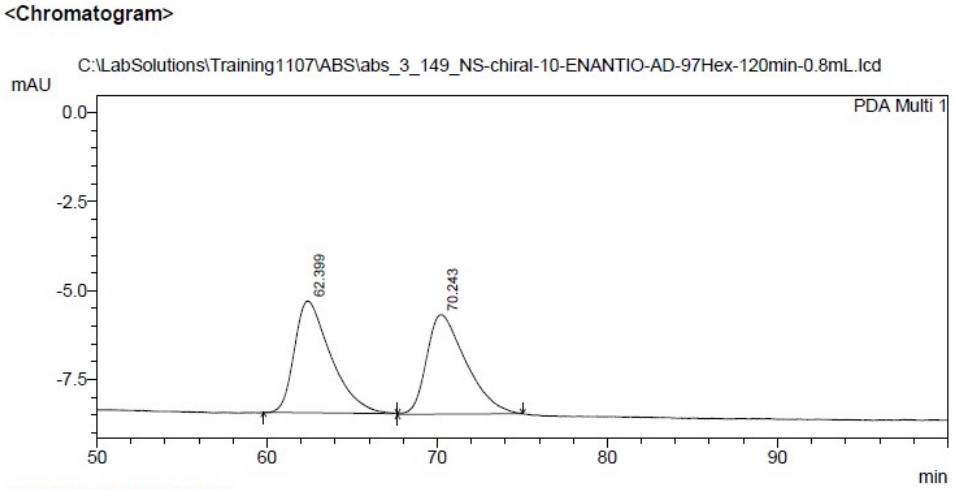

< Peak Table >

PeakTable C:\LabSolutions\Training1107\ABS\abs_3_149_NS-chiral-10-ENANTIO-AD-97Hex-120min-0.8mL.lcd

PDA Ch1 254nm 4nm

Peak#	Ret. Time	Area	Height	Area %	Height %
1	62.399	467545	3139	50.976	52.891
2	70.243	449647	2796	49.024	47.109
Total		917192	5935	100.000	100.000

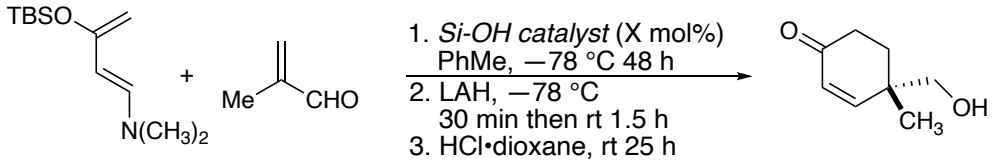

3.48 **3.49** **3.50**

(*S*)-4-(hydroxymethyl)-4-methylcyclohex-2-en-1-one (3.50)

To a flame-dried microwave vial was added methacrolein **3.49** (1.0 equiv) and catalyst (X mol%) and dissolved in toluene (0.67 M). The reaction mixture was cooled to –78 °C, the aminosiloxydiene **3.48** (2.0 equiv) was added. The reaction mixture was allowed to stir in the Cryocool at –78 °C for 48 h. Then, the reaction was quenched with lithium aluminum hydride (4.0 M, 4.0 equiv). Note: see Table **3.7** in this chapter for amounts of each reagent. After stirring for 30 min and 1.5 h at room temperature (23 °C) the reaction was quenched with Rochelle's

salts (1 mL). The supernatant liquid was decanted, combined with extraction, and concentrated *in vacuo.* The resulting oil was cooled to 0 °C and HCl•dioxane (4.0M in 1,4-dioxane, 0.36 equiv) was added as an alternative[70] and the resulting mixture was allowed to stir for 24 h. The reaction mixture was concentrated *in vacuo* and purified using flash chromatography (SiO_2, hexanes/EtOAc, 7:3 *v/v*) to yield **3.55** as a yellow oil and matched literature precedent.[53] Note: For reported yields, see Table **3.7** in this chapter.

^{1}H NMR (400 MHz, $CDCl_3$) δ 6.70 (d, J = 9.3 Hz, 1H), 5.99 (d, J = 9.7 Hz, 1H), 4.12 (q, J = 7.1 Hz, 2H), 2.04 (s, 3H), 1.63 (s, 1H), 0.87 (m, 6H).

Racemic Standard for **3.50**, using disiloxanediol **3.48**

<Chromatogram>

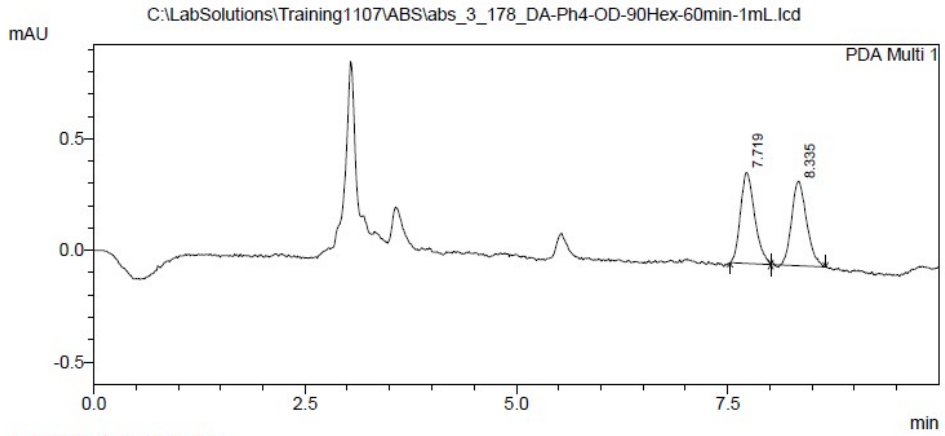

1 PDA Multi 1/254nm 4nm

< Peak Table >

PeakTable C:\LabSolutions\Training1107\ABS\abs_3_178_DA-Ph4-OD-90Hex-60min-1mL.lcd

PDA Ch1 254nm 4nm

Peak#	Ret. Time	Area	Height	Area %	Height %
1	7.719	4782	408	50.558	51.850
2	8.335	4677	379	49.442	48.150
Total		9459	788	100.000	100.000

Enantiomerically enriched, using disiloxanediol **3.57** (63:37 er).

Enantiomeric ratios were determined by HPLC Diacel CHIRALPAK OD-H column (10% IPA/heptanes) 1 mL/min **3.57**–1 = 9.3 min, **3.57**–2 = 10.1 min.

<Chromatogram>

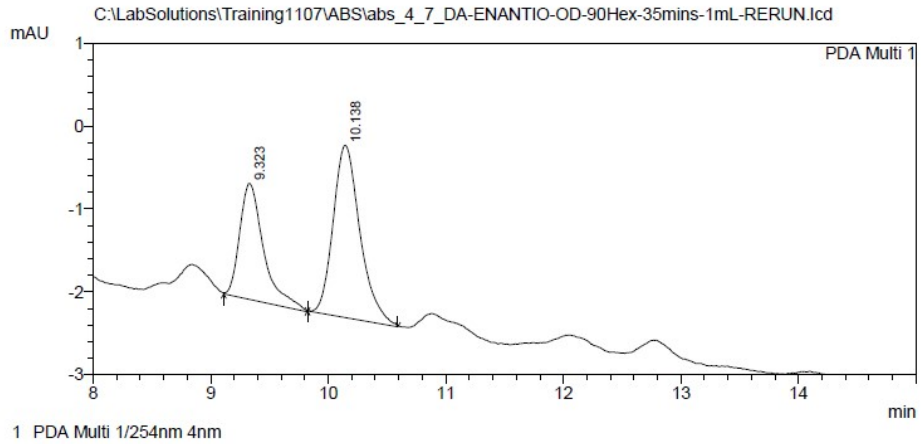

1 PDA Multi 1/254nm 4nm

< Peak Table >

PeakTable C:\LabSolutions\Training1107\ABS\abs_4_7_DA-ENANTIO-OD-90Hex-35mins-1mL-RERUN.lcd

PDA Ch1 254nm 4nm

Peak#	Ret. Time	Area	Height	Area %	Height %
1	9.323	19777	1400	37.478	40.212
2	10.138	32993	2081	62.522	59.788
Total		52770	3481	100.000	100.000

Enantiomerically enriched, using disiloxanediol **3.57** (51:49 er).

Enantiomeric ratios were determined by HPLC Diacel CHIRALPAK OD-H column (10% IPA/heptanes) 1 mL/min **3.57**–1 = 7.3 min, **3.57**–2 = 7.7 min.

<Chromatogram>

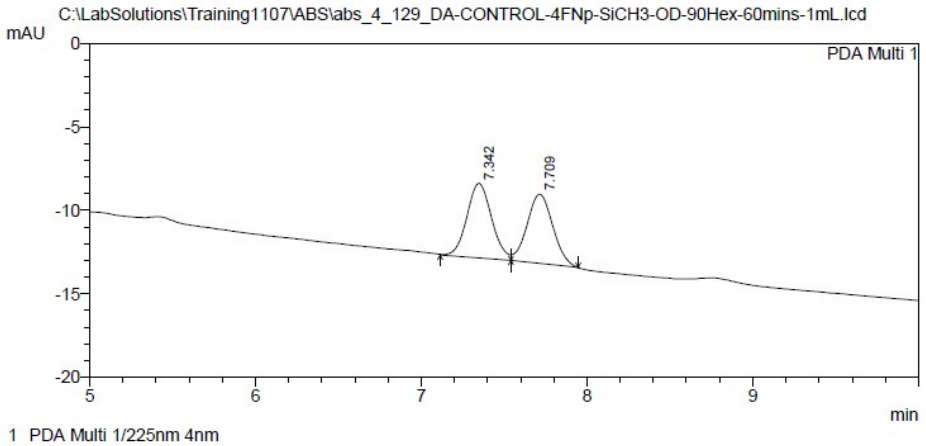

1 PDA Multi 1/225nm 4nm

< Peak Table >

PeakTable C:\LabSolutions\Training1107\ABS\abs_4_129_DA-CONTROL-4FNp-SiCH3-OD-90Hex-60mins-1mL.lcd

PDA Ch1 225nm 4nm

Peak#	Ret. Time	Area	Height	Area %	Height %
1	7.342	46420	4483	51.205	52.001
2	7.709	44235	4138	48.795	47.999
Total		90655	8621	100.000	100.000

Racemic Standard for **3.50**, using disiloxanediol **3.48**

<Chromatogram>

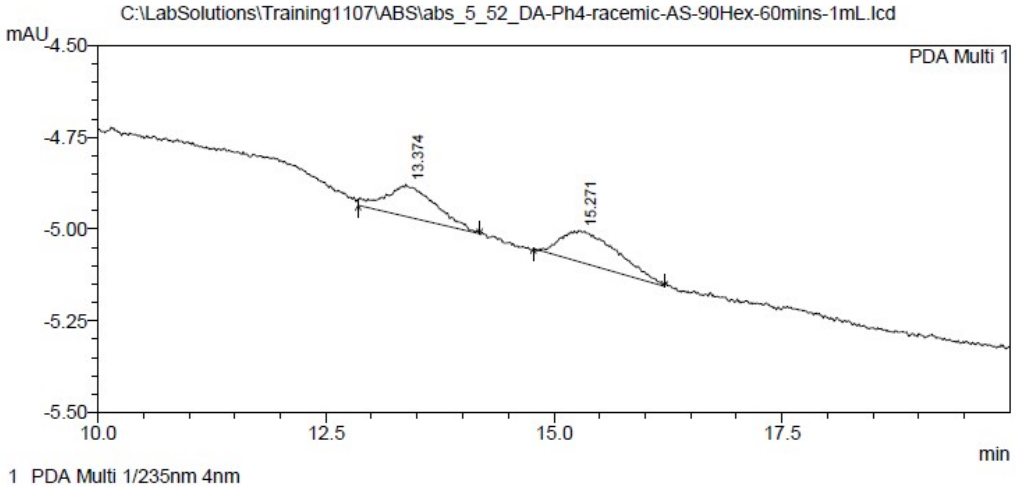

1 PDA Multi 1/235nm 4nm

< Peak Table >

PeakTable C:\LabSolutions\Training1107\ABS\abs_5_52_DA-Ph4-racemic-AS-90Hex-60mins-1mL.lcd

PDA Ch1 235nm 4nm

Peak#	Ret. Time	Area	Height	Area %	Height %
1	13.374	3281	87	46.187	50.456
2	15.271	3822	85	53.813	49.544
Total		7103	172	100.000	100.000

Enantiomerically enriched, using disiloxanediol **3.34b** (55:45 er)

Enantiomeric ratios were determined by HPLC Diacel CHIRALPAK AS-H column (10% IPA/heptanes) 1 mL/min **3.57**–1 = 13.4 min, **3.57**–2 = 15.2 min.

<Chromatogram>

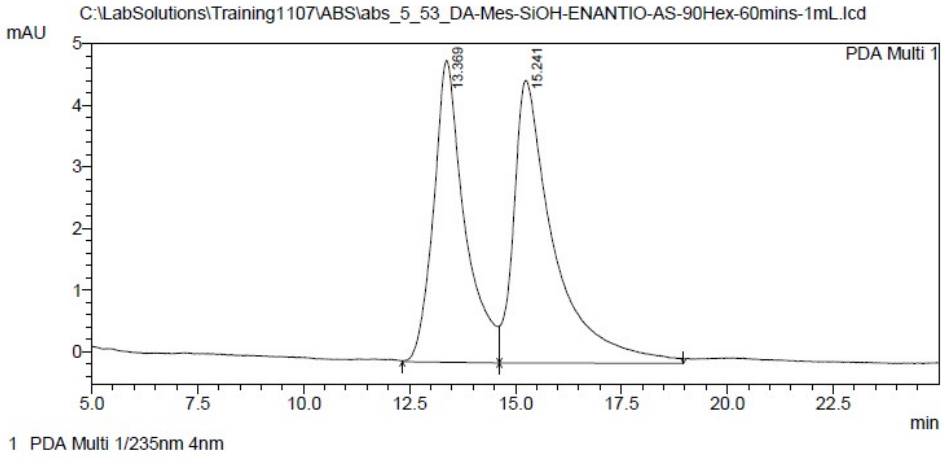

1 PDA Multi 1/235nm 4nm

< Peak Table >

PeakTable C:\LabSolutions\Training1107\ABS\abs_5_53_DA-Mes-SiOH-ENANTIO-AS-90Hex-60mins-1mL.lcd

PDA Ch1 235nm 4nm

Peak#	Ret. Time	Area	Height	Area %	Height %
1	13.369	251142	4902	45.417	51.648
2	15.241	301833	4589	54.583	48.352
Total		552975	9491	100.000	100.000

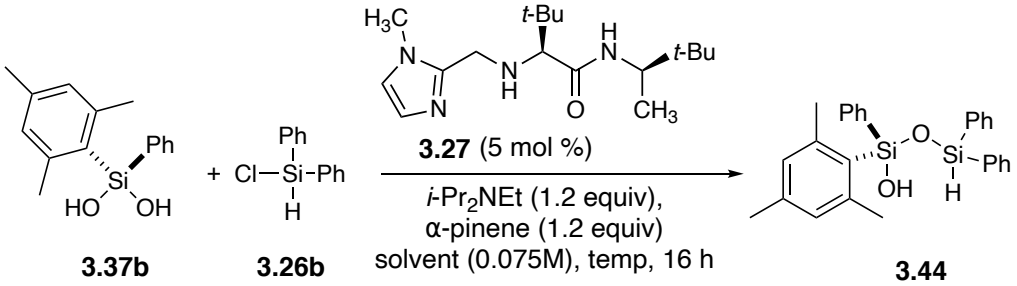

3.37b **3.26b** **3.44**

(*S*)-1-mesityl-1,3,3-triphenyldisiloxan-1-ol (3.44)

General Procedure A was used for the optimization of **3.44**. See Table **3.5** in this chapter for details regarding optimization conditions. Compound **3.44** was purified according to experimental listed in this chapter.

Racemic Standard for **3.44**

<Chromatogram>

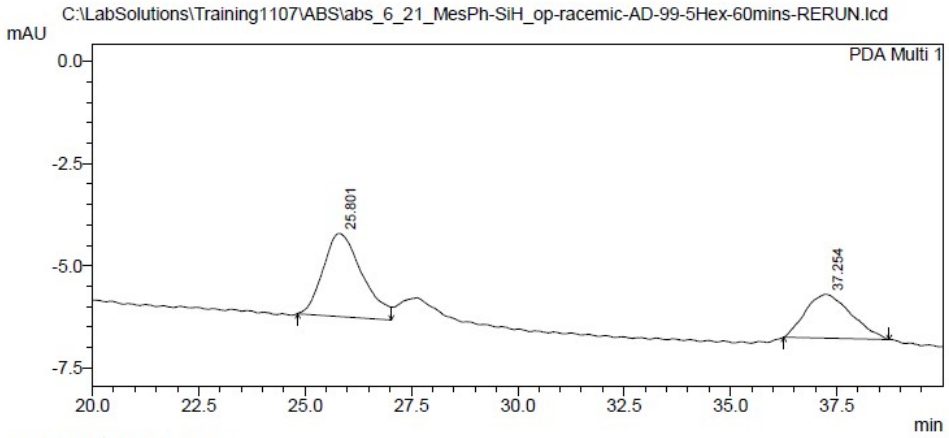

1 PDA Multi 1/225nm 4nm

< Peak Table >

PeakTable C:\LabSolutions\Training1107\ABS\abs_6_21_MesPh-SiH_op-racemic-AD-99-5Hex-60mins-RERUN.lcd

PDA Ch1 225nm 4nm

Peak#	Ret. Time	Area	Height	Area %	Height %
1	25.801	129941	2032	61.808	65.417
2	37.254	80294	1074	38.192	34.583
Total		210235	3105	100.000	100.000

Enantiomerically enriched, PhCl at – 78 °C (66:34 er)

Enantiomeric ratios were determined by HPLC Diacel CHIRALPAK AD-H column (0.5% IPA/heptanes) 1 mL/min **3.44**–1 = 29.3 min, **3.44**–2 = 40.5 min.

<Chromatogram>

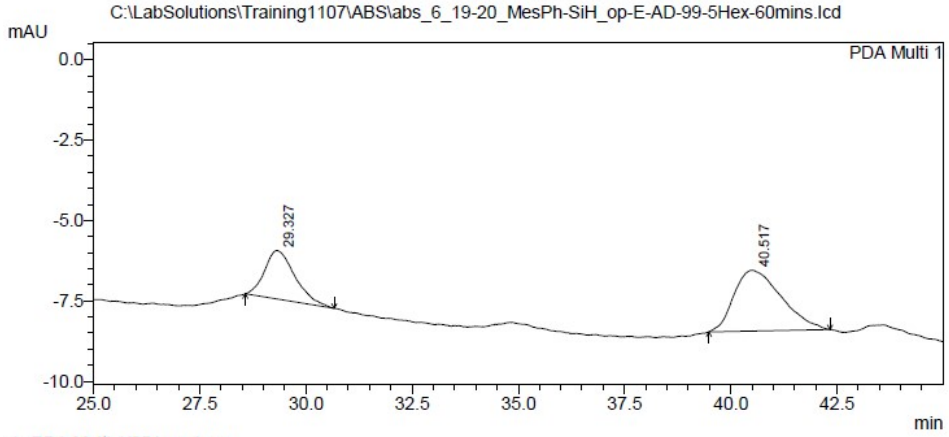

1 PDA Multi 1/254nm 4nm

< Peak Table >

PeakTable C:\LabSolutions\Training1107\ABS\abs_6_19-20_MesPh-SiH_op-E-AD-99-5Hex-60mins.lcd

PDA Ch1 254nm 4nm

Peak#	Ret. Time	Area	Height	Area %	Height %
1	29.327	75147	1513	33.914	44.481
2	40.517	146433	1889	66.086	55.519
Total		221579	3402	100.000	100.000

Enantiomerically enriched, PhMe at – 40 °C (66:34 er)

Enantiomeric ratios were determined by HPLC Diacel CHIRALPAK OD-H column (0.5% IPA/heptanes) 1 mL/min **3.44**–1 = 24.6 min, **3.44**–2 = 35.1 min.

<Chromatogram>

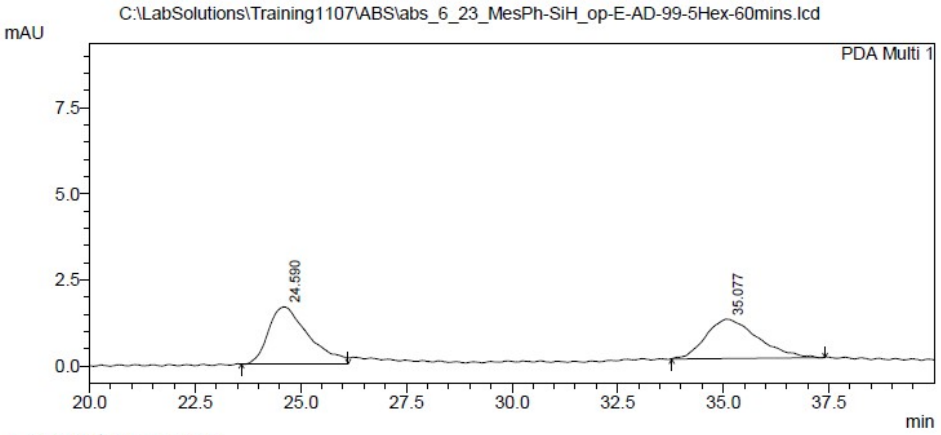

1 PDA Multi 1/225nm 4nm

< Peak Table >

PeakTable C:\LabSolutions\Training1107\ABS\abs_6_23_MesPh-SiH_op-E-AD-99-5Hex-60mins.lcd

PDA Ch1 225nm 4nm

Peak#	Ret. Time	Area	Height	Area %	Height %
1	24.590	108129	1653	52.403	58.974
2	35.077	98212	1150	47.597	41.026
Total		206340	2803	100.000	100.000

General Procedure D: ^{1}H NMR Spectroscopy Binding Studies

Two 20-mL scintillation vials were flame dried and back purged with argon. Each scintillation vial was fitted with a septa and argon balloon. A freshly bought bottle of deuterated solvent (C_6D_6) equipped with activated 4 Å molecular sieves was used. Note: The deuterated solvent (C_6D_6) was left to sit with activated 4 Å molecular sieves for a minimum of 18 h prior to use. NMR tubes were placed in the oven for 1 h prior to use. Two stock solutions were made, (1) with the disiloxanediol, and (2) the Lewis base. The first stock solution was made by dissolving the disiloxanediol in 4 mL of deuterate solvent (C_6D_6). The Lewis base, pyridine (5.0 equiv) was added to the other scintillation vial. To further eliminate any moisture, the deuterated solvent (C_6D_6) was fitted with a septum and argon balloon when being used. A 2 mL aliquot was taken

from the stock solution containing the disiloxanediol and transferred to the stock solution containing the Lewis base. Then different volumes of each stock solution were mixed into the corresponding NMR tubes with the desired equivalents of Lewis base (Table **3.10**).

Table **3.10** Volumes needed for binding studies

NMR tube	Lewis base (equiv)	Volume from (SD solution)	Volume from (Lewis base solution)
A	0	0.50	0
B	1	0.45	0.05
C	2	0.35	0.15
D	3	0.25	0.25
E	4	0.15	0.35
F	5	0	0.50

Each NMR tube was capped with a rubber septum. Then, each NMR tube was back purged with argon. The ^{1}H NMR spectrum of each solution was recorded using the 400 MHz NMR spectrometer after 16 scans at room temperature. Binding constants were calculated using Microsoft Excel Solver to fit a nonlinear curve with the model equation below.[79] The binding affinity *(K_a)* was the only variable optimized and no constraints were used. The error was calculated at a 95% confidence interval based on the NMR data to the model.

$$\Delta\delta_i = \delta_{obs,i} - \delta_{free} = \frac{C}{R_o} \qquad \text{eq. } \mathbf{3.1}$$

$$C = \frac{(K_aR_o+1+K_aS_i) \pm \sqrt{(K_aR_o+1+K_aS_i)^2-4K_a{}^2R_oS_i}}{2K_a} \qquad \text{eq. } \mathbf{3.2}$$

The chemical shift (ppm) of the SiOH proton in the bound Lewis base complex is equal to $\delta_{complex}$, and thus $\Delta\delta = \delta_{complex} - \delta_{free}$ where $\delta_{free} =$ chemical shift (ppm) of the SiOH proton when no Lewis base is present (i.e., NMR tube A). This value ($\Delta\delta$) is estimated from extrapolation of where the binding curve levels off. The remaining values are as follows: $\delta_{obs,i} =$

chemical shift (ppm) of SiOH proton at *i* equivalents of Lewis base, $R_o =$ initial concentration of disiloxanediols, and $S_i =$ concentration of Lewis base at *i* equivalents in M, and $K_a =$ binding constant in M^{-1}.

3.12 References

(1) Pauling, L. *The Nature of the Chemical Bond and the Structure of Molecules and Crystals*, 3rd ed.; Cornell University Press, 1960.

(2) Doyle, A. G.; Jacobsen, E. N. Small-Molecule H-Bond Donors in Asymmetric Catalysis. *Chem. Rev.* **2007**, *107* (12), 5713–5743. https://doi.org/10.1021/cr068373r.

(3) Taylor, M. S.; Jacobsen, E. N. Asymmetric Catalysis by Chiral Hydrogen-Bond Donors. *Angew. Chem. Int. Ed.* **2006**, *45* (10), 1520–1543. https://doi.org/10.1002/anie.200503132.

(4) Schreiner, P. R. Metal-Free Organocatalysis through Explicit Hydrogen Bonding Interactions. *Chem. Soc. Rev.* **2003**, *32* (5), 289–296. https://doi.org/10.1039/B107298F.

(5) Takemoto, Y. Recognition and Activation by Ureas and Thioureas: Stereoselective Reactions Using Ureas and Thioureas as Hydrogen-Bonding Donors. *Org. Biomol. Chem.* **2005**, *3* (24), 4299–4306. https://doi.org/10.1039/B511216H.

(6) Akiyama, T.; Itoh, J.; Fuchibe, K. Recent Progress in Chiral Brønsted Acid Catalysis. *Adv. Synth. Catal.* **2006**, *348* (9), 999–1010. https://doi.org/10.1002/adsc.200606074.

(7) Seayad, J.; List, B. Asymmetric Organocatalysis. *Org. Biomol. Chem.* **2005**, *3* (5), 719–724. https://doi.org/10.1039/B415217B.

(8) Dalko, P. I. *Enantioselective Organocatalysis*; Wiley-VCH, 2007.

(9) Berkessel, A.; Gröger, H. *Asymmetric Organocatalysis- From Biomimetic Concepts to Applications in Asymmetric Synthesis*; Wiley-VCH, 2005.

(10) *Chiral Heterogeneous Scandium Lewis Acid Catalysts for Continuous-Flow Enantioselective Friedel–Crafts Carbon–Carbon Bond-Forming Reactions - Saito - 2021 - Angewandte Chemie International Edition - Wiley Online Library*. https://onlinelibrary.wiley.com/doi/10.1002/anie.202112797 (accessed 2025-04-21).

(11) Keith Hollis, T.; Odenkirk, W.; Robinson, N. P.; Whelan, J.; Bosnich, B. Homogeneous Catalysis. Transition Metal Based Lewis Acid Catalysts. *Tetrahedron.* **1993**, *49* (25), 5415–5430. https://doi.org/10.1016/S0040-4020(01)87259-8.

(12) Zhang, L.; Meggers, E. Chiral-at-Metal Catalysts: History, Terminology, Design, Synthesis, and Applications. *Chem. Soc. Rev.* **2025**, *54* (4), 1986–2005. https://doi.org/10.1039/D4CS01043D.

(13) Zhang, L.; Meggers, E. Steering Asymmetric Lewis Acid Catalysis Exclusively with Octahedral Metal-Centered Chirality. *Acc. Chem. Res.* **2017**, *50* (2), 320–330. https://doi.org/10.1021/acs.accounts.6b00586.

(14) *Titanium(IV)-Catalyzed Dynamic Kinetic Asymmetric Transformation of Alcohols, Silyl Ethers, and Acetals under Carbon Allylation - Braun - 2004 - Angewandte Chemie International Edition - Wiley Online Library*. https://onlinelibrary.wiley.com/doi/abs/10.1002/anie.200352128 (accessed 2025-04-21).

(15) Santelli, M.; Pons, J.-M. *Lewis Acids and Selectivity in Organic Synthesis*, 1st ed.; CRC Press: Boca Raton, Florida, 1996.

(16) Saito, Y.; Kobayashi, S. Chiral Heterogeneous Scandium Lewis Acid Catalysts for Continuous-Flow Enantioselective Friedel–Crafts Carbon–Carbon Bond-Forming Reactions. *Angew. Chem. Int. Ed.* **2021**, *60* (51), 26566–26570. https://doi.org/10.1002/anie.202112797.

(17) Ryu, D. H.; Zhou, G.; Corey, E. J. Enantioselective and Structure-Selective Diels−Alder Reactions of Unsymmetrical Quinones Catalyzed by a Chiral Oxazaborolidinium Cation.

Predictive Selection Rules. *J. Am. Chem. Soc.* **2004**, *126* (15), 4800–4802. https://doi.org/10.1021/ja049323b.
(18) Sibi, M. P.; Ma, Z.; Jasperse, C. P. Exo Selective Enantioselective Nitrone Cycloadditions. *J. Am. Chem. Soc.* **2004**, *126* (3), 718–719. https://doi.org/10.1021/ja039087p.
(19) Braun, M.; Kotter, W. Titan(IV)-Katalysierte Dynamisch-Kinetische Asymmetrische Umwandlung von Alkoholen, Silylethern Und Acetalen Unter Kohlenstoff-Allylierung. *Angew. Chem.* **2004**, *116* (4), 520–523. https://doi.org/10.1002/ange.200352128.
(20) Walsh, P. J.; Kozlowski, M. Lewis Acid and Lewis Base Catalysis. In *Fundamentals of Asymmetric Catalysis*; University Science Books, 2009.
(21) Walsh, P. J.; Kozlowski, M. Beyond Lewis Acid and Lewis Base Catalyzed Activation. In *Fundamentals of Asymmetric Catalysis*; University Science Books, 2009; p 674.
(22) Hine, J.; Linden, S. M.; Kanagasabapathy, V. M. 1,8-Biphenylenediol Is a Double-Hydrogen-Bonding Catalyst for Reaction of an Epoxide with a Nucleophile. *J. Am. Chem. Soc.* **1985**, *107* (4), 1082–1083. https://doi.org/10.1021/ja00290a067.
(23) Friedel, C.; Crafts, J.-M. *R.Acad. Sci.* **1884**, 449–532.
(24) Pihko, P. M. Activation of Carbonyl Compounds by Double Hydrogen Bonding: An Emerging Tool in Asymmetric Catalysis. *Angew. Chem. Int. Ed.* **2004**, *43* (16), 2062–2064. https://doi.org/10.1002/anie.200301732.
(25) Krause, N.; Hoffmann-Röder, A. Recent Advances in Catalytic Enantioselective Michael Additions. *Synthesis* **2001**, *2001* (2), 171–196. https://doi.org/10.1055/s-2001-10803.
(26) Das, T.; Mohapatra, S.; Mishra, N. P.; Nayak, S.; Raiguru, B. P. Recent Advances in Organocatalytic Asymmetric Michael Addition Reactions to α, β-Unsaturated Nitroolefins. *ChemistrySelect.* **2021**, *6* (15), 3745–3781. https://doi.org/10.1002/slct.202100679.
(27) Zhang, Y.; Wang, W. Recent Advances in Organocatalytic Asymmetric Michael Reactions. *Catal. Sci. Technol.* **2011**, *2* (1), 42–53. https://doi.org/10.1039/C1CY00334H.
(28) Berner, O. M.; Tedeschi, L.; Enders, D. Asymmetric Michael Additions to Nitroalkenes. *Eur. J. Org. Chem.* **2002**, *2002* (12), 1877–1894. https://doi.org/10.1002/1099-0690(200206)2002.
(29) Okino, T.; Hoashi, Y.; Takemoto, Y. Enantioselective Michael Reaction of Malonates to Nitroolefins Catalyzed by Bifunctional Organocatalysts. *J. Am. Chem. Soc.* **2003**, *125* (42), 12672–12673. https://doi.org/10.1021/ja036972z.
(30) Herrera, R. P.; Sgarzani, V.; Bernardi, L.; Ricci, A. Catalytic Enantioselective Friedel–Crafts Alkylation of Indoles with Nitroalkenes by Using a Simple Thiourea Organocatalyst. *Angew. Chem. Int. Ed.* **2005**, *44* (40), 6576–6579. https://doi.org/10.1002/anie.200500227.
(31) Tsogoeva, S. B.; Wei, S. Highly Enantioselective Addition of Ketones to Nitroolefins Catalyzed by New Thiourea–Amine Bifunctional Organocatalysts. *Chem. Commun.* **2006**, No. 13, 1451–1453. https://doi.org/10.1039/B517937H.
(32) Terada, M.; Ube, H.; Yaguchi, Y. Axially Chiral Guanidine as Enantioselective Base Catalyst for 1,4-Addition Reaction of 1,3-Dicarbonyl Compounds with Conjugated Nitroalkenes. *J. Am. Chem. Soc.* **2006**, *128* (5), 1454–1455. https://doi.org/10.1021/ja057848d.
(33) Huang, H.; Jacobsen, E. N. Highly Enantioselective Direct Conjugate Addition of Ketones to Nitroalkenes Promoted by A Chiral Primary Amine−Thiourea Catalyst. *J. Am. Chem. Soc.* **2006**, *128* (22), 7170–7171. https://doi.org/10.1021/ja0620890.

(34) Diels, O.; Alder, K. Synthesen in Der Hydroaromatischen Reihe. *Justus Liebigs Ann. Chem.* **1928**, *460* (1), 98–122. https://doi.org/10.1002/jlac.19284600106.
(35) Huang, Y.; Unni, A. K.; Thadani, A. N.; Rawal, V. H. Single Enantiomers from a Chiral-Alcohol Catalyst. *Nature.* **2003**, *424* (6945), 146–146. https://doi.org/10.1038/424146a.
(36) Unni, A. K.; Takenaka, N.; Yamamoto, H.; Rawal, V. H. Axially Chiral Biaryl Diols Catalyze Highly Enantioselective Hetero-Diels−Alder Reactions through Hydrogen Bonding. *J. Am. Chem. Soc.* **2005**, *127* (5), 1336–1337. https://doi.org/10.1021/ja044076x.
(37) Danishefsky, S.; Kitahara, T. Useful Diene for the Diels-Alder Reaction. *J. Am. Chem. Soc.* **1974**, *96* (25), 7807–7808. https://doi.org/10.1021/ja00832a031.
(38) Tonoi, T.; Mikami, K. Chiral Bis-Trifluoromethanesulfonylamide as a Chiral Brønsted Acid Catalyst for the Asymmetric Hetero Diels–Alder Reaction with Danishefsky's Diene. *Tetrahedron Lett.* **2005**, *46* (37), 6355–6358. https://doi.org/10.1016/j.tetlet.2005.07.043.
(39) Rajaram, S.; Sigman, M. S. Design of Hydrogen Bond Catalysts Based on a Modular Oxazoline Template: Application to an Enantioselective Hetero Diels−Alder Reaction. *Org. Lett.* **2005**, *7* (24), 5473–5475. https://doi.org/10.1021/ol052300x.
(40) Lou, S.; Schaus, S. E. Asymmetric Petasis Reactions Catalyzed by Chiral Biphenols. *J. Am. Chem. Soc.* **2008**, *130* (22), 6922–6923. https://doi.org/10.1021/ja8018934.
(41) Das, A.; Ayad, S.; Hanson, K. Enantioselective Protonation of Silyl Enol Ether Using Excited State Proton Transfer Dyes. *Org. Lett.* **2016**, *18* (20), 5416–5419. https://doi.org/10.1021/acs.orglett.6b02820.
(42) Lou, S.; Moquist, P. N.; Schaus, S. E. Asymmetric Allylboration of Ketones Catalyzed by Chiral Diols. *J. Am. Chem. Soc.* **2006**, *128* (39), 12660–12661. https://doi.org/10.1021/ja0651308.
(43) Chandrasekhar, V.; Boomishankar, R.; Nagendran, S. Recent Developments in the Synthesis and Structure of Organosilanols. *Chem. Rev.* **2004**, *104* (12), 5847–5910. https://doi.org/10.1021/cr0306135.
(44) Beemelmanns, C.; Husmann, R.; Whelligan, D. K.; Özçubukçu, S.; Bolm, C. Planar-Chiral Bis-Silanols and Diols as H-Bonding Asymmetric Organocatalysts. *Eur. J. Org. Chem.* **2012**, *2012* (18), 3373–3376. https://doi.org/10.1002/ejoc.201200548.
(45) Oishi, M.; Kawakami, Y. A Stereoselective Approach to Optically Active Bifunctional 1,3-Dimethyl-1,3-Diphenyldisiloxanes. *Org. Lett.* **1999**, *1* (4), 549–552. https://doi.org/10.1021/ol990068n.
(46) Dalton, J. J.; Bernal Sánchez, A.; Kelly, A. T.; Fettinger, J. C.; Franz, A. K. Organocatalytic Asymmetric Synthesis of Si-Stereogenic Siloxanols. *ACS Catal.* **2024**, *14* (2), 1005–1012. https://doi.org/10.1021/acscatal.3c03932.
(47) Diemoz, K. M.; Wilson, S. O.; Franz, A. K. Synthesis of Structurally Varied 1,3-Disiloxanediols and Their Activity as Anion-Binding Catalysts. *Chem. Eur. J.* **2016**, *22* (51), 18349–18353. https://doi.org/10.1002/chem.201604103.
(48) Diemoz, K. M.; Hein, J. E.; Wilson, S. O.; Fettinger, J. C.; Franz, A. K. Reaction Progress Kinetics Analysis of 1,3-Disiloxanediols as Hydrogen-Bonding Catalysts. *J. Org. Chem.* **2017**, *82* (13), 6738–6747. https://doi.org/10.1021/acs.joc.7b00875.
(49) Diemoz, K. M. Design, Synthesis and Investigation of Siloxanol Hydrogen-Bonding Catalysts and Chiral Silanol Ligands, 2011.
(50) Schafer, A. G.; Wieting, J. M.; Mattson, A. E. Silanediols: A New Class of Hydrogen Bond Donor Catalysts. *Org. Lett.* **2011**, *13* (19), 5228–5231. https://doi.org/10.1021/ol2021115.

(51) Tran, N. T. Design, Synthesis, and Study of Silanediols as Homogenous, Hydrogen-Bonding Organocatalysts for Asymmetric Transformation, 2014.
(52) Kannengießer, J.-F.; Briesenick, M.; Meier, D.; Huch, V.; Morgenstern, B.; Kickelbick, G. Synthesis and Hydrogen-Bond Patterns of Aryl-Group Substituted Silanediols and -Triols from Alkoxy- and Chlorosilanes. *Chem. Eur. J.* **2021**, *27* (66), 16461–16476. https://doi.org/10.1002/chem.202102729.
(53) Tran, N. T.; Min, T.; Franz, A. K. Silanediol Hydrogen Bonding Activation of Carbonyl Compounds. *Chem. Eur. J.* **2011**, *17* (36), 9897–9900. https://doi.org/10.1002/chem.201101492.
(54) Crawford, C. J.; Qiao, Y.; Liu, Y.; Huang, D.; Yan, W.; Seeberger, P. H.; Oscarson, S.; Chen, S. Defining the Qualities of High-Quality Palladium on Carbon Catalysts for Hydrogenolysis. *Org. Process Res. Dev.* **2021**, *25* (7), 1573–1578. https://doi.org/10.1021/acs.oprd.0c00536.
(55) Tran, N. T.; Min, T.; Franz, A. K. Silanediol Hydrogen Bonding Activation of Carbonyl Compounds. *Chem. Eur. J.* **2011**, *17* (36), 9897–9900. https://doi.org/10.1002/chem.201101492.
(56) Simons, R. S.; Haubrich, S. T.; Mork, B. V.; Niemeyer, M.; Power, P. P. The Syntheses and Characterization of the Bulky Terphenyl Silanes and Chlorosilanes 2,6-$Mes_2C_6H_3SiCl_3$, 2,6-$Trip_2C_6H_3SiCl_3$, 2,6-$Mes_2C_6H_3SiHCl_2$, 2,6-$Trip_2C_6H_3SiHCl_2$, 2,6-$Mes_2C_6H_3SiH_3$, 2,6-$Trip_2C_6H_3SiH_3$ and 2,6-$Mes_2C_6H_3SiC1_2SiC1_3$. *Main Group Chem.* **1998**, *2* (4), 275–283. https://doi.org/10.1080/10241229812331341469.
(57) Suzuki, H.; Tokitoh, N.; Okazaki, R.; Harada, J.; Ogawa, K.; Tomoda, S.; Goto, M. Synthesis and Structures of Extremely Hindered and Stable Disilenes. *Organometallics.* **1995**, *14* (2), 1016–1022. https://doi.org/10.1021/om00002a056.
(58) Södner, M.; Sandor, M.; Schier, A.; Schmidbaur, H. Synthesis Structure and Photoluminescence of 1,2-Disila-Acenaphthene $Si_2C_{10}H_{10}$ and 1,2-Diaryldisilane Reference Compounds. *Chem. Ber.* **1997**, *130* (11), 1671–1676. https://doi.org/10.1002/cber.19971301119.
(59) Barnes, G. H. Jr.; Daughenbaugh, N. E. The Preparation of Organosilanols via the Metal-Catalyzed Reaction of Organosilicon Hydrides with Water. *J. Org. Chem.* **1966**, *31* (3), 885–887. https://doi.org/10.1021/jo01341a056.
(60) Lee, M.; Ko, S.; Chang, S. Highly Selective and Practical Hydrolytic Oxidation of Organosilanes to Silanols Catalyzed by a Ruthenium Complex. *J. Am. Chem. Soc.* **2000**, *122* (48), 12011–12012. https://doi.org/10.1021/ja003079g.
(61) Kelly, A. T.; Franz, A. K. Metal-Free Synthesis of 1,3-Disiloxanediols and Aryl Siloxanols. *ACS Omega.* **2019**, *4* (4), 6295–6300. https://doi.org/10.1021/acsomega.9b00121.
(62) Lee, Y.; Seomoon, D.; Kim, S.; Han, H.; Chang, S.; Lee, P. H. Highly Efficient Iridium-Catalyzed Oxidation of Organosilanes to Silanols. *J. Org. Chem.* **2004**, *69* (5), 1741–1743. https://doi.org/10.1021/jo035647r.
(63) Tran, N. T.; Wilson, S. O.; Franz, A. K. Cooperative Hydrogen-Bonding Effects in Silanediol Catalysis. *Org. Lett.* **2012**, *14* (1), 186–189. https://doi.org/10.1021/ol202971m.
(64) Shumaila, A. M. A.; and Kusurkar, R. S. Silica Gel, an Effective Catalyst for the Reaction of Electron-Deficient Nitro-Olefins with Nitrogen Heterocycles. *Synth. Commun.* **2010**, *40* (19), 2935–2940. https://doi.org/10.1080/00397910903340694.

(65) Mesa, K. M.; Hibbard, H. A.; Franz, A. K. Sodium-Catalyzed Friedel–Crafts Reactions and Mechanistic Insight. *Org. Lett.* **2019**, *21* (11), 3877–3881. https://doi.org/10.1021/acs.orglett.9b00747.
(66) Liu, M.; Tran, N. T.; Franz, A. K.; Lee, J. K. Gas-Phase Acidity Studies of Dual Hydrogen-Bonding Organic Silanols and Organocatalysts. *J. Org. Chem.* **2011**, *76* (17), 7186–7194. https://doi.org/10.1021/jo201214x.
(67) Unno, M.; Matsumoto, T.; Matsumoto, H. Synthesis of Laddersiloxanes by Novel Stereocontrolled Approach. *J. Organomet. Chem.* **2007**, *692* (1), 307–312. https://doi.org/10.1016/j.jorganchem.2006.08.068.
(68) Kondo, S.; Fukuda, A.; Yamamura, T.; Tanaka, R.; Unno, M. Anion Recognition by a Disiloxane-1,3-Diol in Organic Solvents. *Tetrahedron Lett.* **2007**, *48* (45), 7946–7949. https://doi.org/10.1016/j.tetlet.2007.09.067.
(69) Dalton, J. J. Development and Mechanistic Analysis of the Organocatalytic Asymmetric Synthesis of Stereogenic Siloxanols from Prochiral Silanediols, 2024.
(70) Zhao, Y.; Rodrigo, J.; Hoveyda, A. H.; Snapper, M. L. Enantioselective Silyl Protection of Alcohols Catalysed by an Amino-Acid-Based Small Molecule. *Nature* **2006**, *443* (7107), 67–70. https://doi.org/10.1038/nature05102.
(71) Gutmann, V. *The Donor-Acceptor Approach to Molecular Interactions*, 1st ed.; Springer New York, NY, 2012.
(72) Denmark, S. E.; Jacobs, R. T.; Dai-Ho, G.; Wilson, S. Synthesis, Structure, and Reactivity of an Organogermanium Lewis Acid. *Organometallics.* **1990**, *9* (12), 3015–3019. https://doi.org/10.1021/om00162a006.
(73) Wilson, S. O.; Tran, N. T.; Franz, A. K. NMR and X-Ray Studies of Hydrogen Bonding for Amide-Containing Silanediols. *Organometallics.* **2012**, *31* (19), 6715–6718. https://doi.org/10.1021/om300736n.
(74) DiVerdi, J. A.; Kobayashi, T.; Maciel, G. E. Molecular Dynamics of Pyridine Adsorbed on the Silica Surface. *J. Phys. Chem. C* **2007**, *111* (16), 5982–5989. https://doi.org/10.1021/jp067353q.
(75) Nikiel, L.; Zerda, T. W. Adsorption of Pyridine on Silica Gels. *J. Phys. Chem.* **1991**, *95* (10), 4063–4069. https://doi.org/10.1021/j100163a033.
(76) Gurinov, A. A.; Mauder, D.; Akcakayiran, D.; Findenegg, G. H.; Shenderovich, I. G. Does Water Affect the Acidity of Surfaces? The Proton-Donating Ability of Silanol and Carboxylic Acid Groups at Mesoporous Silica. *ChemPhysChem* **2012**, *13* (9), 2282–2285. https://doi.org/10.1002/cphc.201200204.
(77) Dib, E.; Medeiros Costa, I.; Vayssilov, G. N.; Aleksandrov, H. A.; Mintova, S. Complex H-Bonded Silanol Network in Zeolites Revealed by IR and NMR Spectroscopy Combined with DFT Calculations. *J. Mater. Chem. A* **2021**.
(78) Södner, M.; Sandor, M.; Schier, A.; Schmidbaur, H. Synthesis Structure and Photoluminescence of 1,2-Disila-Acenaphthene Si2C10H10 and 1,2-Diaryldisilane Reference Compounds. *Chem. Ber.* **1997**, *130* (11), 1671–1676. https://doi.org/10.1002/cber.19971301119.
(79) Thordarson, P. Determining Association Constants from Titration Experiments in Supramolecular Chemistry. *Chem. Soc. Rev.* **2011**, *40* (3), 1305–1323. https://doi.org/10.1039/C0CS00062K.